Universidad Autónoma de Madrid

Faculty of Science

Department of Molecular Biology

Functional characterization of AmpC β-lactamase and role of LMM-PBPs in peptidoglycan composition, β-lactam resistance and *ampC* regulation in *Pseudomonas aeruginosa*

Doctoral Thesis

Alaa Ropy Mahmoud Sayed

Madrid 2014

Department of Molecular Biology

Faculty of Science

Universidad Autónoma de Madrid

Functional characterization of AmpC β-lactamase and role of LMM-PBPs in peptidoglycan composition, β-lactam resistance and *ampC* regulation in *Pseudomonas aeruginosa*

A dissertation presented

by

Alaa Ropy Mahmoud Sayed

to obtain the ***Ph.D. degree*** *in Biochemistry, Molecular Biology, Biomedicine and Biotechnology.*

Director

Dr. Juan Alfonso Ayala Serrano

This work was done at

Centro de Biología Molecular "Severo Ochoa" (CBMSO)

C/ Nicolás Cabrera nº 1; Campus de la Universidad Autónoma de Madrid, 28049, Madrid, Spain.

CENTRO DE BIOLOGÍA MOLECULAR
"SEVERO OCHOA"

JUAN ALFONSO AYALA SERRANO, Scientific Researcher A2 from Superior Council for Scientific Research (CSIC) and Honorary Professor in the Department of Molecular Biology at the Autonoma University of Madrid, group leader in the Department of Microbiology and Virology of the Centre for Molecular Biology "Severo Ochoa", CSIC -UAM,

CERTIFIES that

the doctoral thesis titled "**Functional characterization of Pae-AmpC β-lactamase and role of LMM-PBPs in peptidoglycan composition, β-lactam resistance and *ampC* regulation in *Pseudomonas aeruginosa*"** presented by Mr. **Alaa Ropy Mahmoud Sayed** to obtain the Ph.D. degree in Biochemistry, Molecular Biology, Biomedicine and Biotechnology has been performed at the Centre of Molecular Biology "Severo Ochoa", under my supervision

And to serve for the appropriate purpose, to authorize his presentation and evaluation by the corresponding committee, I sign this certification in Madrid the 17th September, 2014.

Sig. **Juan A. Ayala**

UNIVERSIDAD AUTONOMA
28049 CANTOBLANCO
MADRID, ESPAÑA
Tel: 91 196 44 97
Fax: 91 196 44 20

e-mail: jayala@cbm.csic.es

To My Beloved Father, Mother, Brother and Sisters

Acknowledgments

With the highest appreciation, I would like express my great thanks to Dr. Juan A. Ayala (CBMSO) for his supervision of my Ph. D. study and for guiding me in my thesis work.

Many thanks to Dr. Antonio Oliver (IdISPa) for accepting me to do some work in his Lab; also, I would like to thank his entire lab group (Dr. Bartolome Moya, Gabriel Cabot and all the others) for their cooperation.

Many thanks to Dr. Miguel A. De Pedro (CBMSO), Dr. Marina González-Leiza, Cristian Aguilera (CBMSO), Dr. Miguel Vicente (CNB), Dr. Alicia Sánchez (CNB) and Dr. Juan A. Hermoso (IQFR-CSIC) for their help.

Many thanks to all of those who gave me a hand during my Ph. D. study inside and outside the Centre of Molecular Biology (CBMSO).

This work was supported by a pre-doctoral scholarship (JAE) from the Spanish National Research Council (CSIC).

Finally, I would like to express my great thanks and gratitude to my parents who are always supporting and encouraging me.

Summary (in English) & Resumen (in Spanish)

Summary

Pseudomonas aeruginosa is one of the most problematic versatile Gram-negative bacteria in causing opportunistic human infections which are particularly difficult to treat because of its intrinsic resistance to antibiotics, as a consequence of many intervening resistance mechanisms involving the ability to overproduce the chromosomally encoded cephalosporinases, Pae-AmpC, which are periplasmic enzymes, belong to group I class C serine β-lactamases and are also responsible of bacterial resistance in many bacteria. In *P. aeruginosa*, *ampC* expression is regulated mainly by AmpG permeases, AmpD amidases, AmpR, NagZ, and two competing AmpR-binding muropeptides [UDP-MurNAc-pentapeptides (*ampC* suppressor) and 1,6-anhydromuropeptides (*ampC* inducer)]. Low molecular mass penicillin-binding proteins [LMM-PBP; e.g. PBP4 (DacB), PBP5 (DacC), PBP7 (PbpG)] are a group of periplasmic enzymes that have DD-carboxypeptidase and/or DD-endopeptidase activities which participate in cell separation, peptidoglycan (PG) maturation and recycling. Binding of β-lactams (e.g. penicillin) with LMM-PBPs causes an increase in anhydromuropeptides and periplasmic AmpC overproduction to hydrolyze that external unwelcome inducer. This study aims to highlight and to characterize the functions of Pae-AmpC and the role of LMM-PBPs PBP4, PBP5 and PBP7 in PG composition and bacterial resistance in *P. aeruginosa*; also, to study the role of these LMM-PBPs in Pae-*ampC* regulation and to see if they are needed for the recovery of rod shape of imipenem-induced round cells in *P. aeruginosa.* To fulfill this study we characterized several Pae-AmpC forms (wild type and mutants) in wild type and mutants of *E. coli* and in *P. aeruginosa* PAO1 strain which were tested for their PG composition by HPLC analysis and for bacterial resistance by disc diffusion method. Also, we constructed single and combined mutants of *dacB*, *dacC*, *pbpG* and *ampC* in PAO1 strain which were tested for their PG composition, *ampC* expression by RT-PCR, β-lactams susceptibility and their PBPs pattern by Bocillin-FL binding test. We analyzed PG composition and PBPs pattern in imipenem-induced round cells and their rod shape recovered cells in PAO1. We found that some Pae-AmpC mutants had a very low β-lactamase activity (AmpC-F4:C3 and AmpC-F4:C6); the mature form of Pae-AmpC had a high β-lactamase activity and a secondary DD-endopeptidase and DD-carboxypeptidase activities; only *dacB* single and combined mutations produced high *ampC* expression and β-lactam resistance; only *dacC* single and combined mutations produced maximum increase of PG pentapeptides. The triple mutant of *dacB*, *dacC* and *pbpG* displayed the largest increase in *ampC* expression and β-lactams resistance. Microscopic examination of all the constructed Pae mutants showed that they still retain their rod shape morphology similar to their parental PAO1 strain. Also, we found that activities of DacB, DacC and PbpG are not essential for recovery of rod shape in imipenem-induced spheres in *P. aeruginosa*.

P. aeruginosa es una de las bacterias Gram-negativas versátiles y más problemáticas causantes de infecciones oportunistas en humanos y que son particularmente difíciles de curar debido a su resistencia intrínseca a los antibióticos, como consecuencia de los muchos mecanismos de resistencia intervinientes, y que implica la capacidad de sobreproducir las cefalosporinas codificados cromosómicamente, Pae-AmpC. En *P. aeruginosa*, la expresión de *ampC* se rige principalmente por la permeasa AmpG, la amidasa AmpD, AmpR, NagZ y dos muropéptidos competidores fijadores de AmpR [UDP-MurNAc-pentapéptido (supresor de *ampC*) y 1,6-anhidro-muropéptidos (inductor de *ampC*)]. Las proteínas (de baja masa molecular) fijadoras de penicilina [LMM-PBP; por ejemplo PBP4 (DacB), PBP5 (DacC), PBP7 (PbpG)] son un grupo de enzimas periplásmicas que tienen actividades DD-carboxipeptidasa/DD-endopeptidasa y que participan en la separación celular, y en la maduración y reciclaje del peptidoglicano (PG). La unión de un β-lactámicos (por ejemplo, penicilina) a las LMM-PBP provoca un aumento en anhidro-muropéptidos y sobreproducción de AmpC en periplasma para hidrolizar este inductor externo no deseado. Este estudio tiene como objetivo destacar y caracterizar las funciones de Pae-AmpC y la implicación de PBP4, PBP5 y PBP7 en la composición del PG y la resistencia bacteriana en *P. aeruginosa* y además, analizar el papel de estas LMM-PBPs en la regulación de Pae-ampC y determinar si son necesarias para la recuperación de la forma bacilar a partir de esferoplastos de *P. aeruginosa* inducidos por imipenem. Para realizar este estudio hemos caracterizado varias formas de Pae-AmpC en *E. coli* y *P. aeruginosa* PAO1 que se ensayaron mediante la determinación de su composición del PG por análisis de HPLC y su resistencia bacteriana por el método de difusión en disco en agar. Además, hemos construido mutantes individuales y combinados de *dacB, dacC, pbpG* y *ampC* en la cepa PAO1. Además, se analizó la composición del PG y los patrones de PBP en esferoplastos inducidos por imipenem y de sus formas bacilares recuperadas en PAO1. Hemos encontrado que algunos mutantes de Pae-AmpC tenían una actividad muy baja β-lactamasa (AmpC-F4: C3 y AmpC-F4: C6); que el tipo silvestre de Pae-AmpC (AmpC-F4) tenía una alta actividad β-lactamasa y unas actividades secundarias de DD-endopeptidasa y DD-carboxipeptidasa; que sólo mutaciones individuales en *dacB* y combinadas producen una alta expresión de *ampC* y resistencia a β-lactámicos; que sólo mutaciones individuales en *dacC* y combinadas producen un aumento máximo de pentapéptidos en el PG. El triple mutante de *dacB, dacC* y *pbpG* mostró el mayor aumento en la resistencia a β-lactámicos y en la expresión de *ampC*. El examen microscópico de todos los mutantes construidos en PAO1 mostró que todavía conservan sus formas morfologías bacilares similar a su cepa parental PAO1. Las actividades de DacB, DacC y PbpG no son esenciales para la recuperación de la forma bacilar en los esferoplastos de *P. aeruginosa* inducidos por imipenem.

Index

Index

Contents	**Page**
Acknowledgements	**i**
Summary (in English)	**ii**
Resumen (in Spanish)	**iii**
List of abbreviations	**7**
List of figures	**9**
List of tables	**13**
1. Introduction	**15**
1.1. *Pseudomonas aeruginosa* & high challenge	**17**
1.2. Penicillin-binding proteins (PBPs)	**18**
1.2.1. High molecular mass HMM-PBPs (class A, B)	**18**
1.2.2. Low molecular mass LMM-PBPs (class C)	**19**
1.3. Peptidoglycan (PG, murein, cell wall)	**20**
1.3.1. PG structure & chemical and physical properties	**21**
1.3.2. PG biosynthesis and remodeling	**22**
1.4. Antibiotics targeting cell wall biosynthesis & bacterial resistance	**23**
1.4.1. Inhibitors of Mur family and PG precursors	**25**
1.4.2. β-Lactam antibiotics	**27**
1.4.3. Bacterial resistance to β-Lactams	**28**
1.4.4. β-lactamase inhibitors	**29**
1.5. β-Lactamases	**29**
1.5.1. Classification of β-lactamases	**29**
1.5.2. Group 2 and 3 β-lactamases	**30**
1.5.3. AmpC β-lactamases	**30**
1.5.4. Mechanism of action	**31**
1.5.5. AmpC structure	**34**

1.5.6. AmpC regulation in *Pseudomonas aeruginosa* **34**

2. Objectives of this study **39**

3. Materials & methods **41**

3.1. Bacterial strains and plasmids **43**

3.2. Primers **47**

3.3. Culture media for cell growth **47**

3.4. DNA manipulation **50**

3.4.1. DNA purification and sequencing **50**

3.4.2. Agarose DNA electrophoresis **50**

3.4.3. PCR amplification **50**

3.4.4. *ampC* cloning and expression using pET28b plasmid **52**

3.4.5. *ampC* cloning and expression using pUCP24 plasmid **53**

3.4.6. Bacterial transformation **56**

3.5. Protein manipulation **56**

3.5.1. Estimation of protein concentration **56**

3.5.2. SDS-PAGE electrophoresis **56**

3.5.3. Western blot **57**

3.5.4. β-lactamase activity assay **57**

3.5.5. Bocillin-FL test **58**

3.5.6. MALDI-TOF **58**

3.5.7. Cell fractionation for protein localization **58**

3.6. AmpC purification **59**

3.7. Construction PAO1 mutants **61**

3.8. Estimation of *ampC* expression by RT-PCR **62**

3.9. Antimicrobial susceptibility testing **63**

3.10. Production of imipenem-induced round cells of PAO1 wild type and mutants **65**

3.11. Confocal microscopic analysis **65**

3.12. Peptidoglycan (PG) manipulation **66**

3.12.1. Preparation of PG **66**

3.12.2. HPLC analysis **67**

3.12.3. Effect of Pae-AmpC on the whole PG and individual muropeptides in vitro **67**

4. Results **69**

4.1. Functional characterization of Pae-AmpC β-lactamase in *E. coli* and *P. aeruginosa* PAO1 strains **71**

4.1.1. Summary **71**

4.1.2. Pae-*ampC* cloning **72**

4.1.3. Pae-*ampC* expression **76**

4.1.4. Pae-AmpC purification and characterization **85**

4.1.5. Pae-AmpC structure and crystallization **85**

4.1.6. Effect of Pae-*ampC* expression on bacterial resistance **88**

4.1.7. Effect of Pae-*ampC* expression on PG composition (in vivo) **91**

4.1.8. Effect of the purified Pae-AmpC forms on PG composition and individual muropeptides (in vitro) **92**

4.2. Role of LMM-PBPs in *ampC* regulation, β-lactam resistance and peptidoglycan structure in *P. aeruginosa* **103**

4.2.1. Summary **103**

4.2.2. The constructed PAO1 mutants **103**

4.2.3. Growth rates and microscopic examination of PAO1 mutants **106**

4.2.4. Bocillin-FL test of PAO1 mutants **106**

4.2.5. Effect of LMM-PBPs inactivation on *ampC* expression and β-lactam resistance in *P. aeruginosa* PAO1. **107**

4.2.6. PG composition of the constructed PAO1 mutants **116**

4.3. Activities of DacB, DacC and PbpG are not essential for recovery of rod shape in imipenem-induced spheroplasts in *P. aeruginosa*. **119**

4.3.1. Summary **119**

4.3.2. Microscopic examination of imipenem-induced spheroplasts of PAO1 wild type and mutants. **120**

4.3.3. PG composition of imipenem-induced spheroplasts PAO1 wild type and mutants **120**

4.3.4. Bocillin-FL test of imipenem-induced spheroplasts of PAO1 wild type and PAOΔ*ampC* **121**

5. Discussion **127**

5.1. Motivation and design of this study **129**

5.2. Functional characterization of Pae-AmpC β-lactamase **130**

5.2.1. Various forms of Pae-AmpC were produced **130**

5.2.2. Interpretation AmpC production using pET28b and pUCP24 vectors **130**

5.2.3. Mutations, sub-cellular localization and solubility can largely affect AmpC β-lactamase activity **131**

5.2.4. The secondary DD-peptidase activity was clear with AmpC-F3 rather than the other studied AmpC forms **133**

5.2.5. AmpC-F3 crystallization & obstacles on the way! **134**

5.3. Role of *Pseudomonas aeruginosa* LMM-PBPs in PG composition, β-lactam resistance and *ampC* regulation in *P. aeruginosa* **135**

5.3.1. Role of *P. aeruginosa* LMM-PBPs in cell wall physiology **135**

5.3.2. Role of *P. aeruginosa* LMM-PBPs in AmpC regulation and β-lactam resistance **136**

5.4. Activities of DacB, DacC and PbpG are not essential for recovery of rod shape in imipenem-induced spheroplasts in *P. aeruginosa* **138**

6. Conclusions (in English) **143**

Conclusiones (in Spanish) **145**

Bibliography **149**

Addendum **161**

Lists of abbreviations, figures and tables

List of abbreviations

AMC	Amoxacillin/clavulanic acid
AmpD	anhMurNAc-L-Ala amidases
AmpG	Permease-muropeptide transporter
AmpR	LysR-type transcriptional regulator
AN	Amikacin
anhMurNAc	1,6-anhydro-*N*-acetylmuramic acid
AnmK	AnhMurNAc kinase
ATM	Aztreonam
C	Chloramphenicol
CPase(s)	Carboxypeptidase(s)
CRO	Ceftriaxone
CTX	Cefotaxim
Eco	*E. coli*
EPase(s)	Endopeptidase(s)
ESACs	Extended-spectrum AmpC cephalosporinases
ESBLs	Extended-Spectrum β-lactamases
FOX	Cefoxitin
Fru-6-P	Fructose-6-phosphate
GlcNAc	*N*-acetylglucosamine
GlmM	Phosphoglucosamine mutase
GlmU	Bifunctional *N*-acetylglucosamine-1-phosphate Uridyltransferase/glucosamine-1-phosphate acetyltransferase
TGase(s)	Transglycosylase(s)
HMM-PBPs	High molecular mass penicillin-binding proteins
IMI	Imipenem
LdcA	LD-Carboxypeptidase
lipid I	Undecaprenoyl-pyrophosphoryl-MurNAc–pentapeptide
lipid II	Undecaprenoyl-pyrophosphoryl-GlcNAc-MurNAc-pentapeptide
LMM-PBPs	Low molecular mass penicillin-binding proteins
LTs	Lytic transglycosylases
MBLs	Metallo-β-lactamases

***m*-DAP& m-A2pm**	*meso*-diaminopimelic acid
Moe A	Moenomycins A
Mpl	Murein tripeptide ligase
MppA	Muropeptides binding protein
MraY	UDP-MurNAc–pentapeptide phosphotransferase
MurA	UDP-GlcNAc enolpyruvyl transferase
MurB	UDP-MurNAc dehydrogenase
MurC	UDP-MurNAc–L-Ala ligase
MurD	UDP-MurNAc-L-Ala–D-Glu ligase
MurE	UDP-MurNAc-L-Ala-D-Glu–meso-Dap ligase
MurF	UDP-MurNAc-tripeptide–D-alanyl–D-Alal ligase
MurG	UDP-GlcNAc-undecaprenoyl-pyrophosphoryl–MurNAc–pentapeptide transferase
MurI	Glu racemase
MurNAc	N-acetylmuramic acid
MurP	N-acetylmuramic acid transporter
MurQ	MurNAc-6-phosphate etherase
NagA	*N*-acetylglucosamine-6-phosphate deacetylase
NagB	Glucosamine-6-phosphate deaminase
NagE	PTS phosphotransferase system
NagZ	*N*-acetylglucosaminidase
OMPs	Outer membrane proteins
Opp	Oligopeptide permease
Pae	*Pseudomonas aeruginosa*
PB	Penicillin-binding domain
PBP(s)	Penicillin binding protein(s)
PBS	Phosphate-buffered saline
PG	Peptidoglycan
RBS	Ribosome binding site
TIC	Ticarcillin
TPase	Transpeptidase
UDP-GlcNAc	Uridine diphosphate *N*-acetylglucosamine
UDP-MurNAc	Uridine diphosphate *N*-acetylmuramic acid

List of figures

No.	Chapter/ *Description*	Page
	Introduction (section 1)	
1.1	*Common 3-4 crosslinks between glycan strands of PG*	**22**
1.2	*Outline of PG biosynthesis, PG recycling and ampC regulation in Gram-negative bacteria*	**24**
1.3	*Sub-cellular targets for antibiotic actions*	**26**
1.4	*Mechanism of antibiotic inhibition of bacterial cell wall biosynthesis*	**26**
1.5	*Chemical structures of penicillins and cephems*	**27**
1.6	*Chemical structures of penems, carbapenems, aztreonam, sulbactam and tazobactam*	**28**
1.7	*Mechanism of action of β-lactamases and PBPs on β-lactams*	**33**
	Methods (section 3)	
3.1	*Outline of Pae-ampC cloning region in pET28b vector*	**54**
3.2	*Outline of Pae-ampC cloning region in pUCP24 vector*	**55**
3.3	*Outline for gene-knockout inactivation of pbpG and dacC in P. aeruginosa by cre-lox method*	**64**
	Results (section 4)	
4.1	*Schematic outline of general structures and amino acid sequences of the studied Pae-AmpC forms*	**75**
4.2	*Detection of AmpC-F1, AmpC-F1:C3, AmpC-F1:C6 and AmpC-F2 in cellular fractions (total sonicate, cell extract and cell membrane) of Bl21(DE3)*	**78**
4.3	*Detection of AmpC-F4, AmpC-F4:C3, AmpC-F4:C6 and AmpC-F3 in cellular fractions (total sonicate, cell extract and cell membrane) of Bl21(DE3)*	**79**
4.4	*Detection of AmpC-F4, AmpC-F4:C3, AmpC-F4:C6, AmpC-F2*	

	and AmpC-F3 in cellular fractions (total sonicate, cell extract and cell membrane) of DV900(DE3)	**80**
4.5	*Expression and production of AmpC-F3, AmpC-F3-TEV and AmpC-F4-TEV in Bl21(DE3) transformants*	**81**
4.6	*Pae-ampC expression in PAO1 mutants transformed with pUCP-F3 and pUCP-F4*	**83**
4.7	*Analysis of the purified Pae-AmpC forms by SDS-PAGE and western blot*	**87**
4.8	*Muropeptides structures and chromatograms of HPLC analysis of PG of E. coli Bl21(DE3) and DV900(DE3)*	**94**
4.9	*Effect of AmpC-F3(b) activity on individual muropeptides M4, M5, D44 and D45 at 37 and 42°C (in vitro)*	**101**
4.10	*Effect of AmpC-F3(a) activity on individual muropeptides M4, M5, D44 and D45 at 42°C (in vitro)*	**102**
4.11	*Growth curves of the constructed PAO1 mutants*	**108**
4.12	*Microscopic examination of the constructed PAO1 mutants*	**109**
4.13	*Bocillin-FL binding test of cell membranes of PAO1 mutants under non-induction conditions*	**112**
4.14	*Bocillin-FL binding test of cell membranes of PAO1 mutants previously induced with cefoxitin*	**113**
4.15	*Microscopic examination of spheroplasts of imipenem-induced PAO1 wild type, PAOΔampC and PAOΔdacBΔdacCΔpbpG ΔampC mutants*	**124**
4.16	*Bocillin-FL binding of Pae spheroplasts membranes of IMI-induced PAO1 wild type and PAOΔampC mutant*	**126**

Addendum

A.1	*Colony-PCR amplifications of the different ampC forms displaying their DNA fragment sizes*	**161**
A.2	*Confirmation of the constructed pbpG and dacC gene-specific mutagenesis vectors*	**162**
A.3	*Verification of the constructed mutants PAOΔpbpG, PAOΔdacB ΔpbpG and PAOΔpbpGΔampC by colony PCR and agarose gel*	

	electrophoresis	**163**
A.4	*Verification of the constructed mutants PAOΔdacCΔampC, PAOΔdacCΔpbpG, PAOΔdacC, PAOΔdacBΔdacC and PAOΔdacBΔdacCΔpbpG*	**164**
A.5	*Verification of the constructed mutants PAOΔdacBΔampC and PAOΔdacBΔpbpGΔampC*	**165**
A.6	*Verification of the constructed mutants PAOΔdacBΔdacCΔampC, PAOΔdacCΔpbpGΔampC and PAOΔdacBΔdacCΔpbpGΔampC*	**166**
A.7	*Verification of the constructed mutant PAOΔdacBΔpbpGΔampC ΔdacC*	**167**

List of tables

No.	Chapter/ *Description*	Page
	Introduction (section 1)	
1.1	*Various cephalosporin generations*	**28**
1.2	*Functional and structural classification of β-lactamases*	**32**
	Material & Methods (section 3)	
3.1	*Bacterial strains and plasmids*	**44**
3.2	*Primers used for PCR amplification and DNA sequencing.*	**48**
3.3	*Primers used for the construction of knockout mutants of ampC, dacB, dacC and pbpG in PAO1*	**49**
3.4	*Conditions used for PCR amplification of different ampC forms*	**51**
	Results (section 4)	
4.1	*Mutations and changes in the main sequence of the cloned Pae-ampC constructs*	**74**
4.2	*β-lactamase activity of different forms of AmpC expressed in BL21(DE3) and DV900(DE3) after IPTG induction*	**82**
4.3	*β-lactamase activity of some PAO1 mutants transformed with pUCP-F3 and pUCP-F4*	**84**
4.4	*Characterization of the purified Pae-AmpC Forms*	**86**
4.5	*Disc diffusion assay for Pae-AmpC expression in Bl21(DE3)/pET-ampC*	**89**
4.6	*Disc diffusion assay for complementation of ampC deletion in some PAO1 mutants*	**90**
4.7	*HPLC analysis of muropeptides prepared from PG of induced E. coli Bl21(DE3)/pET-ampC*	**96**
4.8	*HPLC analysis of muropeptides prepared from PG of induced E. coli DV900(DE3)/pET-ampC*	**97**
4.9	*HPLC analysis of muropeptides prepared from PG of*	

	PAO1/pUCP24-ampC	**98**
4.10a	*HPLC PG analysis of E. coli DV900 and CS109 after incubation with different forms of Pae-AmpC in vitro*	**99**
4.10b	*Selected muropeptides from HPLC analysis of PG of DV900 after incubation with different forms of Pae-AmpC in vitro*	**100**
4.11	*Estimated IC_{50} values for cefoxitin with cell membranes of the wild type and some PAO1 mutants using Bocillin-FL test*	**111**
4.12	*MICs and ampC expression under basal and cefoxitin induction conditions for all studied mutants*	**114**
4.13	*HPLC analysis of muropeptides prepared from PG of the constructed Pae mutants under non-induction conditions*	**117**
4.14	*HPLC analysis of muropeptides prepared from PG of the constructed Pae PAO1 mutants treated with FOX*	**118**
4.15a	*HPLC analysis of muropeptides prepared from PG of imipenem-induced Pae spheroplasts*	**122**
4.15b	*Selected muropeptides produced from PG of imipenem-induced Pae spheroplasts*	**123**

Introduction

1. ***Introduction***
   - *1.1. Pseudomonas aeruginosa & high challenge*
   - *1.2. Penicillin-binding proteins (PBPs)*
     - *1.2.1. High molecular mass HMM-PBPs (class A, B)*
     - *1.2.2. Low molecular mass LMM-PBPs (class C)*
   - *1.3. Peptidoglycan (PG, murein, cell wall)*
     - *1.3.1. PG structure & chemical and physical properties*
     - *1.3.2. PG biosynthesis and remodeling*
   - *1.4. Antibiotics targeting cell wall biosynthesis & bacterial resistance*
     - *1.4.1. Inhibitors of Mur family and PG precursors*
     - *1.4.2. β-Lactam antibiotics*
     - *1.4.3. Bacterial resistance to β-Lactams*
     - *1.4.4. β-lactamase inhibitors*
   - *1.5. β-Lactamases*
     - *1.5.1. Classification of β-lactamases*
     - *1.5.2. Group 2 and 3 β-lactamases*
     - *1.5.3. AmpC β-lactamases*
     - *1.5.4. Mechanism of action*
     - *1.5.5. AmpC structure*
     - *1.5.6. AmpC regulation in Pseudomonas aeruginosa*

1. Introduction

1.1. *Pseudomonas aeruginosa* & high challenge

Classification

Bacteria (Super-kingdom); Proteobacteria (Phylum); Gammaproteobacteria (Class); Pseudomonadales (Order); Pseudomonadaceae (Family); Pseudomonas (Genus), aeruginosa (Species) (Benson et al, 2009; Sayers et al, 2009).

Genetic complexity and diversity & clinical challenge

The complete genome of *P. aeruginosa* PAO1 strain was sequenced and displayed 6.3 Mbp with 5570 predicted open reading frames (ORFs) which are mostly larger than sequenced genomes of 25 bacterial strains showing how complex is *P. aeruginosa*. This massive number of ORFs has only a few gene clusters duplicated and lacks recent gene duplications referring to high functional diversity, genetic complexity and evolutionary adaptations of this microorganism which can explain its versatility and wide occurrence in soil, water, as well as on plant and animal tissues as a pathogen (Stover et al, 2000). PAO1 strain is considered as the major reference strain for research *P. aeruginosa*, where new genomic sequences of other Pseudomonas strains are being discovered, annotated and compared with PAO1 reference to reveal the function and genetic variations (SNPs) of the new ORFs (Klockgether et al, 2010; Winsor et al, 2011). *P. aeruginosa* is considered as one of the most challenging versatile Gram negative bacteria in causing opportunistic human infections which are particularly difficult to treat because of its intrinsic resistance to antibiotics, as a consequence of many intervening resistance mechanisms; its low outer membrane permeability (OprD porin), active drug efflux pumps and mutations leading overproduction of the chromosomally encoded cephalosporinase, AmpC. While the incidences of concerning transferable resistance determinants, such as those encoding class B carbapenemases are increasing, especially in other pathogens, the current global threat of antimicrobial resistance in *P. aeruginosa* mainly still results from the extraordinary capacity of this microorganism to develop resistance to almost any available antibiotic by the selection of mutations in chromosomal genes. This enables *P. aeruginosa* to produce multidrug-resistance strains through combinations of the previous resistance mechanisms beside accumulation of multiple chromosomal changes overtime. So, treatment of *P. aeruginosa* is a serious therapeutic challenge (Lister et al, 2009; Stover et al, 2000; Strateva & Yordanov, 2009). *P. aeruginosa* secretes several virulence factors (e.g. pili, flagella, lipopolysaccharides, quorum sensing, toxins, lipases and proteases), (Lyczak et al, 2000; Stover et al, 2000). Also, *P. aeruginosa* is able to develop biofilm which is surface-attached microbial

populations with distinctive construction and phenotypic and biochemical properties different from their free-swimming, planktonic counterparts. Bacterial biofilm is characterized by a very high antibiotic resistance when compared with planktonic cells (Mah et al, 2003). AmpC overproduction is the main mechanism in *P. aeruginosa* to develop resistance to most of β-lactams, with the exception of carbapenems and cefepime which require additional mechanisms to develop resistance [e.g., AmpC mutations, downregulation of porin production] (Cabot et al, 2014; Lister et al, 2009). It was reported that *P. aeruginosa* is the second common pathogen to be clinically isolated after *E. coli* and it was reported that among 56 random isolates of *P. aeruginosa* there were 41.1% non-multidrug resistant (non-MDR) strains, 37.5% extensively drug resistant (XDR) strains and 21.4% multidrug resistant (MDR) strains (Gomila et al, 2013); such a study highlights how dangerous are the resistant mutants of this microorganism. Therefore, finding more effective antibiotics to cure infections with resistant (MDR and XDR) *P. aeruginosa* pathogens is a public necessity.

1.2. Penicillin-binding proteins (PBPs)

PBPs are a group of enzymes responsible for PG polymerization, crosslinking and remodeling in the periplasmic compartment (section 1.3.2; Fig.1.2). They have a common penicillin-binding domain although they may have different overall structures and activities. According to their molecular masses and structures, PBPs were classified into class A (HMM-PBPs), class B (HMM-PBPs) and class C (LMM-PBPs) referring to *E. coli* type which has twelve PBPs involving three class A PBPs (PBP1a, PBP1b and PBP1c), two class B PBPs (PBP2 and PBP3) and seven class C LMM-PBPs (PBP4, PBP5, PBP6, PBP6b, PBP7, PBP4b and AmpH) (Sauvage et al, 2008). Penicillin-binding proteins in *E. coli* are the best characterized, both at molecular and functional level, and the PBPs from most other microorganisms are always referred to those one, including Gram-positive that have a different peptidoglycan structure (Sauvage et al, 2008).

1.2.1. High molecular mass HMM-PBPs (class A, B)

HMM-PBPs are multimodular enzymes (>60 kDa) which catalyze PG polymerization and/or crosslinking by glycosyltransferase (TGase) and transpeptidase (TPase) activities respectively. They mainly act to construct a new PG strands by TGase activity from muropeptide subunits carried by lipid II and then to crosslink these new strands into the old PG mesh by TPase activity. They have a cytoplasmic tail, a transmembrane anchor and two periplasmic domains whose C-terminal one is called penicillin-binding (PB) domain, due to the ability to bind β-lactams, and is responsible for TPase activity. HMM-PBPs were further

classified into class A and class B depending on the structures and the catalytic activity of the N-terminal domain (Sauvage et al, 2008; Vollmer & Bertsche, 2008).

Class A PBPs (e.g. Eco-PBP1a and Eco-PBP1b) are bifunctional enzymes with TGase and TPase activities as their N-terminal domain has TGase activity. Eco-PBP1a and Eco-PBP1b are the main bifunctional TGase-TPase enzymes in *E. coli* (Sauvage et al, 2008). Inactivation of both of PBP1a and PBP1b was lethal to *E. coli*; indicating their vital role in PG synthesis and cell life (Denome et al, 1999; Kong et al, 2010; Sauvage et al, 2008). Penicillin-binding proteins Pae-PBP1a and Pae-PBP1b of Pseudomonas belong to this class (Sauvage et al, 2008).

Class B PBPs (e.g. Eco-PBP2 and Eco-PBP3) are monofunctional TPase enzymes. They are involved in cell elongation complex (elongase), cell division complex (divisome) and cell morphogenesis. Their N-terminal domain may interact with some other proteins involved in the cell cycle and in turn affects cell morphogenesis. It was reported that Eco-PBP2 is essential for cell elongation and shape maintenance, while Eco-PBP3 is essential for cell division in *E. coli* (Sauvage et al, 2008). Penicillin-binding proteins Pae-PBP2, Pae-PBP3 and Pae-PBP3b of Pseudomonas belong to this class (Sauvage et al, 2008).

1.2.2. Low molecular mass, LMM-PBPs (class C)

LMM-PBPs include periplasmic proteins (<60 kDa) that are either soluble or associated with the cytoplasmic membrane. They are not essential for bacterial viability under laboratory conditions (Clarke et al, 2009; Sauvage et al, 2008). Their PB domain has carboxypeptidase (CPase) and/or endopeptidase (EPase) activities which enable them to participate in PG maturation and recycling and cell separation. LMM-PBPs were sub-divided into 4 sub-groups (Type-4, type-5, type-7 and type-AmpH) referring to *E. coli* type concerning structural and functional similarities (Sauvage et al, 2008).

Type-4 class C LMM-PBPs (e.g. Eco-PBP4): *E. coli* PBP4 with solved crystal structure was reported to have both DD-EPase and DD-CPase activities (Clarke et al, 2009; Kishida et al, 2006). Type-4 PBPs are very loosely associated with the cytoplasmic membrane and may be involved in cell morphology, daughter cell separation and biofilm formation. (Sauvage et al, 2008). Inactivation of PBP4 in *P. aeruginosa* was reported to cause AmpC overproduction triggering high β-lactam resistance (Moya et al, 2009). Penicillin-binding protein Pae-DacB of Pseudomonas belongs to this class (Sauvage et al, 2008).

Type-5 class C LMM-PBPs [e.g. Eco-PBP5, Eco-PB6 and Eco-PBP6b (DacD)]: Type-5 LMM-PBPs have DD-CPase activity, being Eco-PBP5 the prototype and it is the most abundant LMM-PBP with major DD-CPase. Type-5 LMM-PBPs are associated with the cytoplasmic membrane by amphipathic helix and play an important role in determining the cell

diameter and the correct septum formation (Chowdhury & Ghosh, 2011; Chowdhury et al, 2010; Ghosh et al, 2008; Sauvage et al, 2008). It was suggested that Eco-PBP5 (but not Eco-PBP6 and Eco-DacD) may have a role in intrinsic β-lactam resistance (Sarkar et al, 2011). Recently, it has been described that the soluble form of PBP5 from PA01 (Pae-sPBP5) displayed in vitro bifunctional DD-CPase and expanded-spectrum β-lactamase activities even for carbapenems which is unusual when compared with the monofunctional DD-CPase Eco-PBP5 in *E. coli*. This behavior was explained by the flexibility and enlargement of the active site to share the same catalytic apparatus and similar mechanisms. This may be helpful for understanding the evolution of β-lactamase activity from the PBP enzymes (Smith et al, 2013). Penicillin-binding protein Pae-DacC of Pseudomonas belongs to this class (Sauvage et al, 2008).

Type-7 class C LMM-PBPs (e.g. Eco-PBP7): PBP7 enzymes are loosely associated to the cytoplasmic membrane and have DD-EPase activity. It was found that *E. coli* double mutant ΔPBP5-ΔPBP7 had more abnormality than the single mutant ΔPBP5; however the single mutant ΔPBP7 showed no morphological change (Sauvage et al, 2008). It was suggested that PBP4 and PBP7 affect cell shape in concert with PBP 5 (Meberg et al, 2004). Penicillin-binding protein Pae-PpbG of Pseudomonas belongs to this class (Sauvage et al, 2008).

Type-AmpH class C LMM-PBPs (e.g. Eco-AmpH): It was described that AmpH from *E. coli* showed a bifunctional behavior of EPase and CPase activities (Gonzalez-Leiza et al, 2011). Type-AmpH PBPs have a close structural similarity to class C-β-lactamase. It was suggested that AmpH and AmpC may participate in the normal PG synthesis, remodeling or recycling (Pratt, 2008; Sauvage et al, 2008). No penicillin-binding proteins of this class are identified in Pseudomonas (Sauvage et al, 2008).

1.3. Peptidoglycan (PG, murein, cell wall)

PG and murein are synonyms for the periplasmic sacculus surrounding the cytoplasmic membrane as mesh-like envelope. Furthermore, PG is the main structural component of the bacterial cell wall and mainly acts to maintain the bacterial cell shape and integrity (bacilli, cocci …) protecting the cell from its turgor and acts as a support for some other envelope components like proteins and teichoic acid. Therefore, PG is vital to the bacterial cell life and any major changes in its composition can affect the bacterial cell shape. Moreover, PG deformation or degradation can lead to cell lysis (Vollmer & Bertsche, 2008; Vollmer et al, 2008a; Vollmer & Holtje, 2004; Vollmer & Seligman, 2010).

1.3.1. PG structure& chemical and physical properties

PG is a heterogeneous elastic biopolymer of muropeptides which are linked together by β-1,4-bonds to form a long glycan strands cross-linked by bridges between its peptide stems. Each muropeptide subunit is composed of disaccharide derivatives of *N*-acetylglucosamine (GlcNAc) and *N*-acetylmuramic acid (MurNAc) in addition to a peptide stem of di-, tri-, tetra- or pentapeptides. Moreover, the glycan chains of muropeptides are crosslinked together frequently by 3-4 crosslinks which can be either direct as in most Gram-negative bacteria (e.g. *E. coli*) or through an inter-peptide bridge within most Gram-positive bacteria (e.g. *Staphylococcus aureus*) (fig. 1.1). The peptide stem in PG of *E. coli* and most Gram-negative bacteria is composed of amino acids L-Ala, D-Glu, Dap, D-Ala and D-Ala which occupy positions of numbers 1, 2, 3, 4 and 5, respectively, where amino acid number 1 (L-Ala) is linked to the D-lactyl group of MurNAc. The same was reported for PG peptide stem in most of Gram-positive bacteria except for positions number 2 and 3 which are occupied by D-Gln and L-Lys, respectively. (Vollmer & Bertsche, 2008; Vollmer et al, 2008a; Vollmer & Holtje, 2004; Vollmer & Seligman, 2010). D-amino acids in peptide stems provide PG with resistance against auto-degradation by cellular proteases because D-amino acids are not common in natural proteins and peptides (Cava et al, 2011). PG composition can change from one strain to another and even within the same strain because it is sensitive to changes in growth conditions (e.g. growth media, temperature and growth phase). These changes may involve variations in the length of the glycan strands, types and degree of cross-linkage, amino acids of the peptide stem and PG layers which are almost one layer in Gram-negative bacteria while several PG layers occur frequently in Gram-positive bacteria. PG of *E. coli* was used for long time for HPLC analysis to understand its chemical structure beyond its purification and digestion with muramidase which cleaves β-1,4-glycosidic bonds between MurNAc and GlcNAc residues liberating the constituting muropeptide subunits which can be separated and analyzed by HPLC (Glauner, 1988; Glauner et al, 1988). Knowing PG chemical composition provides important data concerning cell wall structure which in turns may explain variations in cell shapes (Cava et al, 2013). Atomic Force Microscopy and TEM tomography were used to track the mechanics and spatial architecture of PG from different bacteria (Cava et al, 2013; Vollmer & Seligman, 2010; Yao et al, 1999). Additionally, it was concluded that the glycan strands in Gram-negative bacteria (e.g. *E. coli* and *P. aeruginosa*) run almost in parallel to the cell membrane in the direction of the short axis of the cell, while the PG peptide-stems are oriented mostly in the direction of the long axis. Also, It was found that the PG is thinner and shorter with less crosslinks and larger pores in *Pseudomonas aeruginosa* than in *E. coli* (Vollmer & Seligman, 2010).

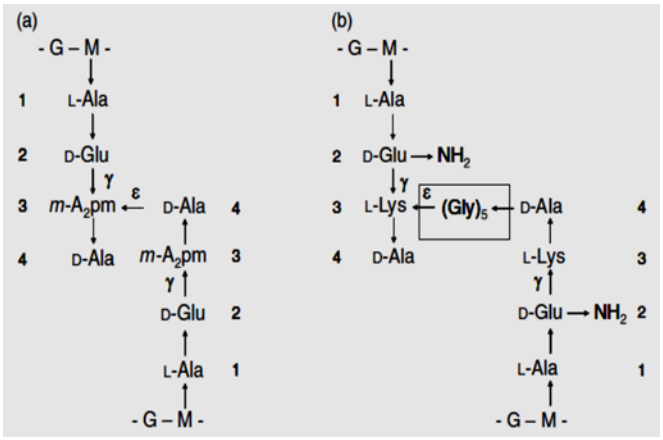

Figure 1.1. Common 3-4 crosslinks between glycan strands of PG (Vollmer et al, 2008a).

(a) *Direct 3-4 crosslinks in E. coli between D-Ala and m-A2pm.* ***(b)*** *3–4 cross-link with a penta-glycine bridge between D-Ala and L-Lys in Staphylococcus aureus.*

M: *N-acetylmuramic acid,* ***G:*** *N-acetylglucosamine. Numbers refer to positions of amino acids in peptide stems where the 1st amino acid, L-Ala, is linked to N-acetylmuramic acid.*

1.3.2. PG biosynthesis and remodeling

Biosynthesis of PG takes place in three cellular compartments (cytoplasm, cytoplasmic membrane and periplasm) beginning in the cytoplasm where UDP-MurNAc-pentapeptide (fig. 1.2; 2) is constructed from Fructose-6-P (fig. 1.2; 1), free tri-, tetra- or pentapeptides (fig. 1.2; 7a-c), GlcNAc-6-P, MurNAc-6-P and anhMurNAc (fig. 1.2; 10) by consecutive activities of AnmK, MurQ, NagA, GlmS, GlmM, GlmU, MurA-F and Mpl. The next step occurs at the cytoplasmic membrane in the cytoplasmic side where PG precursor carriers (Lipid I and II) are formed by the action of MraY and MurG on UDP-MurNAc-pentapeptide, undecaprenoyl phosphate carrier and UDP-GlcNAc. Then, lipid II (disaccharide pentapeptide carrier) is turned out by flippase activity from cytoplasm into the periplasmic side where muropeptide subunits are liberated from lipid II and incorporated into newly formed PG chains by glycosyltransferase action of TGase HMM-PBPs (fig. 1.2; 3) and then newly formed PG strands are crosslinked with the old PG network by transpeptidase activity of TPase HMM-PBPs (fig. 1.2; 4). Meanwhile, PG pentapeptide stems (fig. 1.2; 3c, 4c) are trimmed into tetrapeptide stems by the action of DD-CPases. Also, undecaprenoyl phosphate carriers are recycled for new lipid II synthesis (Fisher & Mobashery, 2014; Johnson et al, 2013; Typas et al, 2012). Normally, many bacterial cells remodel about half of their PG per generation which aids in insertion of newly PG strands in PG mesh and cell elongation and division. PG turnover starts in the periplasm by the action of PG hydrolases (fig. 1.2; steps 1-5) where endopeptidases (EPases LMM-PBPs) hydrolyze the peptide crosslinks between peptide stems of PG strands; DD-carboxypeptidases (DD-CPases LMM-PBPs) convert pentapeptide stems into tetrapeptides by elimination of the terminal D-Ala (fig. 1.2; 5b; step 1); Lytic transglycosylases (LTs) hydrolyze 1,4-β-glycosidic bonds within glycan strands releasing anhydromuropeptides GlcNAc-anhMurNAc-peptides [tri-

, tetra- or pentapeptides; (fig. 1.2; 6a-c; step 2)]. Moreover, periplasmic amidases AmiA-D in *E. coli* or AmpDh2 and AmpDh3 in *P. aeruginosa* cleave the peptide stem releasing free tri-, tetra- and pentapeptides from the muropeptide subunits in PG strands (fig. 1.2; 7a-c). After that, free GlcNAc, MurNAc and peptides are passed into cytoplasm by NagE, MurP and Opp and converted into GlcNAc-6-P, MurNAc-6-P and tripeptides, respectively, to be recycled into PG biosynthesis. Also, GlcNAc-anhMurNAc (fig. 1.2; 9) and GlcNAc-anhMurNAc-peptide (tri-, tetra- or penta-peptide; fig. 1.2; 6a-c) are transported into cytoplasm by AmpG permeases (Fig. 1.2; step 3). In cytoplasm, muropeptides (fig. 1.2; 6a-c; step 4) and free disaccharide derivatives (fig. 1.2; 9) are further cleaved by NagZ into anhMurNAc-peptide (tri-, tetra- or pentapeptides; fig. 1.2; 8a-c) and the constituting sugars (GlcNAc and anhMurNAc), respectively. Also, LdcA (LD-CPase) enzymes trim all tetrapeptides (free and sugar-linked) into their corresponding tripeptides (fig. 1.2; 6a, 7a, 8a). Meanwhile, cytoplasmic AmpD amidases eliminate peptide stems from sugar residues releasing free peptides (fig. 1.2; 7a-c; step 5). At the end, free peptides and sugar subunits are recycled in synthesis of lipid II and it seems to be a closed circle of PG biosynthesis and recycling. On the other hand, it was reported that the liberated anhydromuropeptides (*ampC* inducing peptides) accumulate in the cytoplasm and enter in a competition with UDP-MurNAc-pentapeptides (*ampC* repressing peptides) in binding to AmpR (fig. 1.2; step 6) which is a transcription factor for both of *ampR* and *ampC* β-lactamase in many Gram-negative bacteria (e.g. *P. aeruginosa* but not *E. coli*) causing AmpC overproduction and in turn β-lactam resistance (Fisher & Mobashery, 2014; Johnson et al, 2013; Reith & Mayer, 2011; Vollmer et al, 2008b).

1.4. Antibiotics targeting cell wall biosynthesis & bacterial resistance

In general, antibiotics are a group of natural (e.g. penicillin, erythromycin and vancomycin) and synthetic (e.g. linezolid, sulphomethoxazole, cephalosporins and trimethoprim) compounds that have variant inhibitory effects to vital physiological pathways leading to inhibition of bacterial growth (bacteriostatic effect) or cell death (bactericidal effect). As shown in figure 1.3, the main targets for antibiotic inhibition are DNA replication, folate metabolism, biosynthesis of bacterial proteins and cell wall; and so antibiotics were classified according to their target and mechanism of action and further sub-divided concerning their molecular structure (Becker, 2013; Bolhuis & Aldrich-Wright, 2014; Pucci & Bush, 2013; Walsh, 2003) As peptidoglycan precursor are important component for the biosynthesis of PG and also important for induction of ampC-type beta-lactamases, we will describe in some details some of the inhibitors of this cellular target.

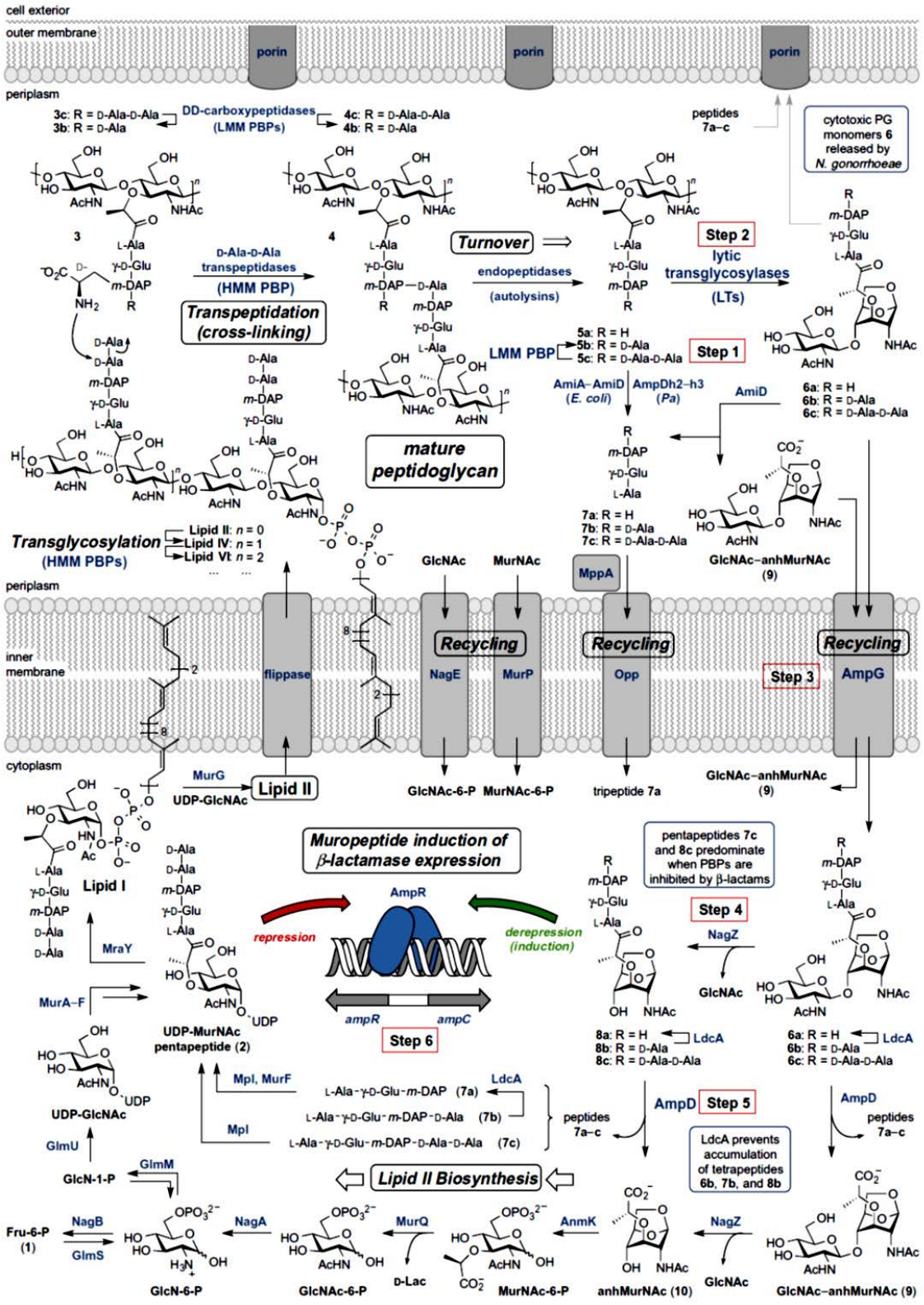

Figure 1.2. Outline of PG biosynthesis, PG recycling and *ampC* regulation in Gram-negative bacteria (Fisher & Mobashery, 2014; Johnson et al, 2013).

*Three main physiological events, described on the text, are summarized in this figure; **1st event** is PG biosynthesis which occurs in the three cellular compartments (cytoplasm, inner membrane and periplasm), starting in cytoplasm (1,2) where UDP-MurNAc-pentapeptide is*

formed by the action of AnmK, MurQ, NagA,GlmS, GlmM, GlmU, MurA-F and Mpl. Then lipid I and II are formed at the inner membrane by the action of MraY and MurG which is followed by the action of flippase which cause turning of lipid II from cytoplasmic side into the periplasmic side where PG precursors are added into PG strands (3) and inter-crosslinked (4) by the activity of HMM-PBPs (TGases, TPases); also, PG-pentapeptides are converted into tetrapeptides by the action of DD-CPases (LMM-PBPs). ***The 2nd event*** *is PG turnover and recycling (steps 1-5) starting in the periplasm by the action of PG hydrolases (EPases, DD-CPases, LTs and amidases AmiA-D in E. coli or AmpDh2-h3 in P. aeruginosa) producing free tri-, tetra- and pentapeptides (7a-c), GluNAc, MurNAc, GluNAc-anhMurNAc (9) and GluNAc-anhMurNAc-peptides (tri-, tetra- or pentapeptides; 6a-c) which are transported into cytoplasm through NagE, MurP, Opp and AmpG. In cytoplasm, muropeptides (6a-c) are further degraded into anhMurNAc-peptides (tri-, tetra- or pentapeptides; 8a-c), free tri-, tetra- or pentapeptides (7a-c), GluNAc-anhMurNAc (9) and anhMurNAc and GluNAc (10) by the action of NagZ, LdcA and AmpD. Free peptides and sugar derivatives are then recycled into synthesis of lipid II (PG precursors).* ***The 3rd event*** *is regulation of expression of AmpC β-lactamase (step 6) in P. aeruginosa (but not in E. coli) by the action of UDP-MurNAc-pentapeptide (repression, basal AmpC level) and anhydromuropeptides (derepression, AmpC overproduction) upon binding to AmpR. Meanings of all symbols (e.g. MurA-G, PBPs, LTs, LdcA, etc.) are described in the text and in the abbreviation list.*

1.4.1. Inhibitors of Mur family and PG precursors

Inhibition of Mur family and PG precursors lead to blocking of PG synthesis, cell wall degradation and bacterial cell death. Fosfomycin is a natural antibacterial compound produced by various *Streptomyces* and *Pseudomonas* species to inhibit MurA (fig. 1.3) and stops the construction of UDP-MurNAc and consequently, decreases in PG synthesis and cell growth, and ultimately cell lysis (Borisova et al, 2014; Nikolaidis et al, 2014). Tunicamycin blocks transglycosylation step of MurG while mersacidin (Type-B lantibiotics) inhibits PG biosynthesis by tight interaction with lipid II (Islam et al, 2012; Walsh, 2003). Ramoplanin and enduracidin (lipoglycodepsipeptides) have a higher affinity for Lipid II over lipid I which results in blocking the transglycosylation reaction of PG biosynthesis as shown in figure 1.3 (Fang et al, 2006; Walsh, 2003). MoenomycinsA (MoeA) is a phosphoglycolipid which inhibits PG synthesis by blocking transglycosylase (TGase) subunit, while vancomycin is a glycosylated heptapeptide which blocks transpeptidation reaction (TPases) by binding D-Ala–D-Ala of the peptide stems of PG precursors (Lipid II) and lead to inhibition of PG synthesis (fig. 1.3; 1.4) (Jia et al, 2013; Ostash & Walker, 2010; Tseng et al, 2014; Walsh, 2003).

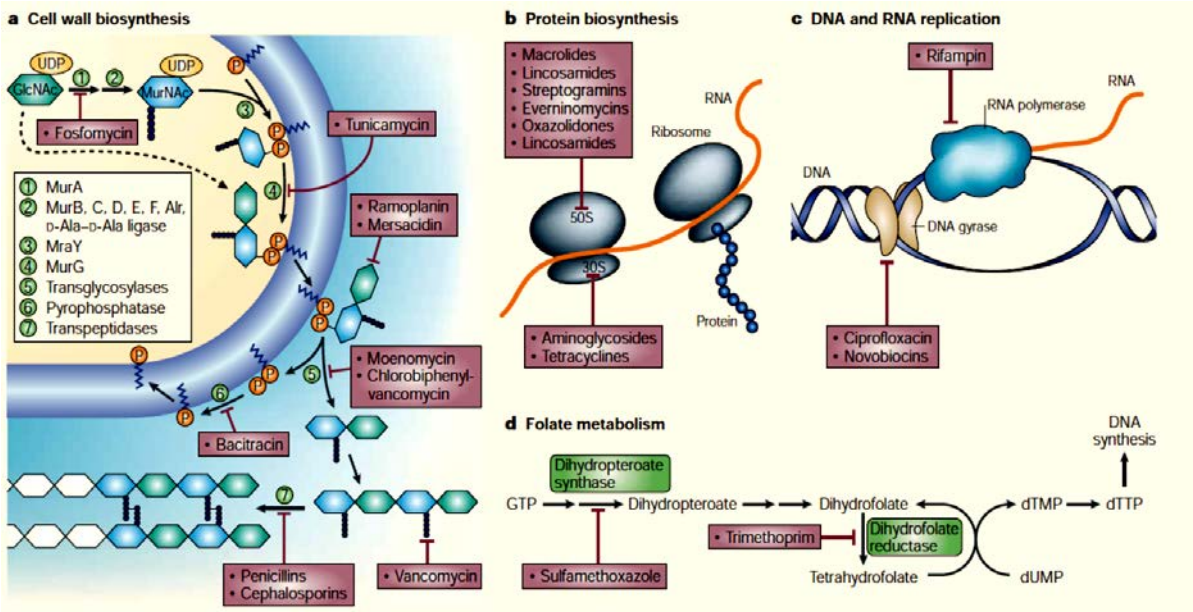

Figure 1.3. Sub-cellular targets for antibiotic actions (Walsh, 2003).

Different antibiotics *with different targets [inhibition of cell wall biosynthesis (a), protein biosynthesis (b), DNA and RNA replication (c), and folate metabolism (d)] are shown.* ***Vancomycin*** *inhibits transpeptidase reaction by binding the peptide stem of PG.* ***β-lactam*** *antibiotics (e.g. penicillins and cephalosporins) bind and inhibit transpeptidases; and so inhibit cell wall biosynthesis. Also, cell-wall biosynthesis can be inhibited by* ***fosfomycin*** *which inhibits MurA;* ***tunicamyin*** *which inhibits MurG TGase and* ***moenomycin*** *which inhibits transglycosylases (TGases).*

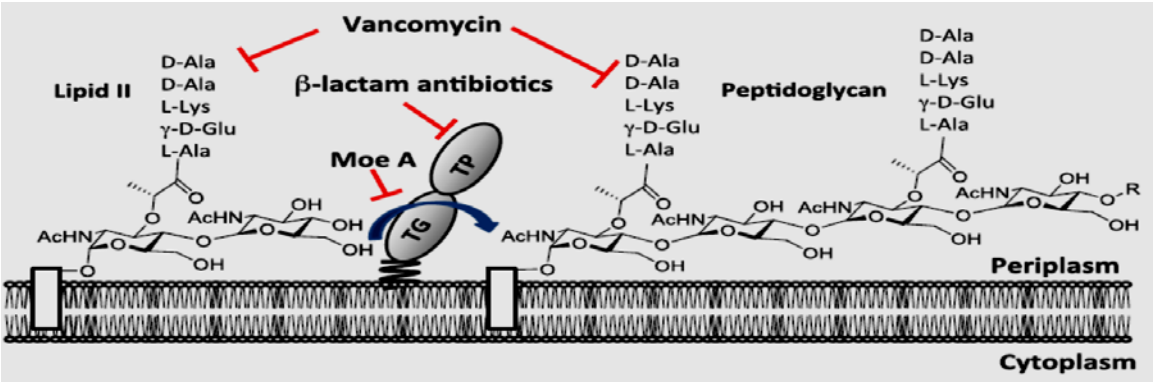

Figure 1.4. Mechanism of antibiotic inhibition of bacterial cell wall biosynthesis (Tseng et al, 2014).

Vancomycin *binds D-Ala–D-Ala of the pentapeptide stem in PG. β-lactam antibiotics bind the transpeptidase subunit (TPase) of PBPs.* ***Moenomycins A*** *(Moe A) blocks transglycosylation reaction by binding to the transglycosylase subunit (TGase) of PBPs.* ***β-lactams*** *block the active site of transpeptidase subunits of PBPs. Red colored T-shaped lines identify the target site for each of vancomycin, β-lactam antibiotics and Moe A.*

1.4.2. β-lactam antibiotics

They are a group of antimicrobial agents targeting PBPs in order to inhibit PG synthesis pathway by blocking TPase subunits and consequently inhibit bacterial growth (fig. 1.4; 1.3). They have various β-lactam ring systems (penam, cefem, penem, carbapenem and monobactam) involving a highly strained and reactive cyclic amide which mimics the terminal D-Ala–D-Ala in the muropeptides. Hence they can bind to PBPs and cause irreversible inhibition of these PBPs by blocking their active site Ser [Fig. 1.7; i] (Fernandes et al, 2013; Johnson et al, 2013; Tseng et al, 2014; Walsh, 2003). β-lactam antibiotics are produced either by isolation of fermented natural compounds (e.g. penicillin) or by further synthetic or enzymatic modification of fermented natural compounds like many penicillins and most of cephalosporins (Elander, 2003; Hamed et al, 2013; Kong et al, 2010).

Penams (e.g. Penicillins): Penicillins have a bicyclic nucleus, 6-aminopenicillanic acid, 6-APA (Fig. 1.5) (Kong et al, 2010). Ampicillin, amoxicillin, cloxacillin, floxacillin, mezlocillin, nafcillin and oxacillin are different derivatives of penicillin G and penicillin V which are sensitive to penicillinase (β-lactamase) action (fig. 1.7; ii), while methicillin and dicloxacillin are more stable forms against penicillinase. Also, carbenicillin and ticarcillin are penicillins more stable against *P. aeruginosa* and many Gram-negative rods (Elander, 2003; Tan & File, 1995). Penicillin G is active against *Neisseria gonorrhoeae* and *Treponema pallidum.* Both of penicillin G and V are susceptible to *S. aureus.* On the other hand, some penicillinase-stable derivatives (e.g. oxacillin, dicloxacillin and floxacillin) that were developed are less effective (in blocking PBPs) than their parental sources (Becker, 2013; Fernandes et al, 2013).

Cephems (e.g. Cephalosporins): Several generations (table 1.1) of cephalosporins were developed with an enhanced spectrum reaching 4th generation (e.g. cefepime, cefpirome) and 5th generation (e.g. Ceftobiprole, Ceftaroline) with the broadest spectrum activities which are more effective against *P. aeruginosa* than antipseudomonal penicillins (Fernandes et al, 2013). They are derivatives of cephalosporin C (fig. 1.5) produced from *Cephalosporium acremonium*, and have a nucleus of 7-aminocephalosporinic acid, 7-ACA, (Kong et al, 2010). Also, They are not susceptible to β-lactamases produced by *S. aureus* (Becker, 2013).

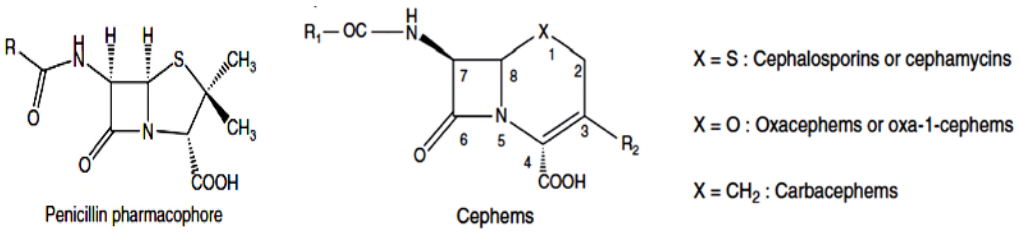

Figure 1.5. Chemical structures of penicillins and cephems (Fernandes et al, 2013).

Table 1.1. Various cephalosporin generations (Fernandes et al, 2013).

First-generation	Second-generation	Third-generation	Fourth-generation	Fifth-generation
Cephalothin	Cefamandole	Cefotaxime	Cefepime	Ceftobiprole
Cephapirin	Cefuroxime	Ceftizoxime	Cefpirome	Ceftaroline
Cefazolin	Cefonicid	Ceftriaxone		
Cephalexin[a]	Ceforanid	Ceftazidime		
Cephradine[a]	Cefoxitin[b]	Cefoperazone		
Cefadroxil[a]	Cefmetazole[b]	Cefixime[a]		
	Cefminox[b]	Ceftibuten[a]		
	Cefotetan[b]	Cefdinir[a]		

[a]Oral cephalosporins; all the others are parental cephalosporins. [b]Besides being cephamycins (chemical classification), they are usually included in the microbiological classification as second-generation cephems.

Penems: have the broadest spectrum of antibacterial activity which make them resistant to hydrolysis by many β-lactamases including ESBL and AmpC enzymes (fig. 1.7) (Dalhoff et al, 2006; Papp-Wallace et al, 2011). According to structural differences, penems were sub-divided into penems (e.g. faropenem) and carbapenems (e.g. doripenem, imipenem and meropenem, fig. 1.6) which are more effective than faropenem against *P. aeruginosa* and Enterobacteriaceae, (Dalhoff et al, 2006).

Monobactams: They are monocyclic, N-sulfonated β-lactams, produced by bacteria. Aztreonam is a synthetic monobactam (fig. 1.6) resistant to hydrolysis by chromosomally encoded cephalosporinases and many plasmid-mediated β-lactamases such as TEM-1, TEM-2, OXA-2, and SHV-1 (Drawz & Bonomo, 2010).

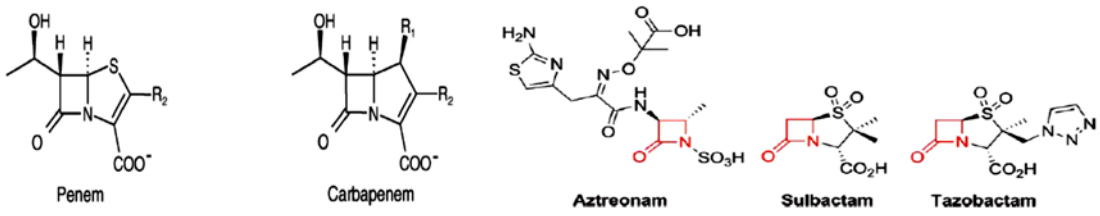

Figure 1.6. Chemical structures of penems and carbapenems (Dalhoff et al, 2006)**; aztreonam, sulbactam and tazobactam** (Hamed et al, 2013).

1.4.3. Bacterial resistance to β-lactams

Antibiotic resistance is the ability of bacteria to accommodate and to grow in presence of challenging compounds like antibiotics. The intensive and prolonged clinical and agricultural use and misuse of antibiotics have triggered the worldwide spread of highly resistant pathogenic bacteria (Rodriguez-Rojas et al, 2013). Many resistance mechanisms were previously described like production of β-lactamase which is common in many Gram-negative bacteria; changes in β-lactam targets (PBPs), e.g. Methicillin resistance in *S. aureus* (MRSA); decreased production of

outer membrane proteins (OMPs), e.g. loss of OprD increased resistance to some carbapenems in *P. aeruginosa*; increased efflux pumps and reduced membrane permeability which facilitate multidrug resistance in many Gram-negative pathogens especially in *P. aeruginosa* and *Acinetobacter spp* (Drawz & Bonomo, 2010). β-lactam hydrolysis and emergence of a broad spectrum β-lactamases are basic keys for bacterial resistance (Bush & Jacoby, 2010).

1.4.4. β-lactamase inhibitors

The developed bacterial resistance to most of clinically used β-lactam antibiotics pushed the investigators to search for some natural or synthetic compounds that can inhibit β-lactamases, even though they may have a weak antibiotic effect (Hamed et al, 2013). Clavulanic acid, sulbactam, and tazobactam are clinically used as β-lactamase inhibitors. They share structural similarity with penicillin (fig. 1.6) and are effective against class A β-lactamases (including CTX-M and the ESBL derivatives of TEM-1, TEM-2, and SHV-1); and are generally less effective against class B, C, and D β-lactamases (fig. 1.7; table 1.2). Metallo-β-lactamases (MBLs) are resistant to all the mechanism-based inhibitors of the serine enzymes (Drawz & Bonomo, 2010; Hamed et al, 2013). It was found that the use of β-lactam inhibitors in combinations with β-lactam antibiotics (e.g. Amoxicillin/clavulanate, ampicillin/sulbactam, pipericillin/tazobactam, ticarcillin/clavulanate, cefoperazone/sulbactam) was more effective than their individual use (Drawz & Bonomo, 2010; Hamed et al, 2013; Pucci & Bush, 2013)

1.5. β-lactamases

1.5.1. Classification of β-lactamases

β-lactamases are a group of chromosomally-encoded or plasmid-mediated enzymes that can hydrolyze β-lactam antibiotics. They were classified according to their molecular structure by Ambler into molecular classes A, B, C and D, where serine β-lactamases were grouped in classes A, C and D, while MBLs were grouped in class B. (Ambler, 1980; Hall & Barlow, 2005; Kong et al, 2010). Recently, functional classification was reported and divided β-lactamases concerning their activity behavior towards substrates and inhibitors (e.g. β-lactams, clavulanic acid, tazobactam and EDTA) into groups 1, 2, 3 and further divided into subgroups (a, b …). Also, in that study, both functional and molecular classifications of β-lactamases were mentioned in parallel (table 1.2). New candidates of β-lactamases emerged due to mutations in the existing ones and showed a broad spectrum activity (e.g. ESACs, group1e and ESBLs, group 2b). Functional classification of β-lactamases is very helpful in clinics to characterize and to deal with bacterial resistance challenges (Bush & Jacoby, 2010; Bush et al, 1995).

1.5.2. Group 2 and 3 β-lactamases

Functional group 2 β-lactamases (molecular classes A and D) is the largest group of β-lactamases, due to emerging of new of ESBLs. This group is subdivided into subgroup 2a which include β-lactamases (e.g. PC1; predominant in Gram-positive cocci) with a relatively limited spectrum of hydrolytic activity; Subgroup 2b includes β-lactamases (e.g. TEM-1, TEM-2, and SHV-1) readily hydrolyze penicillins and early cephalosporins (e.g. cephaloridine and cephalothin); Subgroup 2be β-lactamases (e.g. TEM-3, SHV-2 and CTX-M-15) are active on penicillins, extended spectrum cephalosporins and monobactams; Subgroup 2br β-lactamases (e.g. TEM-30 and SHV-10) are active on penicillins; Subgroup 2ber β-lactamases (e.g. TEM-50) are active on penicillins, extended spectrum cephalosporins and monobactams; Subgroup 2c β-lactamases (e.g. PSE-1, CARB-3) showed improved activity on carbencicillin; Subgroup 2ce β-lactamases (e.g. RTG-4) showed improved activity on carbenicillin and cefepime; Subgroup 2d β-lactamases (e.g. OXA-1, OXA-10) showed improved activity on cloxacillin or oxacillin; Subgroup 2de β-lactamases (e.g. OXA-11, OXA-15) hydrolyze cloxacillin or oxacillin and oxyimino-β-lactams; Subgroup 2df β-lactamases (e.g. OXA-23, OXA-48) hydrolyze cloxacillin or oxacillin and carbapenems; Subgroup 2e β-lactamases (e.g. CepA) are active extended spectrum cephalosporins; Subgroup 2f β-lactamases (e.g. KPC-2, IMI-1,SME-1) displayed increased hydrolysis of carbapenems, oxyimino-β-lactams, cephamycins with variable profiles with clavulanic acid and tazobactam. β-lactamases of subgroups 2a, 2b, 2be, 2c, 2ce and 2e are inhibited by clavulanic acid or tazobactam while subgroups 2br and 2ber are resistant to clavulanic acid, tazobactam and sulbactam. Moreover, subgroups 2d, 2de and 2df displayed variable profiles with clavulanic acid and tazobactam (Bush & Jacoby, 2010).

Functional group 3 (class B) of β-lactamases include subgroubs a and b which are Zn^{2+}-metallo-β-lactamases (MBLs) and can be inhibited by EDTA but not by clavulanic acid and tazobactam. Subgroup 3a β-lactamases (e.g. IMP-1, VIM-1) are active on carbapenems but not monobactams. Subgroup 3b β-lactamases (e.g. CphA, Sfh-1) displayed preferential hydrolysis of carbapenems (Bush & Jacoby, 2010).

1.5.3. AmpC β-lactamases

AmpC β-lactamases are periplasmic enzymes, belong to group 1 class C serine β-lactamases (table 1.2), active on cephamycins (e.g. cefoxitin) and more active on cephalosporins than bezylpenicillin while it showed low affinities to cefepime, cefpirome, and carbapenems (Bush & Jacoby, 2010; Jacoby, 2009). They are not inhibited by clavulanic acid but inhibited by cloxacillin, oxacillin, and aztreonam. AmpC enzymes were reported principally as chromosomally-encoded in many members of Proteobacteria; however plasmid- mediated

AmpC enzymes (e.g. ACT-1, CMY-2, FOX-1 and MIR-1) have emerged in the last two decades. AmpC is inducible by certain β-lactams (e.g. imipenem and cefoxitin) in many organisms (e.g. *P. aeruginosa*), but it is not induced in some others (e.g. *E. coli*). Extended-spectrum AmpC β-lactamases (ESACs) like GC1 in *E. cloacae* and plasmid-mediated CMY-10, CMY-19, CMY-37 are categorized as subgroup 1e (Bush & Jacoby, 2010; Jacoby, 2009). AmpC overproduction confers resistance to most penicillins, β-lactamase inhibitor/β-lactam combinations and resistance to many broad-spectrum cephalosporins (e.g. cefotaxime, ceftazidime, and ceftriaxone) with reduced susceptibilities to carbapenem, cefepime and cefpirome (Jacoby, 2009; Mammeri et al, 2006; Rodriguez-Martinez et al, 2009). Infections due to AmpC-producing bacteria (e.g. *P. aeruginosa*) can be treated with carbapenems unless there is no carbapenem resistance which can arise by mutations that cause loss of outer membrane porin (reduce influx) or increase efflux by efflux pump activation (Jacoby, 2009).

1.5.4. Mechanism of action

The active site of these proteins (PBPs and β-lactamases**)** contains nine highly conserved residues; the catalytic serine is located at the beginning of α2 helix and followed by a lysine to form the S*XXK sequence; a second sequence, SxN, is located in a loop between helix α4 and α5; four conserved residues form the KTG(T/S) form the third sequence; and a ninth residue, a glycine (G) at the back portion of the active site, is also strictly conserved (Sauvage et al, 2008). The reaction between serine β-lactamases or Zn^{2+}-dependent MBLs and common β-lactam substrates (e.g. penicillin) produces labile acyl-enzyme complexes which easily can be hydrolyzed into inactive β-lactams and active enzymes (fig. 1.7 ii and v, respectively) while β-lactam-based inhibitors (e.g. clavulanic acid) or carbapenems (e.g. imipenem) form stable inactive acyl-enzyme complexes with serine β-lactamases due to the formation of stable bond with the active site Ser [fig. 1.7 iii and iv, respectively] (Hamed et al, 2013). Physiologically, active site inactivation of PBPs by β-lactam antibiotics (fig. 1.7 i), follows the same mechanism of reaction producing an inactive acyl-enzyme containing a very stable bond with the active site Ser. Inactivation of some PBPs lead to overexpression of AmpC in many Gram-negative bacteria to hydrolyze the β-lactam antibiotic and to recover the vital activities of the PBPs for maintaining their cell wall (Kong et al, 2010).

Table 1. 2. Functional and structural classification of β-lactamases* (Bush & Jacoby, 2010).

Bush-Jacoby group (2009)	Bush-Jacoby-Medeiros group (1995)	Molecular class (subclass)	Distinctive substrate(s)	Inhibited by		Defining characteristic(s)	Representative enzyme(s)
				CA or TZB[a]	EDTA		
1	1	C	Cephalosporins	No	No	Greater hydrolysis of cephalosporins than benzylpenicillin; hydrolyzes cephamycins	*E. coli* AmpC, P99, ACT-1, CMY-2, FOX-1, MIR-1
1e	NI[b]	C	Cephalosporins	No	No	Increased hydrolysis of ceftazidime and often other oxyimino-β-lactams	GC1, CMY-37
2a	2a	A	Penicillins	Yes	No	Greater hydrolysis of benzylpenicillin than cephalosporins	PC1
2b	2b	A	Penicillins, early cephalosporins	Yes	No	Similar hydrolysis of benzylpenicillin and cephalosporins	TEM-1, TEM-2, SHV-1
2be	2be	A	Extended-spectrum cephalosporins, monobactams	Yes	No	Increased hydrolysis of oxyimino-β-lactams (cefotaxime, ceftazidime, ceftriaxone, cefepime, aztreonam)	TEM-3, SHV-2, CTX-M-15, PER-1, VEB-1
2br	2br	A	Penicillins	No	No	Resistance to clavulanic acid, sulbactam, and tazobactam	TEM-30, SHV-10
2ber	NI	A	Extended-spectrum cephalosporins, monobactams	No	No	Increased hydrolysis of oxyimino-β-lactams combined with resistance to clavulanic acid, sulbactam, and tazobactam	TEM-50
2c	2c	A	Carbenicillin	Yes	No	Increased hydrolysis of carbenicillin	PSE-1, CARB-3
2ce	NI	A	Carbenicillin, cefepime	Yes	No	Increased hydrolysis of carbenicillin, cefepime, and cefpirome	RTG-4
2d	2d	D	Cloxacillin	Variable	No	Increased hydrolysis of cloxacillin or oxacillin	OXA-1, OXA-10
2de	NI	D	Extended-spectrum cephalosporins	Variable	No	Hydrolyzes cloxacillin or oxacillin and oxyimino-β-lactams	OXA-11, OXA-15
2df	NI	D	Carbapenems	Variable	No	Hydrolyzes cloxacillin or oxacillin and carbapenems	OXA-23, OXA-48
2e	2e	A	Extended-spectrum cephalosporins	Yes	No	Hydrolyzes cephalosporins. Inhibited by clavulanic acid but not aztreonam	CepA
2f	2f	A	Carbapenems	Variable	No	Increased hydrolysis of carbapenems, oxyimino-β-lactams, cephamycins	KPC-2, IMI-1, SME-1
3a	3	B (B1)	Carbapenems	No	Yes	Broad-spectrum hydrolysis including carbapenems but not monobactams	IMP-1, VIM-1, CcrA, IND-1
		B (B3)					L1, CAU-1, GOB-1, FEZ-1
3b	3	B (B2)	Carbapenems	No	Yes	Preferential hydrolysis of carbapenems	CphA, Sfh-1
NI	4	Unknown					

[a] CA, clavulanic acid; TZB, tazobactam.
[b] NI, not included.

**Summary of functional classification of β-lactamases (Bush-Jacoby-Medeiros group, 1995), updated functional classification (Bush-Jacoby group, 2009) and structural classification (Molecular class, Ambler classification). β-lactamases were functionally classified (Bush-Jacoby group, 2009; Bush-Jacoby-Medeiros group, 1995) regarding their activity behavior towards substrates and inhibitors (e.g. β-lactams, clavulanic acid (CA), tazobactam (TZB) and EDTA) into groups 1, 2, 3 and further divided into subgroups (a, b …). Also, they were classified according to their similarities in their molecular structure by Ambler into molecular classes A, B, C and D. More details of the activity, functionality, substrate, inhibitors and molecular class are described in the text.*

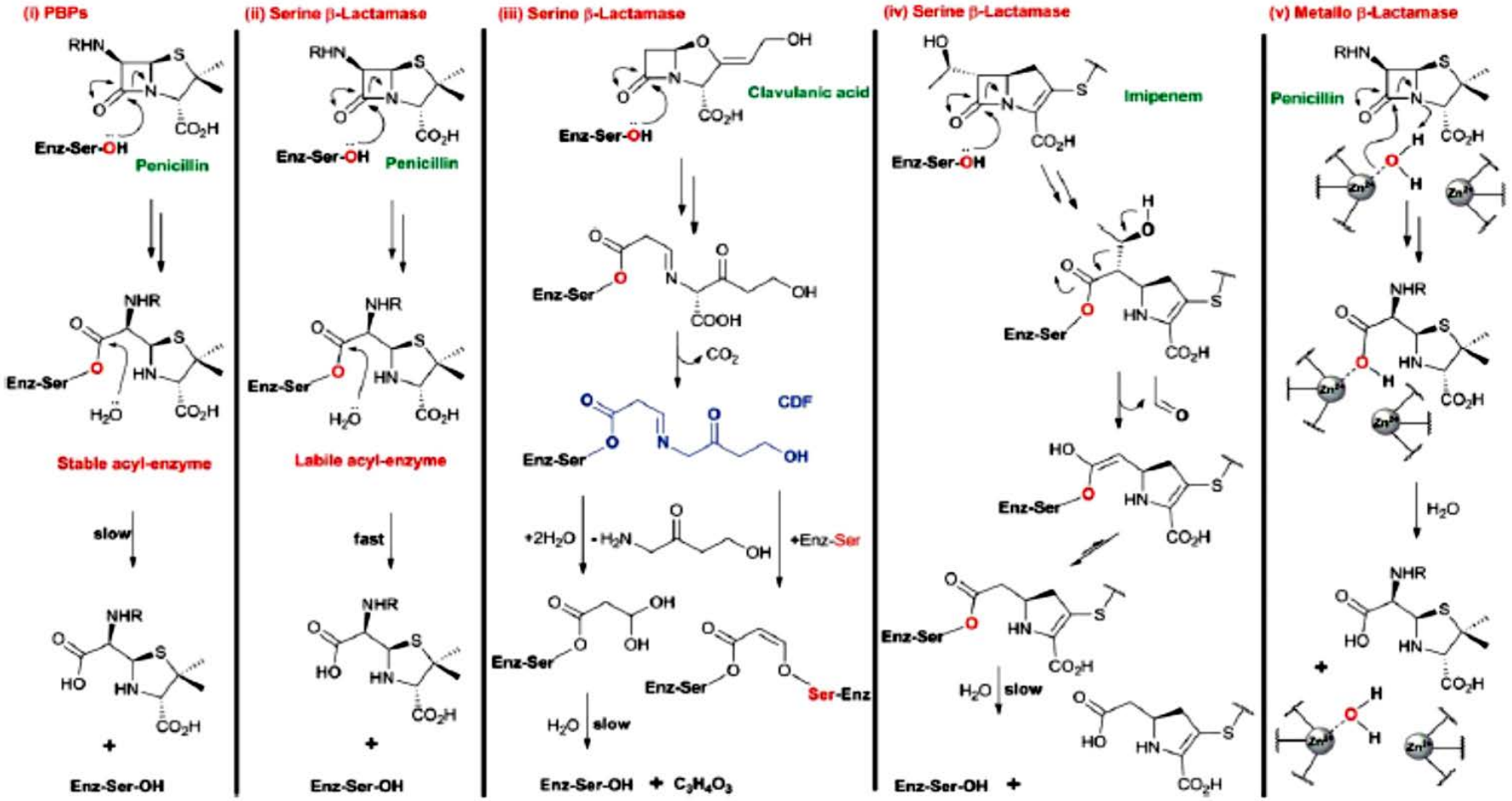

Figure 1.7. Mechanism of action of β-lactamases and PBPs on β-lactams (Hamed et al, 2013). ***(i)*** *The formation of inactive PBP–penicillin complex.* ***(ii)*** *Hydrolysis penicillin by serine β-lactamases.* ***(iii, iv)*** *Inhibition of serine β-lactamases by clavulanic acid and imipenem, respectively.* ***(v)*** *Hydrolysis of penicillin by Zn^{2+}-dependent metallo β-lactamases (MBLs).*

1.5.5. AmpC structure

The 3-D structure of *E. coli* AmpC showed that the active site residues are Ser64* (catalytic residue), Lys67, Gln120, Tyr150, Asn152, Lys315, Thr316 and Ala318 (Ser318 in some other types). These residues are conserved in all class C β-lactamases (Jacoby, 2009; Usher et al, 1998). Recently, 3-D structure of *P. aeruginosa* AmpC was developed and showed active site similarity to the *E. coli* with the exception of having Ser318 (Lahiri et al, 2013). ESACs differ from wild-type AmpC by amino acid substitutions or insertions in some regions in the vicinity of the active site (e.g. the Ω-loop, the H-10 helix, the H-2 helix and the C-terminal end of the protein) which improve affinities and reactions with more β-lactam substrates like broad spectrum cephalosporins [e.g. cefotaxime, ceftazidime] (Rodriguez-Martinez et al, 2009). Concerning their structural similarity, it was found that both class C β-lactamases and class C LMM-PBPs type-AmpH (e.g. R61 DD-peptidase) have a close similarity in their general structure and conserved motifs near the active site serine (Jacoby, 2009; Sauvage et al, 2008). This suggests that both of them have a common ancestor and implies that class C β-lactamases may have a secondary peptidase activity (Bishop & Weiner, 1992; Hall & Barlow, 2004; Joris et al, 1988; Kong et al, 2010).

1.5.6. AmpC regulation in *P. aeruginosa*

In *P. aeruginosa*, ampC is chromosomally encoded, expressed in low basal amount, and can be induced by β-lactam challenge. AmpC expression is regulated mainly by the enzymes; AmpG permease homologs (AmpG and AmpP or ampGh1), ampD amidase homologs (ampD, ampDh2 and ampDh3), ampR (LysR superfamily) and NagZ, and two competing AmpR-binding muropeptides; the first is suppressing peptide, UDP-MurNAc-pentapeptide, which set *ampC* expression at basal level while the second is inducing peptide, 1,6-anhydromuropeptide which triggers high *ampC* expression [fig. 1.2] (Fisher & Mobashery, 2014; Johnson et al, 2013; Lister et al, 2009). Normally, GlcNAc-MurNAc-1,6-anhydromuropeptides shed of from peptidoglycan and find its way to cytoplasm via AmpG permease (fig. 1.2; step 3), where it is processed by NagZ to generate MurNAc-1,6-anhydromuropeptides (fig. 1.2; step 4) which is then cleaved by AmpD to generate anhMurNAc and free tri-, tetra- and pentapeptides (fig. 1.2; step 5). The inducing peptides replace UDP-MurNAc-pentapeptides from AmpR binding which in turn undergoes some conformational changes that lead to overexpression of AmpC (fig. 1.2; step 6). During β-lactam exposure, MurNAc-1,6-anhydromuropeptides accumulate in cytoplasm where AmpD activity is not enough to cleave them. So, these anhydromuropeptides can replace the suppressing peptides from AmpR binding until the β-lactam inducer is removed, and then the conditions can be reversed to the

normal. It is still unidentified the actual and the effector (*ampC* inducing) anhydromuropeptide although it was suggested to be compounds 8a, 8b or 8c in figure 1.2 (Fisher & Mobashery, 2014; Johnson et al, 2013; Lister et al, 2009). As AmpR binds to the *ampR-ampC* intergenic region, mutations in this region and in *ampR* could increase AmpC expression. AmpR plays a dual role, positively regulating *ampC* and negatively regulating the expression levels of chromosomally encoded class D β-lactamase *poxB,* recently described. Also, AmpR has been involved in the regulation of many virulence factors. Moreover, AmpR mutant showed a high constitutive expression of β-lactamases (Balasubramanian et al, 2012; Kong et al, 2010). The three AmpD homologues are responsible for a stepwise *ampC* upregulation mechanism. The inactivation of *ampD* leads to the constitutive hyperproduction (derepression) of AmpC β-lactamase (Juan et al, 2006). It was reported that inactivation of *nagZ* or *ampG* were able to block *ampC* induction and restored the susceptibility of *ampD* or *dacB* laboratory mutants (Zamorano et al, 2010; Zamorano et al, 2011). Recently, mutation of the nonessential *dacB* gene encoding the DD-carboxypeptidase PBP4 was found to elicit AmpC expression in the absence of β-lactams (Moya et al, 2009). *dacB* mutations were also identified in β-lactam-resistant clinical isolates of *P. aeruginosa*, suggesting that loss of PBP4 function is a medically relevant resistance mechanism (Juan et al, 2006). In *Aeromonas spp.*, induction of AmpC expression requires a specific, 1,6-anhydromuropentapeptide (Tayler et al, 2010). These observations suggest that loss of specific enzyme activities, rather than general inhibition of PG turnover, leads to AmpC induction. However, mechanism underlining the loss of PBP4 activity is unknown and it is not yet clear if it is the only one that triggers that response. Lately, two new gene mutants have been reported to be involved in AmpC overproduction through an AmpR-dependent mechanism. The first mutant, YT1677, had an insertion in *mpl*, which encodes UDP-N-acetylmuramate (L-alanyl-γ-D-glutamyl-meso-diaminopimelate ligase) which is involved in the recycling of cell wall components. The second mutant, YT7988, had an insertion in *nuoN*, which encodes NADH dehydrogenase I chain N. For the first mutant, it was considered that AmpC overproduction was related to cytosolic accumulation of cell wall components i.e. 1,6-anhydromuropeptides. However, it is assumed that the mechanism involved for the second mutant was unclear, and although it is AmpR-dependent, it is thought there is another new regulatory mechanism for *ampC* expression or the cell wall recycling system (Tsutsumi et al, 2013). Also it was reported that single or double mutants of PBP4, or some lytic-transglycosylases, LTs, (e.g. SltB1, or MltB) had an increased *ampC* dependent β-lactam resistance, while it decreased with single mutants of other LTs (e.g. Slt or MltF). Also, it was suggested that there are at least two different pathways leading to AmpC expression and β-lactam resistance in *P. aeruginosa* (Cavallari et al, 2013).

Objectives of this study

2. Objectives of this study

There were three main objectives beyond this work;

The 1st objective *was to characterize Pae-AmpC activity not only as a β-lactamase but mainly to study the effect of AmpC expression on the PG composition in both of E. coli and P. aeruginosa, using wild type and mutant strains.*

The 2nd objective *was to track the consequences on bacterial resistance and peptidoglycan composition after gene inactivation of the main LMM-PBPs (dacB, dacC and pbpG) in PAO1 as single and combined constructs and further to study the effects upon ampC inactivation within these mutants. Also, to go closer understanding the mechanism behind the relationship between inactivation of these LMM-PBPs and ampC induction in P. aeruginosa as previously identified for dacB mutant.*

The 3rd objective *was to pursue the physiological role and activities of DacB, DacC and PbpG in the recovery of the rod shape in spheroplasts of P. aeruginosa.*

Materials & Methods

3. Materials & methods

3.1. Bacterial strains and plasmids

3.2. Primers

3.3. Culture media for cell growth

3.4. DNA manipulation

3.4.1. DNA purification and sequencing

3.4.2. Agarose DNA electrophoresis

3.4.3. PCR amplification

3.4.4. ampC cloning and expression using pET28b plasmid

3.4.5. ampC cloning and expression using pUCP24 plasmid

3.4.6. Bacterial transformation

3.5. Protein manipulation

3.5.1. Estimation of protein concentration

3.5.2. SDS-PAGE electrophoresis

3.5.3. Western blot

3.5.4. β-lactamase activity assay

3.5.5. Bocillin-FL test

3.5.6. MALDI-TOF

3.5.7. Cell fractionation for protein localization

3.6. AmpC purification

3.7. Construction PAO1 mutants

3.8. Estimation of ampC expression by RT-PCR

3.9. Antimicrobial susceptibility testing

3.10. Production of imipenem-induced round cells of PAO1 wild type and mutants

3.11. Confocal microscopic analysis

3.12. Peptidoglycan (PG) manipulation

3.12.1. Preparation of PG

3.12.2. HPLC analysis

3.12.3. Effect of Pae-AmpC on the whole PG and individual muropeptides in vitro

3. Materials & Methods

3.1 Bacterial strains and plasmids

We worked in this study only with bacterial strains of *E. coli* and *P. aeruginosa* PAO1 wild type and mutants. All bacterial strains and plasmids used in this study are summarized in table 3.1 where *E. coli* DH5α was used for cloning of Pae-*ampC*-encoding vectors; *E. coli* BL21(DE3) was used for expression, overproduction and purification of Pae-AmpC; *E. coli* CS109, BL21(DE3) and DV900(DE3) were used to study the effect of Pae-AmpC on PG composition in vitro and in vivo; *E. coli* XL1-Blue was used for cloning of (*dacC* and *pbpG*) gene-specific inactivation vectors; *E. coli* S17.1λpyr was used as a carrier of gene-specific inactivation vectors (e.g. pEXTΔ*pbpG*::Gm) for conjugation in the double recombination step during the construction process of mutants in PAO1. PAOΔ*dacC*, PAOΔ*pbpG*, PAOΔ*dacB*Δ*dacC*, PAOΔ*dacB*Δ*pbpG*, PAOΔ*dacB*Δ*ampC*, PAOΔ*dacC*Δ*ampC* and PAOΔ*pbpG*Δ*ampC*, PAOΔ*dacC*Δ*pbpG*, PAOΔ*dacC*Δ*pbpG*Δ*ampC*, PAOΔ*dacB*Δ*dacC*Δ*ampC*, PAOΔ*dacB*Δ*dacC*Δ*pbpG*, PAOΔ*dacB*Δ*pbpG*Δ*ampC*, PAOΔ*dacB* Δ*pbpG*Δ*ampC*Δ*dacC* and PAOΔ*dacB*Δ*dacC*Δ*pbpG*Δ*ampC* are mutants of *P. aeruginosa* PAO1 that were constructed in this study starting from the wild type PAO1 while PAOΔ*dacB* and PAOΔ*ampC* were provided from previous studies (Moya et al, 2009; Moya et al, 2008). These Pae mutants were used for characterization of the role of LMM-PBPs (*dacB, dacC* and *pbpG*) in PG composition, β-lactam resistance and *ampC* regulation in *P. aeruginosa*. Plasmids pEX100Tlink and pUCGmlox were used in generation of gene-specific inactivation vectors. pCM157 plasmid was used for expression of *cre* recombinase after double recombination during the construction of Pae mutants to remove the gentamycin cassette from the constructed mutant genotypes. pEXTΔ*ampC*::Gm (Moya et al, 2008), pEXTΔ*dacB*::Gm (Moya et al, 2009), pEXTΔ*dacC*::Gm and pEXTΔ*pbpG*::Gm are gene-specific inactivation vectors which were used for inactivation of *ampC, dacB, dacC* and *pbpG*, respectively in *P. aeruginosa* PAO1. pET28b plasmid was used in the construction of vectors (e.g. pET-F1, pET-F1:C3, pET-F1:C6, pET-F2, pET-F3, pET-F4, pET-F4:C3, pET-F4:C6, pET-F3-TEV, pET-F3:C3-TEV, pET-F3:C6-TEV and pET-F4-TEV) encoding different forms of Pae-*ampC* (wild type and mutants described in table 4.1 and figure 4.1). These pET28b vectors were used for expression and overproduction of different Pae-AmpC forms in *E. coli*. pUCP24 plasmid was used for cloning and expression of different *ampC* forms (e.g. pUC-F3 and pUCP-F4 for expression of AmpC-F3 and AmpC-4, respectively) in *P. aeruginosa* of wild type PAO1 and mutants.

Table 3.1. Bacterial strains and plasmids.

Bacterial Strain or Plasmid	Genotype/Characteristics	Reference/Source
E. coli		
DH5α	*F⁻ φ80lacZΔM15 Δ(lacZYA-rgF)U169 recA1 endA1 hsdR17(rk⁻, mk⁺) phoA supE44 thi-1 gyrA96 relA1 λ⁻*	Fermentation service, CBMSO
BL21(DE3)	*F⁻, ompT, hsdB (r_B^- m_B^-) gal, dcm (DE3).*Encodes T7 RNA polymerase.	Fermentation service, CBMSO
CS109	Wild type *E. coli*	Laboratory collection
DV900	CS-109 Δ[*ponB dacA dacB dacC dacD pbpG ampH ampC pbp4b*]	(Vega & Ayala, 2006)
DV900(DE3)	DV900 lysogenized by λDE3 lysogenization kit (Novagen, Merck KGaA, Darmstadt, Germany)	This study
XL1-Blue	F´::Tn*10 proA+proB_+lacI*^{q} Δ (*lacZ*)M15/*recA1 endA1 gyrA96* (Nal^r) *thi hsdR17* (r_k + m_k +) *mcrB1*	Laboratory collection
S17.1λpyr	recA pro (RP4-2Tet::Mu Kan::Tn7)	Laboratory collection
P. aeruginosa		
PAO1	Wild type reference strain.	Laboratory collection
PAOΔ*ampC*	PAO1 Δ*ampC*::*lox*	(Moya et al, 2008)
PAOΔ*dacB*	PAO1 Δ*dacB*::*lox*	(Moya et al, 2009)
PAOΔ*dacC*	PAO1 Δ*dacC*::*lox*	This study
PAOΔ*pbpG*	PAO1 Δ*pbpG*::*lox*	This study
PAOΔ*dacB*Δ*dacC*	PAO1 Δ*dacB*::*lox* Δ*dacC*::*lox*	This study
PAOΔ*dacB*Δ*pbpG*	PAO1 Δ*dacB*::*lox* Δ*pbpG*::*lox*	This study
PAOΔ*dacC*Δ*pbpG*	PAO1 Δ*dacC*::*lox* Δ*pbpG*::*lox*	This study

PAOΔ*dacB*Δ*dacC*Δ*pbpG*	PAO1 Δ*dacB*::*lox* Δ*dacC*::*lox* Δ*pbpG*::*lox*	This study
PAOΔ*dacB*Δ*ampC*	PAO1 Δ*dacB*::*lox* Δ*ampC*::*lox*	This study
PAOΔ*dacC*Δ*ampC*	PAO1 Δ*dacC*::*lox* Δ*ampC*::*lox*	This study
PAOΔ*pbpG*Δ*ampC*	PAO1 Δ*pbpG*::*lox* Δ*ampC*::*lox*	This study
PAOΔ*dacB*Δ*dacC*Δ*ampC*	PAO1 Δ*dacB*::*lox* Δ*dacC*::*lox* Δ*ampC*::*lox*	This study
PAOΔ*dacB*Δ*pbpG*Δ*ampC*	PAO1 Δ*dacB*::*lox* Δ*pbpG*::*lox* Δ*ampC*::*lox*	This study
PAOΔ*dacC*Δ*pbpG*Δ*ampC*	PAO1 Δ*dacC*::*lox* Δ*pbpG*::*lox* Δ*ampC*::*lox*	This study
PAOΔ*dacB*Δ*pbpG*Δ*ampC*Δ*dacC*	PAO1 Δ*dacB*::*lox* Δ*pbpG*::*lox* Δ*ampC*::*lox* Δ*dacC*::*lox*	This study
PAOΔ*dacB*Δ*dacC*Δ*pbpG* Δ*ampC*	PAO1 Δ*dacB*::*lox* Δ*dacC*::*lox* Δ*pbpG*::*lox* Δ*ampC*::*lox*	This study
Plasmids		
pEX100Tlink	Ap^r *sacB*, pUC19-based gene replacement vector with an MCS	(Quenee et al, 2005)
pUCGmlox	Apr Gm^r, pUC18-based vector containing the lox-flanked *aacC1* gene	(Quenee et al, 2005)
pCM157	Tc^r, *cre* expression vector	(Quenee et al, 2005)
pEXTΔ*ampC*::Gm	pEX100Tlink containing 5´and 3´ flanking sequence of *ampC*::Gm *lox*	(Moya et al, 2008)
pEXTΔ*dacB*::Gm	pEX100Tlink containing 5´and 3´ flanking sequence of *dacB*::Gm *lox*	(Moya et al, 2009)
pEXTΔ*dacC*::Gm	pEX100Tlink containing 5´and 3´ flanking sequence of *dacC*::Gm *lox*	This study
pEXTΔ*pbpG*::Gm	pEX100Tlink containing 5´and 3´ flanking sequence of *pbpG*::Gm *lox*	This study
pET28b+	Kan^r, expression by T7 RNA polymerase. Fusion with poly His at amino terminal.	Novagen
pET-F1	pET28b expressing AmpC-F1 with C-terminal poly-His tag.	This study
pET-F1:C3	pET28b expressing AmpC-F1:C3 with C-terminal poly-His tag.	This study
pET-F1:C6	pET28b expressing AmpC-F1:C6 with C-terminal poly-His tag.	This study
pET-F2	pET28b expressing AmpC-F2 with C-terminal poly-His tag.	This study

pET-F3	pET28b expressing AmpC-F3 with C-terminal poly-His tag.	This study
pET-F4	pET28b expressing AmpC-F4 with C-terminal poly-His tag.	This study
pET-F4:C3	pET28b expressing AmpC-F4:C3 with C-terminal poly-His tag.	This study
pET-F4:C6	pET28b expressing AmpC-F4:C6 with C-terminal poly-His tag.	This study
pET-F3-TEV	pET28b expressing AmpC-F3-TEV with C-terminal poly-His tag and TEV protease recognition site.	This study
pET-F3:C6-TEV	pET28b expressing AmpC-F3:C6-TEV with C-terminal poly-His tag and TEV protease recognition site.	This study
pET-F3:C3-TEV	pET28b expressing AmpC-F3:C3-TEV with C-terminal poly-His tag and TEV protease recognition site.	This study
pET-F4-TEV	pET28b expressing AmpC-F4-TEV with C-terminal poly-His tag and TEV protease recognition site.	This study
pUCP24	Amp^r, cloning and expression vector for *P. aeruginosa.*	Laboratory collection
pUCP-F4	pUCP24 expressing AmpC-F4 with C-terminal poly-His tag.	This study
pUCP-F3	pUCP24 expressing AmpC-F3 with C-terminal poly-His tag.	This study

3.2 Primers

Pae-*ampC* (PA4110) was targeted by this study for functional characterization in bacterial resistance and PG composition of *E. coli* and *P. aeruginosa*. So, primers were designed for PCR amplification of PA4110 *ampC* gene of wild type and mutant forms in order to be cloned and expressed by recombinant vectors (e.g. pET28b and pUCP24) in the target bacterial strains.

Primers used for PCR amplification of different forms of Pae-*ampC* (table 4.1; fig. 4.1) are summarized in table 3.2 and their uses in PCR-amplifications are summarized in table 3.4. All the PCR amplifications were cloned in pET28b plasmid. Primers T7-Fw and pET-Rv-PaeI were used to amplify *ampC*-F3 and *ampC*-F4 using the templates pET-F3 and pET-F4, respectively, to be cloned in the plasmid pUCP24 for *ampC* cloning and expression in *P. aeruginosa*. Primers T7-Fw and T7-Rv were used for sequencing of *ampC* forms cloned in pET28b vector while primers M13-Fw (-21), M13-Rv and M13-Rv2 were used for sequencing of *ampC* forms cloned in pUCP24 vector. Primers PBP5-Fw and PBP5-Rv were used for amplification and sequencing of *dacC* gene (Pae-PBP5).

Primers used for amplification of upstream (PCR1) and downstream (PCR2) regions of the target genes (*ampC*, *dacB*, *dacC* and *pbpG*) to be used in the construction of knock out mutants in PAO1 are summarized in table 3.3. All the used primers were synthesized by Sigma.

3.3 Culture media for cell growth

Luria-Bertani (LB) and SOC media were prepared as described previously (Wiley & Sons, 2002). Agar, yeast extract, and tryptone were purchased from CONDA Pronadisa Micro & Molecular Biology, Spain while glucose and NaCl were purchased from Merck, EMD Millipore Corporation. Mueller-Hinton media (MHA) and cation adjusted Mueller-Hinton broth (CAMHB) were prepared following the provider´s instructions (Becton Dickinson, France S.A). For *ampC* expression, *E. coli* and *P. aeruginosa* strains transformed with recombinant vectors (encoding Pae-*ampC*) were grown in LB liquid media (with a proper antibiotic) at 37°C with agitation (180 rpm). Also, for the construction of Pae mutants LB media was used with a proper antibiotic. For disc diffusion assay MHA plates were used. Mostly, LB media was used in this study, otherwise it will be mentioned. CAMHB media was used for production of imipenem-induced spheroplasts in *P. aeruginosa*.

Table 3.2. Primers used for PCR amplification and DNA sequencing.

Name*	Sequence (5´- 3´)	Restriction Site*	Reference/ Source
ampC-Fw1	TTTCCATGGATGCGCGATACCAGATTCC	NcoI	This study
ampC-Fw2	TTTCCATGGGCGATACCAGATTCCCCT		
ampC-Fw3	TTTCCATGGCCGGCGAGGCCCCGG		
ampC-Fw4	TTTCCATGGCCATGCGCGATACCAGATTCC		
ampC-Rv	TTTGAATTCCGCTTCAGCGGCACCTTGC	EcoRI	This study
ampC-Rv-TEV	TTTGAATTCCCCTGAAAATACAGGTTTTC-CGCTTCAGCGGCACCTTGC	EcoRI+ TEV site	This study
pET-Rv-PaeI	GCATGCT TGTTAGCAGCCGGATCTCAG	PaeI (SphI)	This study
T7-Fw	TAATACGACTCACTATAG	-	Laboratory collection
T7-Rv	GCTAGTTATTGCTCAGCGG	-	Laboratory collection
M13-Fw (-21)	TGTAAAACGACGGCCAGT	-	Parque Científico de Madrid
M13-Rv	CAGGAAACAGCTATGACC	-	
M13-Rv2	ACACTTTATGCTTCCGGCTCG	-	This study
PBP5-Fw	GATCGGTTCGGCGGACGAGGT	-	This study
PBP5-Rv	ACGCTCGCAGGGGAATTCGAT	-	This study

** Fw and Rv refer in the primer direction, forward and reverse, respectively. * Restriction sites used for cloning are underlined.*

Table 3.3. Primers used for the construction of knockout mutants of *ampC*, *dacB*, *dacC* and *pbpG* in PAO1.

Target gene	Primer Name*	Primer Sequence, 5´→3´	PCR Product (bp)	Reference
pbpG	pbpG-F1-ERI	-TCGAATTCCACTTTCAAAGCCCTACGTGC-	PCR1= 375	This study
	pbpG-RI- HDIII	-TCAAGCTTGCAGTTTCGAGTCGAGCACG-		
	pbpG-F2-HDIII	-TCAAGCTTCACTGCGATCCCGGCCGC-	PCR2= 318	
	pbpG-R2-BHI	-TCGGATCCCAGTACCGGACCCAGGAGC-		
dacC	dacCF-ERI	-TCGAATTCACCTTGGCCAGCCGACGC-	PCR1= 500	This study
	dacCIR-HDIII	-TCAAGCTTCTCGGCCAGGGCGACGC-		
	dacCIF-HDIII	-TCAAGCTTGAAGTGAAAGCCGGCCTCG-	PCR2= 400	
	dacCR-BHI	-TCGGATCCACGCTCGCAGGGGAATTCG-		
dacB	dacB-F1-ERI	-TCGAATTCCGACCATTCGGCGATATGAC-	PCR1= 571	(Moya et al, 2009)
	dacB-R1-HDIII	-TCAAGCTTGTCGCGCATCAGCAGCCAG-		
	dacB-F2-HDIII	-TCAAGCTTGCCAGGGCAGCGTACCGC-	PCR2= 693	
	dacB-R2-BHI	-TCGGATCCCGCGTAATCCGAAGATCCATC-		
ampC	AmpC-F-ERI	-TCGAATTCGCGCGCAGGGCGTTCAG-	PCR1= 415	(Moya et al, 2008)
	AmpC-I-R-HDIII	-TCAAGCTTCGTCCTCTTACGAGGCCAGC-		
	AmpC-I-F-HDIII	-TCAAGCTTCAGGGCAGCCGCTTCGAC-	PCR2= 448	
	AmpC-R-BHI	-TCGGATCCCAGGTTGGCATCGACGAAG-		

*Primers used for PCR amplification of both upstream (PCR1) and downstream (PCR2) regions of target genes (pbpG, dacC, dacB and ampC) in P. aeruginosa PAO1 strain. * In each primer name, ERI, HDIII and BHI refer to the presence of the restriction sites (underlined sequences) of EcoRI, HindIII and BamHI; while F and R refer to the direction, forward and reverse, respectively.*

3.4 DNA manipulation

3.4.1 DNA purification and sequencing

DNA purification was achieved by following the manufacturer's instructions using the kits; Wizard® genomic DNA purification kit (Promega) for purification of chromosomal DNA; Wizard® Plus SV minipreps DNA purification system (Promega) for purification of plasmid DNA, while Wizard® SV gel and PCR clean-up system (Promega) was used for purification of PCR product and DNA fragments separated by agarose gel electrophoresis. The concentration of purified DNA was measured by NanoDrop N-1000 (Thermoscientific). Sequencing of PCR products and cloned genes was done at the Parque Científico de Madrid; sequence data were analyzed by Chromas LITE program and online NCBI blast tools.

3.4.2 Agarose DNA electrophoresis

This technique was used for separation, identification and purification of DNA fragments using 1x TAE electrophoresis buffer, 0.5 µg/ml ethidium bromide (for visualization of DNA bands) and 0.8-1.0 g% Agarose gel were used (Wiley & Sons, 2000). The used system units were Mini-sub® cell GT (BIO-RAD) and sub-cell GT WIDE MINI (BIO-RAD). After run, DNA bands were visualized on DNA-gel scanner (Slite 140, ETNA, European Technological Network Aliance).

3.4.3 PCR amplification

For PCR amplification of the different forms of Pae-*ampC*, a 50 µl reaction contained 0.2 mM dNTPs (BIOTOOLS, Spain), 0.2-1 µM forward and reverse primers (Sigma), 100ng DNA and1.25 U Pfu or GoTaq polymerase (Promega), (table 3.4).

For colony PCR, each of the selected colonies was resuspended in 30 µl sterile distilled water and boiled for 10 min at 100°C. After that, cell suspensions were centrifuged at 14000 rpm for 5 min and then 1µl form the supernatant was used in the PCR reaction without the addition of any DNA or plasmid templates. Usually GoTaq (Promega) was used for colony PCR, while *Pfu* was used for PCR-mediated cloning.

Table 3.4. Conditions used for PCR amplification of different *ampC* forms.[a]

Amplified *ampC*	DNA template	Forward primer	Reverse primer	Annealing Temp., °C
***ampC*-F1**	chromosomal DNA, PAO1	0.2 µM ampC-Fw1	0.2 µM ampC-RV	62
***ampC*-F1:C3**	pET-F1:C3 (pGEM-19)	0.2 µM ampC-Fw1	0.2 µM ampC-RV	62
***ampC*-F1:C6**	pET-F1:C6 (pGEM-13)	0.2 µM ampC-Fw1	0.2 µM ampC-RV	62
***ampC*-F2**	chromosomal DNA, PAO1	0.2 µM ampC-Fw2	0.2 µM ampC-RV	62
***ampC*-F3**	chromosomal DNA, PAO1	1 µM ampC-Fw3	0.2 µM ampC-RV	68
***ampC*-F4**	chromosomal DNA, PAO1	0.2 µM ampC-Fw4	0.2 µM ampC-RV	65
***ampC*-F4:C3**	pET-F1:C3	0.2 µM ampC-Fw4	0.2 µM ampC-RV	65
***ampC*-F4:C6**	pET-F1:C6	0.2 µM ampC-Fw4	0.2 µM ampC-RV	65
***ampC*-F4-TEV**	pET-F4	0.2 µM ampC-Fw4	0.2 µM ampC-Rv-TEV	65
***ampC*-F3-TEV**	pET-F3	1 µM ampC-Fw3	0.2 µM ampC-Rv-TEV	68
***ampC*-F3:C3-TEV**	pET-F3:C3	1 µM ampC-Fw3	0.2 µM ampC-Rv-TEV	68
***ampC*-F3:C6-TEV**	pET-F3:C6	1 µM ampC-Fw3	0.2 µM ampC-Rv-TEV	68
ampC*-F3	pET-F3	1 µM T7-Fw	0.2 µM pET-Rv-PaeI	57
ampC*-F4	pET-F4	1 µM T7-Fw	0.2 µM pET-Rv-PaeI	57

[a] *For all PCR amplifications of ampC, we used 100 ng of DNA template except for some cases (*) where 300 ng of pET-F3 and pET-F4 were used. The extension temperature was 72°C for all reactions. * Only those two amplifications were used for ampC-F3 and ampC-F4 cloning in pUCP24 plasmid to be cloned in P. aeruginosa. All the other amplifications were cloned in pET28b plasmid to be cloned and expressed in E. coli.*

3.4.4 *ampC* cloning and expression using pET28b plasmid

The plasmid pET28b was used for cloning, expression of various Pae-*ampC* forms (wild type and mutants) in *E. coli* to characterize the effect of AmpC activity on PG composition and bacterial resistance. pET28b plasmid has kanamycin resistance marker (Kn^r) and multiple cloning sites. Expression of *ampC* from pET28b recombinant vectors was achieved under the control of T7 promoter of T7 RNA polymerase and *lac* operator for control of induction with IPTG. Cloning within pET28b can provide the cloned gene with N-terminal and/or C-terminal poly-His tag.

In this study, cloning of different forms of Pae-*ampC* in pET28b was done in the restriction sites of EcoRI and NcoI (fig. 3.1). Moreover, all the developed AmpC proteins were designed to have C-terminal His-tag. The plasmid pET28b was digested with EcoRI and NcoI (Fermentas life sciences) overnight at 37°C, and then they were purified by the proper kit (section 3.4.1). After that, the digested and purified pET28b was then incubated overnight with alkaline phosphatase (Calf Intestinal, CIAP, Promega) at 37°C, and then purified as mentioned above. The purified pET28b was then ligated by T4 DNA ligase (Promega) overnight at 16°C with each of the purified and digested (with EcoRI and NcoI) PCR products of *ampC*-F1, *ampC*-F1:C3, *ampC*-F1:C6 *ampC*-F2, *ampC*-F3, *ampC*-F4, *ampC*-F4:C3, *ampC*-F4:C6, ampC-F3-TEV, ampC-F3:C3-TEV, ampC-F3:C6-TEV and ampC-F4-TEV to produce pET-F1, pET-F1:C3, pET-F1:C6, pET-F2, pET-F3, pET-F4, pET-F4:C3, pET-F4:C6, pET-F3-TEV, pET-F3:C3-TEV, pET-F3:C6-TEV and pET-F4-TEV, respectively (table 3.1). These recombinant vectors were used to transform DH5α which then was platted on LB plates containing a 30 µg/ml kanamycin and incubated overnight at 37°C. Selected transformants were examined by colony-PCR (addendum, fig. A.1), digestion with EcoRI and NcoI and finally DNA sequencing. After that, the recombinant vectors carrying the confirmed *ampC* sequence were used to transform *E. coli* BL21(DE3) and DV900(DE3) for AmpC expression, functional characterization and PG analysis. Restriction and ligation conditions were followed according to the manufacturer´s recommendations. For expression of the different AmpC forms from pET-*ampC* recombinant vectors, Bl21(DE3) and DV900(DE3) transformants of pET-*ampC* were cultivated in LB media supplemented with different concentrations of IPTG (indicated in results), for different incubation periods at 37°C with agitation. Where, pET-*ampC* was used to refer to the different pET28b recombinant vectors encoding for various *ampC* forms mentioned above.

3.4.5 *ampC* cloning and expression using pUCP24 plasmid

The plasmid pUCP24 was used for cloning in the wild type and some mutants of *P. aeruginosa* PAO1; for functional characterization of some Pae-AmpC forms on β-lactam resistance and PG composition in *P. aeruginosa*. pUCP24 has a gentamycin resistance marker (*aacC1*) and multiple cloning sites as those present in the plasmid pUCP18 (West et al, 1994). Also pUCP24 has *lac* promoter and *lacZα* gene which encodes for β-galactosidase that cleaves X-Gal producing blue colored transformants while interruption of *lacZα* gene by gene cloning develops white transformants when X-Gal is supplemented into the growth medium. Cloning of *ampC*-F3 and *ampC*-F4 in pUCP24 was done in the restriction sites of XbaI and PaeI (fig. 3.2). Using pET-F4 and pET-F3 as a templates, T7-Fw and pET-Rv-PaeI primers and *Pfu* polymerase, PCR products For *ampC*-F4 and *ampC*-F3 were produced (table 3.4) which were then digested as well as the pUCP24 vector with PaeI (Thermo Scientific) in buffer B for two hours at 37°C and then for another 2 hours with 2-fold excess XbaI (Thermo Scientific) and then purified as mentioned in section 3.4.1. After that they were ligated with T4 DNA ligase (Thermo Scientific) to produce pUCP-F4 and pUCP-F3, respectively. The ligation products were transformed into DH5α and then platted on LB plates containing 10 µg/ml gentamycin, 10 mg/ml X-Gal (Sigma) and 0.5 mM IPTG and incubated overnight at 37°C, and then white colonies were selected and tested for having pUCP-F3 and pUCP-F4 by colony PCR and DNA sequencing. The verified pUCP-F3 and pUCP-F4 recombinant plasmids were used to transform the wild type PAO1 and some of the constructed Pae mutants to study the complementation in *ampC* mutants and to follow the expression effect of AmpC on bacterial resistance and PG composition of *P. aeruginosa*. For expression of *ampC*-F3 and *ampC*-F4 in *P. aeruginosa*, transformants of pUCP24-F3 and pUCP-F4 were cultivated in LB media supplemented with 10 µg/ml gentamycin and different concentrations of IPTG (indicated in results), for different incubation periods at 37°C with agitation.

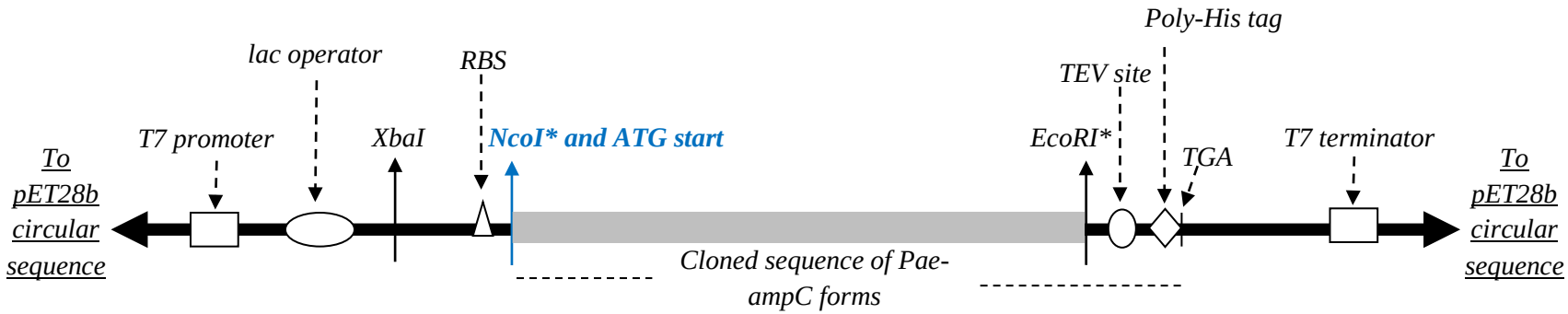

Figure 3.1. Outline of Pae-*ampC* cloning region in pET28b vector.

All the ampC forms described in table 4.1 and figure 4.1 were cloned in pET28b vector in the restriction sites of EcoRI and NcoI (*). Expression in pET28b is achieved under the control of T7 promoter (T7 RNA polymerase) and lac operator. The pET28b plasmid (5368 bp) has a kanamycin resistance marker, and multiple cloning sites. All the cloned ampC forms (ampC-F1, ampC-F1:C3, ampC-F1:C6 ampC-F2, ampC-F3, ampC-F4, ampC-F4:C3, ampC-F4:C6, ampC-F3-TEV, ampC-F3:C3-TEV, ampC-F3:C6-TEV and ampC-F4-TEV) have C-terminal poly-His tag, but only ampC-F3-TEV, ampC-F3:C3-TEV, ampC-F3:C6-TEV and ampC-F4-TEV have the TEV site upstream to the C-terminal His-tag. The site of ATG initiation codon of various AmpC forms is colored in blue.

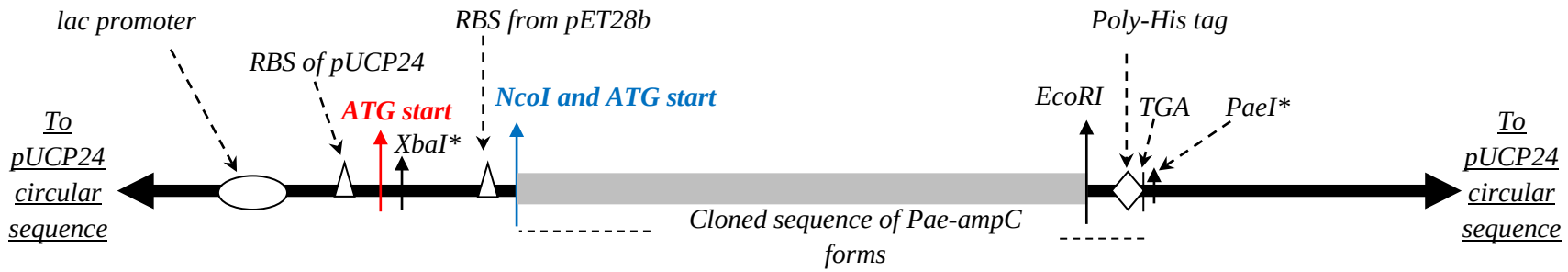

Figure 3.2. Outline of Pae-*ampC* cloning region in pUCP24 vector.

Expression in pUCP24 is achieved under the control of lac promoter. pUCP24 plasmid (4036 bp) has gentamycin resistance marker, multiple cloning sites and lacZα for white/blue colony discrimination. Both of ampC-F3 and ampC-F4 were retrieved from pET28-F3 and pET-F4, respectively (fig. 3.1), by PCR amplification (table 3.4) and then were cloned in pUCP24 vector within the restriction sites of XbaI and PaeI (*). As shown, pUCP-F3 and pUCP-F4 which encode ampC-F3 and ampC-F4, respectively, have two RBS (and two ATG starting codons) one is original from pUCP24 plasmid and the other is external from pET28b. Using these recombinant vectors (pUCP-F3 and pUCP-F4), ampC expression from the first ATG (in red color) with the 1st RBS (of pUCP24) will not produce ampC sequence but rather a short ended and different sequence; only the 2nd ATG starting codon (in blue color) can produce ampC expression.

3.4.6 Bacterial transformation

Transformation is one way and an important step in gene cloning to introduce the recombinant vectors (encoding the gene under study) into bacterial cells for further gene characterization, expression and overproduction. Competent cells were provided from the fermentation service at CBMSO or prepared as described previously (Wiley & Sons, 1997). For transformation by heat-shock, 5 µl of the ligation product was mixed with 100 µl of competent cells of *E. coli* strain (e.g. DH5α, DV900 (DE3), XL1-Blue or S17.1 strains) and kept on ice for 30 minutes and then heat chocked at 42 ºC for 1 minute, and then was left on ice for 2 minutes. After that, 1 ml LB was added and cell suspension was incubated at 37ºC and 180 rpm for 1 hour. Finally, the culture was plated into LB plates, with a proper antibiotic, overnight at 37ºC. For transformation by electroporation, 1-5 µl of the plasmid (e.g. pEXTΔpbpG::Gm) was mixed with 100 µl of competent cells of *P. aeruginosa* or *E. coli* Bl21(DE3) and left on ice for 10 minutes. The mixture was transferred to a chilled 0.2 cm electroporation cuvette and electroporated at 25 µF, 2.5 kV and 200 Ω, and then 1 ml SOC media was added immediately to the cell suspension mixture and incubated at 37ºC and 180 rpm for 1 hour. The culture was plated into LB plates, with the proper antibiotic overnight at 37ºC.

3.5 Protein manipulation

3.5.1 Estimation of protein concentration

It was achieved using BIO-RAD™ DC protein assay by following the provider´s instructions. Standard curve was developed with each assay using BSA (Sigma). Absorbance was measured at 750 nm on U-2000 spectrophotometer (HITACHI).

3.5.2 SDS-PAGE electrophoresis

Polyacrylamide gel electrophoresis technique was used to separate mixture of proteins which can be visualized by direct Coomassie staining or by western blot. The different buffers (Tris-Glycine-SDS) and run conditions were done as described (Wiley & Sons, 2006). 8-10% acrylamide gels and Tris-glycine/SDS were used as electrophoresis buffer. The used system was MINI PROTEAN® TETRA CELL (BIO-RAD). Also, Pre-stained molecular markers (SeeBlue® Plus-2, Invitroen) were utilized.

3.5.3 Western blot

After SDS-PAGE electrophoresis run, proteins were transferred from gel into immobilon-P transfer membrane (Millipore Co.) using the system Criterion™ blotter (BIO-RAD). Briefly, after 2 h blotting at 45 V and 350 mA using blotting buffer (Tris/Gly/SDS/Methanol), the membrane was immersed in blocking buffer (Tris-buffered saline-0.05% Tween 20, TBS-T) containing 3% (W/V) nonfat dry milk for 1h with shaking. Then, the membrane was incubated for 1h at room temperature with 3000 fold diluted antibody, anti-His-tagged rabbit IgG (SC-803; Santa Cruz Biotechnology, Heidelberg, Germany), in TBS-T buffer. After that, the membrane was washed three times by incubation with fresh TBS-T for 10 min with shaking. Then, the blot was incubated overnight at 4°C with the 2nd antibody goat anti-rabbit IgG–horseradish peroxidase (HRPO, 3000 fold diluted in TBS-T; GAR-HRPO 170-651; Bio-Rad, Hercules, CA), with shaking. After that, the blot was washed three times as mentioned above, then it was incubated for 30 seconds with visualization solution for HRPO and then it was exposed to X-ray in KODAK X-OMAT 2000 processor. The visualization solution was prepared just before its use and it was prepared as two 1 ml solutions of 100mM Tris-HCL, pH 8.0; the 1st contained 5 µl luminol [200x stock solution, 88.6mg luminol (Sigma) in 1ml DMSO] and 4.3 luciferin [218x stock solution, 10 mg D-luciferin (Roche Diagnostics) in 2.1 ml 100mM Tris-HCL, pH 8.0]; the 2nd solution contained 15% H_2O_2 (Merck). Before use, both solutions were mixed together to form the visualization solution for HRPO. Photographs of both of X-ray films and stained gels were developed by gel scanner (GS-800 BIO-RAD) using Quantity One program.

3.5.4 β-lactamase activity assay

This assay was used to characterize β-lactamase activities of wild type Pae-AmpC and some mutants. For each assay, 2 µl sample was mixed with 988 µl PBPs (1x, pH 7.5) and 10 µl nitrocefin stock solution (500 µg/ml, Oxoid, Cambridge, United Kingdom), then incubated in a dark place at 23° for 15 min then centrifuged at 14000 rpm for 2 min. The supernatant absorbance was measured at 486 nm on U-2000 spectrophotometer (HITACHI). One milliunit β-lactamase activity is defined as 1 nanomole of nitrocefin hydrolyzed per min per microgram of protein. It was modified from a previous method (Kong et al, 2005).

Values of V_{max} and K_m of purified AmpC forms were identified (using nitrocefin as a substrate) from a plot of the equation of Lineweaver-Burk double reciprocal plot which was driven from the Michaelis-Menten equation (Crowe & Bradshaw, 2010);

$$(1 / v) = (1 / V_{max}) + (K_m / V_{max}) (1 / [S])$$

Where (1 / v) is y-axis; (1 / [S]) is x-axis; (1 / V_{max}) is y-intercept and (K_m / V_{max}) is plot slope. Also, V_{max} is the maximum reaction velocity (activity); K_m is Michaelis constant and is defined by the substrate concentration producing half of maximum activity on a given enzyme substrate.

3.5.5 Bocillin-FL test

Bocillin-FL test was done to analyze the cellular PBPs pattern by fluorescence scanning after incubation of cell membrane fraction with Bocillin-FL which has the ability to bind HMM-PBPs (e.g. PBP1a, PBP1b, PBP2 and PBP3) and LMM-PBPs (e.g. DacB, DacC and PbpG). Briefly, 100µg membrane proteins were incubated with 10 µM Bocillin-FL (Invitrogen, Carlsbad, CA) in 1x PBS (pH 7.5) at 37°C for 30 min and then, a proper volume of loading sample buffer was added. The samples were left at 100°C for 10 min, centrifuged in Eppendorf centrifuge at maximum speed for 5 min and loaded to 8% acrylamide gels in SDS-PAGE system and run at 90V. After the run was complete, the gels were being left in fixing solution (10% methanol and 7% acetic acid) for 1-2 hours then visualized on a Thyphon 9410 variable-mode imager (General Electric) at 588 nm, with a 520BP40 emission filter. For the determination of the cefoxitin 50% inhibitory concentrations (IC50) for the different PBPs, 100µg membrane proteins were incubated firstly with serial concentrations from 0 to 1500 µg/ml of cefoxitin at 37°C for 30 min and then they were incubated with Bocillin-FL at 20 µM at 37ºC for 30 min and processed as described above. IC50 was calculated as the cefoxitin concentration producing a 50% reduction of Bocillin-FL binding for each individual PBP. In this assay a previously described method was used with some modifications (Gonzalez-Leiza et al, 2011).

3.5.6 MALDI-TOF

It is a mass spectrometric analysis-based technique which was used to identify protein bands (e.g. AmpC precursor and mature forms) separated by SDS-PAGE. Also, it was used to identify unknown muropeptides produced from PG analysis by HPLC. MALDI-TOF was done by the unit of proteomics at the Center of Molecular Biology "Severo Ochoa" (CBMSO).

3.5.7 Cell fractionation for protein localization

Fresh LB cultures of Bl21(DE3), DV900(DE3) and PAO1 strains, harboring inducible *ampC* vector, were induced at OD=0.3 with IPTG for 1-3 h at 37°C with 180 rpm agitation. The cells were collected by centrifugation at 5000 rpm for 15 min at 4°C. The cells were re-

suspended in ice-cold 1x PBS, pH 7.5, and lysed by sonication on ice. A small portion of the total sonicate was left on ice, while the other portion was centrifuged at 85000 rpm for 40 min at 4°C. The cell extract (supernatant) was left on ice. The cell pellet (membranes) was re-suspended in a proper volume of ice-cold 1x PBS, pH 7.5. Ice-reserved cell fractions were checked for AmpC presence by SDS-PAGE, western blot and β-lactamase activity, and then stored at -20°C.

3.6 AmpC purification

Purification of an overproduced cellular protein from other contaminating proteins is very important especially for activity characterization and protein X-ray crystallization. Purification can be achieved by various chromatographic techniques. In this study, we have used Ni^{2+}-affinity chromatography to purify AmpC proteins which have poly-His tag where Ni^{2+}-carrying beads trap Poly-His tag-containing AmpC proteins which can be eluted later by high concentration of imidazole after removal of the contaminating proteins by washing buffer (Wiley & Sons, 1996).

All AmpC forms were over-produced by IPTG induced pET28b-*ampC* recombinant vectors in Bl21(DE3). For large AmpC production, transformed Bl21(DE3) cells were grown with agitation in a 30 L fermenter (Biostat UD30, B. Braun Biotech) in LB medium supplemented with 30 µg/ml kanamycin (Kn) at 37°C and induced at OD_{600} ~ 0.3 with 1 mM IPTG for 3 h in case of AmpC-F3 and AmpC-F3-TEV; and induced with 0.1 mM IPTG for 1 h in case of AmpC-F2, AmpC-F4, AmpC-F4:C3 and AmpC-F4:C6. After that, cells were collected, resuspended in 1x phosphate buffer (43 mM Na_2HPO_4 and 14 mM KH_2PO_4, pH 7.5), broken within French pressure cell (American Instrument co, Urbana, III) at 20000 psi and further centrifuged at 50000 rpm for 30 min at 4°C. Both of supernatant and pellet were either stored at -20°C or used in the next step of purification.

The proteins, **AmpC-F3** and **AmpC-F3-TEV**, were purified from the supernatant which passed twice through the Ni-NTA column equilibrated with 1x phosphate buffer (10 mM imidazole, pH7.5). Unbound proteins were washed away with 1x phosphate buffer (50 mM imidazole, pH7.5). Bound AmpC was then eluted with 250 mM imidazole (Merck, Germany) in phosphate buffer, pH 7.5. The Ni-NTA column (QIAGEN GmbH) was regenerated with 500-1000 mM imidazole, and then it was recharged with $NiSO_4.6H_2O$ and equilibrated for another purification cycle (Wiley & Sons, 1996). The eluted fractions were then dialyzed against 20 mM Tris HCl, pH 7.5 with three buffer changes (for 2 h each and the third was left overnight) at 4°C with agitation. Analyzing the purified samples with SDS-PAGE revealed that there was three other faint protein bands which were eliminated by passing the previous purification batch through Sephadex G-25-80 (Pharmacia Fine Chemicals Co.) column equilibrated with 20 mM

Tris HCl (500 mM NaCl, pH7.5). Highly purified fractions were mixed and concentrated using Amicon® Ultra Centrifugal Filters (Ultracel®-30K; Millipore Ireland Ltd) on Megafuge 2.0 R Heraeus (SEPATECH) at 4° C. The concentrated AmpC-F3 and AmpC-F3-TEV were stored at -20°C. The peptide sequence of AmpC-F3 was identified by MALDI-TOF analysis. For elimination of His-tag from AmpC-F3-TEV, it was incubated with TEV protease (1 mg enzyme for 80 mg protein) with rotation at 4°C. We found that after 1 h the produced AmpC-F3-TEV, that had His-tag eliminated, was formed as insoluble precipitate although the precursor AmpC-F3-TEV (with His-tag) was soluble. The insoluble AmpC-F3-TEV (without His-tag) was collected by centrifugation and resuspended in 20 mM tris-HCl, 0.5% Sarkosyl, 100 mM NaCl, pH7.5, and then it was dialyzed three times as described above against the buffer 20 mM tris-HCl, 100 mM NaCl, pH7.5. The purified AmpC-F3-TEV (without His-tag) was tested for successful His-tag loss by western blot. Both AmpC-F3 and AmpC-F3-TEV (without His-tag) were sent to be crystalized. The proteins AmpC-F3:C3-TEV, AmpC-F3:C6-TEV and AmpC-F4-TEV were not purified.

The majority of **AmpC-F2, AmpC-F4, AmpC-F4:C3** and **AmpC-F4:C6** were found insoluble in the membrane pellet fraction. They were extracted by resuspension of the pellet fraction in phosphate buffer containing 3 M guanidine HCl (Gn-HCl; Sigma) at pH 7.5 and centrifuged at 50000 rpm for 15 min at 4°C. The extract was passed directly through Ni-NTA column equilibrated with 1x phosphate buffer (3 M imidazole, pH 7.5). Unbound proteins were washed away by 1x phosphate buffer (3 M Gn-HCl, 20 mM imidazole, pH 7.5) while bound AmpC was then eluted by 250 mM imidazole (in the equilibration buffer) and dialyzed against 20 mM Tris HCl, pH 7.5 as mentioned above. We found that all of these AmpC forms re-precipitated during the first dialysis incubation. So, they were harvested by centrifugation, resuspended in 20 mM tris-HCl, 2% Sarkosyl (Sigma), 100 mM NaCl, pH7.5 and dialyzed against buffer 20 mM tris-HCl, 0.2% Triton X-100 (Sigma), 100 mM NaCl, pH7.5 or buffer 20 mM Tris, 300 mM NaCl, 0.15% sarkosyl, pH 7.5. SDS-PAGE and western blot showed that AmpC-F2, AmpC-F4, AmpC-F4:C3 and AmpC-F4:C6 were highly purified. After their purification, all purified AmpC samples were stored at -20°C.

Theoretical isoelectric points and molecular masses of purified AmpC forms were identified using online ExPASy tools. The purified AmpC proteins were used for characterization of their β-lactamase activities on nitrocefin, X-ray crystallography and for in vitro reactions with the purified PG and individual muropeptides as described later.

3.7 Construction of PAO1 mutants

Our goal is to construct several mutants of LMM-PBPs [*dacB* (gene PA3047), *dacC* (gene PA3999), *pbpG* (gene PA0869)] and *ampC* (gene PA4110) in *P. aeruginosa* PAO1 strain wild type and mutants to pursue their physiological role in PG composition, bacterial resistance and *ampC* regulation in *P. aeruginosa*. The procedure is based on using *cre-lox* method (fig. 3.3) which depends on double recombination between gene-specific inactivation vector and the target chromosomal gene (in PAO1). The used gene-specific inactivation vector in this study is pEX100Tlink vector which has a cloned DNA fragment (PCR1-*lox*-*aacC1*-*lox*-PCR2) containing PCR1 (gene upstream sequence), PCR2 (gene downstream sequence), two *lox* sequences and gentamycin resistance marker (*aacC1*). Also, pEX100Tlink vector has ampicillin resistance marker and *sacB* for sucrose sensitivity. After double recombination, the next step is to eliminate the gentamycin cassette (*aacC1*) by *cre* recombinase (Moya et al, 2009; Quenee et al, 2005).

Previously constructed gene-specific inactivation vectors (pEXTΔ*ampC*::Gm and pEXTΔ*dacB*::Gm) were used for the generation of *dacB* and *ampC* mutants in *P. aeruginosa* PAO1strain (Moya et al, 2009; Moya et al, 2008). These two gene-specific inactivation vectors and single mutants of *dacB* and *ampC* were used in this study also to construct double and multiple mutants in PAO1 strain. In this study we have constructed the gene-specific inactivation vectors for *pbpG* and *dacC* which were used for the generation of many single and combined mutants of LMM-PBPs and *ampC* (described below).

Construction of gene-specific mutagenesis vectors

For amplification of both upstream (PCR1) and downstream (PCR2) regions of the gene to be deleted, a 50 µl PCR reaction contained 1.5 mM MgCl2 (sigma), 0.2mM dNTPs (Bioline), 1µM forward and reverse primers (Sigma), 10% DMSO (sigma), 2.5 U AmpliTaq GoldTM (Roche), 1x Buffer for AmpliTaq and 100ng DNA. For the construction of *pbpG* and *dacC* gene-specific mutagenesis vectors, both upstream (PCR1) and downstream (PCR2) regions of each gene were amplified using the corresponding primers in table 3.3. Then, the product, PCR1 was digested with EcoRI (HF, New England Biolabs) and HindIII (HF, New England Biolabs), while PCR2 was digested with BamHI (HF, New England Biolabs) and HindIII. In the same time pEX100Tlink (with deleted HindIII site) was digested with EcoRI and BamHI. The three digestion products were ligated in one reaction using T4 DNA ligase (New England Biolabs) to produce pEXTΔ*pbpG* and pEXTΔ*dacC*. The ligation products were used to transform *E. coli* XL1-Blue strain by heat chock. The colonies were selected with 50 µg/ml ampicillin LB agar plates and tested by colony PCR. The plasmids, pEXTΔ*pbpG* and pEXTΔ*dacC* were digested with HindIII. The *lox*-flanked gentamicin resistance cassette

(*aacC1*) was extracted from pUCGmlox after digestion with HindIII, using High pure PCR product purification kit (Roche). The *aacC1* fragment was ligated within the linearized pEXTΔ*pbpG* and pEXTΔ*dacC* to produce both *pbpG* and *dacC* gene-specific mutagenesis vectors which will have the formula: pEXTΔ*pbpG*::Gm and pEXTΔ*dacC*::Gm respectively which were used to transform XL1-blue strain. Transformants were selected with 50 µg/ml ampicillin and 10 µg/ml gentamicin LB agar plates. The extracted plasmids, pEXTΔ*pbpG*::Gm and pEXTΔ*dacC*::Gm were used to transform *E. coli* S17.1 λ pyr helper strain and selected as done previously. The right clones were verified by digestion with restriction enzymes, colony PCR (addendum, fig. A.2) and DNA sequencing.

Double recombination and removal of gentamycin cassette

Knockout mutants were generated by conjugation between PAO strain (receptor) and *E. coli* S17.1 λ harboring gene-specific mutagenesis vector (donor), followed by selection of double recombinants using LB plates supplemented with 5% sucrose, 1 µg/ml cefotaxime and 30 µg/ml gentamicin. Double recombinants were checked by first screening for carbenicillin (200 µg/ml) susceptibility and afterwards by PCR amplification and sequencing. For the removal of the gentamicin resistance cassettes, plasmid pCM157 was electroporated into the different mutants. Transformants were selected in LB plates containing a 250 µg/ml tetracycline. One transformant for each mutant was grown overnight in 250 µg/ml tetracycline LB broth in order to allow the expression of the *cre* recombinase. Plasmid pCM157 was then cured from the strains by successive passages in LB broth. Selected colonies were then screened for their tetracycline (250 µg/ml) and gentamicin (30 µg/ml) susceptibilities and checked by PCR amplification and DNA sequencing. Double, triple, and quadruple mutants were then generated sequentially following the same procedure (addendum, Fig. A.3→A.7).

3.8 Estimation of *ampC* expression by RT-PCR

The expression of *ampC* in *P. aeruginosa* was determined by RT-PCR for the constructed mutants and PAO1 (as a control) following previously described protocols (Juan et al, 2006). For the quantification of *ampC* induction, the strains were incubated in the presence of 50 µg/ml of cefoxitin. Briefly, total RNA from logarithmic-phase-grown LB cultures was obtained with an RNeasy minikit (Qiagen, Hilden, Germany). 50 ng of purified RNA was then used for one-step reverse transcription and real-time PCR using a QuantiTect SYBR green reverse transcription-PCR kit (Qiagen) in a SmartCycler II apparatus (Cepheid, Sunnyvale, CA). Previously described conditions and primers were used (Juan et al, 2006). The *rpsL* housekeeping gene was used to normalize the expression levels, and results were always

referenced against PAO1 basal expression. All RT-PCRs were performed in duplicate, and the mean values of mRNA expression resulting from three independent experiments were considered in all cases. *This assay was done as a cooperative work by Gabriel Cabot, Irina Sánchez-Diener, Bartolome Moya and Antonio Oliver (Servicio de Microbiología and Unidad de Investigación, Hospital Universitario Son Espases, Palma de Mallorca, Spain).*

3.9 Antimicrobial susceptibility testing

Disk diffusion was used for determination of bacterial resistance to β-lactams in Bl21 (DE3) and PAO1 mutants transformed with pET-*ampC* and pUCP-*ampC* respectively using antibiotic disks; cefoxitin (FOX-30 µg), ceftriaxone (CRO-30 µg), imipenem (IMI-10 µg), chloramphenicol (C-30 µg), aztreonam (ATM-30 µg), amoxacillin/clavulanic acid (AMC-20+10 µg), Amikacin (AN-30 µg) and ticarcillin (TIC-75 µg) (BioMerieux® sa, France). Inoculum was prepared using growth method and used to inoculate MHA plates as described previously (CLSI, 2012b). For determination of antimicrobial susceptibility of the constructed PAO1 mutants, MICs of ampicillin, piperacillin, aztreonam, cefotaxime, ceftazidime, cefepime, cefoxitin, imipenem, meropenem, and vancomycin were determined by microdilution in 100 µl of cation-adjusted Müller-Hinton broth following the Clinical Laboratory Standards Institute guidelines (CLSI, 2012a).

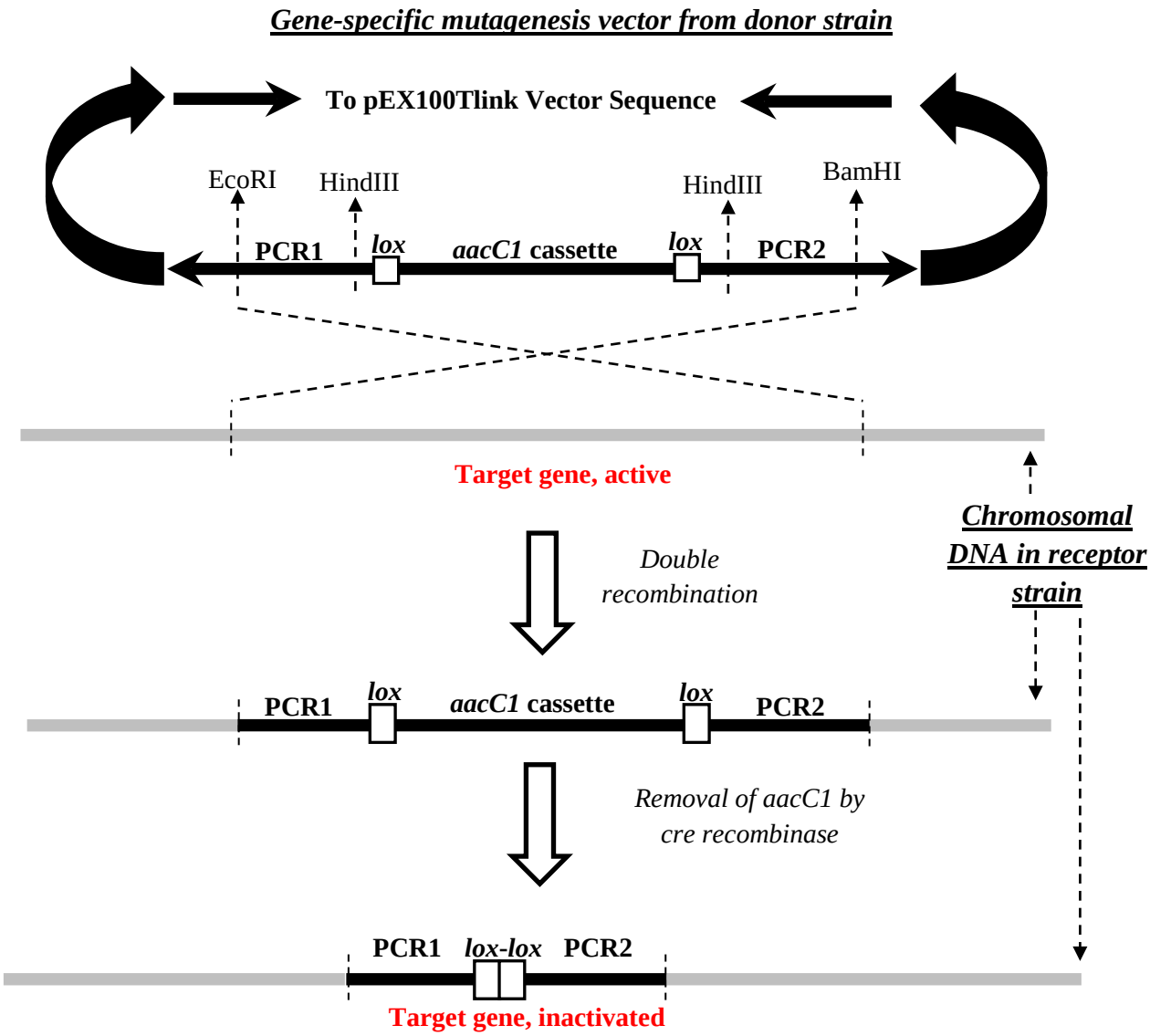

Figure 3.3. Outline for gene-knockout inactivation of *pbpG* and *dacC* in *P. aeruginosa* by *cre-lox* method.

The target gene in red color (e.g. pbpG or dacC) was knocked out and substituted by a DNA fragment having PCR1, 2 lox sequences and PCR2 within two steps, firstly the chromosomal target gene (pbpG or dacC) in the receptor strain (P. aeruginosa) was exchanged for the fragment PCR1-lox-aacC1-lox-PCR2 of the gene-specific mutagenesis vector from the donor strain (e.g. S17/pEXTΔpbpG::Gm) by double recombination. The second step is the elimination of the gentamycin cassette (aacC1) by cre recombinase. The gene-specific mutagenesis vector is a recombinant pEX100Tlink vector having the fragment PCR1-lox-aacC1-lox-PCR2 within the multicloning region where PCR1 and PCR2 are the upstream and downstream DNA sequences of the target gene. The pEX100Tlink and gene-specific inactivation vectors has genes of sacB (sucrose sensitivity) and bla (ampicillin resistance).

3.10 Production of imipenem-induced round cells of PAO1 wild type and mutants

The objective of this experiment is to identify the physiological role of LMMs-PBPs in the recovery of rod shape after elimination of imipenem from the culture media. This effect of imipenem on *P. aeruginosa* was reported in a previous study (Monahan et al, 2014).

Spheroplasts of the wild type PAO1 and all the constructed Pae mutants including the quadruple mutant PAOΔ*dacB*Δ*dacC*Δ*pbpG*Δ*ampC* were obtained after incubation with 5x MICs of IMI in CAMHB media supplemented with 0.5 M sucrose for 4 hours at 37°C without agitation. After that round cells were collected at 6000 rpm for 10 min and resuspended in 0.5 M sucrose supplemented CAMHB medium without imipenem and left for recovery overnight at 37°C without agitation. Both round and recovered cells were tested for their PG composition by HPLC, their morphology by phase-contrast and fluorescence microscopy and their pattern of PBPs by Bocillin-FL binding test.

3.11 Confocal microscopic analysis

Cell preparation for microscopic examination was carried out from overnight cultures of PAO1 wild type and mutant strains. They were used to inoculate new LB media and left to grow at 37°C and 180 rpm for about 8 hours. The optical density was measured at 600 nm every one hour on U-2000 spectrophotometer (HITACHI). Also at different time intervals, the cell morphology was tested in vivo (phase-contrast) using equipment of fluorescence resonance energy transfer (FRET) comprising Axiovert200 inverted microscope (Zeiss) coupled to a monochrome CCD camera. Also, imipenem-induced round cells and their recovered rods of PAO1 wild type and mutants were tested by phase-contrast and fluorescence microscopy using CYTO 9 dye (green fluorescence staining) following the provider´s instructions (LIVE/DEAD® BacLight Bacterial Viability Kit; Molecular Probes, Inc.) where cells stained with CYTO 9 produce green color and considered to be viable.

3.12 Peptidoglycan (PG) manipulation

3.12.1 Preparation of PG

PG was prepared from *E.coli* and *P. aeruginosa* wild type and mutants to be analyzed by HPLC in order to study the effect of AmpC activity on PG composition; also, to highlight the role of LMM-PBPs (DacB, DacC and PbpG) on PG composition. The used method was adapted from a previous study (Gonzalez-Leiza et al, 2011).

For *P. aeruginosa*, wild type and the different mutants of PAO1 were cultured in LB medium treated with and without 50 µg/ml cefoxitin (FOX) at 37°C and 185 rpm agitation until OD_{600} ~0.75-0.8 was achieved, the cells were collected by centrifugation at 5000 rpm/min at 4°C and resuspended in 1x PBS buffer, pH 7.5. One fraction from this cell suspension was left at -20°C for membrane preparation (see below). The rest of cell suspension was added drop by drop to an equal volume of boiling 6% SDS (Merck, Germany) solution with strong stirring. The final cell-SDS suspension was left under boiling conditions for 12 hours with stirring.

For *E coli* (e.g. Bl21(DE3), DV900(DE3), CS109), overnight culture of one colony was 1:100 diluted in fresh LB media with specific antibiotic and left growing at 37°C and 185 rpm agitation until the exponential phase (OD_{600} ~ 0.75-0.8) was achieved, then the cells were harvested and added to boiling SDS solution as described above. The cell-SDS suspension was left under boiling conditions with stirring for 3-4 hours and overnight at room temperature.

The cell-SDS suspensions were centrifuged at 60000 rpm for 10 min to collect the sacculi from the pellet fraction which was then washed with warm sterile milli-Q water, three or more times, until no SDS was detected (no foam appears). Sacculi were suspended in 10 ml of 10 mM Tris-HCl (pH 7.2) and digested with 100 µg/ml α-amylase (EC 3.2.1.1; Sigma-Aldrich, Saint Louis, MO) for 1 h at 37°C and then with 100 µg/ml pre-activated pronase E (EC 3.4.24.4; Merck, Darmstadt, Germany) at 60°C for 90 min. The enzymes were inactivated by boiling for 20 min in 1% (final concentration) SDS. PG was collected and washed as described above. One part of undigested PG was stored at 4°C for in vitro assays. The other part of PG was digested with 100 µg/ml Cellosyl muramidase (Hoechst AG, Frankfurt, Germany) in 50 mM phosphate buffer (pH 4.9) at 37°C overnight. The enzyme was inactivated by boiling the sample for 10 min in a water bath and centrifuged in Eppendorf centrifuge at 14000 rpm for 5 min to remove insoluble debris. The supernatant was mixed with 1/3 volume of 0.5 M sodium borate buffer (pH 9.0) and reduced with excess sodium borohydride (NaBH4) for 30 min at room temperature. The pH was tested with pH indicator strips (Acilit, Merck) and adjusted to pH 3 with orthophosphoric acid. All samples were filtered (Millex-GV filters; 0.22-µm pore size, 2.5-mm diameter; Millipore, Cork, Ireland) or centrifuged at maximum speed for 10 min., then stored at -20°C until its injection in the HPLC.

3.12.2 HPLC analysis

Breeze 2 HPLC System (Waters Breeze™ 2 HPLC System, with 1525 Binary HPLC Pump) was used. Sodium phosphate buffers (A) pH4.35 with 0.2% sodium azide and sodium phosphate buffer (B), pH 4.95 with 15% methanol (Merck, Germany) were used. It was modified from previously reported method (Glauner, 1988; Gonzalez-Leiza et al, 2011). During the HPLC run of digested PG, some unknown peaks (muropeptides) were collected, lyophilized and sent to be identified by MALDI-TOF. Some other well-known muropeptides (e.g. M5, M4, D44 and D45) were collected for in vitro reactions. Quantification of muropeptides was achieved from their integrated areas in the HPLC chromatogram.

3.12.3 Effect of Pae-AmpC on the whole PG and individual muropeptides in vitro

To confirm if Pae-AmpC has DD-peptidase activity in vitro, the purified AmpC proteins (wild type and mutants) were incubated with purified muropeptides or whole peptidoglycan.

In vitro assay using the whole PG

A 250 µl reaction contained about 160 µg of undigested purified PG with various concentrations (indicated in results) of purified AmpC at 37 or 42°C for variable periods (1→24 h) in buffer 20 mM tris-HCl, pH7.5, and then boiled for 15 min. After that, muramidase was added to the reaction mixture which was incubated at 37°C overnight. Reduction of digested PG was done as described before (Section 3.11.1) and then it was subjected to HPLC analysis.

In vitro assay using individual muropeptides

A 250 µl reaction contained purified AmpC of various concentrations (indicated in results) were incubated in buffer 20 mM tris-HCl, pH7.5 with a different amounts (indicated in results) of the individual purified muropeptides (e.g. M4, M5, D44 and D45) at 37 or 42°C for variable periods (1→24 h), then the reaction was boiled for 2 min, centrifuged at 14000 rpm for 10 min and injected into the HPLC or stored at -20°C until being used.

4. Results

4.1. Functional characterization of Pae-AmpC β-lactamase in E. coli and P. aeruginosa PAO1 strains

4.1.1. Summary

4.1.2. Pae-ampC cloning

4.1.3. Pae-ampC expression

4.1.4. Pae-AmpC purification and characterization

4.1.5. Pae-AmpC structure and crystallization

4.1.6. Effect of Pae-ampC expression on bacterial resistance

4.1.7. Effect of Pae-ampC expression on PG composition (in vivo)

4.1.8. Effect of the purified Pae-AmpC forms on PG composition and individual muropeptides (in vitro)

4.2. Role of LMM-PBPs in ampC regulation, β-lactam resistance and peptidoglycan structure in P. aeruginosa

4.2.1. Summary

4.2.2. The constructed PAO1 mutants

4.2.3. Growth rates and microscopic examination of PAO1 mutants

4.2.4. Bocillin-FL test of PAO1 mutants

4.2.5. Effect of LMM-PBPs inactivation on ampC expression and β-lactam resistance in P. aeruginosa PAO1

4.2.6. PG composition of the constructed PAO1 mutants

4.3. Activities of DacB, DacC and PbpG are not essential for recovery of rod shape in imipenem-induced spheroplasts in P. aeruginosa

4.3.1. Summary

4.3.2. Microscopic examination of imipenem-induced spheroplasts of PAO1 wild type and mutants.

4.3.3. PG composition of imipenem-induced spheroplasts PAO1 wild type and mutants

4.3.4. Bocillin-FL test of imipenem-induced spheroplasts of PAO1 wild type and PAOΔampC

4. Results

4.1. Functional characterization of Pae-AmpC β-lactamase in some *E. coli* and *P. aeruginosa* PAO1 strains

4.1.1. Summary

The aim of this chapter is to characterize the activity of AmpC β-lactamase (Pae-AmpC) of *Pseudomonas aeruginosa* PAO1 strain; also to study the effect of *ampC* expression in bacterial resistance and PG composition and to analyze the effect of some uncharacterized mutations on the activity of Pae-AmpC and on the profile of bacterial resistance. For that purpose we did the next steps: a) cloning of the wild type Pae-*ampC* [precursor form (*ampC*-F1) and mature form (*ampC*-F3 and *ampC*-F3-TEV)] and wild type Pae-AmpC having modified signal peptide sequence (*ampC*-F2, *ampC*-F4 and *ampC*-F4-TEV) and some mutants of Pae-*ampC* having single nucleotide mutation [T^{728}→C (e.g. *ampC*-F4:C3), C^{152}→T (e.g. *ampC*-F4:C6)] in some wild type and mutant strains of *E. coli* and *P. aeruginosa* PAO1; b) pursuing AmpC activity and expression by SDS-PAGE, western blot, β-lactamase activity assay; c) analyzing the change in bacterial resistance after *ampC* expression using disc diffusion assay; d) purification of some AmpC forms by Ni-affinity chromatography for functional characterization and X-ray crystallization; and e) pursuing the effect of AmpC activity on PG composition of *E. coli* and *P. aeruginosa* by HPLC analysis of their PG after *ampC* expression (in vivo assay). Also, AmpC effect on PG was analyzed by HPLC after direct reaction of purified Pae-AmpC with both the whole PG and individual muropeptides which were purified from the given bacterial strains (in vitro assays). Most remarkable data are: 1) we found that *ampC*-F1, *ampC*-F1:C3 and *ampC*-F1:C6 were not expressed; 2) AmpC-F4 had the highest β-lactamase activity and caused the largest increase in bacterial resistance; 3) the two mutants AmpC-F4:C3 and AmpC-F4:C6 had a very low β-lactamase activity and a little effect on the profile of bacterial resistance; 4) data obtained from HPLC analysis of PG composition in vivo support the previous suggestion that AmpC can have DD-carboxypeptidase or DD-endopeptidase activity (due to structural similarities). Also, in vitro assays showed and confirmed that only AmpC-F3 had DD-peptidase activity.

4.1.2. Pae-*ampC* cloning

Outline of the cloned Pae-ampC forms

The cloned forms of Pae-*ampC* from PAO1 are *ampC*-F1 (the wild type *ampC*, precursor form); *ampC*-F2 is an *ampC* mutant with $G^4 \rightarrow C$ single nucleotide mutation which corresponds to $R^2 \rightarrow G$ amino acid mutation in the signal peptide; *ampC*-F3 is the mature form of Pae-*ampC* with an insertion of ATG as initiation codon; *ampC*-F4 is a designed *ampC* form with insertion of two codons (ATG GCC) before the starting codon of wild type *ampC* sequence inserting the two amino acids M^1 A^2 to the AmpC protein; *ampC*-F3-TEV and *ampC*-F4-TEV have the same sequence of *ampC*-F3 and *ampC*-F4 respectively but with extra sequence at C-terminal which encodes amino acids (E N L Y F Q G) that constitute the recognition site for TEV protease; *ampC*-F1:C3, *ampC*-F3:C3-TEV and *ampC*-F4:C3 have the same sequence of *ampC*-F1, *ampC*-F3-TEV and *ampC*-F4, respectively, but with $T^{728} \rightarrow C$ single nucleotide mutation (we called it C3 mutation) which correspond to single amino acid change ($P^{243} \rightarrow L$); *ampC*-F1:C6, *ampC*-F3:C6-TEV and *ampC*-F4:C6 have the same sequence of *ampC*-F1, *ampC*-F3-TEV and *ampC*-F4, respectively, but with $C^{152} \rightarrow T$ single nucleotide mutation (we called it C6 mutation) which correspond to single amino acid change $I^{51} \rightarrow T$. All these *ampC* forms have a sequence for poly-His tag at C-terminal. Only *ampC*-F3:C3-TEV, *ampC*-F3:C6-TEV and *ampC*-F4-TEV have TEV site sequence upstream to the sequence of the C-terminal poly-His tag (fig. 4.1; table 4.1). As described above, the nomenclature of each *ampC* form involves *ampC* at the beginning then F1, F2, F3 and F4 (referring to the Forward primer used in amplification, table 3.2); C3 and C6 referring to the mutations $T^{728} \rightarrow C$ and $C^{152} \rightarrow T$ which were first observed in a previous unpublished study (our laboratory collection), respectively. The nomenclature also involved the word TEV referring to the presence of a sequence coding for recognition site of TEV protease. In figure 4.1, we have an illustrative diagram for the different forms of Pae-AmpC proteins that were produced by expression of all the above described *ampC* constructs. All AmpC forms produced were expected to be periplasmic, except AmpC-F2 having a charge defect in the signal peptide, and AmpC-F3, AmpC-F3-TEV, AmpC-F3:C3-TEV and AmpC-F3:C6-TEV that were produced as cytoplasmic forms because they do not have the signal peptides.

Cloning of Pae-ampC in pET28b

All *ampC* forms *ampC*-F1, *ampC*-F2, *ampC*-F3, *ampC*-F4, *ampC*-F1:C3, *ampC*-F1:C6, *ampC*-F4:C3, *ampC*-F4:C6, *ampC*-F3-TEV, *ampC*-F3:C3-TEV *ampC*-F3:C6-TEV and *ampC*-F4-TEV were successfully cloned in pET28b plasmid producing respectively the recombinant vectors pET-F1, pET-F2, pET-F3, pET-F4, pET-F1:C3, pET-F1:C6, pET-F4:C3, pET-F4:C6,

pET-F3-TEV, pET-F3:C3-TEV, pET-F3:C6-TEV and pET-F4-TEV (table 3.1). All of these clones were transformed in DH5α (for cloning) and Bl21(DE3) [for *ampC* expression and characterization]. Due to their high *ampC* expression profile and other interesting results (described later), only the recombinant vectors pET-F2, pET-F4, pET-F4:C3, pET-F4:C6 and pET-F3 were used to transform DV900 for functional characterization of *ampC* in this strain. All clones were confirmed by DNA electrophoresis of their colony PCR (addendum, figure A. 1) and by DNA sequencing. For simplification we used pET-*ampC* to refer to all the cloned Pae-*ampC* forms in the vector pET28b unless there is something special to describe for any of these constructs.

Cloning of Pae-ampC in pUCP24

From all previously cloned *ampC* forms in *E. coli*, only *ampC*-F3 and *ampC*-F4 were selected to be cloned in *P. aeruginosa* because both forms produced relevant results (described later) respect to β-lactamase activity, bacterial resistance and effect on PG composition. Both of *ampC*-F3 and *ampC*-F4 were cloned in pUCP24 vector producing the recombinant vectors pUCP-F3 and pUCP-F4 respectively which were transformed into DH5α and some PAO1 mutant strains and were confirmed by colony PCR and by DNA sequencing.

The selected PAO1 mutant strains used for cloning of pUCP-F3 and pUCP-F4 are PAOΔ*ampC*, PAOΔ*dacB*Δ*pbpG*Δ*ampC*, PAOΔ*dacB*Δ*dacC*Δ*ampC* and PAOΔ*dacB*Δ*dacC* Δ*pbpG*Δ*ampC*. These mutants have *ampC* deletion and some special characteristics concerning their PG composition where PAOΔ*dacB*Δ*dacC*Δ*pbpG*Δ*ampC* has a very large amount of penta muropeptides resembling PG composition of *E. coli* DV900 with which *ampC*-F3 produced some DD-peptidase activity (section 4.1.8) and it was interesting to compare this activity with a similar PG composition from *P. aeruginosa*; also, PAOΔ*dacB*Δ*dacC*Δ*ampC* has a considerable increase in penta muropeptides but with larger amounts of tetra muropeptides; both of PAOΔ*ampC* and PAOΔ*dacB*Δ*pbpG*Δ*ampC* have a normal penta and tetra muropeptides and they were selected because *ampC* complementation in PAOΔ*ampC* would give us the normal effect of AmpC activity without interfering with the effect of inactivation of PBPs, also PAOΔ*dacB*Δ*pbpG*Δ*ampC* is a special mutant because it lacks the activity of the main DD-endopeptidases (*dacB* and *pbpG*) and it was interesting to pursue the effect of *ampC* expression in this mutant; more detailed information about these mutants is described in section 4.2.

Table 4.1. Mutations and changes in the main sequence of the cloned Pae-*ampC* constructs.

Pae-*ampC* form/ name[a]	Nucleotide change[b]	Amino acid change[c]
***ampC*-F1**	-	-
***ampC*-F1:C3**	T^{728}→C mutation	P^{243}→L
***ampC*-F1:C6**	C^{152}→T mutation	I^{51}→T
***ampC*-F2**	G^{4}→C	R^{2}→G
***ampC*-F3**	A^{1}TG insertion as a start codon	M insertion before A^{26}
***ampC*-F3-TEV**	A^{1}TG insertion as a start codon	M insertion before A^{26}
***ampC*-F3:C3-TEV**	T^{728}→C mutation	P^{243}→L
***ampC*-F3:C6-TEV**	C^{152}→T mutation	I^{51}→T
***ampC*-F4**	A^{1}TG GCC insertion	M A insertion before M^{1}
***ampC*-F4-TEV**	A^{1}TG GCC insertion	M A insertion before M^{1}
***ampC*-F4:C3**	T^{728}→C mutation and ATG GCC insertion	P^{243}→L mutation and M A insertion before M^{1}
***ampC*-F4:C6**	C^{152}→T mutation and ATG GCC insertion	I^{51}→T mutation and M A insertion before M^{1}

[a] The cloned Pae-ampC forms from PAO1 were named referring to their corresponding forward primers (F1→F4), the presence of C3 or C6 mutations[b] and the presence of recognition site of TEV protease. Nucleotide changes[b] and its corresponding amino acid changes[c] within different ampC constructs are shown compared to the wild type PAO1 ampC where ampC-F1 is the wild type Pae-ampC; ampC-F2 is an ampC mutant with G^{4}→C single nucleotide mutation; ampC-F3 is the mature form of ampC with an insertion of ATG as initiation codon while ampC-F4 is a designed ampC form with insertion of two codons (ATG GCC) before the starting codon of wild type Pae-ampC sequence. All ampC constructs that have C3 or C6 in their nomenclature refer to mutations that were previously found (laboratory collection) in transformants colonies number 3 and 6 with sense single nucleotide mutations, T^{728}→C and C^{152}→T, respectively. All ampC constructs were designed to have C-terminal His-tag. More information about these constructs is shown in figure 4.1.

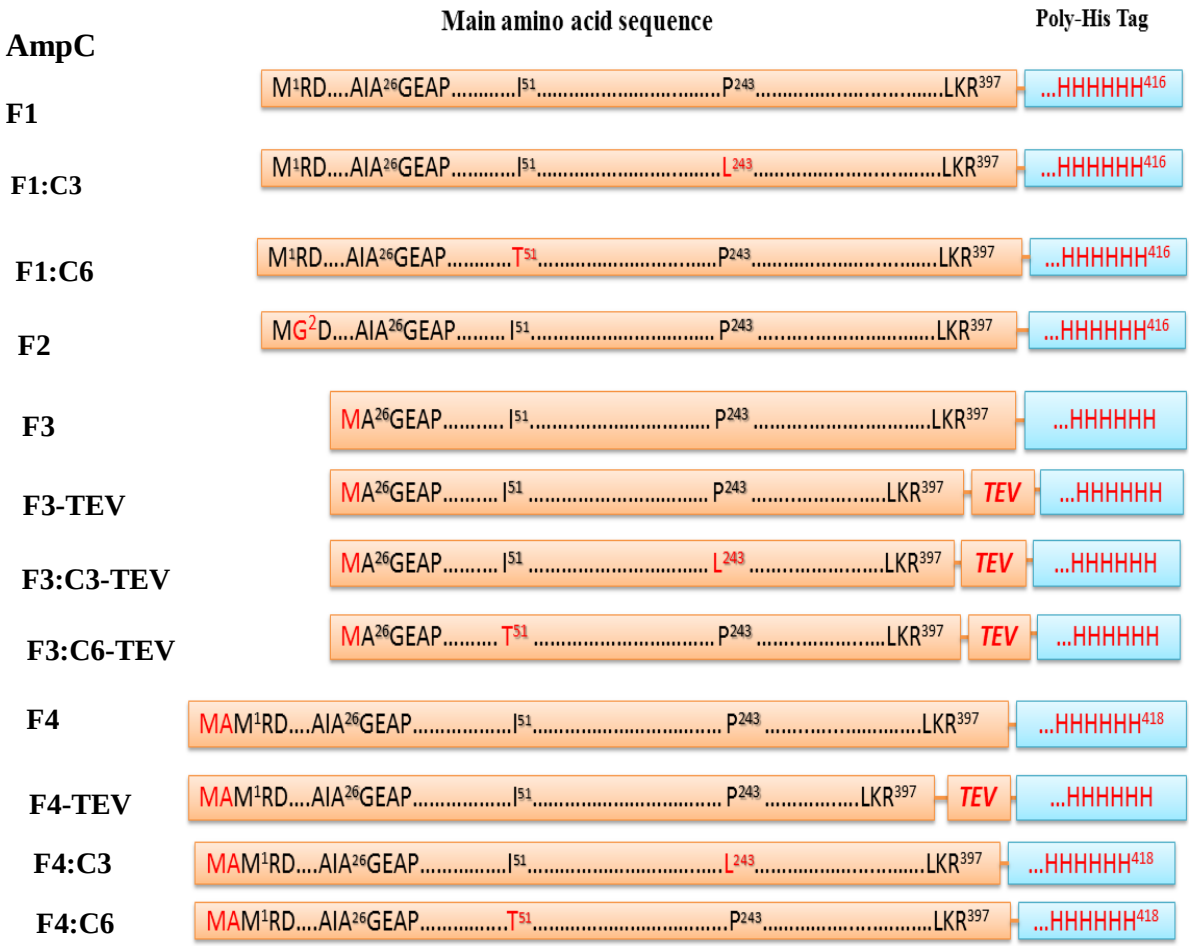

Figure 4.1. Schematic outline of general structures and amino acid sequences of the studied Pae-AmpC forms.

Main amino acid sequences of AmpC forms are colored in black while amino acid changes and extra-amino acids are colored in red. ***TEV****: Cleavage site for TEV protease. Nomenclature of AmpC forms was described within table 4.1. AmpC-F1 is the wild type Pae-AmpC; AmpC-F2 is AmpC mutant with* $R^{2}\rightarrow G$ *point amino acid mutation; AmpC-F3 is the mature form of Pae-AmpC with an insertion of amino acid M as a peptide initiator in translation; while AmpC-F4 is AmpC form with insertion of two amino acids (M A) before* M^{1} *of the main amino acid sequence of wild type AmpC. All AmpC forms that have C3 or C6 in their nomenclature refer to the presence of point amino acid mutation* $P^{243}\rightarrow L$ *and* $I^{51}\rightarrow T$*, respectively, compared to the wild type AmpC.*

4.1.3. Pae-*ampC* expression

Pae-ampC expression in E. coli Bl21(DE3) and DV900(DE3)

The recombinant vectors of pET-*ampC* were used for expression of their encoded *ampC* forms in Bl21(DE3) and DV900(DE3) under IPTG induction. Bl21(DE3)/pET-*ampC* and DV900(DE3)/pET-*ampC* were used to refer respectively to Bl21(DE3) and DV900(DE3) transformed with some pET28b recombinant vectors encoding for various *ampC* forms which were described in table 4.1. For detection of the expressed AmpC form by SDS-PAGE and western blot after induction with IPTG, cell fractionation was done as described in section 3.5.7 and samples from total sonicate, cell extract and cell membrane pellet were loaded to detect and to localize AmpC forms in these fractions (fig. 4.2, 4.3, 4.4, 4.5). For overproduction of AmpC forms in transformants of Bl21(DE3) (fig. 4.2, 4.3, 4.5) harboring pET-F1, pET-F2, pET-F3, pET-F4, pET-F1:C3, pET-F1:C6, pET-F4:C3 and pET-F4:C6 and transformants of DV900(DE3) (fig. 4.4) harboring pET-F2, pET-F4, pET-F4:C3 and pET-F4:C6; cells were induced with 0.1 mM IPTG in LB media for 1 h at 37°C with agitation. DV900(DE3) transformed with pET-F3 was induced with 1 mM IPTG (fig. 4.4) due to low production of AmpC-F3 with 0.1 mM IPTG in Bl21(DE3) (fig. 4.3). The production of AmpC-F1, AmpC-F1:C3 and AmpC-F1:C6 was too low and cannot be detected by SDS-PAGE and western blot (fig. 4.2), while, all of AmpC-F2, AmpC-F4, AmpC-F4:C3 and AmpC-F4:C6 were produced in a large amount which can be detected by SDS-PAGE and western blot (fig. 4.2, 4.3, 4.4). AmpC-F3 was produced in a low amount that can be detected only by western blot (fig. 4.4). For transformants of Bl21(DE3) harboring pET-F3, pET-F3-TEV, pET-F3:C3-TEV, pET-F3:C6-TEV and pET-F4-TEV we found that the best production conditions for AmpC-F3 was induction with 1 mM IPTG for three hours; while, AmpC-F3-TEV, AmpC-F3:C3-TEV and AmpC-F3:C6-TEV were produced after induction with 2 mM IPTG for 3 h at 37 °C. On the other hand, 0.1 mM IPTG was enough to overproduce AmpC-F4-TEV in two hours (fig 4.5). Induction with 1 mM IPTG caused overproduction of AmpC-F2, AmpC-F4, AmpC-F4:C3 and AmpC-F4:C6 which were too lethal to both of Bl21(DE3) and DV900(DE3) causing a decrease in cell growth and some cell lysis.

Detection of AmpC proteins of cellular fractions of Bl21(DE3)/pET-*ampC* by SDS-PAGE and western blot showed that under induction conditions the majority of AmpC-F2 was produced as a precursor form and was present in membrane fraction (fig. 4.2); AmpC-F4:C3 and AmpC-F4:C6 (precursor and mature forms) were found only in the membrane fraction (fig. 4.3). Most of mature form AmpC-F4 was found in the cell extract while the majority of its precursor form was found in the membrane fraction (fig. 4.3). Mature form AmpC-F3 was not detected under these conditions (0.1mM IPTG induction for 1 h) but it was found in a low

amount in the cell extract after induction with 1 mM IPTG for 1h (fig. 4.3, 4.4, 4.5). No AmpC form of the different constructs was found in fractions of non-induced Bl21(DE3) cells. Equivalent results were obtained from cellular fractions of DV900(DE3)/pET-*ampC* with IPTG induction (fig. 4.4), with the exception of a considerable soluble amount of the mature and a dimeric AmpC forms in all non-induced samples, indicating some escape from the T7 promoter on those strains. Another difference with expression on DV900(DE3) transformants is that most of the precursor and mature form of AmpC-F4 were found in the membrane fractions of induced cells (fig. 4.4).

Cellular fractions were tested for β-lactamase activity (table 4.2) where fractions of Bl21(DE3)/pET-F4 showed the highest activity in fractions of total sonicate and cell extract; cellular fractions of Bl21(DE3)/pET-F2 displayed a medium β-lactamase activity; cellular fractions of Bl21(DE3)/pET-F3, Bl21(DE3)/pET-F4:C3 and Bl21(DE3)/pET-F4:C6 displayed lower β-lactamase activities. Concerning transformants of DV900(DE3), cellular fractions of DV900(DE3)/pET-F4 and DV900(DE3)/pET-F2 showed high β-lactamase activities in fractions of total sonicate and cell extract; cellular fractions of DV900 (DE3)/pET-F3 displayed a low β-lactamase activities while cellular fractions of DV900(DE3)/pET-F4:C3 and DV900 (DE3)/pET-F4:C6 showed very low β-lactamase activities.

Pae-ampC expression in PAO1

The vectors pUCP-F3 and pUCP-F4 were used for complementation studies in some PAO1 mutants (PAOΔ*dacB*Δ*pbpG*Δ*ampC*, PAOΔ*dacB*Δ*dacC*Δ*ampC*, PAOΔ*dacB*Δ*dacC* Δ*pbpG*Δ*ampC* and PAOΔ*ampC*) which have *ampC* deletion. We observed a low production of AmpC-F3 and AmpC-F4 from Pae (*P. aeruginosa)* transformants of pUCP-F3 and pUCP-F4, respectively, after induction with 1mM IPTG for 3 hours in LB media at 37 °C with agitation. In this case both of AmpC-F3 and AmpC-F4 were detected only by western blot and they were not detected by SDS-PAGE; western blots of samples from cellular fractions of total sonicate displayed the bands of both of AmpC-F3 and AmpC-F4 in both of induced and non-induced fractions with no difference, indicating that IPTG induction did not help in AmpC production from pUCP-F3 and pUCP-F4; also, blots shows that there is a basal production of AmpC-F3 and AmpC-F4 (fig.4.6).

β-lactamase activity assays of cellular fractions from total sonicate of all above described Pae transformants showed that activity of AmpC-F4 was also very high when compared with AmpC-F3 in all Pae transformants, as has been shown previously with *E. coli* transformants. The values of β-lactamase activity (table 4.3) were very close in cellular fractions with IPTG induction compared with those without induction which are in perfect accordance with data obtained from their production in figure 4.6.

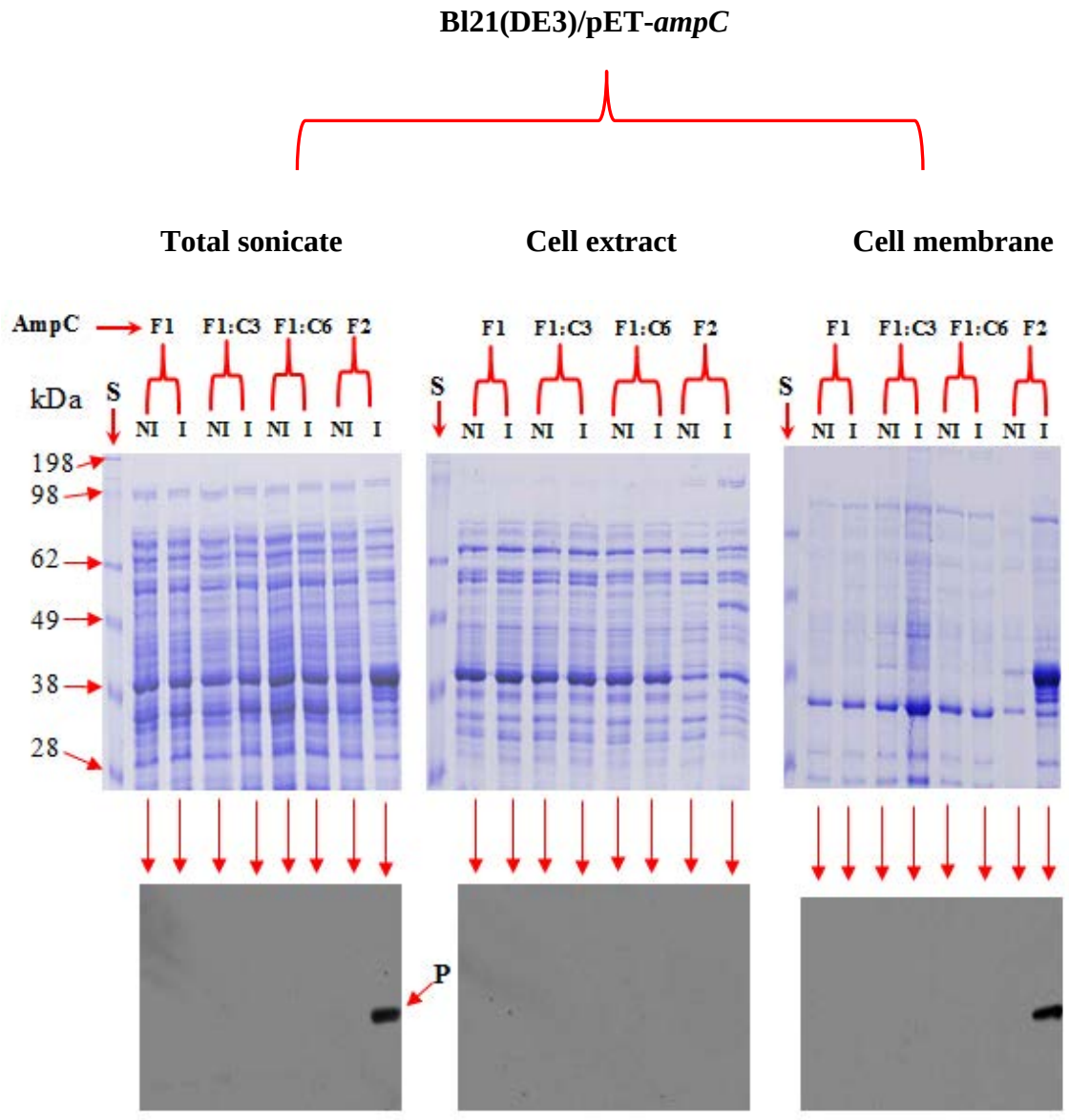

Figure 4.2. Detection of AmpC-F1, AmpC-F1:C3, AmpC-F1:C6 and AmpC-F2 in cellular fractions (total sonicate, cell extract and cell membrane) of Bl21(DE3).

*After 1 h of induction (37 °C) by 0.1mM IPTG of Bl21(DE3) harboring pET-F1, pET-F1:C3, pET-F1:C6 and pET-F2, cells were collected, sonicated and fractionated (section 3.5.7). AmpC forms were then detected in Coomassie-stained 8% SDS-PAGE gels (upper panel) and in the corresponding western blot (lower panel). An equivalent of 0.2 UOD was loaded from each fraction of both of non-induced (**NI**) and induced (**I**) cells. AmpC-F1, AmpC-F1:C3 and AmpC-F1:C6 were not detected while AmpC-F2 was found mostly in the pellet fraction as a precursor form (**P**). **S**: standard protein molecular mass markers.*

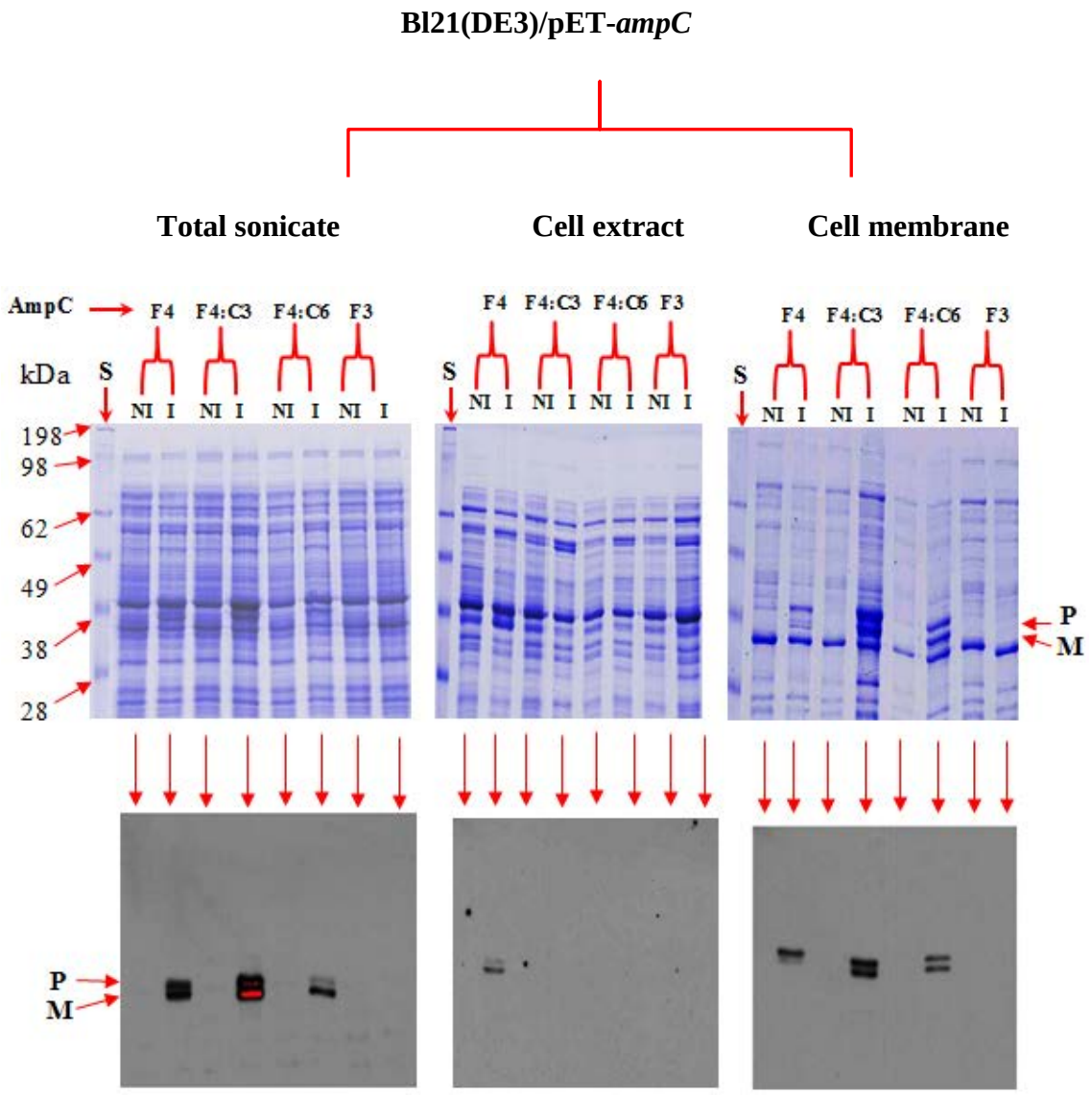

Figure 4.3. Detection of AmpC-F4, AmpC-F4:C3, AmpC-F4:C6 and AmpC-F3 in cellular fractions (total sonicate, cell extract and cell membrane) of Bl21(DE3).

*After 1 h of induction (at 37 °C) by 0.1mM IPTG of Bl21 (DE3) harboring pET-F4, pET-F4:C3, pET-F4:C6 and pET-F3, cells were collected, sonicated and fractionated (section 3.5.7). AmpC forms were then detected in Coomassie-stained 8% SDS-PAGE gels (upper panel) and in the corresponding western blot (lower panel). An equivalent of 0.2 UOD was loaded from each fraction of both of non-induced (**NI**) and induced (**I**) cells. Mature form of AmpC-F4 was detected mainly in cell extract while its precursor form was detected mostly in the membrane fraction; both precursor (**P**) and mature (**M**) forms of AmpC-F4:C3 and AmpC-F4:C6 were observed mainly in the membrane fraction while AmpC-F3 was not detected under these conditions. **S**: standard protein molecular mass markers.*

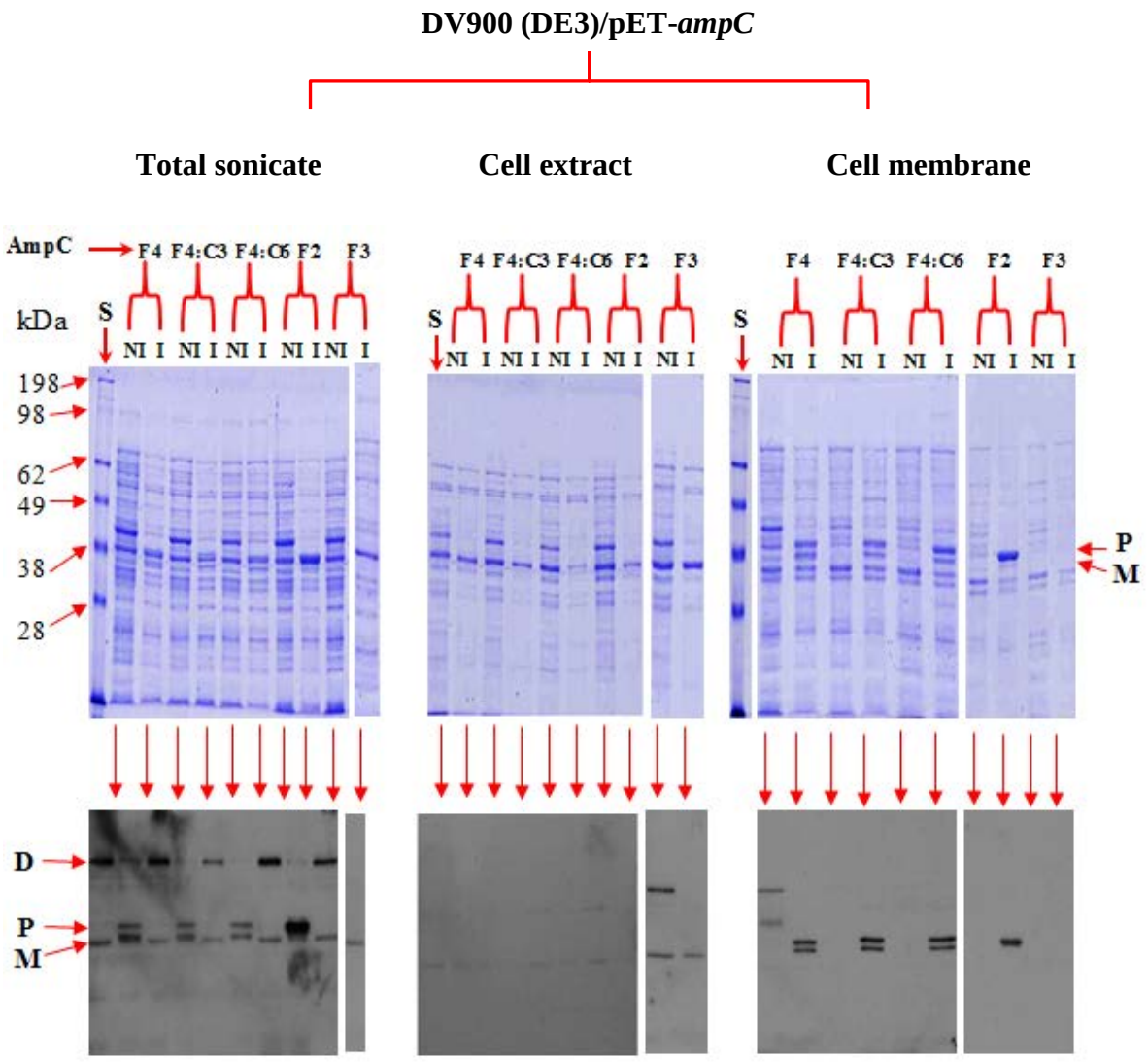

Figure 4.4. Detection of AmpC-F4, AmpC-F4:C3, AmpC-F4:C6, AmpC-F2 and AmpC-F3 in cellular fractions (total sonicate, cell extract and cell membrane) of DV900 (DE3).

*DV900 (DE3) harboring pET-F4, pET-F4:C3, pET-F4:C6 and pET-F2 were induced by 0.1mM IPTG at 37 °C for 1 h and then cells were collected, sonicated and fractionated (section 3.5.7). DV900(DE3)/pET-F3 was induced by 1 mM IPTG for 1 h. AmpC forms were then detected in Coomassie-stained 8% SDS-PAGE gels (upper panel) and in the corresponding western blot (lower panel). An equivalent of 0.2 UOD was loaded from each fraction of both of non-induced (NI) and induced (I) cells. Both of precursor (**P**) and mature (**M**) forms of AmpC-F4, AmpC-F4:C3 and AmpC-F4:C6 were detected mainly in the membrane fraction while AmpC-F3 mature form was detected in the cell extract. **D** is expected to be a dimeric form of AmpC. **S**: standard protein molecular mass markers.*

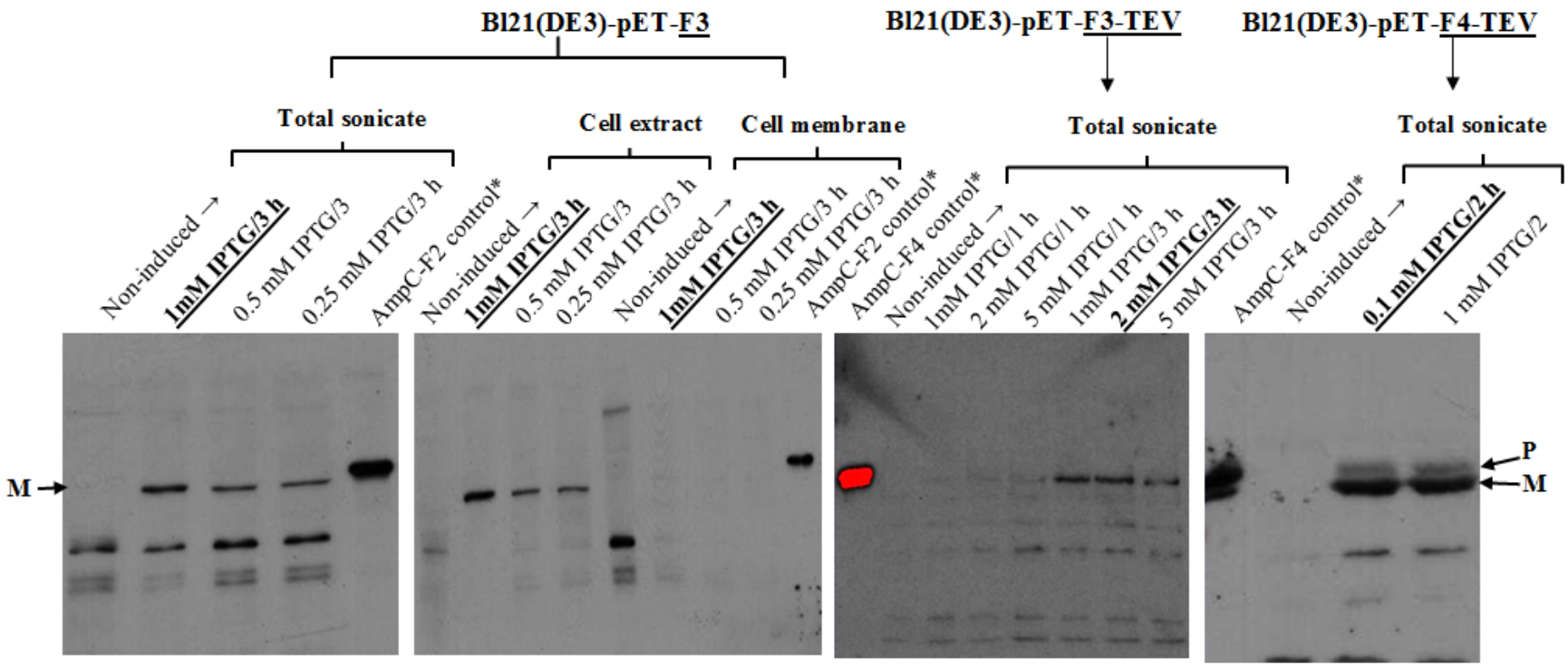

Figure 4.5. Expression of AmpC-F3, AmpC-F3-TEV and AmpC-F4-TEV in Bl21(DE3) transformants.

*Expression of AmpC-F3, AmpC-F3-TEV and AmpC-F4-TEV in Bl21(DE3)/pET-F3, Bl21(DE3)/pET-F3-TEV and Bl21(DE3)/pET-F4-TEV, respectively, was done with different IPTG concentrations and different incubation times (down-up writing) in LB media at 37°C. Different AmpC forms were analyzed by western blot in fractions of total sonicate, cell extract and cell membrane pellet. The best expression conditions (bold; underlined) were 1mM IPTG/3 h, 2 mM IPTG/3 h and 0.1 mM IPTG/2 h for production of AmpC-F3, AmpC-F3-TEV and AmpC-F4-TEV, respectively. The forms ampC-F3:C3-TEV and ampC-F3:C6-TEV were expressed like ampC-F3-TEV with 2 mM IPTG/3 h (fig. not shown for simplification). The bands appearing below the AmpC-F3 band may be due to some protein degradations or other protein background. * Purified AmpC-F2 and AmpC-F4 were used as controls.* ***P*** *stands for precursor form while* ***M*** *stands for the mature form.*

Table 4.2. β-lactamase activity of different forms of AmpC expressed in BL21(DE3) and DV900(DE3) after IPTG induction.

***E. coli* Strain**	**Plasmid**	**IPTG mM**	**µmole/min/UOD[a]**		
			Total sonicate fraction	Cell extract fraction	Cell membrane fraction
BL21(DE3)	pET-F4	0	27.1	25.8	11
		0.1	526.4	329.0	153
	pET-F4:C3	0	1.3	0.7	0.5
		0.1	10.5	3.4	2.5
	pET-F4:C6	0	0.8	0.4	0.3
		0.1	32.1	28.4	5
	pET-F2	0	6.5	5	1.3
		0.1	113.4	36.1	38
	pET-F3	0	1.2	0.8	0.1
		1	28.2	24.4	1
	pET-F1	0	0.8	0.6	0.1
		1	27.5	6.7	1.1
	pET-F1:C3	0	0.7	0.4	0.05
		1	0.9	0.5	0.2
	pET-F1:C6	0	0.9	0.7	0.04
		1	5	2.7	1
DV900(DE3)	pET-F4	0	9.5	6.3	2.6
		0.1	196	75.4	128.2
	pET-F4:C3	0	0.53	0.32	0.16
		0.1	3.5	1.4	2
	pET-F4:C6	0	0.13	0.12	0
		0.1	2.2	0.74	1.5
	pET-F2	0	63.3	52.8	4.2
		0.1	260.3	86.8	181
	pET-F3	0	1.1	0.9	0
		0.1	26.4	23.8	0
		1	46.9	42	0

[a] *β-lactamase Activity using nitrocefin as a substrate was detected in cellular fractions (total sonicate, cell extract and cell membrane) and expressed in µmole/min/UOD. Expression of ampC forms in BL21(DE3) and DV900(DE3) using pET28b-ampC vectors was done under non-induction and induction conditions with 0.1 or 1 mM IPTG for 1 h at 37 °C. UOD stands for Unit of Optical Density.*

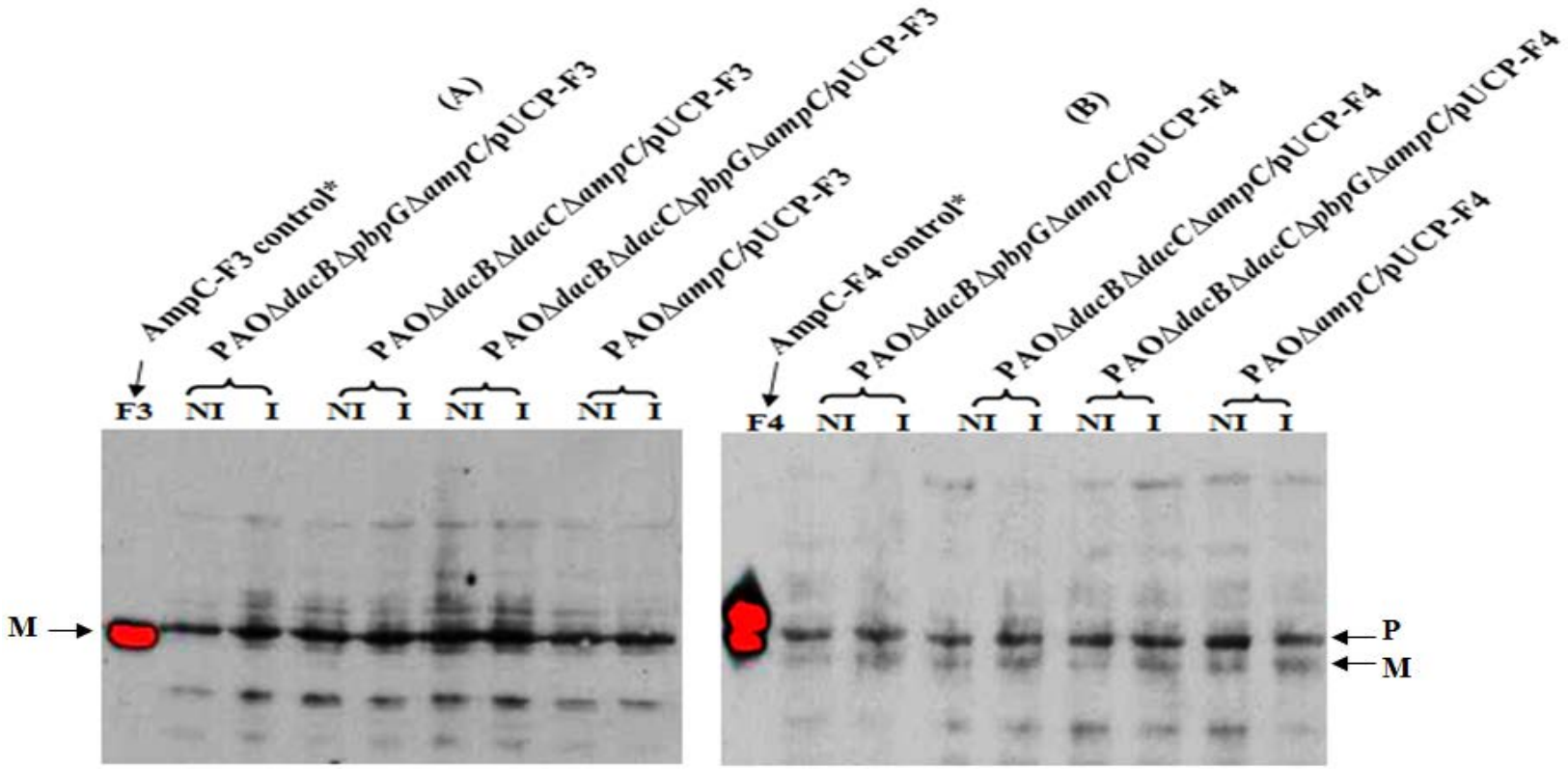

Figure 4.6. Pae-AmpC expression in PAO1 mutants transformed with pUCP-F3 and pUCP-F4.

*Western blot analysis of cellular fractions (total sonicate) of PAO1 mutants (*PAOΔ*dacB*Δ*pbpG*Δ*ampC,* PAOΔ*dacB*Δ*dacC*Δ*ampC,* PAOΔ*dacB*Δ*dacC*Δ*pbpG*Δ*ampC and* PAOΔ*ampC) transformed with pUCP-F3* ***(A)*** *or pUCP-F4* ***(B)*** *after induction by 1mM IPTG for 3 h at 37 °C. The vector pUCP-F3 produces AmpC-F3 while pUCP-F3 produces AmpC-F4. * Both of purified AmpC-F3 (A) and AmpC-F4 (B) were used as positive controls. No difference was observed for production of AmpC-F3 and AmpC-F4 in non-induced* ***(NI)*** *and induced fractions* ***(I)****.* ***P*** *stands for precursor form while* ***M*** *stands for the mature form.*

Table 4.3. β-lactamase activity of some PAO1 mutants transformed with pUCP-F3 and pUCP-F4.

Strain	Plasmid	IPTG (mM)	Sp. Act.[a] µmole /min/mg
PAOΔ*dacB*Δ*pbpG*Δ*ampC*	pUCP-F4	0	673.3
		1	555.6
PAOΔ*dacB*Δ*dacC*Δ*ampC*	pUCP-F4	0	686.8
		1	521.8
PAOΔ*dacB*Δ*dacC*Δ*pbpG*Δ*ampC*	pUCP-F4	0	568.5
		1	518.7
PAOΔ*ampC*	pUCP-F4	0	591.5
		1	526.6
PAOΔ*dacB*Δ*pbpG*Δ*ampC*	pUCP-F3	0	27.2
		1	28.2
PAOΔ*dacB*Δ*dacC*Δ*ampC*	pUCP-F3	0	19.1
		1	19.2
PAOΔ*dacB*Δ*dacC*Δ*pbpG*Δ*ampC*	pUCP-F3	0	27.4
		1	26.5
PAOΔ*ampC*	pUCP-F3	0	38.9
		1	40.4

[a] *β-lactamase specific activities (Sp. Act.) of AmpC-F4 and AmpC-F3 on nitrocefin were detected in cellular fractions (total sonicate) and expressed in µmole/min/mg. Production of AmpC-F4 and AmpC-F3 forms by pUCP-F4 and pUCP-F3 respectively in different transformants of mutants of P. aeruginosa PAO1 was done under non-induction and induction conditions with 1 mM IPTG for 3 h at 37 °C.*

4.1.4. Pae-AmpC purification and characterization

Purification of AmpC-F4, AmpC-F4:C3, AmpC-F4:C6, AmpC-F2, AmpC-F3 (with His tag) and AmpC-F3-TEV (without His-tag; symbol: ΔHis) from transformants of Bl21(DE3) was previously described in section 3.6. The final purified batches of AmpC-F4, AmpC-F2, AmpC-F4:C3 and AmpC-F4:C6 were resuspended in buffer 20 mM Tris-HCl, 0.2% Triton X-100, 100 mM NaCl, pH 7.5 or buffer 20 mM Tris-HCl, 300 mM NaCl, 0.15% sarkosyl, pH 7.5. While, AmpC-F3 (with poly-His tag, symbol: +His) and AmpC-F3-TEV (+His) were solubilized in buffer 20 mM Tris HCl (pH 7.5), and AmpC-F3-TEV (ΔHis) in 20 mM Tris-HCl, 100 mM NaCl, pH 7.5. These final purification batches were analyzed by SDS-PAGE and western blot, which displayed that all of AmpC-F4, AmpC-F4:C3 and AmpC-F4:C6 have two bands where the upper corresponds to the precursor form (large amount) and the lower corresponds to the mature form (lower amount); AmpC-F2 has mostly one band of the precursor form; AmpC-F3 and AmpC-F3-TEV (+His) have one band of the mature form; the band of AmpC-F3-TEV (ΔHis) was not detected by western blot which confirmed the elimination of poly-His tag from AmpC-F3-TEV (+His) upon TEV protease treatment (fig. 4.7).

The purified Pae-AmpC forms were characterized by identification of their molecular masses, theoretical isoelectrical points, K_m and V_{max} in vitro assays as described in section 3.5.4. We found that the mature form AmpC-F3 had the highest activity (V_{max} = 100 µmol/min/mg) on nitrocefin while AmpC-F4, AmpC-F2, AmpC-F4:C3 and AmpC-F4:C6 had V_{max} values 12.5, 5, 2.5 and 2.5 µmol/min/mg, respectively. AmpC-F3, AmpC-F4, AmpC-F2, AmpC-F4:C3 and AmpC-F4:C6 displayed K_m values 10, 11.3, 10.5, 13.5 and 16.8 µM, respectively (table 4.4).

4.1.5. Pae-AmpC structure and crystallization

As shown in figure 4.1, AmpC-F4 (and AmpC-F4-TEV), AmpC-F4:C3 and AmpC-F4:C6 have the same amino acid sequence of AmpC-F1 (Wild type), AmpC-F1:C3 and AmpC-F1:C6, respectively, but with two extra-amino acids (M A) at the N-terminal at the beginning of their amino acid sequence. AmpC-F2, AmpC-F1:C3 (also AmpC-F4:C3 and AmpC-F3:C3-TEV) and AmpC-F1:C6 (also AmpC-F4:C6 and AmpC-F3:C6-TEV) have single amino acid mutations R^{2}→G, P^{243}→L and I^{51}→T respectively. AmpC-F3, AmpC-F3-TEV, AmpC-F3:C3-TEV and AmpC-F3:C6-TEV are soluble forms of AmpC without signal peptides. AmpC-F1, AmpC-F1:C3, AmpC-F1:C6, AmpC-F4, AmpC-F4-TEV, AmpC-F4:C3, AmpC-F4:C6 and AmpC-F2 are periplasmic forms having signal peptide of AmpC which involves the first 26 amino acids up to A^{26}. All produced AmpC forms have poly-His tag at their C-terminal which can be eliminated from those forms that have TEV site by the activity of TEV protease (fig. 4.1). All the produced AmpC

forms except those having TEV site have extra amino acids **(N^{398} S S S V D K L A A A L E H H H H H H^{416})** at their C-terminal which are due to the multiple cloning sites and hexa-His tag from pET28b. Also, AmpC forms that have TEV site, have C-terminal extra amino acids **(E^{398} N L Y F Q G N S S S V D K L A A A L E H H H H H H^{423})** due to the TEV site (underlined), multiple cloning sites and hexa-His tag from pET28b; TEV protease cleaves between the two amino acids Gln (Q) and Gly (G). These amino acid sequences deduced from the sequenced clones and MALDI-TOF analysis correlate perfectly with the expression patterns shown above.

The 3-D structure of AmpC β-lactamase from *P. aeruginosa* (Smith et al, 2013) was solved by X-ray crystallography and is discussed later in section 5.2. Because AmpC-F3 showed a secondary DD-peptidase activity (section 4.1.8), both AmpC-F3 forms (with and without His-tag) were purified and sent for crystallographic analysis to obtain the 3-D structure but unfortunately it has not been achieved any AmpC-F3 crystals by the time of submission of this study.

Table 4.4. Characterization of the purified Pae-AmpC forms.

Purified AmpC	V_{max}	K_m (µM)	M.M. (kDa)	pI
AmpC-F4	12.5	11.3	45.7	8.3
AmpC-F4:C3	2.5	13.5	45.7	8.3
AmpC-F4:C6	2.5	16.8	45.7	8.3
AmpC-F2	5	10.5	45.4	7.8
AmpC-F3	**100**	10	43	7.9

V_{max} is the maximum activity on substrate (nitrocefin) expressed in µmol/min/mg. K_m is the substrate concentration (nitrocefin) producing half of maximum activity. V_{max} and K_m were calculated from the β-lactamase activity of different forms of Pae-AmpC on nitrocefin.
Both of V_{max} and K_m were calculated as described in section 3.5.4. M.M.: molecular mass; pI: theoretical isoelectric point (online ExPASy tools). AmpC-F3 displayed a very high activity as shown in bold for its V_{max} value.

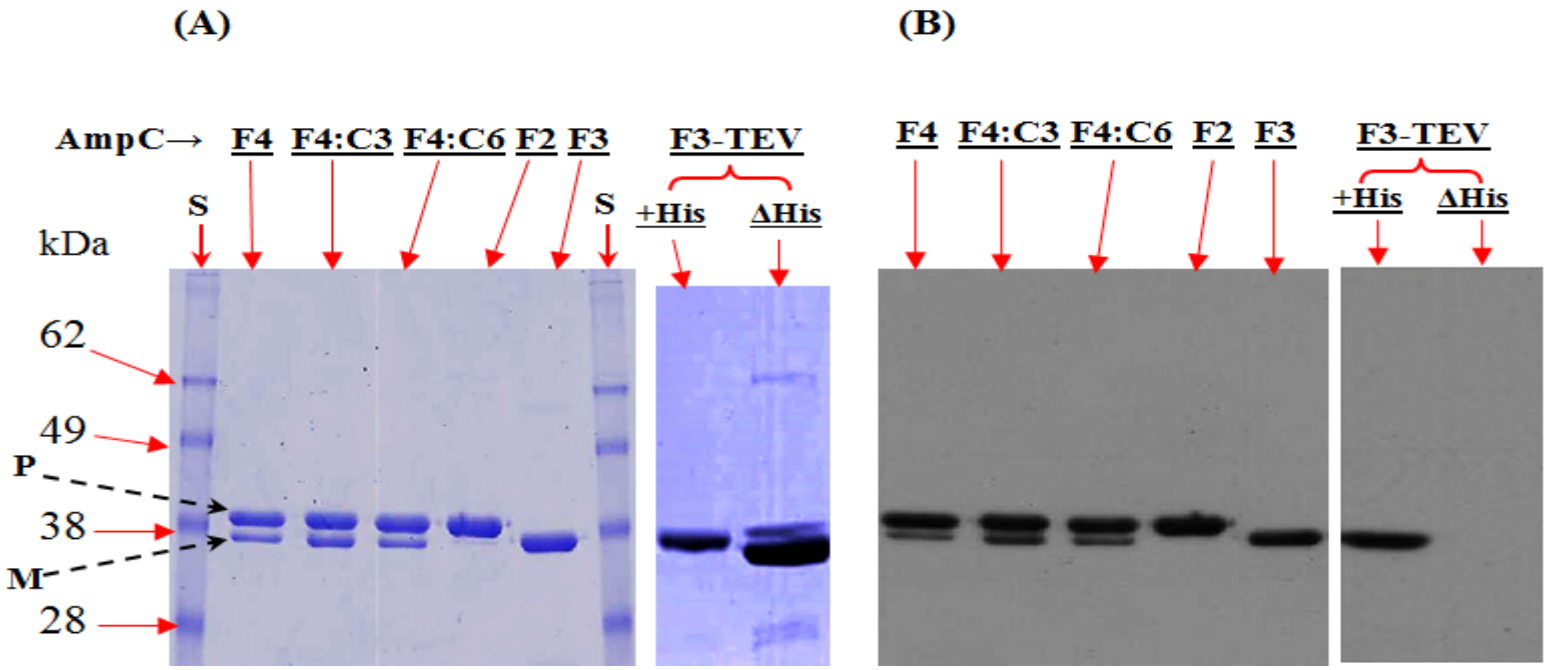

Figure 4.7. Analysis of the purified Pae-AmpC forms by SDS-PAGE and western blot.

*Purified AmpC-F4, AmpC-F4:C3, AmpC-F4:C6, AmpC-F2, AmpC-F3 (with poly-His tag), AmpC-F3-TEV (with poly-His tag; symbol: **+His**) and AmpC-F3-TEV (without poly-His tag; symbol: **ΔHis**) were analyzed by SDS-PAGE (A) and western blot (B); where the Purified AmpC-F4, AmpC-F4:C3 and AmpC-F4:C6 displayed two bands corresponding to precursor (upper band; **P**) and mature (lower band; **M**) forms; AmpC-F2 displayed mostly the precursor form while AmpC-F3 and AmpC-F3-TEV displayed only the mature form. In western blot (B), Band of AmpC-F3 (**ΔHis**) disappeared confirming the loss of poly-His tag. The final preparations of AmpC-F4, AmpC-F2, AmpC-F4:C3 and AmpC-F4:C6 were in buffer 20 mM tris-HCl, 0.2% Triton X-100, 100 mM NaCl, pH7.5 while AmpC-F3 (with poly-His tag) and AmpC-F3-TEV (**+His**) were in buffer 20 mM Tris HCl, pH 7.5 and AmpC-F3-TEV (**ΔHis**) was in 20 mM tris-HCl, 100 mM NaCl, pH7.5. **S**: standard protein molecular mass markers. Black arrows (dashed) refer to bands of precursor (P) and mature forms (M) of AmpC forms.*

4.1.6. Effect of Pae-*ampC* expression on bacterial resistance

Pae-ampC expression and bacterial resistance in E. coli Bl21(DE3)

Disk diffusion assay showed that β-lactamase activities of AmpC forms were variable in Bl21(DE3)/pET28-*ampC* using 0.05 mM IPTG-MHA plates. We found that among the tested AmpC forms, AmpC-F4 was the most active on nitrocefin in total cell extract assay; but strain Bl21(DE3)/pET-F4 showed resistance to amoxacillin/clavulanic acid (AMC) and decreased susceptibilities to cefoxitin (FOX), ceftriaxone (CRO), imipenem (IMI) and ticarcillin (TIC). Bl21(DE3)/pET-F2 showed resistance to AMC and also decreased susceptibilities to cefoxitin (FOX), ceftriaxone (CRO), aztreonam (ATM) and ticarcillin (TIC), while AmpC-F4:C3 and F4:C6 showed very low β-lactamase activities as they only decreased susceptibility to AMC in strains Bl21(DE3)/pET-F4:C3 and Bl21(DE3)/pET-F4:C6. AmpC-F3 did not change the resistance susceptibilities to the used β-lactams even AMC (table 4.5). Also, we found that some clear inhibition zones (Symbol: CZ) were surrounded by a partial growth zone (Symbol: PZ) or had some resistant colonies (symbol: CR) growing inside it (table 4.5, 4.6).

Pae-ampC expression and bacterial resistance in some Pae mutants

Complementation of *ampC* deletion was studied by disk diffusion assay in some Pae mutants, PAOΔ*ampC,* PAOΔ*dacB*Δ*pbpG*Δ*ampC,* PAOΔ*dacB*Δ*dacC*Δ*ampC* and PAOΔ*dacB*Δ*dacC*Δ*pbpG*Δ*ampC* (table 4.6). MHA plates were used without IPTG additions for disk diffusion because data of AmpC production from Pae transformants of pUCP24-F3 and pUCP24-F4 showed that there was no big difference in the levels of AmpC using IPTG induction conditions and normal basal conditions (fig. 4.6). In this assay, the same Pae mutants transformed with pUCP24 were used as a negative control for β-lactamase level. Basal level of AmpC-F4 expressed by pUCP-F4 showed resistance to AMC, CRO and TIC, and decreased susceptibilities to ATM and IMI in all tested mutants. In the other hand, basal level of AmpC-F3 showed little change and deceased susceptibilities to AMC in all Pae mutants, and only to CRO and TIC in the four deletions Pae mutant (table 4.6).

Table 4.5. Disc diffusion assay for Pae-AmpC expression in Bl21(DE3)/pET-*ampC*.

BL21 (DE3)/ pET-*ampC* [b]	IPTG (mM)[c]	Diameter of inhibition zone (mm)[a]							
		AMC	ATM	IMI	C	FOX	CRO	TIC	AN
pET-F4	**0**	**17**	**34**	**27**	**33**	**22**	**28**	**27**	**26**
	0.05	0	34	24	35	18	20	25	27
pET-F4:C3	**0**	**22**	**32**	**31**	**38**	**23**	**33**	**30**	**28**
	0.05	14(CZ), 27(PZ)	33	31	38	23	30	29	28
pET-F4:C6	**0**	**24**	**38**	**31**	**34**	**28**	**36**	**31**	**28**
	0.05	18(CZ), 23(PZ)	38	31	34	28	36	31	28
pET-F2	**0**	**14**	**33**	**26**	**32**	**24**	**28**	**29**	**26**
	0.05	0 (CZ), 19(PZ)	31(CZ), 38(PZ)	28	34	17(CZ), 22(PZ)	18(CZ), 27(PZ)	18(CZ), 29(PZ)	28
pET-F3	**0**	**24**	**35**	**30**	**33**	**25**	**32**	**29**	**26**
	0.05	23	38	30	35	25	32	33	29

[a] Amoxacillin/clavulanic acid (AMC), aztreonam (ATM), imipenem (IMI), chloramphenicol (C), cefoxitin (FOX), ceftriaxone (CRO), ticarcillin (TIC) and amikacin (AN). CZ: clear inhibition zone; PZ: partial growth zone occurred around the clear inhibition zone; all values that are not marked by CZ or PZ are considered CZ. [b] E. coli Bl21(DE3) harboring pET-F4, pET-F2, pET-F3, pET-F4:C3 and pET-F4:C6 produce AmpC-F4, AmpC-F2, AmpC-F3, AmpC-F4:C3 and AmpC-F4:C6, respectively. [c] The assay was done using MHA plates without IPTG (non-induction conditions; values shown in bold) and with 0.05 mM IPTG (induction conditions) for 16 hours.

Table 4.6. Disc diffusion assay for complementation of *ampC* deletion in some PAO1 mutants.

Transformant Pae Strain[b]	Diameter of inhibition zone (mm)[a]									
	FOX		AMC		ATM	CRO		TIC		IMI
	CZ	PZ	CZ	PZ	CZ	CZ	PZ	CZ	PZ	CZ
PAOΔ*ampC*/ pUCP24*	**0**	**10**	**21**	**23**	**22**	**17**	**24**	**12**	**18**	**36**
PAOΔ*ampC*/ pUCP24-F4	0	-	0	-	15	0	-	0	-	26
PAOΔ*ampC*/ pUCP24-F3	0	-	17 CR	-	26	21 CR	-	2	-	37
PAOΔ*dacB*Δ*pbpG*Δ*ampC*/ pUCP24*	**0**	**12**	**22**	**26**	**25**	**19**	**26**	**19**	**29**	**36**
PAOΔ*dacB*Δ*pbpG*Δ*ampC*/ pUCP24-F4	0	-	0	-	13	0	-	0	-	25
PAOΔ*dacB*Δ*pbpG*Δ*ampC*/ pUCP24-F3	0	-	17 CR	-	26	1.8 CR	-	17 CR	-	36
PAOΔ*dacB*Δ*dacC*Δ*ampC*/ pUCP24*	**0**	**10**	**22**	**-**	**27**	**22**	**-**	**20**	**-**	**37**
PAOΔ*dacB*Δ*dacC*Δ*ampC*/ pUCP24-F4	0	-	0	-	18	0	-	0	-	28
PAOΔ*dacB*Δ*dacC*Δ*ampC*/ pUCP24-F3	0	-	18 CR	-	27	20	-	21	-	38
PAOΔ*dacB*Δ*dacC*Δ*pbpG*Δ*ampC*/ pUCP24*	**0**	**10**	**20**	**23**	**25**	**22**	**-**	**20**	**-**	**36**
PAOΔ*dacB*Δ*dacC*Δ*pbpG*Δ*ampC*/ pUCP24-F4	0	-	0	-	14	0	-	0	-	22
PAOΔ*dacB*Δ*dacC*Δ*pbpG*Δ*ampC*/ pUCP24-F3	0	-	15 CR	-	24	10	-	14	23	35

*[a] Cefoxitin (FOX), ceftriaxone (CRO), imipenem (IMI), aztreonam (ATM), amoxacillin/clavulanic acid (AMC), and ticarcillin (TIC). **CZ**: clear inhibition zone; **PZ**: partial growth zone occurred around the clear inhibition zone; **CR**: resistant colonies appeared in the clear inhibition zone. The assay was done using MHA plates without IPTG for 16 hours. [b] Transformants of pUCP-F3 and pUCP-F4 produce AmpC-F3 and AmpC-F4, respectively. * Pae mutants transformed with pUCP24 vector used as a negative control for AmpC production whose data are shown in bold values.*

4.1.7. Effect of *Pae-ampC* expression on PG composition (in vivo)

HPLC analysis of muropeptides and PG structure

HPLC analysis of muropeptides prepared by digestion of PG described in section 3.12 is important information because it gives us an image about PG structure and its main constituents (muropeptides) as shown in figure 4.8. Muropeptides can be classified according to their structures into monomers (e.g. M2, M3, M4 and M5), Dimers (e.g. D43, D44 and D45), Trimers (e.g. T443, T444 and T445), anhydro-muropeptides (e.g. M4N, D44N and T44N), lipo-muropeptides, having a link to Braun's lipoprotein (e.g. M3L), and Dap-Dap (D-D) muropeptides, having a LD type crosslink between the Dap of adjacent glycan chains (e.g. D34D). Chromatograms of HPLC analysis of PG from the wild type *E. coli* Bl21(DE3) showed that PG is composed mainly of monomers muropeptides (M3, M4G, M4, M2, M5, M3L), dimers muropeptides (D33D, D34D, D43, D44, D45), trimers muropeptides (T443, T444), and anhydromuropeptides (D44N and T444N); while PG of *E. coli* DV900(DE3) is composed of monomers muropeptides (M3, M4, M5G, M2, M5, M3L), dimers muropeptides (D34D, D43, D44, D45G, D45), trimers muropeptides (T443, T445), and anhydromuropeptides (D45N and T445N). Muropeptides M4N, M5N, D43N, D44N, D45N, T443N, T444N, T445N have the same structures of M4, M5, D43, D44, D45, T443, T444, T445, respectively, but with anhydro-N-acetylmuramic acid instead of N-acetylmuramic acid (fig. 4.8). PG analysis of the wild type *E. coli* CS109 and the wild type *P. aeruginosa* PAO1 displayed a similar HPLC chromatograms like the wild type *E. coli* Bl21(DE3) while the constructed PAO1 mutants PAOΔ*dacB*Δ*dacC*Δ*pbpG* and PAOΔ*dacB*Δ*dacC*Δ*pbpG*Δ*ampC* displayed a similar HPLC chromatograms like *E. coli* mutant DV900(DE3) (not shown).

Pae-ampC expression and PG composition in E. coli Bl21(DE3) and DV900(DE3) in vivo

E. coli Bl21(DE3) and DV900(DE3) transformants of pET-F4, pET-F4:C3, pET-F4:C6, pET-F2 and pET-F3 were grown in LB media +/- IPTG at 37°C with agitation; then PG was prepared at the exponential phase and analyzed by HPLC. No big differences were found in all transformants under no-induction, indicating no major effect of the presence of the different plasmids in any of the two reference strains. In Bl21(DE3)/pET-F4, Bl21(DE3)/pET-F4:C3 and Bl21(DE3)/pET-F4:C6, we found that under IPTG induction conditions, PG analysis of transformants showed that there was an increase in monomers, anhydro-muropeptides and pentapeptides and a decrease dimers and trimers beside low crosslinking degree and lower cell length, but actually small changes in Bl21(DE3)/pET-F2 and Bl21(DE3)/pET-F3 (table 4.7).

As modifications in PG reflect a global structural change, these data may indicate, not a direct and specific activity of the produced proteins on the metabolism of PG, but most probably an effect of the overproduction, or IPTG induction itself. PG analysis of IPTG-induced DV900(DE3)/pET-F4, DV900(DE3)/pET-F4:C3 and DV900(DE3)/pET-F4:C6 transformants displayed only small increases in anhydro-muropeptides and crosslinking, and also small decrease in cell length, while no significant change on pentapeptides was encountered (table 4.8). And, again no differences were found in DV900(DE3)/pET-F2 or DV900(DE3)/pET-F3 under induction conditions. These changes do not suggest any enzymatic activity for Pae-AmpC on PG of this heterologous strain.

Pae-ampC expression and PG composition in PAO1 in vivo

Transformants of PAOΔ*ampC*, *PAO*Δ*dacB*Δ*dacC* Δ*ampC*, *PAO*Δ*dacB*Δ*pbpG*Δ*ampC* and *PAO*Δ*dacB*Δ*dacC*Δ*pbpG*Δ*ampC* harboring pUCP24, pUCP-F3 and pUCP-F4 were grown in LB media without IPTG addition at 37°C with agitation where pUCP24 transformants were used as a negative control for AmpC production, while transformants of pUCP-F3 and pUCP-F4 were used for expression of ampC-F3 and ampC-F4, respectively. For the control strains (plasmid pUCP24), there was no changes in PG structure, is spite of those changes already seen in the PG of the parental mutants strains. HPLC analysis of PG of these transformants shows that there was some increase in crosslinking and anhydro-muropeptides and a slight decrease in cell length compared with the control strains (table 4.9). Also, these data indicate no major effect of Pae-AmpC-F3 and Pae-AmpC-F4 on the whole PG structure of Pae, in spite of the large β-lactamase activity displayed by Pae-AmpC-F4 (table 4.3) on these strains, and the low expression level of these proteins (fig. 4.6).

4.1.8. Effect of the purified Pae-AmpC forms on PG composition and individual muropeptides (in vitro)

Effect of Pae-AmpC on whole PG composition (in vitro)

In vitro activity of purified AmpC forms on PG of *E. coli* CS109 and DV900 was followed. We found that incubation of (0.4-2 µg/µl) AmpC-F4, AmpC-2, AmpC-F3, AmpC-F4:C3 and AmpC-F4:C6 with the whole PG of each of CS109 and DV900 at 37°C for up to 24 hours (as described in section 3.12.3) produced no significant structural change while extending incubation

(42 h) time at 37°C produced some interesting changes in PG composition especially with AmpC-F3; indicating that AmpC may has a secondary DD-peptidase activity (table 4.10a).

In case of incubation with PG of the wild type ***E. coli* CS109** for 42 hours there was a decrease in anhydro-muropeptides, correlated with the decrease in crosslinking and produced an increase in monomers and a decrease in dimers and trimers only with AmpC-F3(b) (three month old purified sample) (table 4.10a). Moreover, analysis of individual muropeptides revealed there were a decrease in D44 and an increase in M4 beside the decrease in the crosslinking degree which indicates that there was some DD-EPase activity (table 4.10a).

In case of incubation of different AmpC forms with PG of **DV900** for 42 hours, there was also an increase in monomers and decrease in dimers and trimers only with AmpC-F3 (table 4.10a). Again, analysis of individual muropeptides after treatment with AmpC-F3 of PG of DV900 shows a large increase in M4 and D44 and a decrease in M5, D45, T445, D45N and T445N (table 4.10b). This indicates that AmpC-F3 acted as DD-CPase and DD-EPase on the whole PG of *E. coli* DV900. The fact that in the old preparation of AmpC-F3 the decrease of M5 is higher and the decrease of D45 is smaller, and the increase of M4 and D44 are smaller, compared with the fresh preparation of AmpC-F3, indicates that freezing may favor the DD-EPase activity of the sample.

Effect of Pae-AmpC on individual purified muropeptides (in vitro)

Trying to reinforce or confirm data on isolated whole PG in vitro described in the previous paragraph, we performed analysis with individual purified muropeptides. The reaction involved incubation of (0.4-2 µg/µl) AmpC-F4, AmpC-2, AmpC-F3, AmpC-F4:C3 and AmpC-F4:C6 with each of the individual purified muropeptides (M4, M5, D44 and D45) within different conditions [temperature (37 and 42°C) and +/- 50 mM NaCl addition, various AmpC concentrations] and was continued as described in section 3.12.3. The results showed that a concentration of up to 2 µg/µl of AmpC-F4, AmpC-F2, AmpC-F4:C3 and AmpC-F4:C6 had no activity on the muropeptides; while 0.4 µg/µl AmpC-F3 (b) [three-month old purified AmpC-F3] displayed DD-EPase activity on D44 (5 ng/µl) and D45 (10 ng/µl) at 42°C for 24 hours however there was no activity on M4 (4ng/µl) and M5 (16 ng/µl), (fig. 4.9 and 4.10). Newly purified AmpC-F3(a) (fig. 4.10) was less active than the three-month old purified AmpC-F3(b) which also showed some protein degradation (fig. 4.9). These data confirm the DD-EPase activity of AmpC-F3 on isolated muropeptides, but it was not detected DD-CPase activity on the purified monomers muropeptide. As this last activity was clearly seen on whole isolated PG of DV900, it may indicate that particular conformations of the muropeptides on the whole structure are required for bringing out that activity.

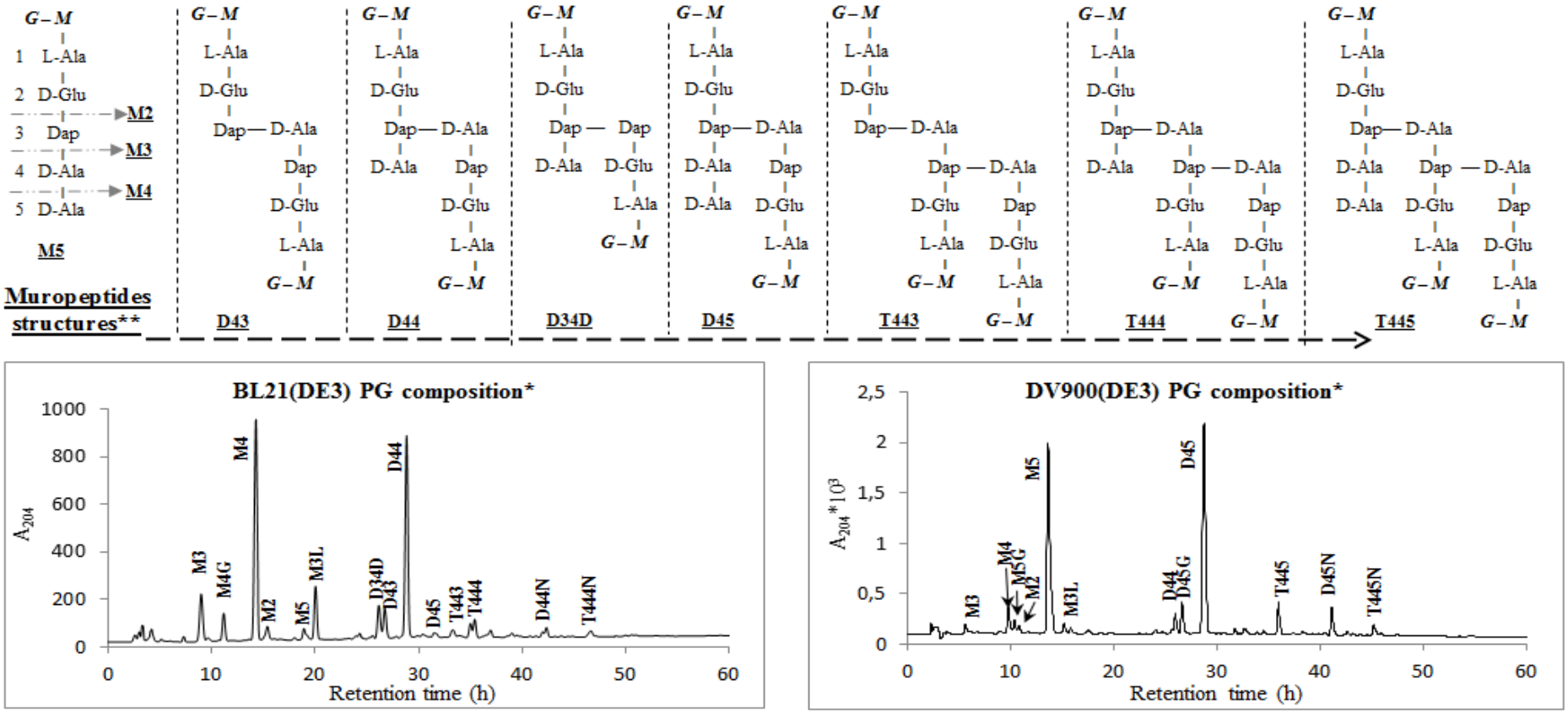

Figure 4.8. Muropeptides structures and chromatograms of HPLC analysis of PG of *E. coli* Bl21(DE3) and DV900(DE3).

** Chromatograms of HPLC analysis (lower panel) of PG from E. coli Bl21(DE3) showed that PG is composed of muropeptides M3, M4G, M4, M2, M5, M3L, D34D, D43, D44, D45, T443, T444, D44N and T444N while PG of E. coli DV900(DE3) is composed of muropeptides M3, M4, M5G, M2, M5, M3L, D34D, D43, D44, D45G, D45, T445, D45N and T445N. ** In the upper panel, there are chemical structures of common*

muropeptides in PG of E. coli and P. aeruginosa; where, ***G:*** *N-acetylglucosamine;* ***M:*** *N-acetylmuramic Acid;* ***M2:*** *disaccharide dipeptide* ***M3:*** *disaccharide tripeptide;* ***M4:*** *disaccharide tetrapeptide;* ***M4G:*** *disaccharide tetrapeptide with Gly at position number 4 (not shown);* ***M5:*** *disaccharide pentapeptide where L-Ala, D-Glu, Dap, D-Ala and D-Ala occupy positions of numbers 1, 2, 3, 4 and 5, respectively, also L-Ala is linked to N-acetylmuramic acid ;* ***M5G:*** *disaccharide pentapeptide with Gly at position number 5 (not shown);* ***M3L:*** *disaccharide tripeptide bound to Braun's lipoprotein (not shown);* ***D44:*** *crosslinked-dimer of disaccharide tetrapeptide-disaccharide tetrapeptide;* ***D34D:*** *Dap-Dap crosslinked-dimer of disaccharide tripeptide-disaccharide tetrapeptide;* ***D43:*** *crosslinked-dimer of disaccharide tetrapeptide-disaccharide tripeptide;* ***D45:*** *cross-linked-dimer of disaccharide tetrapeptide-disaccharide pentapeptide;* ***T443:*** *crosslinked-trimer of disaccharide tetrapeptide-disaccharide tetrapeptide-disaccharide tripeptide;* ***T444:*** *crosslinked-trimer of disaccharide tetrapeptide-disaccharide tetrapeptide-disaccharide tetrapeptide;* ***T445:*** *crosslinked-trimer of disaccharide tetrapeptide-disaccharide tetrapeptide-disaccharide pentapeptide;* ***anhydro-muropeptides*** *M4N, M5N, D43N, D44N, D45N, T443N, T444N, T445N have the same structures of muropeptides M4, M5, D43, D44, D45, T443, T444, T445, respectively, but with anhydro-N-acetylmuramic acid instead of N-acetylmuramic Acid (not shown for simplification).*

Table 4.7. HPLC analysis of muropeptides prepared from PG of induced *E. coli* Bl21 (DE3)/pET-*ampC*.

BL21(DE3)/pET-*ampC*[b]	IPTG	Muropeptides (% Molar)[a]							Crosslink	D-D/T	Length
		Mono	Di	Tri	D-D	Lpp	Anhy	Penta			
pET-F4	0	64.62	33.16	2.22	5.63	12.43	1.94	0.51	37.6	14.96	51.55
	0.1	**73.72**	**25.8**	**0.48**	7.01	18.22	**5.25**	**8.3**	**26.76**	26.18	**19.06**
pET-F4:C3	0	66.22	31.69	2.09	5.07	11.96	2.13	0.76	35.86	14.15	46.88
	0.1	**71.32**	**27.99**	**0.69**	9.71	15.39	**5.71**	**6.31**	29.37	33.07	**17.3**
pET-F4:C6	0	66.07	32.76	1.17	8.69	6.83	2.16	0.75	35.1	24.75	46.75
	0.1	**83.53**	**15.75**	**0.71**	3.23	24.87	**5.88**	**3.57**	**17.18**	18.79	**17.02**
pET-F2	0	61.93	35.61	2.46	8.91	12.7	3.38	0.92	40.52	21.98	29.62
	0.1	62.05	36.19	1.76	8.13	8.75	**4.6**	1.6	39.71	20.46	21.74
pET-F3	0	63.37	33.79	2.85	5.9	9.16	3.08	0.92	39.48	14.93	32.46
	1	61	36.32	2.68	7.83	6.95	3.5	1.31	41.68	18.78	28.78

[a] *Relative abundance in % molar of different types of muropeptides; Mono: monomeric muropeptides (e.g. M4, M5); Di: dimeric muropeptides (e.g. D43, D44, D45); Tri: trimeric muropeptides (e.g. T444 and T445); Lpp: Muropeptides bound to Braun's Lipoproteins (e.g. M3L); Anhy: anhydromuropeptides (e.g. D44N, T444N); Crosslink: degree of crosslinking in percentage; D-D: total muropeptides that have Dap-Dap cross-linking (e.g. D34D); D-D/T: ratio of Dap-Dap crosslinking to the total crosslinking. length: measurement for PG length. PG was prepared as described in section 3.12.* [b] *E. coli Bl21(DE3) transformed with pET-F4, pET-F4:C3, pET-F4:C6, pET-F2 and pET-F3 which were induced with 0.1 or 1 mM IPTG as indicated in the table. Relevant changes in PG composition are shown in bold.*

Table 4.8. HPLC analysis of muropeptides prepared from PG of induced *E. coli* DV900 (DE3)/pET-*ampC*.

DV900(DE3)/pET-*ampC*[b]	IPTG (mM)	Muropeptides (% Molar)[a]									
		Mono	Di	Tri	D-D	Lipo	Anhy	Penta	crosslink	D-D/T	Length
pET-F4	0	59.6	35.2	2.7	1.1	1.2	5.1	71	40.7	2.6	19.6
	0.1	57	37.4	3.3	1.3	1.5	**8.2**	71	44.1	2.9	**12.2**
pET-F4:C3	0	63.5	32.8	2.1	0.9	1	4.1	75.7	36.9	2.3	24.3
	0.1	60.4	36.6	1.2	0.9	0.8	**7.1**	**76.4**	39	2.3	**14**
pET-F4:C6	0	67.8	28.7	1.9	0.7	1.6	3.9	76.7	32.4	2.2	25.9
	0.1	64.6	32	1.9	0.7	1.5	**7.9**	77	35.8	1.9	**12.7**
pET-F2	0	58.8	36.2	2.8	1.2	3.3	5.5	69.1	41.7	2.9	18.3
	0.1	58.1	37.4	2.5	1.1	2.1	**6.9**	73.7	42.4	2.5	14.5
pET-F3	0	60.6	35.4	2	0.7	1	4.8	76.2	39.5	1.7	20.7
	1	59.3	36.5	2	1	0.6	4.6	81.1	40.6	2.4	21.9

[a] As described previously within table 4.7. Induced (0.1 or 1 mM IPTG) and non-induced cells were collected. [b] DV900(DE3) transformed with pET-F4, pET-F4:C3, pET-F4:C6, pET-F2 and pET-F3.

Table 4.9. HPLC analysis of muropeptides prepared from PG of PAO1/pUCP24-*ampC*.

PAO1 Mutant[b]	Harboring Plasmid	Muropeptides (% Molar)[a]							Crosslink	D-D/T	Length
		Mono	Di	Tri	D-D	Lpp	Anhy	Penta			
PAOΔ*ampC*	**pUCP24**	62.6	34.2	3.2	1.4	1.4	9.6	2.6	40.6	3.5	10.4
PAOΔ*ampC*	pUCP24-F4	59.8	36.4	3.7	1.6	1.3	**11**	2.1	**43.9**	3.6	9.1
PAOΔ*ampC*	pUCP24-F3	57.4	38.3	4.3	2.2	1.9	**11.7**	2	**46.8**	4.6	**8.5**
PAOΔ*dacB*Δ*dacC* Δ*ampC*	**pUCP24**	58.8	36.3	4.9	2.2	3.6	12.4	31	46.1	4.7	8.1
PAOΔ*dacB*Δ*dacC* Δ*ampC*	pUCP24-F4	57.8	38	4.2	1.3	1.8	11.8	28.9	46.4	2.9	8.5
PAOΔ*dacB*Δ*dacC* Δ*ampC*	pUCP24-F3	56.8	38.5	4.8	1.5	2.6	12.4	34	48	3.1	8.1
PAOΔ*dacB*Δ *pbpG* Δ*ampC*	**pUCP24**	54.5	39.9	5.6	2.3	3.6	11.8	5.4	51.2	4.5	8.5
PAOΔ*dacB*Δ *pbpG* Δ*ampC*	pUCP24-F4	49.7	43.2	7.1	2.4	3.1	**13.5**	3.5	**57.4**	4.1	**7.4**
PAOΔ*dacB*Δ *pbpG* Δ*ampC*	pUCP24-F3	48.5	44	7.4	2.6	3.6	**13.6**	3.6	**58.9**	4.5	**7.4**
PAOΔ*dacB*Δ*dacC pbpG* Δ*ampC*	**pUCP24**	54.2	40.2	5.6	0.8	1.9	9.9	66.9	51.5	1.5	10.1
PAOΔ*dacB*Δ*dacC pbpG* Δ*ampC*	pUCP24-F4	51.4	42.2	6.5	0.8	2.2	**11.5**	69.1	**55.1**	1.4	**8.7**
PAOΔ*dacB*Δ*dacC pbpG* Δ*ampC*	pUCP24-F3	52.1	41.7	6.2	1	2.2	10.3	68.6	**54.1**	1.8	9.7

[a] As described previously within table 4.7. [b] Different PAO1 mutants transformed with pUCP24, pUCP-F4 and pUCP-F3 vectors where transformants of pUCP24 vector were used as a control negative for AmpC production. The vectors pUCP-F3 and pUCP-F4 encode ampC-F3 and ampC-F4, respectively.

Table 4.10a. HPLC PG analysis of *E. coli* DV900 and CS109 after incubation with different forms of Pae-AmpC in vitro.

Reaction with CS109 PG[b]	T (°C)	Time (h)	Muropeptides (% Molar)[a]										crosslink	D-D/T	Length
			Mono	Di	Tri	Gly	D-D	Lpp	Anhy	Penta	M4*	D44*			
DV900-CTRL	37	42	60	35.9	4.1	5.3	0.9	1.5	4	85	3.3	4	44.1	1.9	25.11
AmpC-F4	37	42	59.5	36.2	4.3	5.6	0.9	0.9	4.1	85	3.4	4.1	44.8	2.1	24.5
AmpC-F4:C3	37	42	60	36	4.1	5.6	0.9	0.7	3.9	85.3	3.5	3.9	44.1	2	25.9
AmpC-F4:C6	37	42	60.4	35.8	3.8	5.5	0.9	1.1	3.7	85.2	3.4	3.8	43.4	2	26.9
AmpC-F2	37	42	59.5	36.6	4	5.6	0.6	0.7	3.8	86.4	3	4.3	44.5	1.5	26.5
AmpC-F3(a)	37	42	**61.7**	35.3	3.1	5.2	0.7	1.3	2.8	**67.8**	**13.5**	**5.3**	41.4	1.8	35.3
AmpC-F3(b)	37	42	**68.6**	**28.8**	**2.5**	5	0.8	1	**1.3**	**67.1**	**15.4**	**5.9**	33.9	2.4	74.2
CS109-CTRL	*37*	***42***	*60.3*	*37*	*2.7*	*7.7*	*4.4*	*16.6*	*5.5*	*0*	*22.1*	*18.5*	*42.4*	*10.3*	*18.3*
AmpC-F3(a)	*37*	***42***	***61.1***	*36.5*	*2.4*	*6.3*	***4.3***	*15.8*	*5.3*	*0*	*23.2*	*18.9*	*41.4*	*10.5*	*18.7*
AmpC-F3(b)	*37*	***42***	***71***	***27.9***	***1.1***	*6.9*	***3.5***	*14.9*	***3.1***	*0*	***31***	***15.5***	***30.1***	*11.6*	***32.7***

*[a] As described previously within table 4.7. [b] In vitro reactions (250 µl) contained AmpC-F4 (2 µg/µl), AmpC-F2 (2 µg /µl), AmpC-F4:C3 (2 µg /µl), AmpC-F4:C6 (2 µg /µl) or AmpC-F3 (0.4 µg /µl) with whole PG of and E. coli DV900 and E. coli CS109 (italic writing, the last three rows) were left at 37°C for 42 h, and then were manipulated as described in section 3.12.3; where DV900-CTRL: control negative without AmpC treatment; CS109-CTRL: negative control without AmpC addition; AmpC-F3(a) is a newly purified AmpC-F3 while AmpC-F3(b) is a purified AmpC-F3 stored for 3 months (or more) at -20 °C. *selected muropeptides (M4 and D44) were included due to some relevant changes.*

Table 4.10b. Selected muropeptides from HPLC analysis of PG of DV900 after incubation with different forms of Pae-AmpC in vitro.

Reaction with DV900 PG[b]	T (°C)	Time (h)	Selected Muropeptides (% Molar)[a]						
			M4*	M5	D44*	D45	T445	D45N	T445N
DV900-CTRL	37	42	3.3	29.7	4	32.3	3.7	3.4	1.6
AmpC-F4	37	42	3.4	28.8	4.1	31.8	3.7	3.4	1.7
AmpC-F4:C3	37	42	3.5	29.1	3.9	31.9	3.5	3.3	1.5
AmpC-F4:C6	37	42	3.4	28.8	3.8	31.7	3.3	3.1	1.5
AmpC-F2	37	42	3	30.5	4.3	33.6	3.5	3.3	1.6
AmpC-F3 (a)	37	42	**13.5**	**20.4**	**5.3**	**31.2**	2.9	**2.6**	0.8
AmpC-F3 (b)	37	42	**15.4**	**25.6**	**5.9**	**27.4**	2.5	**1.3**	0.4

*[a] Relative abundance in % molar of some selected muropeptides (M4, M5, D44, D45, T445, D45N and T445N) due to the presence of some interesting changes in their occurrence in PG of DV900 upon AmpC treatment in vitro. [b] The same reactions described in table 4.10a. *Data are mentioned before in table 4.10a and was repeated in this table to be compared with the other muropeptides.*

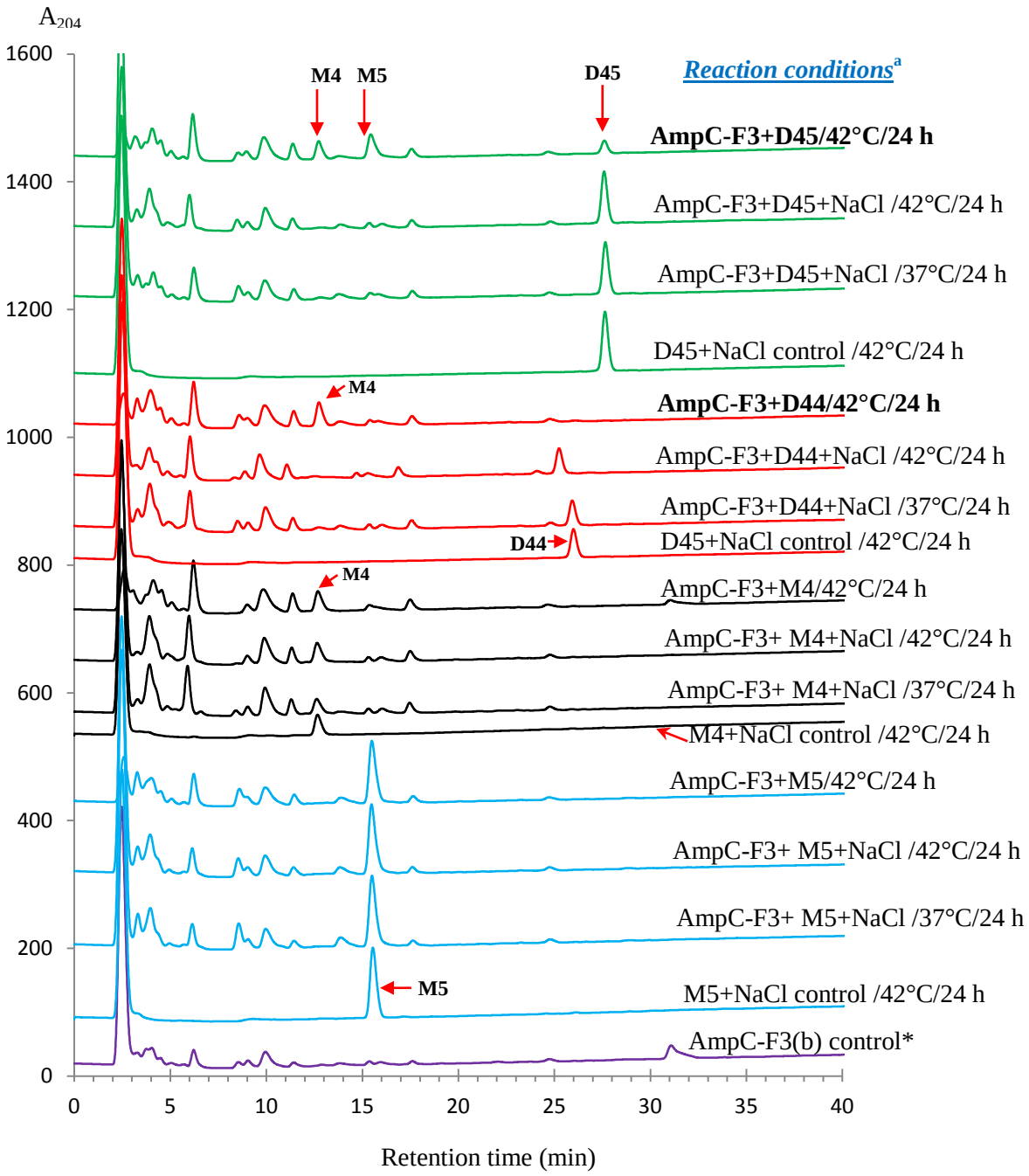

Figure 4.9. Effect of AmpC-F3(b) activity on individual muropeptides M4, M5, D44 and D45 at 37 and 42°C (in vitro). *In vitro reactions (250 µl) contained AmpC-F3(b) (0.4 µg /µl) with each of individual muropeptides M4 (4ng/ µl), M5 (16 ng/ µl), D44 (5 ng/ µl) and D45 (10 ng/ µl) were left at 37 or 42°C for 24 h, and then were manipulated as described in section 3.12.3. * AmpC-F3(b) is a purified AmpC-F3 stored for 3 months (or more) at -20 °C, which showed by HPLC analysis some protein degradations. [a] Reaction conditions were described over each data series where the ones that displayed considerable changes were shown on bold letters; where 42°C for 24 h was the best conditions for yielding some DD-endopeptidase activities on D44 and D45. Some other reactions contained individual muropeptides without any AmpC additions to be a negative control for DD-peptidase activities.*

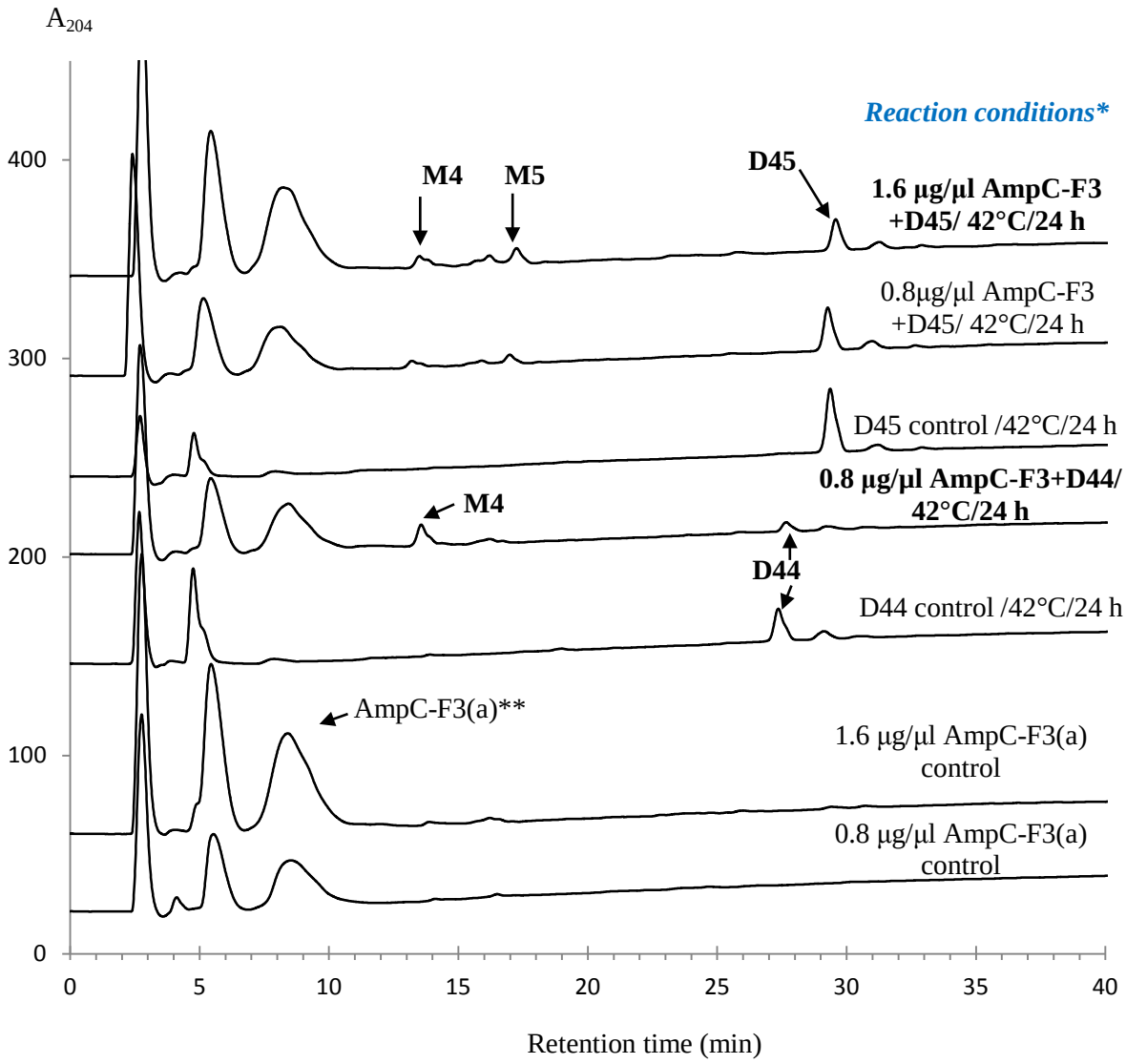

Figure 4.10. Effect of AmpC-F3(a) activity on individual muropeptides M4, M5, D44 and D45 at 42°C (in vitro).

** In vitro reactions of 250 µl, contained freshly prepared AmpC-F3(a) (0.8 or 1.6 µg/µl) with each of individual muropeptides D44 (2 ng/ µl) and D45 (4 ng/ µl) were left at 42°C for 24 h, and then were manipulated as described in section 3.12.3. ** AmpC-F3(a) is a freshly purified AmpC-F3 which showed less DD-endopeptidase activity than AmpC-F3(b) on D44 and D45 at 42°C for 24 h. AmpC-F3(a) displayed no activity on M4 and M5 (not shown).*

4.2. Role of LMM-PBPs in *ampC* regulation, β-lactam resistance and peptidoglycan structure in *P. aeruginosa*

4.2.1.Summary

The aim of this chapter is to highlight the role of the LMM-PBPs PBPs [DacB (PBP4), DacC (PBP5) and PbpG (PBP7)] in peptidoglycan structure, AmpC regulation and β-lactam resistance and morphology in *P. aeruginosa*. To fulfill this objective, we constructed several mutants as single and combined constructs of *dacB*, *dacC*, *pbpG* and *ampC* in *P. aeruginosa* PAO1 strain to compare the effect of inactivation of these LMM-PBPs in presence and in absence of AmpC activity on PG composition, *ampC* regulation and bacterial resistance. The constructed mutants were further checked by microscopy to identify morphological changes, tested for their PG composition by HPLC analysis and tested for their *ampC* expression by RT-PCR. Bocillin-FL test was done to confirm the inactivation of these LMM-PBPs in the constructed mutants and also to identify affinities to cefoxitin to LMM-PBPs. The results showed that mutants having single and combined *dacB* deletions had high *ampC* expression with the increase in bacterial resistance to β-lactam antibiotics except for imipenem and meropenem. Single mutations of *dacC* and *pbpG* did not changed the profile of *ampC* expression, and only *dacC* single and combined mutations produced maximum increase of PG pentapeptides. DacB and PbpG had higher affinities than DacC to cefoxitin. The triple mutant of *dacB*, *dacC* and *pbpG* displayed the largest increase in *ampC* expression and bacterial resistance to β-lactams. Microscopic examination of all the constructed mutants showed that they still retain their rod shape morphology similar to their parental PAO1 strain.

4.2.2.The constructed PAO1 mutants

Single and combined double and multiple mutants of *dacB*, *dacC*, *pbpG* and *ampC* were constructed (section 3.7) in *P. aeruginosa* PAO1 strain to study their physiological role in PG composition and bacterial resistance in *P. aeruginosa*. Also, it was aimed to study the role of the LMM-PBPs *dacB*, *dacC* and *pbpG* in *ampC* expression and regulation *P. aeruginosa*.

The constructed gene-specific inactivation vectors

Gene-specific mutagenesis vectors for inactivation of *ampC* and *dacB* were constructed in previous studies (Moya et al, 2009; Moya et al, 2008) and were used also in this study to knock out *ampC* and *dacB* and to form combined and multiple mutants of *dacB, dacC, pbpG* and *ampC*. Both of *pbpG* and *dacC* gene-specific mutagenesis vectors (pEXTΔ*pbpG*::Gm and pEXTΔ*dacC*::Gm) were constructed in this study, transformed in *E. coli* XL1 and S17λ and confirmed by colony PCR, digestion by restriction enzymes and DNA sequencing. Both of

pEXTΔ*pbpG*::Gm and pEXTΔ*dacC*::Gm have a lox flanked gentamycin resistance cassette (Gm, *aacC1* gene), PCR1 (*pbpG* or *dacC* gene upstream fragment) and PCR2 (*pbpG* or *dacC* gene downstream fragment) which were cloned in the vector pEX100Tlink (Fig. 3.3). These two vectors were used for inactivation of *pbpG* and *dacC* genes, respectively, in *P. aeruginosa* PAO1 wild type and mutants. Confirmation of *pbpG* gene-specific mutagenesis vector (pEXTΔ*pbpG*::Gm) was done by agarose gel electrophoresis of colony PCR of its transformants in *E. coli* XL1 blue with the vector pEXTΔ*pbpG*::Gm whose PCR amplification product has a size (>1.5 kbp) higher than the positive controls for PCR amplification of *pbpG* gene using PAO1 DNA (addendum, figure A. 2a). Also, pEXTΔ*pbpG*::Gm was confirmed by treatment with restriction enzymes HindIII, EcoRI and BamHI (not shown). Also, the verification of *dacC* gene-specific mutagenesis vector (pEXTΔ*dacC*::Gm) was done by treatment with restriction enzymes HindIII, EcoRI and BamHI, where treatment with HindIII only produced two fragments, correspond to pEXTΔ*dacC* Opened Vector (higher size, >7 kbp) having the vector pEX100Tlink with PCR1 and PCR2 in one DNA fragment and the other was *aacC1* fragment of gentamycin cassette (lower size <1.5 kbp). Digestion of pEXTΔ*dacC*::Gm with three enzymes HindIII, EcoRI and BamHI produced the 4 fragments [(lane 4): pEX100Tlink Opened Vector (~6.17 kbp), aacC1 fragment (<1.5 kbp), dacC-PCR1 (0.5 kbp) and dacC-PCR2 (0.4 kbp) (addendum, figure A. 2b)]. Confirmation of pEXTΔ*pbpG*::Gm and pEXTΔ*dacC*::Gm was done by colony PCR and restriction enzymes also in *E. coli* S17λ b. Also, DNA sequencing was done for all the constructs.

Double recombination, removal of gentamycin cassette and verification of Pae mutants

The construction of mutants in *P. aeruginosa* PAO1 was done using two bacterial strains; the first was donor strain (*E. coli* S17λ) having the gene-specific mutagenesis vectors S17/pEXTΔ*dacB*::Gm, pEXTΔ*dacC*::Gm, pEXTΔ*pbpG*::Gm and S17/pEXTΔ*ampC*::Gm for inactivation of *dacB, dacC, pbpG* and *ampC*, respectively. The second strain was the receptor strain which was either of PAO1 wild type or mutant having the target gene to be inactivated. The construction of mutants in *P. aeruginosa* by *cre-lox* method depended on double recombination between the chromosomal target gene and DNA fragment (PCR1-*lox-aacC1-lox*-PCR2) of the gene-specific inactivation vector. The gentamycin cassette (*aacC1*) was then eliminated by *cre* recombinase (fig.3.3).

The two mutants **PAOΔ*ampC*** and **PAOΔ*dacB*** were constructed from the wild type PAO1 in previous in studies (Moya et al, 2009; Moya et al, 2008). All the other Pae mutants summarized in table 3.1 were constructed in this study and confirmed for their gene inactivation by colony PCR amplification and agarose DNA electrophoresis. So that, single, double, triple

and quadruple PAO1 mutants of *dacB, dacC, pbpG* and *ampC* deletion were constructed from PAO1 and confirmed by colony PCR amplification of the target gene (addendum, figure A. 3-7).

The mutants **PAOΔ*pbpG***, **PAOΔ*dacB*Δ*pbpG*** and **PAOΔ*pbpG*Δ*ampC*** were constructed from the wild type PAO1, PAOΔ*dacB* and PAOΔ*ampC*, respectively, by double recombination with pEXTΔ*pbpG*::Gm which produced the positive genotypes PAOΔ*pbpG*::Gm, PAOΔ*dacB*Δ*pbpG*::Gm and PAOΔ*ampC*Δ*pbpG*::Gm, respectively, which were then confirmed by colony PCR for removal of their gentamycin cassette producing the genotypes PAOΔ*pbpG*, PAOΔ*dacB*Δ*pbpG* and PAOΔ*pbpG*Δ*ampC*, respectively.

The mutants **PAOΔ*dacC*Δ*ampC***, **PAOΔ*dacC*Δ*pbpG***, **PAOΔ*dacC***, **PAOΔ*dacB*Δ*dacC*** and **PAOΔ*dacB*Δ*dacC*Δ*pbpG*** were constructed from PAOΔ*ampC*, PAOΔ*pbpG*, PAO1, PAOΔ*dacB* and PAOΔ*dacB*Δ*pbpG*, respectively, by double recombination with pEXTΔ*dacC*::Gm which produced the positive genotypes PAOΔ*ampC*Δ*dacC*::Gm, PAOΔ*pbpG*Δ*dacC*::Gm, PAOΔ*dacC*::Gm, PAOΔ*dacB*Δ*dacC*::Gm and PAOΔ*dacB*Δ*pbpG*Δ*dacC*::Gm, respectively, which were then confirmed by colony PCR for removal of their gentamycin cassette producing the genotypes PAOΔ*dacC*Δ*ampC*, PAOΔ*dacC*Δ*pbpG*, PAOΔ*dacC*, PAOΔ*dacB*Δ*dacC* and PAOΔ*dacB*Δ*dacC*Δ*pbpG*, respectively.

The mutants **PAOΔ*dacB*Δ*ampC*** and **PAOΔ*dacBΔpbpGΔampC*** were constructed from PAOΔ*dacB* and PAOΔ*dacBΔpbpG*, respectively, by double recombination with pEXTΔ*ampC*::Gm which produced the positive genotypes PAOΔ*dacB*Δ*ampC*::Gm, and PAOΔ*dacBΔpbpGΔampC*::Gm, respectively, which were then confirmed by colony PCR for removal of their gentamycin cassette producing the genotypes PAOΔ*dacB*Δ*ampC* and PAOΔ*dacBΔpbpGΔampC*, respectively.

The mutants **PAOΔ*dacB*Δ*dacC*Δ*ampC***, **PAOΔ*dacC*Δ*pbpG*Δ*ampC*** and **PAOΔ*dacB* Δ*dacC*Δ*pbpG*Δ*ampC*** were constructed from PAOΔ*dacB*Δ*dacC*, PAOΔ*dacC*Δ*pbpG and* PAOΔ*dacB*Δ*dacC*Δ*pbpG*, respectively, by double recombination with pEXTΔ*ampC*::Gm which produced the positive genotypes PAOΔ*dacB*Δ*dacC*Δ*ampC*::Gm, PAOΔ*dacC*Δ*pbpG*Δ*ampC*::Gm *and* PAOΔ*dacB*Δ*dacC*Δ*pbpG*Δ*ampC*::Gm, respectively, which were then confirmed by colony PCR for removal of their gentamycin cassette producing the genotypes PAOΔ*dacB*Δ*dacC*Δ*ampC*, PAOΔ*dacC*Δ*pbpG*Δ*ampC and* PAOΔ*dacB* Δ*dacC*Δ*pbpG*Δ*ampC*, respectively.

The mutant **PAOΔ*dacB*Δ*pbpG*Δ*ampC*Δ*dacC*** was constructed from PAOΔ*dacB* Δ*pbpG*Δ*ampC* by double recombination with pEXTΔ*dacC*::Gm which produced the positive genotype PAOΔ*dacB*Δ*pbpG*Δ*ampC*Δ*dacC*::Gm which was then confirmed by colony PCR for removal of its gentamycin cassette producing the genotypes PAOΔ*dacB*Δ*pbpG*Δ*ampC*Δ*dacC*.

The constructed mutants were checked for loss of DacB, DacB and PbpG by Bocillin-FL test as described in section 4.2.4.

4.2.3. Growth rates and microscopic examination of PAO1 mutants

The growth rates in LB media at 37°C with agitation of single, double and multiple PAO1 mutants were not affected by deletion of *dacB*, *dacC*, *pbpG* and *ampC* when compared with the wild type (fig. 4.11). Microscopic examination (phase-contrast) was performed after 2, 3, 4, and 5 hours and overnight growth for all the constructed mutants and the wild type PAO1. By comparing with the wild type, all mutants showed a rod shape with little differences in cellular width and diameter in some of them; only microscopic images after 4 hours were shown in figure 4.12 but the other images of all the constructed mutants at 2, 3 and 5 hours and overnight displayed a close morphological similarity to the wild type.

4.2.4. Bocillin-FL test of PAO1 mutants

The Bocillin-FL binding pattern of PBPs [PBP1a, PBP1b, PBP2, PBP3, PBP4 (DacB), PBP 5 (DacC) and PBP 7 (PbpG)] were checked up through fluorescence scanning of SDS-PAGE of membrane extracts from the different mutants; the Bocillin-FL binding reaction involved incubation of 100 µg of cell membrane proteins (from FOX-induced and non-induced cells) with 10 µM Bocillin-FL in 1x PBS (pH 7.5) at 37°C for 30 min (section 3.5.5). The observed patterns of the PBPs in both of membranes of non-induced (fig. 4.13) and FOX-induced cells (fig. 4.14) were almost similar and these PBPs patterns correlated perfectly with the loss of the expected LMM-PBP for each mutant except for the two mutants *PAOΔdacB* and *PAOΔdacBΔpbpG* which had unpredictably undetected DacC even thought that DacC was clearly detected in their corresponding mutants with *ampC* deletion (i.e. PAOΔ*dacB*Δ*ampC* and PAOΔ*dacB*Δ*pbpG*Δ*ampC*) respectively. Therefore, these results strongly suggests that the high amounts of AmpC produced by DacB mutants (see below) significantly compromises the Bocillin-FL concentration required for DacC visualization. For analysis of the cefoxitin affinity for PBPs in cell membranes of PAO1, PAOΔ*ampC* and PAOΔ*dacB*Δ*pbpG*Δ*ampC*, 100 µg of cell membrane proteins were incubated with serial concentrations of cefoxitin for 30 min at 37°C and then incubated with 10 µM Bocillin-FL in 1x PBS (pH 7.5) at 37°C for 30 min; the results displayed that LMM-PBPs (e.g. DacB, DacC and PbpG) had higher affinity to FOX than HMM-PBPs (e.g. PBP3, PBP2, PBP1a and PBP1b); DacB (PBP4) and PbpG (PBP7) are more sensitive to FOX than DacC (PBP5) which displayed a close behavior similar to PBP3; while PBP1b has the lowest affinity to FOX. IC_{50} values of FOX binding affinity for DacB, PbpG and DacC were of 1.45, <1.5 and 9.1 µg/ml, respectively in the wild type while they were 1.3, <1.5 and 6.5, respectively in PAOΔ*ampC*. IC_{50} for FOX and DacC of PAOΔ*dacB*Δ*pbpG*Δ*ampC* was 7.7 µg/ml (table 4.11). These data demonstrates that DacB and PbpG were very sensitive to

FOX while DacC was more resistant. Gene sequencing of *dacC* in PAOΔ*dacB* and PAOΔ*dacB*Δ*pbpG* showed no mutations; indicating that the disappearance of DacC in Bocillin-FL binding test was not due to a genetic-driven structural change but rather was due to high AmpC production in these two mutants (see next section).

4.2.5. Effect of LMM-PBPs inactivation on *ampC* expression and β-lactam resistance in PAO1 mutants

We have found that among the studied LMM-PBPs in PAO1, *dacB* mutant is the only single LMM-PBP mutant that was able to produce high basal *ampC* expression which caused a marked increase in the MICs for the antipseudomonal penicillins (piperacillin), cephalosporins (cefotaxime, ceftazidime, and cefepime) and monobactams (aztreonam) (table 4.12). The double mutant of *dacB* and *dacC* produced 10-fold increase in *ampC* expression compared to *dacB* mutant alone. The triple mutant of *dacB*, *dacC* and *pbpG* had the maximum basal increase in *ampC* expression and β-lactam resistance. Under FOX induction, there was a basal-level related increase in *ampC* expression in all of single, double and triple mutants which can be explained mainly by FOX blocking of DacB activity. The data suggest that *dacC* inactivation can largely turn on *ampC* expression only when DacB is inactive. The mutants PAOΔ*dacB*Δ*dacC*Δ*pbpG* and PAOΔ*dacB*Δ*dacC* had the highest and the same MICs for CAZ (16µg/ml), ATM (16µg/ml), PIP (128 µg/ml) and CTX (512 µg/ml). Also PAOΔ*dacB* and PAOΔ*dacB*Δ*pbpG* had high MICs [CAZ (8 µg/ml), ATM (8 µg/ml), PIP (16 µg/ml) and CTX (256 µg/ml)] but it was less than that of the mutant PAOΔ*dacB*Δ*dacC*Δ*pbpG* which showed maximum *ampC* expression. However, all of PAOΔ*dacB*, PAOΔ*dacB*Δ*pbpG*, PAOΔ*dacB* Δ*dacC*Δ*pbpG* and PAOΔ*dacB*Δ*dacC* had the same MIC for CEF (4 µg/ml). The wild type PAO1 and all mutants with active AmpC seemed to have the same MIC for FOX (1026 µg/ml) indicating that *ampC* induction in the wild type was enough to produce the maximal MIC for FOX. There was no change in MICs of MER and IMI within the different PAO1 mutants. MICs of vancomycin correlated to the level of pentapeptides and not to *ampC* expression. The wild type PAO1 and all mutants with active AmpC had the same MIC for AMP (1024 µg/ml) with the exception of the two mutants PAOΔ*dacC* and PAOΔ*dacB*Δ*pbpG* having MICs for AMP of 1536 and 2048 µg/ml, respectively. Both of *dacC* and *pbpG* mutants had no significant MIC change except for the decrease in piperacillin susceptibility in the PAOΔ*dacC* mutant. We found that the MICs for nearly all β-lactams decreased in the PAOΔ*dacC*Δ*ampC* mutant compared to PAOΔ*ampC* mutant, and this effect was further enhanced in the PAOΔ*dacB*Δ*dacC*Δ*pbpG*Δ*ampC* mutant, suggesting that LMW PBPs, particularly DacC, play a role in the intrinsic level of β-lactam resistance in *P. aeruginosa* (table 4.12).

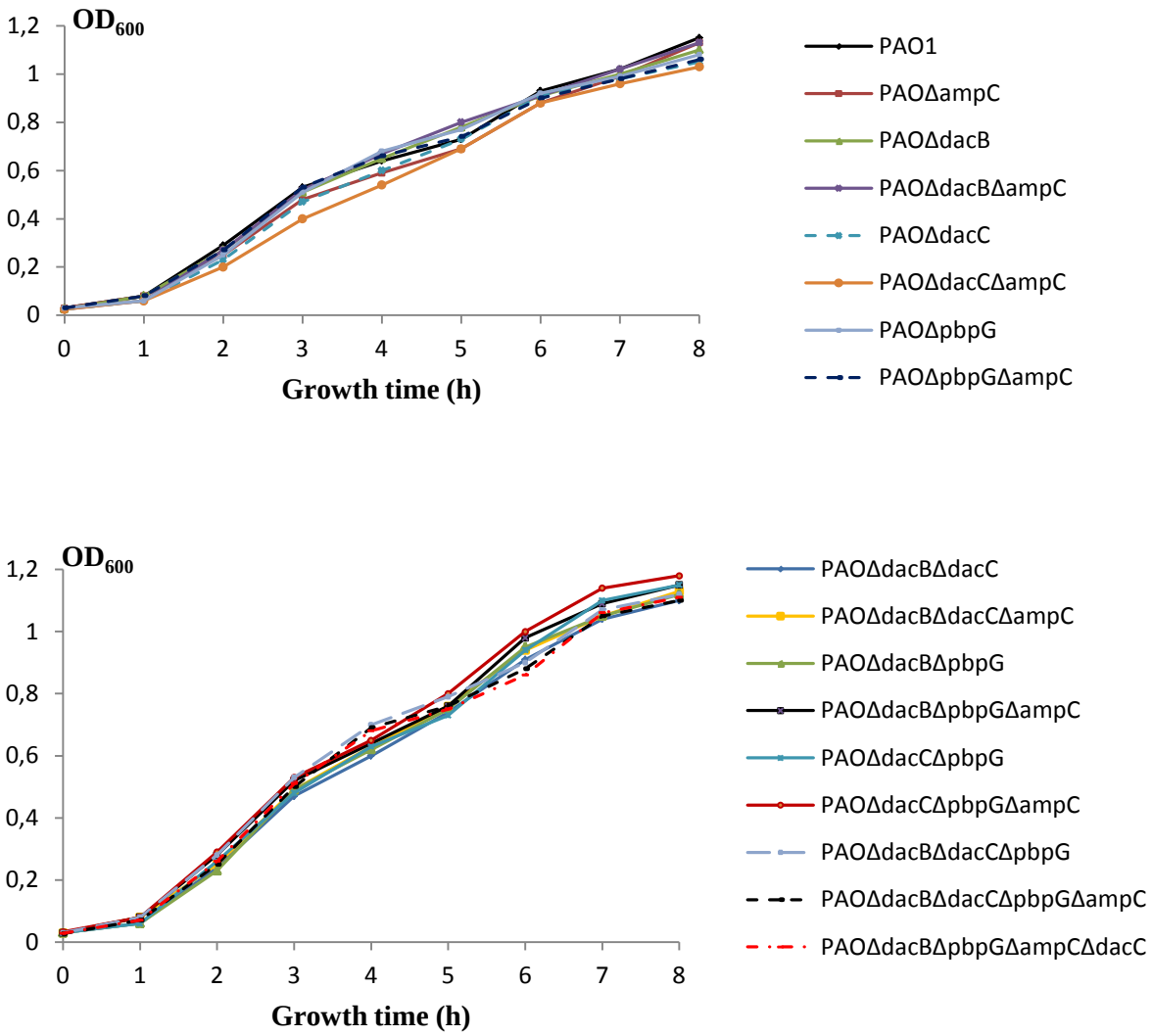

Figure 4.11. Growth curves of the constructed PAO1 mutants.

Optical densities at 600 nm of cellular growth of the wild type and all constructed PAO1 mutants, in LB media at 37°C with agitation (180 rpm), were recorded every one hour (h). Results show that profiles of cellular growth of all constructed mutants in PAO1 are of close similarity to the one displayed by the wild type PAO1.

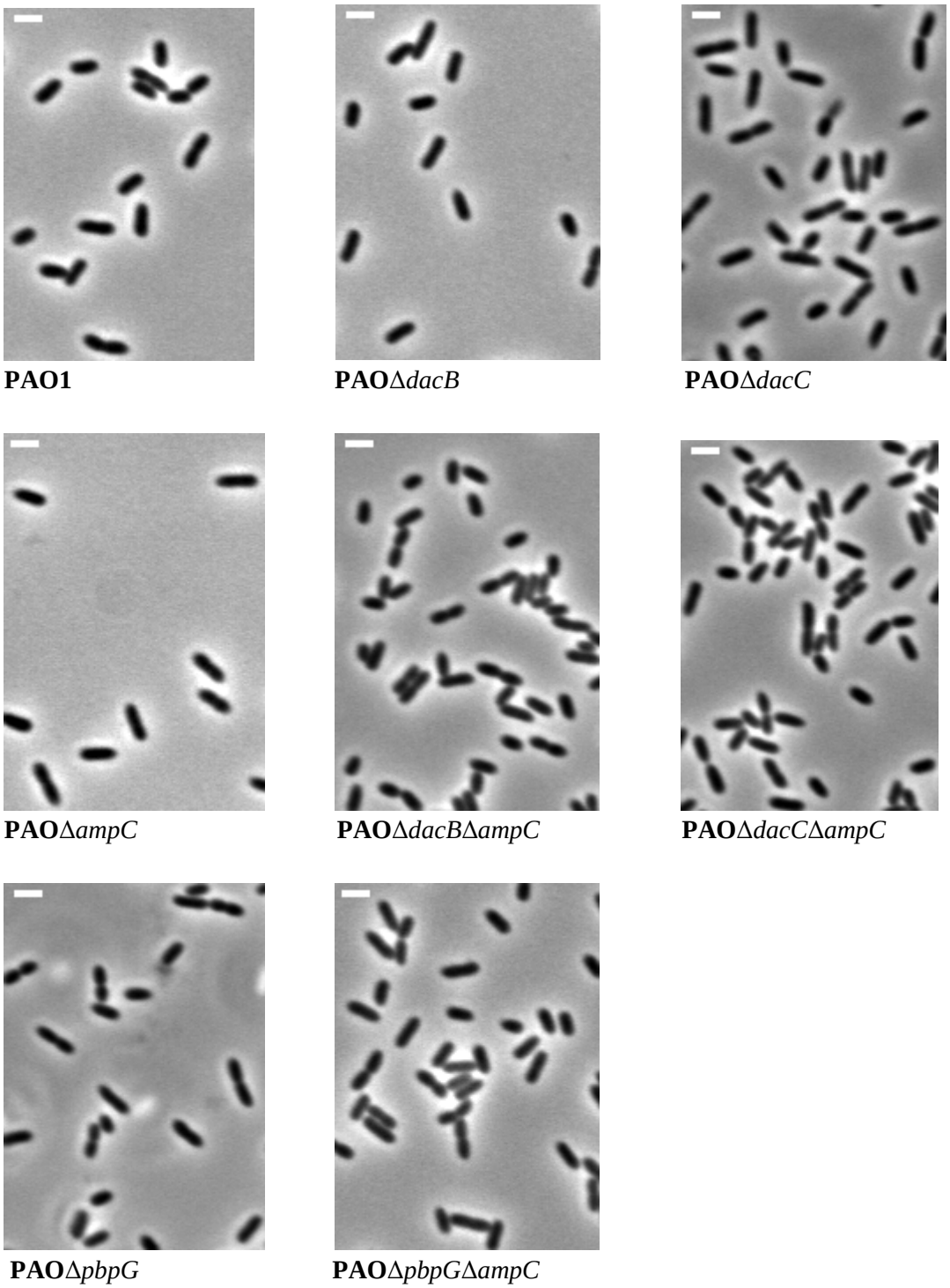

Figure 4.12. Microscopic examination of the constructed PAO1 mutants.
*Phase-contrast microscopic images of the constructed mutants are shown. Scale bars (white color) are 2 µm. As shown on this page and on the next page, all the constructed Pae mutants including the triple mutant (**PAO**ΔdacBΔdacCΔpbpG) and the quadruple mutants (**PAO**ΔdacBΔdacCΔpbpGΔampC and **PAO**ΔdacBΔpbpGΔampCΔdacC) still retain their rod shape phenotype similar to the wild type PAO1.*

Fig. is continued on the next page.

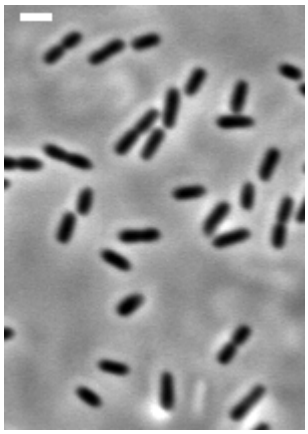

PAOΔ*dacB*Δ*dacC*

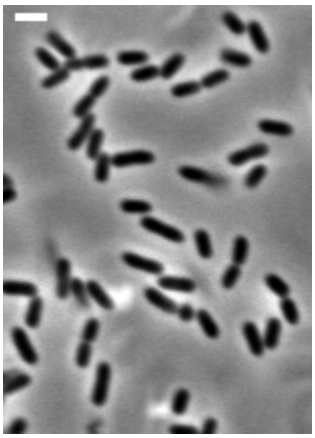

PAOΔ*dacB*Δ*pbpG*

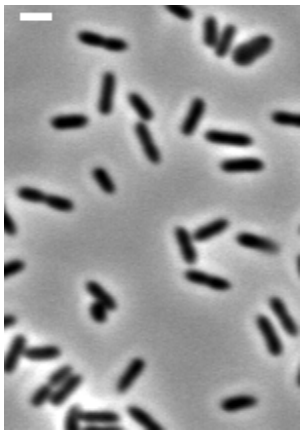

PAOΔ*dacC*Δ*pbpG*

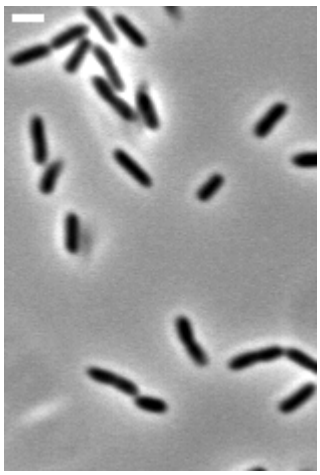

PAOΔ*dacB*Δ*dacC*Δ*ampC*

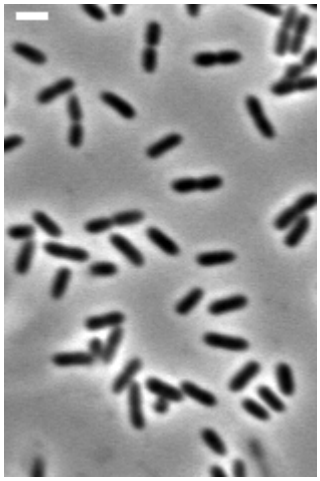

PAOΔ*dacB*Δ*pbpG*Δ*ampC*

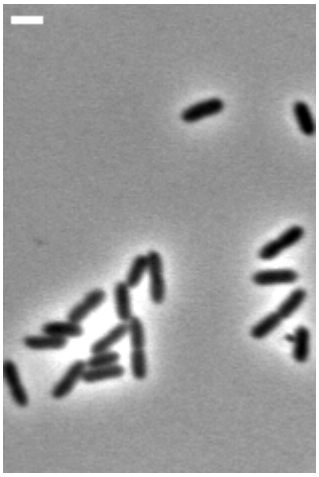

PAOΔ*dacC*Δ*pbpG*Δ*ampC*

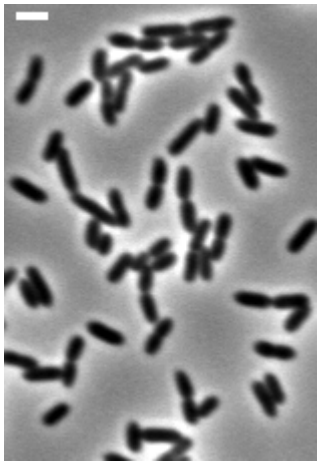

PAOΔ*dacB*Δ*dacC*Δ*pbpG*

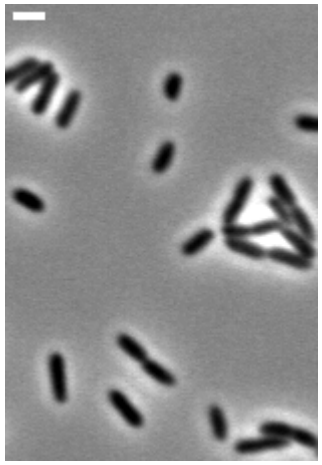

PAOΔ*dacB*Δ*dacC*Δ*pbpG*Δ*ampC*

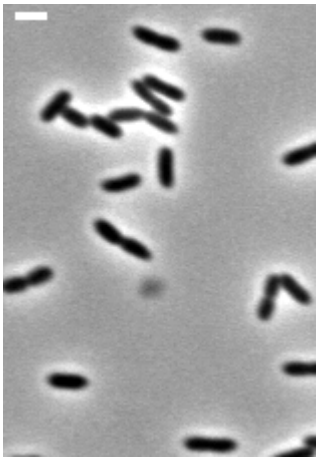

PAOΔ*dacB*Δ*pbpG*Δ*ampC*Δ*dacC*

Figure 4.12 continued. Microscopic examination of the constructed PAO1 mutants.

The wild type and all constructed PAO1 mutants were grown in LB media at 37°C while their microscopic examination was done after 4 hours in vivo using equipment of fluorescence resonance energy transfer (FRET) comprising Axiovert200 inverted microscope (Zeiss) coupled to a monochrome CCD camera. The images of the constructed mutants are of close similarity to the wild type PAO1. Scale bars (white color) are 2 µm.

Table 4.11. Estimated IC_{50} values for cefoxitin within cell membranes of the wild type and some PAO1 mutants using Bocillin-FL test.

Strain	IC_{50}- FOX (µg/ml)[a]						
	PBP1a	PBP1b	PBP2	PBP3	DacB	DacC	PbpG
PAO1	6.4	30.7	16.4	8	1.45	9.1	< 1.5
PAOΔ*ampC*	4.75	27.2	15.4	7.7	1.3	6.5	< 1.5
PAOΔ*dacB*Δ*pbpG*Δ*ampC*	4.25	29	13.1	6.2	0	7.7	0

[a] *IC_{50}- FOX is the cefoxitin (FOX) concentration producing a 50% reduction of Bocillin-FL binding for each individual PBP. The reaction contained 100 µg membrane proteins which were incubated with serial concentrations of cefoxitin for 30 min at 37°C then incubated with 10 µM Bocillin-FL in PBS (1x-pH 7.5) at 37°C for 30 min. The results show that LMM-PBPs (e.g. DacB, DacC and PbpG) have high affinity to FOX than HMM-PBPs (e.g. PBP3, PBP2, PBP1a and PBP1b); DacB (PBP4) and PbpG (PBP7) are more sensitive to FOX than DacC (PBP5) while PBP1b have the least affinity to FOX.*

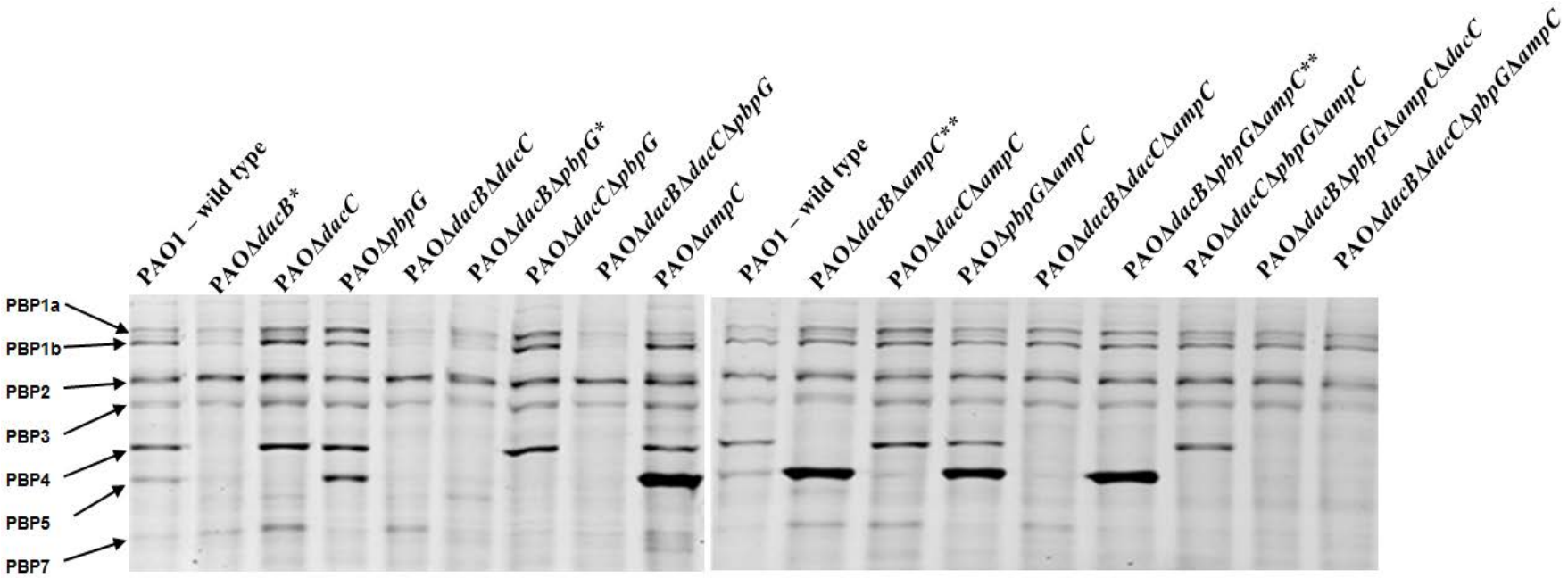

Figure 4.13. Bocillin-FL binding test of cell membranes of PAO1 mutants under non-induction conditions.

The Pattern of PBPs (at left) of all the constructed mutants and their parental wild type PAO1are shown. The reactions contained 100 µg membrane proteins which were incubated with 10 µM Bocillin-FL in 1x PBS (pH 7.5) at 37°C for 30 min. Bocillin-FL binding of cell membranes from Pae mutants that were grown without induction confirms the deletions of dacB, DacC and pbpG in the construed mutants. In case of the wild type we can see the bands corresponding to PBP1a, PBP1b, PBP2, PBP3, PBP4 (DacB), PBP5 (DacC) and PBP7 (PbpG). DacC was not detected in the mutants PAOΔdacB and PAOΔdacBΔpbpG (*) but it was detected in their corresponding mutants with ampC deletion PAOΔdacBΔampC and PAOΔdacBΔpbpGΔampC (**), respectively; also, DacC was highly increased in PAOΔampC and PAOΔpbpGΔampC when compared with the wild type PAO1 and PAOΔpbpG. The data shows that DacC occurs in a higher proportion when compared with the other PBPs in mutants of ampC.

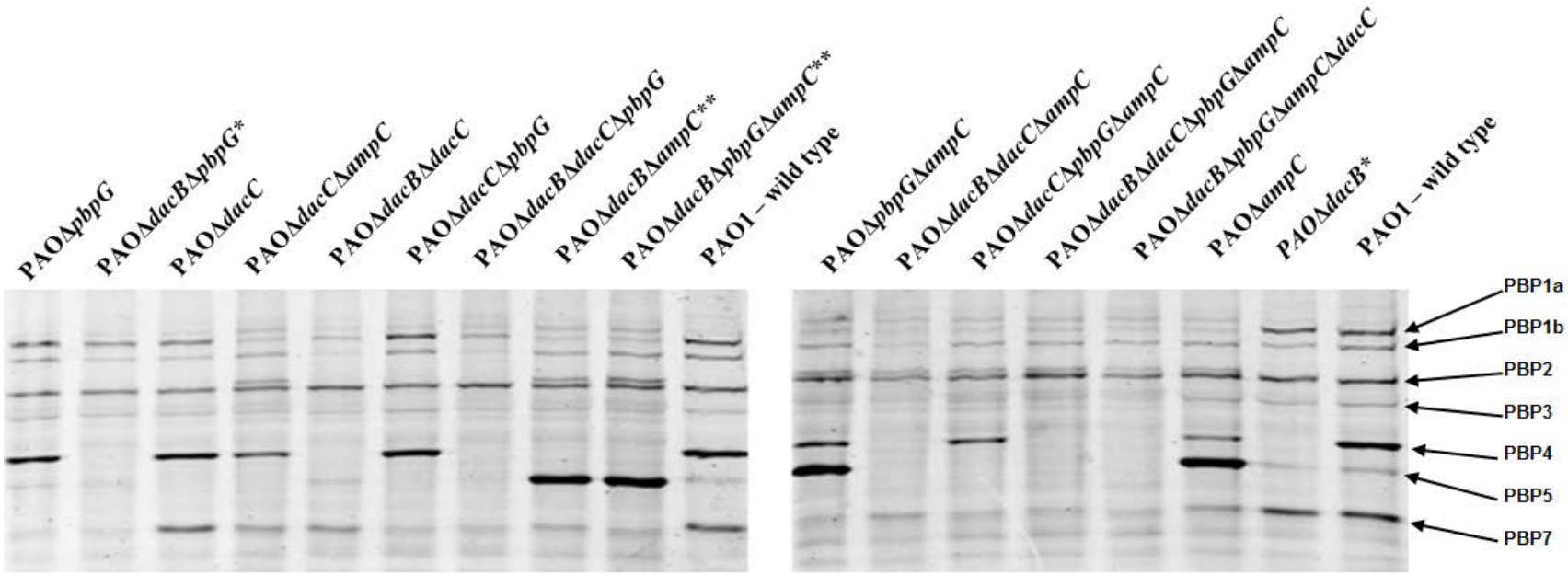

Figure 4.14. Bocillin-FL binding test of cell membranes of PAO1 mutants previously induced with cefoxitin.
**, ** Bocillin-FL assay of cell membranes from mutants pre-treated with FOX showed the same results without induction, described previously (Fig. 4.13).*

Please, take in your account that the order of the samples is not as shown in figure 4.13

Table 4.12. MICs and *ampC* expression under basal and cefoxitin induction conditions for all studied mutants [a].

Strain	MICs (µg/mL)[b]										*ampC* expression[c]	
	CAZ	CEF	ATM	PIP	IMI	MER	CTX	FOX	VAN	AMP	Basal	Induced*
PAO1	1	1	4	2	0.5	0.5	12	1024	512	**1024**	-	347 ± 59
PAOΔ*ampC*	1	1	4	2	≤0.12	0.25	8	64	512	32	-	-
PAOΔ*dacB*	**8**	**4**	**8**	**16**	**1**	0.5	**256**	1024	512	**1024**	**47 ± 29**	**569 ± 166**
PAOΔ*dacB*Δ*ampC*	1	0.5	2	2	≤0.12	0.25	8	96	512	32	-	-
PAOΔdacC	0.75	0.5	2	**4**	0.5	0.5	8	1024	**1024**	**1536**	1.3 ± 0.4	**542 ± 380**
PAOΔ*dacC*Δ*ampC*	0.75	0.5	2	2	≤0.12	0.25	4	64	**4096**	16	-	-
PAOΔ*pbpG*	1	1	4	**4**	**1**	0.5	**16**	1024	512	512	0.6 ± 0.3	305 ± 152
PAOΔ*pbpG*Δ*ampC*	1	0.5	3	**4**	≤0.12	0.25	8	96	512	32	-	-
PAOΔ*dacB*Δ*dacC*	**16**	**4**	**16**	**128**	0.5	0.5	**512**	1024	**2048**	**1024**	**478 ± 5.1**	**840 ± 245**
PAOΔ*dacB*Δ*dacC*Δ*ampC*	1	0.5	2	2	≤0.12	0.25	4	64	**4096**	16	-	-
PAOΔ*dacB*Δ*pbpG*	**8**	**4**	**8**	**16**	0.5	0.25	**256**	1024	512	**2048**	**45 ± 32**	326 ± 106
PAOΔ*dacB*Δ*pbpG*Δ*ampC*	0.75	0.5	2	2	≤0.12	0.5	6	64	**4096**	32	-	-
PAOΔ*dacC*Δ*pbpG*	1	0.5	2	**6**	0.5	0.25	8	1024	**1024**	**1024**	1.4 ± 0.7	162 ± 87
PAOΔ*dacC*Δ*pbpG*Δ*ampC*	0.75	0.5	2	**3**	≤0.12	0.25	4	64	**4096**	24	-	-
PAOΔ*dacB*Δ*dacC*Δ*pbpG*	**16**	**4**	**16**	**128**	0.5	0.5	**512**	**1024**	**4096**	**1024**	**1207 ± 193**	**5742 ± 1975**
PAOΔ*dacB*Δ*pbpG*Δ*ampC*Δ*dacC*	0.5	0.5	2	2	≤0.12	≤0.12	4	64	**4096**	16	-	-
PAOΔ*dacB*Δ*pbpG*Δ*dacC*Δ*ampC*	0.5	0.5	1	2	≤0.12	≤0.12	4	64	**4096**	16	-	-

[a] ***Cooperative work was done by Gabriel Cabot, Irina Sánchez-Diener, Bartolome Moya and Antonio Oliver*** *(Servicio de Microbiología and Unidad de Investigación. Hospital Universitario Son Espases. Palma de Mallorca. Spain).* [b] *MICs of ceftazidime (CAZ), cefepime (CEP), aztreonam (ATM), piperacillin (PIP), imipenem (IMI), meropenem (MER), cefotaxim (CTX), cefoxitin (FOX), vancomycin (VAN) and ampicillin (AMP).* [c] *Expression of ampC was determined by RT-PCR for non-induced (basal) and 50 μg/ml cefoxitin treated (induced) PAO1 wild type and mutants. Median values of 3 experiments are shown. Relevant data are shown in bold letters. dacB mutant caused large increase in ampC expression and bacterial resistance (to β-lactams except IMI and MER) which increased by further deletion of dacC and pbpG. Data of ampC expression show that the increase in bacterial resistance to β-lactams was related to a parallel increase in ampC expression except for VAN which was related to the level of penta peptides in PG of each PAO1 strain. The triple mutant PAOΔdacBΔdacCΔpbpG displayed the largest ampC expression. Both of PAOΔdacBΔdacCΔpbpG and PAOΔdacBΔdacC displayed the same resistance profile with the examined β-lactam antibiotics. PAOΔdacB mutant displayed high ampC expression and β-lactam resistance when compared with other single mutants.*

.

4.2.6. PG composition of the constructed PAO1 mutants

PG composition of cells untreated and treated with FOX was revealed by HPLC analysis (section 3.12) of the constituting muropeptides (tables 4.13 and 4.14, respectively). PG analysis of untreated single mutant cells showed that there was a large increase in penta muropeptides only when DacC was inactivated and this effect was enhanced by further inactivation of DacB and PbpG which produced a maximal penta muropeptides in the triple mutant. The data indicates that DacC has the main role in the DD-CPase activity in *P. aeruginosa*. There was no penta increase within the PG of *dacB* and *pbpG* single mutants, and only small increase (7.1 % mol) in the *dacC* single mutant (table 4.13). However, when those mutants were grown with 50 µg/ml cefoxitin (FOX), only *dacC* mutant shows a large increase in penta (38.8 % mol) most probably due to the inhibition of a DD-CPase activity (table 4.14). This result may indicate a low affinity of DacB or PbpG by cefoxitin, or some enhanced effect of DacC over the two other DD-CPases. Data on the high FOX affinity (IC_{50}) of DacB (1.45 µg/ml) and PbpG (<1.5 µg/ml) (table 4.11) and PG analysis of double mutant indicate that the effect must be mainly due to some kind of interaction of DacC with the two other DD-CPases, because PG analysis of PAOΔ*dacB*Δ*dacC* shows a high increase (28.6 % mol) and PAOΔ*pbpG*Δ*dacC* a moderate increase (9.8 mol%), but double mutant PAOΔ*dacB*Δ*pbpG* had no effect (2.5 % mol) on penta composition of PG (table 4.13). When induced by cefoxitin, the effect is exacerbated with values of 39.8 and 44.0 % mol for both double mutants PAOΔ*dacB*Δ*dacC and* PAOΔ*pbpG*Δ*dacC*, respectively, but again no increase for PAOΔ*dacB*Δ*pbpG* mutant (table 4.14). Without FOX treatment, the penta increase in *PAO*Δ*dacB*Δ*dacC*Δ*ampC* (32.0 % mol) is four times higher than that in *PAO*Δ*dacC*Δ*ampC* (8.0 % mol) (table 4.13), however their corresponding penta increase with FOX treatment is more or less the same (62.3 and 63.1 % mol) and it is very close to that observed in the triple mutant (65.5 % mol) and so did the mutant *PAO*Δ*pbpG*Δ*dacC*Δ*ampC* (64.5 % mol) (table 4.14). This indicates several conclusions: 1) DacB complements the DD-CPase activity when *dacC* is absent, 2) with less efficiency PbpG complements that activity when *dacC* or *dacB* are absent, 3) DacC is the major DD-CPase in *PAO1* because the mutant *PAO*Δ*dacB*Δ*pbpG* has no significant penta increase, and 4) these three PBPs are expected to have an interaction and a synergetic effect respect to the total DD-CPase activity in the cell. PG of the mutant *PAO*Δ*dacB*Δ*pbpG* had less monomers, more dimers, more anhydromuropeptides and a higher crosslinking when compared with the PAO1 wild type; this data must be related to the inhibition of a DD-endopeptidase (DD-EPase) activity, suggesting also these PBPs may have this type of activity (table 4.13).

Table 4.13. HPLC analysis of muropeptides prepared from PG of the constructed Pae mutants under non-induction conditions.

Strain	Muropeptides (% Molar)[a]									
	Mono	Di	Tri	D-D	Lpp	Anh	Penta	**Crosslink**	**D-D/T**	**Length**
PAO1	57.8	38.3	3.9	1.9	3.1	8.7	1.6	46.1	4.1	11.5
PAOΔ*dacB*	56.1	39	4.8	1.5	3.7	9.6	2.4	48.9	3.1	10.5
PAOΔ*dacC*	59.3	37.1	3.6	1.1	3.2	9.1	**7.1**	44.4	2.4	11
PAOΔ*pbpG*	58.7	37.2	4.1	1.5	2.8	9.4	1.4	45.4	3.2	10.7
PAOΔ*dacB*Δ*dacC*	58.4	36.7	4.8	1.1	3.4	9.4	**28.6**	46.6	2.3	10.7
PAOΔ*dacB*Δ*pbpG**	**54.5**	**39.5**	5.9	1.5	3.3	**14.2**	2.5	**51.6**	2.9	**7**
PAOΔ*dacC*Δ*pbpG*	55.9	39.4	4.6	1.2	3.3	8.9	**9.8**	48.8	2.6	11.2
PAOΔ*dacB*Δ*dacCpbpG*	54.7	40	5.2	1.3	2.4	7.6	**66.4**	50.6	2.5	13.2
PAOΔ*ampC*	59.9	36.3	3.8	1.2	3.3	9	2.5	43.8	2.8	11.1
PAOΔ*dacB*Δ*ampC*	54.2	40.3	5.4	2.1	4.1	10.3	2.5	51.2	4.1	9.8
PAOΔ*dacC*Δ*ampC*	59.7	36.6	3.7	1.1	3.2	9.1	8	44.1	2.4	11
PAOΔ*pbpG*Δ*ampC*	56.4	38.6	4.9	1.5	3.7	9.7	2.5	48.5	3.1	10.3
PAOΔ*dacB*Δ*dacC*Δ*ampC*	59.4	36.1	4.4	1	2.5	7.9	32	45.2	2	12.6
PAOΔ*dacB*Δ*pbpG*Δ*ampC**	**49.4**	**43.5**	7	1.7	3.6	11.3	3.7	**57.8**	3	**8.8**
PAOΔ*dacC*Δ*pbpG*Δ*ampC*	54.9	39.9	5.1	1.8	3.7	9.4	**9.4**	50.4	3.5	10.7
PAOΔ*dacB*Δ*dacCpbpG*Δ*ampC*	54.8	40	5.1	0.6	2.1	7.2	**67.6**	50.4	1.1	13.9
PAOΔ*dacB*Δ*pbpG*Δ*ampC*Δ*dacC*	53	40.4	6.5	1.5	2.4	8.8	**65.9**	53.6	2.8	11.4

[a] *As described previously within table 4.7. The interesting changes are shown in bold letters. dacC single and combined mutants displayed large increase in penta peptides in their PG due to inhibition of DD-CPase activity. *dacB and pbpG double mutant showed an increase in monomers, a decrease in dimers and trimers and an increase in crosslinking due to inhibition of DD-EPase activity.*

Table 4.14. HPLC analysis of muropeptides prepared from PG of the constructed Pae mutants treated with FOX.

Strain	Muropeptides (% Molar)[a]									
	Mono.	Di.	Tri.	D-D	Lpp	Anh.	Penta.	Crosslink	D-D/T	Length
PAO1	55.5	39.3	5.1	1.9	3.7	10.1	4.4	49.9	3.7	9.9
PAOΔ*dacB*	57.1	37.2	5.6	1.7	3.4	**13.7**	3.7	48.6	3.5	7.3
PAOΔ*dacC*	55.2	39.6	5.1	1.2	2.5	8.2	**38.8**	50.1	2.3	12.3
PAOΔ*pbpG*	56.6	37.9	5.4	1.9	3.6	8.9	4.2	49	3.9	11.3
PAOΔ*dacB*Δ*dacC*	58.8	36.7	4.4	1.1	3.2	8.1	**39.8**	45.8	2.4	12.4
PAOΔ*dacB*Δ*pbpG*	**51**	**42.1**	6.8	2.1	4.9	**12.3**	4	**56.1**	3.7	**8.2**
PAOΔ*dacC*Δ*pbpG*	54.3	40.3	5.3	1	2.6	7.5	**44**	51.3	1.8	13.4
PAOΔ*dacB*Δ*dacCpbpG*	54.8	39	6	1.1	3.1	9.3	**66**	51.6	2.1	10.8
PAOΔ*ampC*	54.9	40.3	4.6	1.3	2.6	7.2	14	50	2.6	14
PAOΔ*dacB*Δ*ampC*	55.8	39.5	4.5	1.3	3.4	7.7	**16.5**	48.9	2.7	13.1
PAOΔ*dacC*Δ*ampC*	58.1	37	4.8	1.4	3.4	7.5	**62.3**	46.9	3	13.3
PAOΔ*pbpG*Δ*ampC*	53.9	40.6	5.4	1.8	3.1	8.2	14.1	51.7	3.5	12.3
PAOΔ*dacB*Δ*dacC*Δ*ampC*	56.9	37.6	5.3	1.2	2.6	7.5	**63.1**	48.8	2.5	13.3
PAOΔ*dacB*Δ*pbpG*Δ*ampC*	53.4	40.6	5.8	1.9	3.6	8.3	14.7	52.8	3.6	12
PAOΔ*dacC*Δ*pbpG*Δ*ampC*	55.8	38.5	5.5	1.3	2.8	7.3	**64.6**	50.2	2.5	13.7
PAOΔ*dacB*ΔΔ*dacCpbpG*Δ*ampC*	57	37.2	5.6	1.3	2.7	6.7	**63.1**	49.1	2.7	15
PAOΔ*dacB*Δ*pbpG*Δ*ampC*Δ*dacC*	57.2	36.7	5.9	1	2	7.4	**65.5**	49	1.9	13.5

[a] *As described previously within table 4.7 and 4.15. FOX induction caused some increase the level of pentapeptides in all PAO1 wild and mutants. The double mutant of dacC and ampC showed a very close level of penta peptides (maximum penta level) as found in PG of the tripe mutant of dacB, dacC and pbpG and its quadruple mutant with ampC deletion.*

4.3. Activities of DacB, DacC and PbpG are not essential for recovery of rod shape in imipenem-induced spheroplasts in *P. aeruginosa*

4.3.1. Summary

A previous study reported that incubation of *P. aeruginosa* with 5x MIC of imipenem or meropenem with a static growth at 37°C caused the development of spherical shaped cells which were able to recover their shape after elimination of IMI or MER from the growth medium (Monahan et al, 2014). Taking advantage of the different mutant described in the previous section, the role of DacB, DacC and PbpG in the recovery of the rod shape can be studied. Then, we are about to pursue this analysis by producing that round cells by IMI induction and their recovered rod cells (in the wild type PAO1 and all the constructed Pae mutants) following the same procedure described previously (Monahan et al, 2014) and then to analyze their PG composition by HPLC (only for PAO1 and PAOΔ*dacB*Δ*dacC*Δ*pbpG*Δ*ampC*). Bocillin-FL test of round cells and rod shape recovered cells of the wild type PAO1 and the mutant PAOΔ*ampC* was done to identify their changes in PBPs pattern. Also, phase contrast and fluorescence microscopy was used to pursue the change in cell shape and viability. Results of PG analysis showed that by comparing to non-induced cells, PG composition of IMI-induced round cells of both of the wild type and mutant had a decrease in monomers, D-D muropeptides, pentapeptides and length and an increase in dimers, trimers, anhydro-muropeptides and crosslinking degree; also they had a large increase in M3 and decrease in M4, D44 and D45 muropeptides. However, PG composition of rod shape recovered cells had muropeptides with relative abundance similar to that of non-induced cells. Fluorescence microscopy showed that the round cells were viable however there were some unviable cells observed. Bocillin-FL test shows that membranes of round cells of both of the wild type PAO1 and the mutant PAOΔ*ampC* had a low amount of DacC and lost DacB while the rod shape recovered wild type PAO1 had a recovered DacB but DacC was still detected as a low amount; while at the opposite of that, the rod shape recovered PAOΔ*ampC* mutant had a recovered DacC at high amount and DacB at low amount. Also both of overnight recovered and non-induced cells had no PbpG detected.

4.3.2. Microscopic examination of imipenem-induced spheroplasts wild type and mutant PAO1 cells

Round cells were produced after 4 hours incubation of the wild type PAO1 and the constructed Pae mutants in CAMHB media supplemented with 0.5 M sucrose and induced with 5x MICs of IMI for 4 hours at 37°C without agitation (section 3.10). MICs for IMI for the wild type PAO1 and constructed Pae mutants are mentioned in table 4.12. We found that round cells of both of PAO1 and all mutants recovered their rod shape after elimination of IMI from the medium with static overnight growth at 37°C. Non-induction conditions were also performed as a control for the change in the morphological pattern. Phase-contrast and fluorescence microscopy (using green CYTO 9 staining, section 3.11) showed that in both of PAO1, PAOΔ*ampC* and the quadruple mutant (PAOΔ*dacB*Δ*dacC*Δ*pbpG*Δ*ampC*) the round cells were viable and alive. Some dead cells, indicated by white arrows in figure 4.15, were observed also in both strains, but in higher amount for the mutant. Under non-induction conditions cells from wild and quadruple mutant were all viable and alive. Moreover, published data of recovered cells, after removal of IMI in wild type strain, show they had normal morphology and were alive (Monahan et al, 2014); and also quadruple mutant in our assay seemed to have a normal rod shape and cells were all alive. All other constructed single and double Pae mutants displayed the same behavior (under microscope) for IMI-induced spheroplast formation and rod shape recovery after removal of IMI from the growth medium (not shown).

4.3.3. PG composition of imipenem-induced spheroplasts wild type PAO1 and mutants

Only PG of spheroplasts and recovered cells of PAO1wild type and PAOΔ*dacB*Δ*dacC*Δ*pbpG*Δ*ampC* mutant was analyzed by HPLC because we wanted to compare the effect of inactivation of all LMM-PBPs (*dacB*, *dacC* and *pbpG*) on PG composition with that of PAO1 wild type. It is just a way to reveal physiological role of these main Pae DD-CPases and EPases in PG composition during spheroplast formation and rod shape recovery.

IMI-induced round PAO1 cells of wild type and the mutants PAOΔ*dacB*Δ*dacC*Δ*pbpG* Δ*ampC* were grown in CAMHB media supplemented with 0.5 M sucrose and induced with 5x MICs of IMI at 37°C without agitation (section 3.10). After 4 incubation with IMI and 22 h incubation after removal of IMI, PG was collected from round-induced and non-induced cells, digested and analyzed by HPLC (section 3.12). Differences in main general structure of PG were found for both wild type and mutant under non induction conditions, compared with data of the same strains grown in exponential phase in LB and 180 rpm. These changes are expected due to

differences in media and growth conditions. However, major changes were found for round-induced and non-induced for both PAO1 and mutant strains. We found that PG of round cells in both strains had an increase in dimers, trimers, anhydro-muropeptides and crosslinking and a decrease in monomers, D-D muropeptides and length (table 4.15a). Respect to the individual muropeptides, round-shaped PAO1 wild type and the mutant PAOΔ*dacB*Δ*dacC*Δ*pbpG*Δ*ampC* had unusual increase in M3 and decrease in M4, D44 and D45 while M5 was not changed in the quadruple mutant (table 4.15b). After elimination of imipenem the round-shaped cells recovered the original rod shape and PG analysis after recovery showed normal levels of M3 and M4. The given data indicates that the activities DacB, DacC, PbpG and AmpC are not essential for rod shape recovery in *P. aeruginosa*.

4.3.4. Bocillin-FL test of imipenem-induced spheroplasts wild type PAO1 and PAOΔ*ampC*

As the pattern of changes in morphology and PG structure were equivalent in PAO and PAOΔ*dacB*Δ*dacC*Δ*pbpG*Δ*ampC,* indicating no role for the LMM-PBPs on the mechanism of production of round cell, then we decided to analyze the presence of these LMM-PBP on the wild type (complete set of PBPs) and the *ampC* mutant (no AmpC production). Round cells and recovered cells of the wild type PAO1 and the mutant PAOΔ*ampC* were produced as described before (section 3.10) with 5x MICs of imipenem. Bocillin-FL binding reaction involved incubation of a 100 µg of cell membrane proteins of PAO1 and PAOΔ*ampC* with 10 µM Bocillin-FL in PBS (1x-pH 7.5) at 37°C for 30 min. The Bocillin-FL binding pattern of PBPs of membranes of 4 hours non-induced PAO1 and PAOΔ*ampC* displayed a full pattern of PBPs: PBP1a, PBP1b, PBP2, PBP3, PBP4(DacB), PBP5(DacC) and PBP7(PbpG), with higher binding for PBP7 in PAOΔ*ampC*, while overnight non-induced cells of both strains had lost PBP7 band. The Bocillin-FL binding pattern of PBPs of membranes of 4 hours IMI-induced round cells of PAO1 and PAOΔ*ampC* displayed an equivalent pattern with the loss of all PBPs bands, except for small amount of their DacC band. On another hand, overnight recovered PAO1 and PAOΔ*ampC* had regained all PBPs band with the exception of PBP7, but they have a different pattern of expression of PBP4 and PBP5. The given data show that overnight recovered PAO1 had very low PBP5 amount and considerable amount of PBP4, but in the contrary, overnight recovered PAOΔ*ampC* had a low amount of PBP4 and large amount of PBP5 (fig. 4.16).

Table 4.15a. HPLC analysis of muropeptides prepared from PG of imipenem-induced Pae spheroplasts.

Strain	Conditions	Time (h)	Cell shape[c]	Muropeptides (% Molar)[a]									
				Mono	Di	Tri	D-D	Lpp	Anhy	Penta	Crosslink	D-D/T	Length
PAO1	No IMI	4	Normal	63.6	33.9	2.5	3.7	2.1	6.2	5.7	38.8	9.5	16.2
	+ IMI	4	>95% Round	**59.2**	**37.9**	**2.9**	2.3	1.2	**12.3**	**2.1**	**43.8**	**5.2**	**8.1**
	No IMI	22	Normal	62.1	34.9	2.9	8	2.3	5.7	12.9	40.8	19.6	17.7
	Recovery	22	Normal	57.6	39.1	3.3	4.9	2.8	6.8	6.6	45.7	10.7	14.6
PAOΔ*dacB* Δ*dacC* *ΔpbpG*Δ*ampC*	No IMI	4	Normal	60.2	36.3	3.5	1.2	2.9	6	59.6	43.3	2.7	16.7
	+ IMI	4	>95% Round	**52**	**43.2**	**4.8**	1.2	2.2	**14.8**	**55.4**	**52.9**	2.3	**6.8**
	No IMI	22	Normal	52.7	42.8	4.5	1.4	2.7	8.3	66.4	51.7	2.7	12
	Recovery	22	Normal	58.5	37.1	4.4	3.5	3.7	8.3	59.3	45.9	7.7	12.1

[a] *As described previously within table 4.7.* [b] ***No IMI:*** *cells was not treated with imipenem;* ***+IMI:*** *cells were treated with 5x MIC of imipenem; Recovery: cells after removal of imipenem; PG was analyzed from induced and non-induced cells after 4 and 22 hours static growth at 37°C in CAMHB media supplemented with 0.5 M sucrose.* [c] *The wild type PAO1 and the mutant PAOΔdacB ΔdacCΔpbpGΔampC are rod shaped but after their incubation with imipenem by 4 hours, their shapes turned into spheres (Fig. 4.15) and recovered their rod shapes after elimination of IMI in overnight growth. Spheres PG of induced PAO1 cells displayed increase in monomers and decrease in M4, D43 and D44; while, Spheres PG of the quadruple mutant displayed a large increase in M3 and decrease in M4, D43, D44 and D45 and no change in M5. After recovery the PG composition had normal proportions of muropeptides as in non-induced cells.*

Table 4.15b. Selected muropeptides produced from PG of imipenem-induced Pae spheroplasts.

Strain	conditions[b]	Time (h)	Cell Shape[c]	Muropeptides (% Molar)[a]											
				M3	M4	M5	D43	D44	D45	T444	T445	D44N	D45N	T444N	T445N
PAO1	No IMI	4	Normal	8.7	22.7	0.4	3.9	19.1	0.7	1.4	0.3	3.2	0.1	1	0
	+ IMI	4	**> 95% Round**	**14.3**	**14**	0.2	2	**10.8**	0.3	0.6	0	4.4	0	0.8	0
	No IMI	22	Normal	6.27	14.5	2	3.1	15.1	0.3	1.3	0.3	2.7	0.2	1	0
	Recovery	22	Normal	7.7	21.8	0.6	3.9	23.1	0.8	2.1	0.4	3.9	0.2	1.4	0
PAOΔ*dacB* Δ*dacC* Δ*pbpG*Δ*ampC*	No IMI	4	Normal	4.2	7	13.1	1.5	11.8	17.3	0.9	2	1.3	2.1	0.6	1.3
	+ IMI	4	**>95% Round**	**6.7**	**5.9**	13.1	0.9	**6.2**	**11.3**	0.4	0.9	2.2	3.7	0.3	1
	No IMI	22	Normal	3.1	5.1	16.1	1.5	12	22.4	1	2.8	1.9	2.9	0.7	1.9
	Recovery	22	Normal	2.7	5.1	12.5	1.9	8	14.5	1	2	1.7	2	0.5	1.1

[a] *As described previously within table 4.10b.* [b] *As described within table 4.15a. This table shows the molar abundance of common muropeptides in PG of imipenem-induced PAO1 cells which displayed large increase in M3 and decrease in M4, D43 and D44 in the wild type PAO1. While, PG of the quadruple mutant Spheroplasts displayed a large increase also in M3 and decrease in M4, D43, D44 and D45 and displayed no change in M5. After overnight recovery, the PG composition had normal proportions of muropeptides as in non-induced cells.*

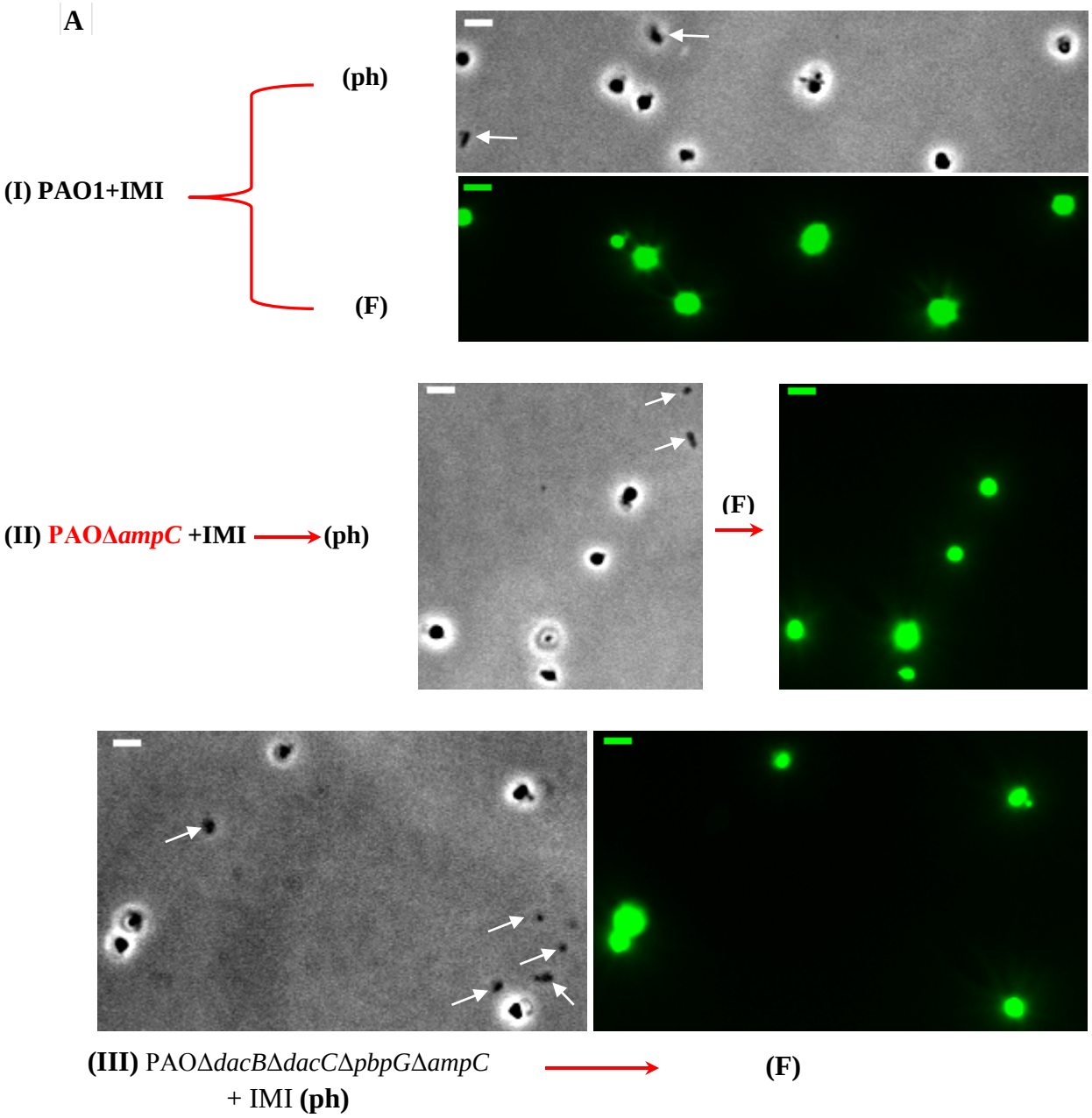

Figure 4.15. Microscopic examination of spheroplasts of imipenem-induced PAO1 wild type, PAOΔ*ampC* and PAOΔ*dacB*Δ*dacC*Δ*pbpG*Δ*ampC* mutants.

A. *Microscopic images of phase-contrast* ***(ph)*** *and fluorescence with CYTO 9* ***(F)*** *of the wild type PAO1* ***(I)*** *PAOΔampC* ***(II)*** *and PAOΔdacBΔdacCΔpbpGΔampC* ***(III)*** *showing spheroplasts which were obtained after incubation with 5x MICs of imipenem* ***(+IMI)*** *in CAMHB media supplemented with 0.5 M sucrose for 4 hours at 37°C without agitation; where the green colored spheres and their corresponding phase-contrast are supposed to be alive cells while the others pointed by white arrows are supposed to be dead cells. Scale bars are 2 µm.*

Fig. is continued on the next page.

B.

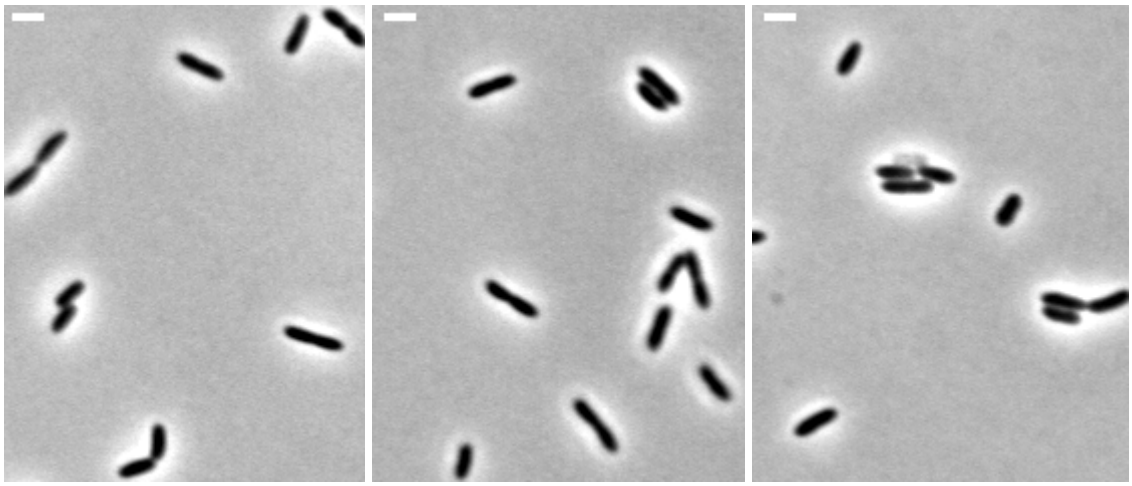

PAO1 **(before IMI)** | PAOΔ*ampC* **(before IMI)** | PAOΔ*dacB*Δ*dacC*Δ*pbpG* Δ*ampC* **(before IMI)**

C.

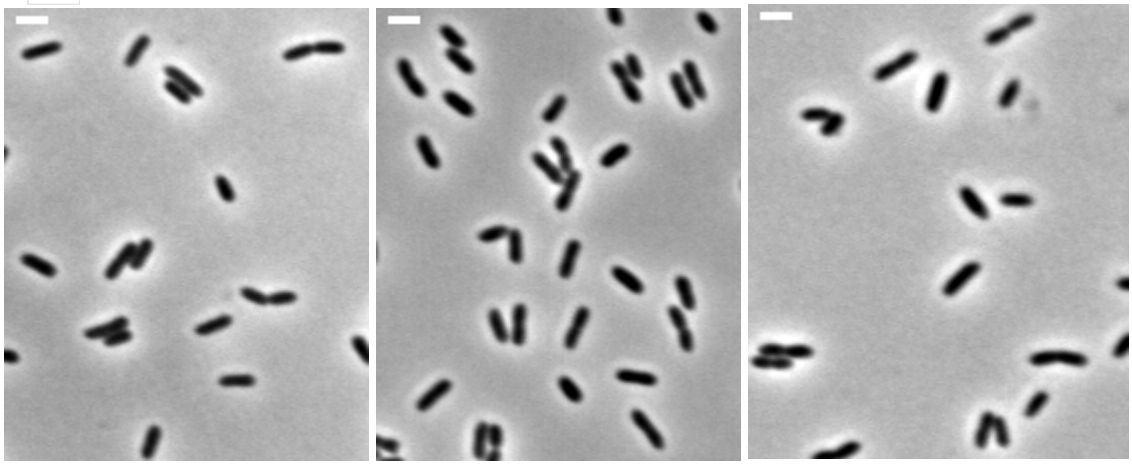

PAO1 **(RE)** | PAOΔ*ampC* **(RE)** | PAOΔ*dacB*Δ*dacC*Δ*pbpG* Δ*ampC* **(RE)**

Figure 4.15 continued. Microscopic examination of spheroplasts of imipenem-induced PAO1 wild type, PAOΔ*ampC* and PAOΔ*dacB*Δ*dacC*Δ*pbpG*Δ*ampC* mutants.

B. *Phase-contrast images of wild type wild type PAO1, PAOΔampC and PAOΔdacBΔdacCΔpbpGΔampC before addition of imipenem (IMI) to the growth medium (CAMHB media supplemented with 0.5 M sucrose at 37°C without agitation).* ***C.*** *Phase-contrast images of wild type wild type PAO1, PAOΔampC and PAOΔdacBΔdacCΔpbpGΔampC after elimination of IMI from the medium (CAMHB media supplemented with 0.5 M sucrose) and overnight incubation at 37°C without agitation.* ***RE:*** *recovery of rod shape from Pae spheroplasts (A) after elimination of IMI from the growth medium. Scale bars (white color) are 2 µm.*

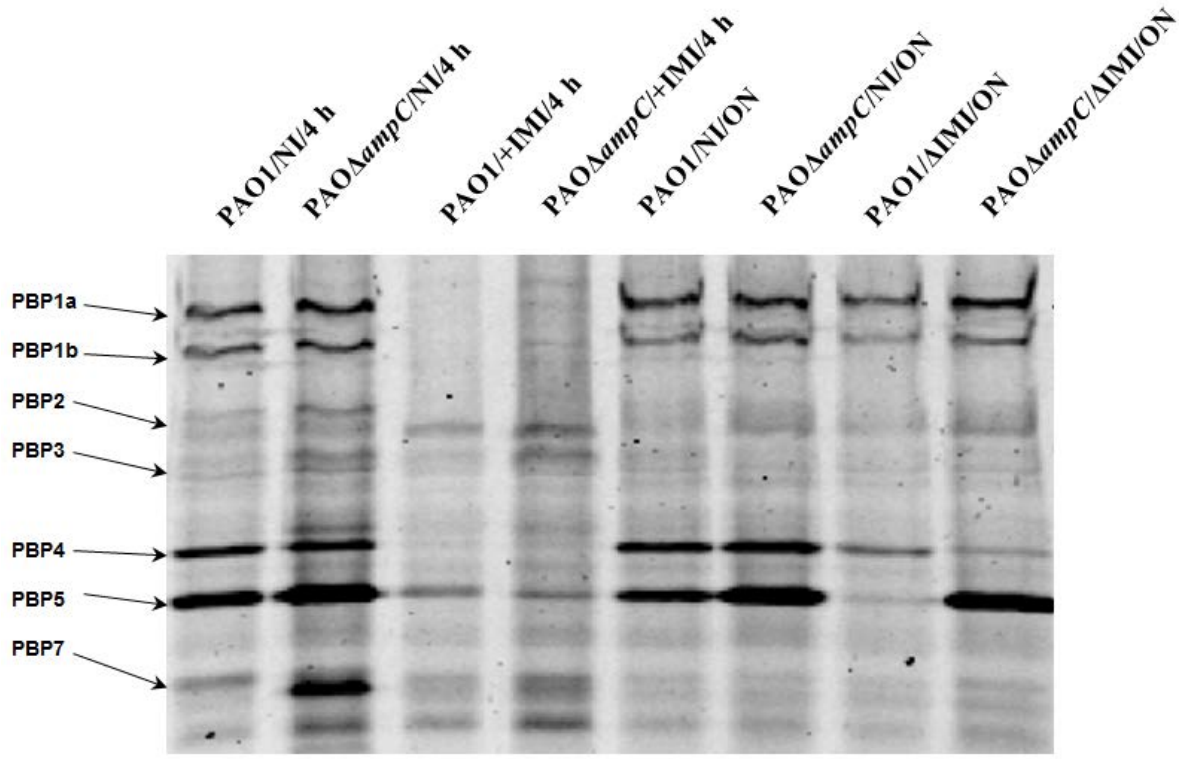

Figure 4.16. Bocillin-FL binding test of Pae spheroplasts membranes of IMI-induced PAO1 wild type and PAOΔ*ampC* mutant.

The Pattern of PBPs (at left) of PAOΔampC mutant and the wild type PAO1are shown. Assay of Bocillin-FL with cell membranes of PAO1 and PAOΔampC which were grown in CAMHB media supplemented with 0.5 M sucrose at 37°C without agitation. ***PAO1/NI/4 h*** *and* ***PAOΔampC/NI/4 h:*** *non-induced* ***(NI)*** *PAO1 and PAOΔampC after 4 hours of growth;* ***PAO1/+IMI/4 h*** *and* ***PAOΔampC/+IMI/4 h:*** *induced PAO1 and PAOΔampC after 4 hours of growth with 5x IMI which produced round cells ;* ***PAO1/NI/ON*** *and* ***PAOΔampC/NI/ON:*** *non-induced* ***(NI)*** *PAO1 and PAOΔampC after 4 hours of overnight* ***(ON)*** *growth;* ***PAO1/ΔIMI/ON*** *and* ***PAOΔampC/ΔIMI/ON:*** *overnight recovery of rod shape after elimination of IMI* ***(ΔIMI)*** *from the growth medium of PAO1 and PAOΔampC. The reaction contained 100 µg membrane proteins which was incubated with 10 µM Bocillin-FL in 1x PBS (pH 7.5) at 37°C for 30 min.*

Discussion

5. Discussion

5.1. Motivation and design of this study

5.2. Functional characterization of Pae-AmpC β-lactamase

5.2.1. Various forms of Pae-AmpC were produced

5.2.2. Interpretation AmpC production using pET28b and pUCP24 vectors

5.2.3. Mutations, sub-cellular localization and solubility can largely affect AmpC β-lactamase activity

5.2.4. The secondary DD-peptidase activity was clear with AmpC-F3 rather than the other studied AmpC forms

5.2.5. AmpC-F3 crystallization & obstacles on the way!

5.3. Role of Pseudomonas aeruginosa LMM-PBPs in PG composition, β-lactam resistance and ampC regulation in P. aeruginosa

5.3.1. Role of P. aeruginosa LMM-PBPs in cell wall physiology

5.3.2. Role of P. aeruginosa LMM-PBPs in AmpC regulation and β-lactam resistance

5.4. Activities of DacB, DacC and PbpG are not essential for recovery of rod shape in imipenem-induced spheroplasts in P. aeruginosa

5. Discussion

5.1. Motivation and design of this study

Functional characterization of Pae-AmpC from *P. aeruginosa* has a significant importance because AmpC overproduction and emergence of AmpC mutants (e.g. ESACs) are considered as one of the basic resistance tools used by this clinically problematic microorganism to overcome the inhibitory effect of most of β-lactam antibiotics (Bush & Jacoby, 2010; Jacoby, 2009; Lister et al, 2009). AmpC enzymes are historically known as β-lactamases but they were thought to have a DD-peptidase activity (CPase and/or EPase) due to structural similarities with LMM-PBPs (e.g. Eco-AmpH) that have these activities (Bishop & Weiner, 1992; Gonzalez-Leiza et al, 2011; Hall & Barlow, 2004; Joris et al, 1988; Kong et al, 2010; Sauvage et al, 2008). So, this study (section 4.1) concerned especially with tracking DD-peptidase activity in vivo and in vitro for Pae-AmpC forms (wild type and mutants) in *E. coli* and in *P. aeruginosa* by HPLC analysis of their PG and muropeptides; that was beside characterization of β-lactamase activity, β-lactam resistance and the effect of Pae-AmpC overproduction in these bacterial strains.

In addition to their structural similarities, LMM-PBPs play a role in *ampC* regulation and β-lactam resistance, likewise it was reported that inhibition of LMM-PBPs by β-lactam antibiotics triggers AmpC overproduction and sometimes mutations that can lead to the emergence of ESACs (Bush & Jacoby, 2010; Kong et al, 2010; Lister et al, 2009). Also, it was found that deletion of *dacB* triggered AmpC overexpression and β-lactam resistance in *P. aeruginosa* (Moya et al, 2009). So that, we aimed also to unveil the physiological role and functional interaction of the main LMM-PBPs (*dacB*, *dacC* and *pbpG*) in *P. aeruginosa* in *ampC* regulation, bacterial resistance and PG composition in *P. aeruginosa* which was achieved by the construction of single and combined mutants of these LMM-PBPs with and without Pae-*ampC* inactivation in PAO1 strain (section 4.2). Then, these Pae mutants were tested for their PG composition by HPLC analysis, their *ampC* expression by RT-PCR and their resistance to some β-lactam antibiotics.

On the other hand it was found that imipenem supplemented growth of *P. aeruginosa* produced spherical shaped cells and elimination of imipenem from the medium helped these round cells to recover their rod shape (Monahan et al, 2014). So, we aimed to characterize LMM-PBPs (DacB, DacC and PbpG) in the round and the recovered cells of *P. aeruginosa* by Bocillin-FL test and to pursue the physiological role of these LMM-PBPs on the recovery of the rod shape from round cells after elimination of imipenem from the growth medium(section 4.3).

5.2. Functional characterization of Pae-AmpC β-lactamase

5.2.1. Various forms of Pae-AmpC were produced

The first main goal was to characterize the function of AmpC-F1 (the wild type Pae-AmpC precursor form), AmpC-F3 (the wild type mature AmpC, without signal peptide) and two uncharacterized AmpC mutants (AmpC-F1:C3 and AmpC-F1:C6) to compare their functional activities and to characterize the effect of the two mutations on AmpC activity in PG composition and bacterial resistance. Because all of AmpC-F1, AmpC-F1:C3 and AmpC-F1:C6 were not produced in large amount from their encoding pET28b vectors in Bl21(DE3) (fig. 4.2), we designed another AmpC forms (AmpC-F4, AmpC-F4:C3, AmpC-F4:C6 and AmpC-F4) in order to overproduce the precursor form of Pae-AmpC and these two mutants using pET28b vectors. Also, some AmpC forms were designed to have C-terminal TEV protease site (e.g. AmpC-F3-TEV, AmpC-F3:C3-TEV, AmpC-F3:C6-TEV and AmpC-F6-TEV) to remove the poly-His tag (by TEV protease) from the purified proteins to be crystallized.

5.2.2. Interpretation of AmpC production using pET28b and pUCP24 vectors

AmpC production from ampC-encoding pET28b recombinant vectors

Detection of the different forms of AmpC proteins by SDS-PAGE and the corresponding western blot analysis is proportional to AmpC production by different recombinant plasmids. AmpC-F1 (the wild type) and the two mutants AmpC-F1:C3 and ampC-F1:C6 were not detected by SDS-PAGE or western blot because they were not actually produced. By returning to the forward primer (ampC-Fw1) of their PCR amplification, it has the sequence (**5'**…TTTCCATGG**ATG**CGCGATACCAGATTCC…**3')** providing the transcription process with two ATG that could be a starting codon for the peptide sequence; the 1st ATG (underlined) is favored rather than at the 2nd one (underlined, bold, the actual AmpC initiation codon) because it is closer to the RBS, which means that the normal AmpC peptide sequence was not produced but rather another short and different amino acid sequence peptide. This explanation is highly supported by the expression profile (detection by SDS-PAGE and western blot) of the other AmpC forms that have the 1st ATG (closer to RBS) and can be used as a start codon for AmpC amino acid sequence (table 3.2; fig 3.1). So, there was protein overproduction in case of AmpC-F2, AmpC-F4, AmpC-F4:C3, AmpC-F4:C6 and AmpC-F4-TEV (periplasmic forms), except for AmpC-F3, AmpC-F3:C3-TEV and AmpC-F3:C6-TEV (cytoplasmic forms, without signal peptides) having a low expression

which may be due to the instability of this forms in the cytoplasm or its degradation by some cytoplasmic proteases (fig. 4.2→4.5). Also we found that all the purified AmpC forms were stable when stored at -20°C except AmpC-F3 which showed some degradation after 3 months or more which was observed during HPLC analysis with muropeptides (fig. 4.9).

AmpC production from ampC-encoding pUCP24 recombinant vectors

AmpC-F3 and AmpC-F4 were detected in a low amount by western blot after IPTG induction of pUCP-F3 and pUCP-F4, respectively, in PAO1 wild type and mutant strains. Also, there was no difference in western blot detection of AmpC-F3 and AmpC-F4 in cases of induction and no-induction with IPTG (fig. 4.6). Also, the β-lactamase activities in Pseudomonas transformants of pUCP-F3 under induction conditions were almost similar compared with the no-induction cases (table 4.3). However, Pseudomonas transformants of pUCP-F4 showed lower β-lactamase activities in induction conditions when compared with non-induction conditions. This can be explained by returning to the design of the cloned sequence of both of *ampC*-F3 and *ampC*-F4 in pUCP24 (fig. 3.2) where two pairs of RBS and starting codon (ATG) are present, the 1st pair (RBS-ATG) is original in pUCP24 vector while the 2nd pair is external and was retrieved from the corresponding sequence of *ampC* in pET28b recombinant vectors. Expression from the 2nd pair will only produce the desired AmpC peptide, however the data indicates that IPTG induction, only affected the 1st RBS-ATG pair which produces a different peptide. Also, expression of *ampC* from the 2nd ATG by means of the 1st RBS is not favored because the 1st ATG is closer to 1st RBS and at the right distance for start of translation.

5.2.3. Mutations, sub-cellular localization and solubility can largely affect AmpC β-lactamase activity

In *E. coli* BL21(DE3)/pET-*ampC*, AmpC-F4 showed the highest β-lactamase activity in cellular fractions of *E. coli* Bl21(DE3)/pET-F4, (table 4.2) and remarkable increase in β-lactam resistance (table 4.5) because it had the majority of its mature form soluble (fig. 4.3). The purified mature form AmpC-F3 showed the highest activity on nitrocefin (table 4.4) however it showed a very low activity in vivo (table 4.2) which may be due to its low expression or degradation. Because AmpC-F3 was produced in the cytoplasm, it did not change the profile of bacterial resistance in Bl21(DE3). AmpC-F2 showed a moderate β-lactamase activity (table 4.2) and decreased the susceptibility to some β-lactams beside resistance to amoxicillin/clavulanic acid, AMC (table 4.5) which may be due to the very low production of the mature form (fig 4.2).

The two mutants AmpC-F4:C3 and AmpC-F4:C6 showed a very low β-lactamase activity in vivo and in vitro (tables 4.2, 4.4) and did not change the profile of bacterial resistance against the tested β-lactams except for amoxicillin/clavulanic acid, AMC (table 4.5); indicating that these two mutations affected largely the β-lactamase activity of Pae-AmpC.

Although both of AmpC-F2 and AmpC-F4 have some modification in the signal peptide (fig. 4.1), both of them would be proficient to produce the wild type of the mature AmpC form by elimination of the signal peptide. By following the β-lactamase activity in cellular fractions of *E. coli* DV900(DE3)/pET-*ampC*, we found that AmpC-F3, AmpC-F4:C3 and AmpC-F4:C6 showed the same behavior as encountered in Bl21(DE3) while AmpC-F2 showed higher activity and AmpC-F4 produced lower activity which could be due to the low production of the soluble mature form (table 4.2; fig. 4.2-4.5). As described before (table 4.1; fig 4.1), AmpC-F2, AmpC-F4:C3 and AmpC-F4:C6 have single amino acid mutations; R^{2}→G, P^{243}→L and I^{51}→T, respectively, which could affect the general protein folding and in turn AmpC activity as demonstrated by low β-lactamase activity of AmpC-F4:C3 and AmpC-F4:C6 and the intermediate activity of AmpC-F2 (tables 4.2, 4.4, 4.5).

On line databases (Benson et al, 2009; Sayers et al, 2009; Winsor et al, 2011) showed that there are a total number of 179 SNPs, which include 80 silent SNPs and 99 missense SNPs, along the total length of Pae-*ampC* (PA4110) gene, representing about 14,99 SNPs, involving 8,29 silent SNPs and 6,70 missense SNPs, per gene length unit. These values are largely about the mean value for Pseudomonas SNPs. Also, it was found that SNPs changes did not take place within the active site residues and neither in amino acids (e.g. N70 and R76) responsible for interaction with C3 and C4 of β-lactam nucleus. It was reported in some *P. aeruginosa* isolates that some amino acid mutations (e.g. A97V and T105A) in the region close to the active site Ser64 in some clinical *ampC* variants (e.g. PDC-2 variant with G27D, A97V, T105A, and V205L substitutions) enhanced the hydrolytic activity of AmpC into an extended spectrum AmpC cephalosporinases activity, ESAC (Rodriguez-Martinez et al, 2009). On the other hand, mutations in active site residues results in decreased β-lactamase activity (Jacoby, 2009). Similarly, K67R mutant displayed lower β-lactamase activity and minimal conformational changes compared to the wild type AmpC (Chen et al, 2009). Conversely, all these missense SNPs must indicate adaptations to change the global structure to adapt the active site to new substrates, without changes on the essential and well conserved catalytic residues.

In Pseudomonas transformants of pUCP-F3 and pUCP-F4, the β-lactamase activity of AmpC-F4 was 10-times higher than that of AmpC-F3, which may be due to the low expression, instability or the misfolding of this second form (table 4.3; fig. 4.6). Although AmpC-F4 was

detected by SDS-PAGE and western blot at a very high level in *E. coli* Bl21(DE3) and very low level in all PAO1 strains , the bacterial resistance of Pae transformants was largely higher than those of BL21(DE3) as seen by resistance of all Pae/pUCP-F4 transformants (table 4.6) to FOX, AMC, CRO and TIC in comparison of resistance of Bl21(DE3)/pET-F4 transformants (table 4.5) to AMC and moderate resistance to FOX which may be explained by more active and higher AmpC folding in homologous PAO1 strains rather than in heterologous Bl21(DE3).

5.2.4. The secondary DD-peptidase activity was clear with AmpC-F3 rather than the other studied AmpC forms

Our data proved basically previous suggestions (Bishop & Weiner, 1992; Hall & Barlow, 2004; Joris et al, 1988; Kong et al, 2010; Sauvage et al, 2008) that AmpC can produce DD-peptidase activity (EPase and/or CPase) which can be inferred or clearly observed from the following observations on the HPLC analysis of PG composition and muropeptides: 1) The DD-EPase activity could be deduced from the increase in monomers, anhydromuropeptides and pentapeptides in parallel with the decrease in dimers upon AmpC expression in Bl21(DE3)/pET-*ampC* in vivo with most of AmpC forms (table 4.7), and also from in vitro analysis with whole PG of CS109 and DV900 with AmpC-F3 form only (table 4.10a). 2) The DD-CPase activity could be inferred from the increase in M4 and decrease in M5, D44, D45, T445, D45N and T445N beyond incubation of purified AmpC-F3 with the whole DV900-PG (table 4.10b) and the hydrolysis of individual dimeric muropeptides, D44 and D45, after incubation with AmpC-F3 (fig. 4.9, 4.10). Our data, also show that the produced mature form (AmpC-F3) has the highest β-lactamase activity in vitro (V_{max}=100 µM) which was very high (8-fold or more) compared to the other AmpC forms (table 4.4), also it was the only AmpC form having DD-peptidase activity (DD-EPase) in vitro and it had inferred DD-CPase and DD-EPase in vitro higher than the other forms. These data indicate that the active site in AmpC-F3 has high accommodation, folding and flexibility permitting higher binding affinity and faster reaction with its β-lactam substrates and also with some PG muropeptides which are substrates for LMM-PBPs (DD-peptidases), the enzymes of the PG metabolism which have a close structural similarity with AmpC β-lactamases (Hall & Barlow, 2004; Sauvage et al, 2008). On the other hand, orthologous of Eco-PBP5 are known as been the main DD-CPases of the different bacteria, and it was reported that the mature form of Pae-PBP5 (PAO sPBP5) was produced and characterized having both a DD-CPase and wide spectrum β-lactamase activity (Smith et al, 2013). That result is in good accordance with our data, and allows highlighting two things; firstly, the production of the soluble mature form can display higher activity to its common substrates and can

increase the affinity to other secondary or low-affinity substrates. Furthermore, these findings may explain that both of class C serine β-lactamases and DD-peptidases have a common ancestor and how β-lactamases were evolved from the DD-peptidases (Hall & Barlow, 2004). Our data highlighted the other side of AmpC activity and physiological function concerning its ancestor DD-peptidases (PBPs) which were clustered together in one grouped (COG1680) by phylogenetic classification of proteins encoded in complete genomes (Tatusov et al, 2003).

5.2.5. AmpC-F3 crystallization & obstacles on the way!

Recently, crystal structures of Pae-AmpC in native form and bound to avibactam (non-β-lactam inhibitor) and bound to aztreonam (β-lactam monobactam) were developed using vapor diffusion in hanging drop setting (Lahiri et al, 2014; Lahiri et al, 2013). These crystal structures showed that conserved domains and active site residues of Pae-AmpC comprise amino acids Ser64* (catalytic residue), Lys67, Gln120, Tyr150, Asn152, Lys315, Thr316 and Asn346 which are conserved in most of AmpC β-lactamases with a little exceptional changes in some amino acids among other species (e.g. Asn346, the most variable residue) (Lahiri et al, 2014). In that study, they used pET-9a vector for cloning, Bl21(DE3) as a host strain which was grown in auto-inducing medium ZYP-5052 at 37 °C for 48 hours and for purification they used cationic chromatography and gel filtration which is somehow different from our procedure for purification of AmpC-F3. Although at the end we had a protein concentration of AmpC-F3 very close to what was used in the former study and crystallographers adopted the same techniques used in that work but, unfortunately we did not get crystals of AmpC-F3 by the time of submission of this thesis, which may be due to the instability and the degradation of this AmpC-F3 form (with poly-His tag). Also, the produced AmpC-F3-TEV (without poly-His tag) after TEV protease treatment was insoluble due to unclear reasons, may be misfolding, (Costa et al, 2014) and we had to use sarkosyl as ionic solvent for resuspension (Seddon et al, 2004), which added another difficulty to AmpC crystallization. His-tag terminal peptide stem may affect the protein structure and in turn the formation of protein crystals (Rosano & Ceccarelli, 2014; Smyth et al, 2003; Terpe, 2003). So, cloning and purification of AmpC-F3 that could produce a stable protein form without His-tag would be required. Moreover, 3D structure for AmpC-F3 would give us a clue for the peptidase activity of this form, and the required adaptation of the active site of a β-lactamase for accommodation a muropeptide substrate.

5.3. Role of *Pseudomonas aeruginosa* LMM-PBPs in PG composition, β-lactam resistance and ampC regulation in *P. aeruginosa*

5.3.1. Role of *P. aeruginosa* LMM-PBPs in cell wall physiology

Previous analyses of the *P. aeruginosa* cell membrane identified eight proteins able to bind H^3-benzylpenicillin or I^{125}-ampicillin, (PBP1a, PBP1b PBP2, PBP3, PBP3b PBP4, PBP5 and PBP7) and in silico analysis revealed the presence of eight open reading frames annotated as potential penicillin-binding proteins (Liao & Hancock, 1997; Song et al, 1998; Weigel et al, 1994). In this study we have used fluorescence-labeled antibiotic (Bocillin-FL) to identified PBPs of wild type and mutants strains of PAO1 (fig. 4.13, 4.14). PBPs patterns of single and multiple deletion mutants correlated perfectly with the loss of the expected PBP for each mutant PBP4 (DacB), PBP5 (DacC) and PBP7 (PbpG) with the exception of the two mutants *PAOΔdacB* and *PAOΔdacBΔpbpG* which had undetected DacC band although it was clearly detected in their corresponding mutants with *ampC* deletion (PAOΔ*dacB*Δ*ampC* and PAOΔ*dacB*Δ*pbpG*Δ*ampC*), respectively. This apparently mysterious lost for DacC in these two mutants may be due to their high AmpC production, that cleaves the Bocillin-FL lowering the needed concentration for detection, mutations on the *dacC* gene, or low *dacC* expression. However, we have confirmed by DNA sequencing that there is no *dacC* mutations on these two mutants (*PAOΔdacB* and *PAOΔdacBΔpbpG*), and data of PG pentapeptide content of these strains, suggest a normal level of DacC (DD-CPase) produced. So, most plausible explanation is high production of β-lactamase activity on these mutant strains. Nevertheless, it will be interesting more future morphological and physiological studies to pursue and to compare the behavior of DacC in these two mutants with their corresponding *ampC* mutants (PAOΔ*dacB*Δ*ampC* and PAOΔ*dacB*Δ*pbpG*Δ*ampC*). Presumably, these data would give information on the implication of the protein on important cellular process, as it has been obtained by the orthologous PBP in *E. coli*. These PBPs (DacB, DacC and PbpG) belong to the class C LMM-PBPs, type 4, type 5 and type 7, respectively. All PBPs in these subclasses have DD-endopeptidase and/or DD-carboxypeptidase. Largest changes in peptidoglycan structure (increase in pentapeptide content) were observed for the triple mutant, DacB-DacC-PbpG, with a structure similar to the nine-PBPs deletion mutant of *E. coli*, where all DD-endopeptidase and DD-carboxypeptidase activities were depleted causing aberrant cellular morphology in *E. coli* (Vega & Ayala, 2006). So, these three PBPs must represent the major endolytic armory of *P. aeruginosa*. Crystal structure of PaePBP5 (DacC) reveals a protein fold that is highly similar to the related *E. coli* PBP5 and PBP6, and also more closely resemble features seen previously only in the class A β-lactamases (Smith et

al, 2013). Gram-negative bacteria most often have a major type-5 PBP which is the most abundant PBP they produce (Sauvage et al, 2008). The most highly expressed PBP in *P. aeruginosa* membranes is also PBP5 (Noguchi et al, 1979) and as it is also shown in this work. It has been recently shown that PBP5 is a DD-carboxypeptidase that preferentially degrades low-molecular-weight substrates (Smith et al, 2013). In this work we confirm that PBP5 is the major DD-carboxypeptidase in *P. aeruginosa*, as evidenced by the fact that of the three single LMM-PBP mutants only *dacC* led significantly increased pentapeptide levels. Moreover, our results indicate that DacB plays a significant role as DD-carboxypeptidase when DacC is absent and that the DD-carboxypeptidase activity of PbpG is only apparent when both, DacC and DacB, are inactivated. On the other hand, the peptidoglycan structure of *dacB* and *pbpG* single and double mutants indicated that *P. aeruginosa* PBP4 and PBP7 have DD-endopeptidase activity as previously suggested for *E. coli* (Korat et al, 1991).

No major effect on cell morphology of growth parameters was seen for any of single, double or triple mutants (fig. 4.12), suggesting that major changes observed in the peptidoglycan structure do not affect significantly the morphology of the cell under laboratory conditions. However in *E. coli*, it was reported that PBP5 inactivation was the only single mutation of LMM PBPs to produce aberrant cellular shape, but further inactivation of PBP6 or PBP4 and PBP7 caused more deformation in cell morphology (Meberg et al, 2004; Nelson & Young, 2000; Nelson & Young, 2001). In parallel to our findings within *P. aeruginosa* (fig. 4.11), it was found in *E. coli* that multiple mutants of all possible LMM PBPs did not affect their growth curves in LB medium at 37°C and the cells were viable (Denome et al, 1999; Vega & Ayala, 2006). However, the *in vivo* role, and particularly the impact on virulence, of *P. aeruginosa* LMW PBPs still needs to be explored.

5.3.2. Role of *P. aeruginosa* LMM-PBPs in AmpC regulation and β-lactam resistance

It was reported previously that inactivation of Pae-*dacB* stimulated AmpR-dependent AmpC overexpression and β-lactam resistance (Cavallari et al, 2013; Moya et al, 2009); in this study, we found that among LMM-PBPs, the only single gene inactivation that triggered AmpC overexpression and β-lactam resistance was *dacB* inactivation but further inactivation of Pae-*dacC* and Pae-*pbpG*, as combined double and multiple deletions with *dacB*, led to an enormous increase on AmpC expression and in turn higher β-lactam resistance in PAO1 (table 4.12). Also, we found that among the constructed double mutants, PAOΔ*dacB*Δ*dacC* was the only one produced AmpC

overexpression (about 10-fold higher) and β-lactam resistance higher than the single mutant PAOΔ*dacB*, inferring a synergetic role of *dacC* in AmpC overexpression and β-lactam resistance. By the same way, *pbpG* inactivation in the double mutant PAOΔ*dacB*Δ*dacC* showed a maximal AmpC overexpression (about 3-fold higher), suggesting a secondary synergetic effect of *pbpG* in AmpC overexpression and β-lactam resistance. Our data showed that the synergetic behaviors of *dacC* and *pbpG* in AmpC expression were not helpful for AmpC overexpression without *dacB* inactivation. The increase of AmpC expression beyond FOX induction in the wild type and all PAO1 mutants was mainly due to the sensitivity of DacB to FOX as demonstrated in table 4.11. It was reported that the increase of anhydro-muropeptides and their binding to AmpR is the main effector of AmpC over-expression which also is regulated by the activities of the permeases AmpG and AmpP, the amidases AmpD, AmpDh2 and AmpDh3 and the hydrolase NagZ and generates β-lactam resistance in *P. aeruginosa* (Balasubramanian et al, 2012; Boudreau et al, 2012; Fisher & Mobashery, 2014; Jacobs et al, 1997; Johnson et al, 2013; Lister et al, 2009). Moreover, we found that the increase in anhydro-muropeptides was mostly accompanied with DacB inactivation (as single and combined forms) during high AmpC expression. Also, our data shows that DacB activity (on/off) alone or in addition to the activities of DacC and PbpG are critical for *ampC* expression in PAO1. Also, our results show however that DacC is the major DD-CPase, and that the DacC mutant is the only single LMM-PBP mutant producing a significant increase in pentapeptide levels (up to 4.4-fold higher than wild-type PAO1). Thus, increased PG pentapeptide levels, and neither apparently any other effect on peptidoglycan structure (table 4.13), do not explain, at least for *P. aeruginosa*, the major role of PBP4 in AmpC induction. Whether the PBP4 effect is driven by significantly increasing periplasmic soluble anhydromuropeptides levels needs still to be explored. Nevertheless, our results suggest that increased peptidoglycan pentapeptide levels, explain the major role of PBP5 in *ampC* expression when PBP4 is absent. Indeed, except for the specific effect of PBP4, a correlation between peptidoglycan pentapeptide levels and *ampC* expression was documented (Tayler et al, 2010).

Our data showed that MICs for the antipseudomonal penicillins (piperacillin), cephalosporins (cefotaxime, ceftazidime, and cefepime) and monobactams (aztreonam) correlated well with *ampC* expression data (table 4.12); they were significantly increased in the DacB mutant and further increased in the DacB-DacC double mutant. On the other hand, unlike for *ampC* expression, β-lactam resistance was not further increased in the triple DacB-DacC-PbpG mutant. Besides the obvious effect on resistance driven by the impact on *ampC* expression, we asked whether *P. aeruginosa* LMM PBPs had a direct effect on β-lactam susceptibility. For this purpose, we analyzed the β-lactams MICs for all combinations of LMM PBPs and AmpC mutants. As

expected (Livermore, 1992; Zamorano et al, 2011), the inactivation of AmpC in wild-type PAO1 produced a marked increase in the susceptibility of strong AmpC-inducer β-lactams, including the carbapenems, cefoxitin and ampicillin, whereas the MICs of weak AmpC-inducer β-lactams (antipseudomonal penicillins, cephalosporins and monobactams) were not significantly modified. Remarkably, the MICs for nearly all β-lactams were lower in the DacC-AmpC mutant compared to the single AmpC mutant, and this effect was further enhanced in the DacB-DacC-PbpG-AmpC mutant, indicating that LMM PBPs, particularly DacC, play a role in the intrinsic level of β-lactam resistance in *P. aeruginosa*. Our results are therefore in agreement with recent studies suggesting that *E. coli* LMM PBPs, particularly PBP5, play a role in intrinsic β-lactam resistance (Sarkar et al, 2010; Sarkar et al, 2011). Purified *E. coli* PBP5 failed to show significant β-lactamase activity and therefore it was concluded that the role of this PBP in intrinsic β-resistance could be consequence of β-lactam trapping. However, interestingly, the recently crystalized *P. aeruginosa* PBP5 does show certain broad spectrum (including penicillins, cephalosporins and carbapenems) β-lactamase activity (Smith et al, 2013). Therefore, the observed effect of PBP5 in *P. aeruginosa* intrinsic resistance is expected to result from both, trapping and hydrolysis of β lactams.

We found that the carbapenems IMI and MER were resistant to hydrolysis by the wild type AmpC as the observed MICs were 0.5 µg/ml for both of them in both of the wild type PAO1 and in the triple mutant PAOΔ*dacB*Δ*dacC*Δ*pbpG* although their corresponding AmpC expression was 347 and 5742, respectively, under induction conditions (table 4.12). Resistance to carbapenems by AmpC overproduction in *P. aeruginosa* requires additional resistance mechanisms efflux pump overproduction, decreased OprD, and/or production of a class A/class B carbapenemase (Lister et al, 2009; Rodriguez-Rojas et al, 2013). Also, it was reported that OprD inactivation alone is known to result in clinical imipenem resistance which supports the previous idea of the ability of combined resistance mechanisms to develop carbapenems resistance (Gutierrez et al, 2007).

5.4. Activities of DacB, DacC and PbpG are not essential for recovery of rod shape in imipenem-induced spheroplasts in *P. aeruginosa*

It was described that imipenem-supplemented media caused transition of the rod shaped wild type *P. aeruginosa* cells into cell wall-defective spherical shaped cell (Monahan et al, 2014). We achieved the same results with the wild type PAO1 and the mutant PAOΔ*dacB*Δ*dacC*Δ*pbpG* Δ*ampC* which were able to produce round cells (spheroplasts) after 4 hours incubation with IMI, and both of them were able to recover their normal rod shape after elimination of IMI, inferring that activities of DacB, DacC and PbpG are not necessary for recovery of rod shape as shown by microscopic examination (fig 4.15). Similarly, all other single and combined Pae mutants of *dacB*,

dacC, *pbpG* and *ampC* that were constructed in this study displayed the same behavior in the ability of IMI-induced spheroplasts formation and rod shape recovery upon growth in imipenem-free media (data not shown). By comparing the PG composition of round cells and the recovered rod shaped ones in the wild type and in the final quadruple mutant, we found that PG of round cells contained unusual high amount of M3, which may be related to the high amount of anhydromuropeptides and shorter PG length. Also we found that after recovery of rod shape, PG contained a normal ratio of M3 and other muropeptides with normal PG length (table 4.15a, 4.15b). Also, we found that analysis of PBPs pattern in round cells by Bocillin-FL of both the wild type PAO1 and PAOΔ*ampC* displayed loss of bands of PBP1a, PBP1b, PBP2, DacB and PbpG with low intensity of DacC, although they were detected in their recovered rod cells (fig 4.16). We found that imipenem was able to block these PBPs in vitro which may explain that they were also blocked in the IMI-induced spheroplasts in vivo. Inhibition of PBPs by imipenem caused spherophast formation due to blocking of PG synthesizing machinery and degradation of their cell wall. PG of these Pae spheroplasts was less than one tenth when compared with normal untreated cells and had large increase in anhydromuropeptides (PG glycan chains ends, susceptible of degradation). Moreover, it has an increase in M3 which can be explained by the activity of increased LD-CPase which are produced when cell walls are degraded (Korza & Bochtler, 2005). Also the decrease in pentapeptides and the increase in PG crosslinking can be explained by blocking of DD-CPase activity (i.e. DacC) and the DD-EPase activity (i.e. DacB and PbpG), respectively. Also, the decrease in pentapeptides (PG donors for transpeptidation reaction) resulted in low values of PG length in spheroplasts. After elimination of imipenem from the growth medium Pae cells, PG synthesizing machinery was back to work normally and was able to re-build the rod shaped PG and so Pae cells were able to revert into shape again. Also, in PG of the recovered Pae cells, M3 returned to its normal level because it was used for the construction of new PG subunits (Johnson et al, 2013). It was reported that inactivation of PBP2 in *E. coli* by amdinocillin (β-lactam antibiotic) led to inhibition of cell elongation and the formation of osmotically stable round cells with one half less in their murein content when compared with normal cells (de Pedro et al, 2001) which is in according to what is described for inhibition of PBP2 by mecillinam in stimulation of round cell formation in both of *E. coli* and *P. aeruginosa* (Noguchi et al, 1979). Similarly, it was reported that inactivation of PBP2 and PBP3 by mecillinam and aztreonam, respectively, produced enlarged spheres however inactivation of both of PBP1a and PB1b was lethal in *E. coli* (Denome et al, 1999). Likewise, it was reported that carbapenems (e.g. imipenem, meropenem) showed strong affinities to PBP2 of *E. coli* and *P. aeruginosa*, PBP1a of *E. coli* and PBP1b of *P. aeruginosa* (Yang et al, 1995).

It was settled that PBP1a, PBP1Bb and PBP2 are responsible for PG elongation and insertion of newly formed PG units into the old PG network; PBP3 is responsible mainly for cell division, and LMM-PBPs (DacB, DacC and PbpG) participate in PG maturation and recycling (Sauvage et al, 2008). In *E. coli*, it was identified that PBP1b, PBP5 and PBP6 are among eight proteins identified for regeneration of normal rod shape from *E. coli* spheroplasts (formed by the effect of lysozyme) which failed in the recovery process by loss of these proteins (Ranjit & Young, 2013; Weiss, 2013). In that study, it was demonstrated that *E. coli* spheroplasts of PBP1b mutant were unable to recover the rod shape but rather become enlarged and lysed; spheroplasts of mutants of PBP5 and PBP6 displayed recovery of defective shapes however spheroplasts of mutant PBP4 or PBP7 regenerated their normal rod shape (Ranjit & Young, 2013). In our study, we described that combined deletions of *dacB*, *dacC* and *pbpG* did not remarkably affect morphology of *P. aeruginosa* and mutants still retain their rod shape. Consequently, we can conclude that the formation of cell wall-defective spheroplasts in *Pseudomonas aeruginosa* after imipenem induction was due to the inhibition of PBPs, especially HMM-PBPs (PBP1a, PBP1b, PBP2 and PBP3). Also, the ability of spheroplasts of the quadruple mutant PAOΔ*dacB*Δ*dacC*Δ*pbpG*Δ*ampC* to revert into rod shape confirms that DacB, DacC and PbpG are dispensable and unessential for this reversion process in *Pseudomonas aeruginosa*.

Conclusions (in English) & Conclusiones (in Spanish)

6. Conclusions

- **The single amino acid mutations P^{243}→L and I^{51}→T, in AmpC-F1:C3 and AmpC-F1:C6, respectively, caused a large decrease β-lactamase activity.**
- **AmpC-F4 (precursor form) produced higher β-lactamase activity in vivo, most probably due to correct localization, while AmpC-F3 (mature form) produced β-lactamase activity of 8-fold higher than AmpC-F4 in vitro.**
- **AmpC β-lactamase in Pseudomonas can comprise a secondary DD-EPase or DD-CPase activity.**
- **The LMM-PBPs DacB and PbpG are more sensitive to FOX (*ampC* inducer) than DacC.**
- **DacC is the main DD-CPase in *P. aeruginosa, and* DacB and PbpG were suggested to elicit some DD-CPase in the mutant PAOΔ*dacC.***
- **Fluctuations in DacB activity are critical for *ampC* regulation.**
- ***dacB* inactivation was the only single mutation of LMM-PBPs found to trigger AmpC overproduction and β-lactam resistance.**
- **Inactivation of both of *dacC* and *pbpG* can stimulate large AmpC overexpression only when *dacB* was inactivated (synergetic effect).**
- **Activities of DacB, DacC and PbpG are not essential for recovery of rod shape in imipenem-induced *P. aeruginosa* spheroplasts.**

- **Las mutaciones individuales de aminoácido P243 → L y I51 → T, en AmpC-F1: C3 y AmpC-F1: C6, respectivamente, causaron una gran disminución de la actividad β-lactamasa.**
- **AmpC-F4 (forma precursora) produjo una mayor actividad de β-lactamasa en vivo, probablemente debido a su correcta locaclización, mientras que AmpC-F3 (forma madura) produjo una actividad β-lactamasa 8 veces superior a AmpC-F4 in vitro.**
- **AmpC en Pseudomonas puede tener una actividad DD-EPase/DD-CPase secundaria.**
- **Las LMM-PBPs DacB y PbpG son más sensibles a FOX (inductor de *ampC*) que DacC.**
- **DacC es la enzima DD-CPase principal en *P. aeruginosa,* mientras que DacB y PbpG pueden compensar la pérdida de actividad DD-CPase en el mutante PAOΔ*dacC***
- **Las fluctuaciones en la actividad enzimática de DacB son críticas para la regulación de *ampC*.**
- **La inactivación de *dacB* fue la única mutación individual de LMM-PBPs capaz de desencadenar la sobreproducción de AmpC y la resistencia a β-lactámicos.**
- **La inactivación de los genes *dacC* y *pbpG* pueden estimular la sobreexpresión de AmpC sólo cuando *dacB* fue simultáneamente inactivado (efecto sinérgico).**
- **Las actividades de DacB, DacC y PbpG no son esenciales para la recuperación de la forma bacilar a partir de esferoplastos de *P. aeruginosa* inducidos por imipenem.**

Bibliography

Bibliography

Ambler RP (1980) The structure of beta-lactamases. *Philosophical transactions of the Royal Society of London Series B, Biological sciences* **289:** 321-331

Balasubramanian D, Schneper L, Merighi M, Smith R, Narasimhan G, Lory S, Mathee K (2012) The regulatory repertoire of Pseudomonas aeruginosa AmpC ss-lactamase regulator AmpR includes virulence genes. *PloS one* **7:** e34067

Becker DE (2013) Antimicrobial drugs. *Anesthesia progress* **60:** 111-123

Benson DA, Karsch-Mizrachi I, Lipman DJ, Ostell J, Sayers EW (2009) GenBank. *Nucleic acids research* **37:** D26-31

Bishop RE, Weiner JH (1992) Coordinate regulation of murein peptidase activity and AmpC beta-lactamase synthesis in Escherichia coli. *FEBS letters* **304:** 103-108

Bolhuis A, Aldrich-Wright JR (2014) DNA as a target for antimicrobials. *Bioorganic chemistry* **55:** 51-59

Borisova M, Gisin J, Mayer C (2014) Blocking peptidoglycan recycling in Pseudomonas aeruginosa attenuates intrinsic resistance to fosfomycin. *Microbial drug resistance* **20:** 231-237

Boudreau MA, Fisher JF, Mobashery S (2012) Messenger functions of the bacterial cell wall-derived muropeptides. *Biochemistry* **51:** 2974-2990

Bush K, Jacoby GA (2010) Updated functional classification of beta-lactamases. *Antimicrobial agents and chemotherapy* **54:** 969-976

Bush K, Jacoby GA, Medeiros AA (1995) A functional classification scheme for beta-lactamases and its correlation with molecular structure. *Antimicrobial agents and chemotherapy* **39:** 1211-1233

Cabot G, Bruchmann S, Mulet X, Zamorano L, Moya B, Juan C, Haussler S, Oliver A (2014) Pseudomonas aeruginosa ceftolozane-tazobactam resistance development requires multiple mutations leading to overexpression and structural modification of AmpC. *Antimicrobial agents and chemotherapy* **58:** 3091-3099

Cava F, Kuru E, Brun YV, de Pedro MA (2013) Modes of cell wall growth differentiation in rod-shaped bacteria. *Current opinion in microbiology* **16:** 731-737

Cava F, Lam H, de Pedro MA, Waldor MK (2011) Emerging knowledge of regulatory roles of D-amino acids in bacteria. *Cellular and molecular life sciences : CMLS* **68:** 817-831

Cavallari JF, Lamers RP, Scheurwater EM, Matos AL, Burrows LL (2013) Changes to its peptidoglycan-remodeling enzyme repertoire modulate beta-lactam resistance in Pseudomonas aeruginosa. *Antimicrobial agents and chemotherapy* **57:** 3078-3084

Clarke TB, Kawai F, Park SY, Tame JR, Dowson CG, Roper DI (2009) Mutational analysis of the substrate specificity of Escherichia coli penicillin binding protein 4. *Biochemistry* **48:** 2675-2683

Costa S, Almeida A, Castro A, Domingues L (2014) Fusion tags for protein solubility, purification and immunogenicity in Escherichia coli: the novel Fh8 system. *Frontiers in microbiology* **5:** 63

Crowe J, Bradshaw T (2010) Kinetcs: what affects the speed of a reaction? In *Chemistry For The Biosciences The Essential Concepts, Second Edition*, pp 439-497.

Chen Y, McReynolds A, Shoichet BK (2009) Re-examining the role of Lys67 in class C beta-lactamase catalysis. *Protein science : a publication of the Protein Society* **18:** 662-669

Chowdhury C, Ghosh AS (2011) Differences in active-site microarchitecture explain the dissimilar behaviors of PBP5 and 6 in Escherichia coli. *Journal of molecular graphics & modelling* **29:** 650-656

Chowdhury C, Nayak TR, Young KD, Ghosh AS (2010) A weak DD-carboxypeptidase activity explains the inability of PBP 6 to substitute for PBP 5 in maintaining normal cell shape in Escherichia coli. *FEMS microbiology letters* **303:** 76-83

Dalhoff A, Janjic N, Echols R (2006) Redefining penems. *Biochemical pharmacology* **71:** 1085-1095

de Pedro MA, Donachie WD, Holtje JV, Schwarz H (2001) Constitutive septal murein synthesis in Escherichia coli with impaired activity of the morphogenetic proteins RodA and penicillin-binding protein 2. *Journal of bacteriology* **183:** 4115-4126

Denome SA, Elf PK, Henderson TA, Nelson DE, Young KD (1999) Escherichia coli mutants lacking all possible combinations of eight penicillin binding proteins: viability, characteristics, and implications for peptidoglycan synthesis. *Journal of bacteriology* **181:** 3981-3993

Drawz SM, Bonomo RA (2010) Three decades of beta-lactamase inhibitors. *Clinical microbiology reviews* **23:** 160-201

Elander RP (2003) Industrial production of beta-lactam antibiotics. *Applied microbiology and biotechnology* **61:** 385-392

Fang X, Tiyanont K, Zhang Y, Wanner J, Boger D, Walker S (2006) The mechanism of action of ramoplanin and enduracidin. *Molecular bioSystems* **2:** 69-76

Fernandes R, Amador P, Prudêncio C (2013) β-Lactams: chemical structure, mode of action and mechanisms of resistance. *Reviews in Medical Microbiology* **24:** 7–17

Fisher JF, Mobashery S (2014) The sentinel role of peptidoglycan recycling in the beta-lactam resistance of the Gram-negative Enterobacteriaceae and Pseudomonas aeruginosa. *Bioorganic chemistry* **56C:** 41-48

Ghosh AS, Chowdhury C, Nelson DE (2008) Physiological functions of D-alanine carboxypeptidases in Escherichia coli. *Trends in microbiology* **16:** 309-317

Glauner B (1988) Separation and quantification of muropeptides with high-performance liquid chromatography. *Analytical biochemistry* **172:** 451-464

Glauner B, Holtje JV, Schwarz U (1988) The composition of the murein of Escherichia coli. *The Journal of biological chemistry* **263:** 10088-10095

Gomila M, Del Carmen Gallegos M, Fernandez-Baca V, Pareja A, Pascual M, Diaz-Antolin P, Garcia-Valdes E, Lalucat J (2013) Genetic diversity of clinical Pseudomonas aeruginosa isolates in a public hospital in Spain. *BMC microbiology* **13:** 138

Gonzalez-Leiza SM, de Pedro MA, Ayala JA (2011) AmpH, a bifunctional DD-endopeptidase and DD-carboxypeptidase of Escherichia coli. *Journal of bacteriology* **193:** 6887-6894

Gutierrez O, Juan C, Cercenado E, Navarro F, Bouza E, Coll P, Perez JL, Oliver A (2007) Molecular epidemiology and mechanisms of carbapenem resistance in Pseudomonas aeruginosa isolates from Spanish hospitals. *Antimicrobial agents and chemotherapy* **51:** 4329-4335

Hall BG, Barlow M (2004) Evolution of the serine beta-lactamases: past, present and future. *Drug resistance updates : reviews and commentaries in antimicrobial and anticancer chemotherapy* **7:** 111-123

Hall BG, Barlow M (2005) Revised Ambler classification of {beta}-lactamases. *The Journal of antimicrobial chemotherapy* **55:** 1050-1051

Hamed RB, Gomez-Castellanos JR, Henry L, Ducho C, McDonough MA, Schofield CJ (2013) The enzymes of beta-lactam biosynthesis. *Natural product reports* **30:** 21-107

Islam MR, Nagao J, Zendo T, Sonomoto K (2012) Antimicrobial mechanism of lantibiotics. *Biochemical Society transactions* **40:** 1528-1533

Jacobs C, Frere JM, Normark S (1997) Cytosolic intermediates for cell wall biosynthesis and degradation control inducible beta-lactam resistance in gram-negative bacteria. *Cell* **88:** 823-832

Jacoby GA (2009) AmpC beta-lactamases. *Clinical microbiology reviews* **22:** 161-182

Jia Z, O'Mara ML, Zuegg J, Cooper MA, Mark AE (2013) Vancomycin: ligand recognition, dimerization and super-complex formation. *The FEBS journal* **280:** 1294-1307

Johnson JW, Fisher JF, Mobashery S (2013) Bacterial cell-wall recycling. *Annals of the New York Academy of Sciences* **1277:** 54-75

Joris B, Ghuysen JM, Dive G, Renard A, Dideberg O, Charlier P, Frere JM, Kelly JA, Boyington JC, Moews PC, et al. (1988) The active-site-serine penicillin-recognizing enzymes as members of the Streptomyces R61 DD-peptidase family. *The Biochemical journal* **250:** 313-324

Juan C, Moya B, Perez JL, Oliver A (2006) Stepwise upregulation of the Pseudomonas aeruginosa chromosomal cephalosporinase conferring high-level beta-lactam resistance involves three AmpD homologues. *Antimicrobial agents and chemotherapy* **50:** 1780-1787

Kishida H, Unzai S, Roper DI, Lloyd A, Park SY, Tame JR (2006) Crystal structure of penicillin binding protein 4 (dacB) from Escherichia coli, both in the native form and covalently linked to various antibiotics. *Biochemistry* **45:** 783-792

Klockgether J, Munder A, Neugebauer J, Davenport CF, Stanke F, Larbig KD, Heeb S, Schock U, Pohl TM, Wiehlmann L, Tummler B (2010) Genome diversity of Pseudomonas aeruginosa PAO1 laboratory strains. *Journal of bacteriology* **192:** 1113-1121

Kong KF, Jayawardena SR, Indulkar SD, Del Puerto A, Koh CL, Hoiby N, Mathee K (2005) Pseudomonas aeruginosa AmpR is a global transcriptional factor that regulates expression of AmpC and PoxB beta-lactamases, proteases, quorum sensing, and other virulence factors. *Antimicrobial agents and chemotherapy* **49:** 4567-4575

Kong KF, Schneper L, Mathee K (2010) Beta-lactam antibiotics: from antibiosis to resistance and bacteriology. *APMIS : acta pathologica, microbiologica, et immunologica Scandinavica* **118:** 1-36

Korat B, Mottl H, Keck W (1991) Penicillin-binding protein 4 of Escherichia coli: molecular cloning of the dacB gene, controlled overexpression, and alterations in murein composition. *Molecular microbiology* **5:** 675-684

Korza HJ, Bochtler M (2005) Pseudomonas aeruginosa LD-carboxypeptidase, a serine peptidase with a Ser-His-Glu triad and a nucleophilic elbow. *The Journal of biological chemistry* **280:** 40802-40812

Lahiri SD, Johnstone M, Ross PL, McLaughlin R, Olivier NB, Alm RA (2014) Avibactam and class C beta-lactamases: mechanism of inhibition, conservation of binding pocket and implications for resistance. *Antimicrobial agents and chemotherapy* **58:** 5704-5713

Lahiri SD, Mangani S, Durand-Reville T, Benvenuti M, De Luca F, Sanyal G, Docquier JD (2013) Structural insight into potent broad-spectrum inhibition with reversible recyclization mechanism: avibactam in complex with CTX-M-15 and Pseudomonas aeruginosa AmpC beta-lactamases. *Antimicrobial agents and chemotherapy* **57:** 2496-2505

Liao X, Hancock RE (1997) Identification of a penicillin-binding protein 3 homolog, PBP3x, in Pseudomonas aeruginosa: gene cloning and growth phase-dependent expression. *Journal of bacteriology* **179:** 1490-1496

Lister PD, Wolter DJ, Hanson ND (2009) Antibacterial-resistant Pseudomonas aeruginosa: clinical impact and complex regulation of chromosomally encoded resistance mechanisms. *Clinical microbiology reviews* **22:** 582-610

Livermore DM (1992) Interplay of impermeability and chromosomal beta-lactamase activity in imipenem-resistant Pseudomonas aeruginosa. *Antimicrobial agents and chemotherapy* **36:** 2046-2048

Lyczak JB, Cannon CL, Pier GB (2000) Establishment of Pseudomonas aeruginosa infection: lessons from a versatile opportunist. *Microbes and infection / Institut Pasteur* **2:** 1051-1060

Mah TF, Pitts B, Pellock B, Walker GC, Stewart PS, O'Toole GA (2003) A genetic basis for Pseudomonas aeruginosa biofilm antibiotic resistance. *Nature* **426:** 306-310

Mammeri H, Poirel L, Fortineau N, Nordmann P (2006) Naturally occurring extended-spectrum cephalosporinases in Escherichia coli. *Antimicrobial agents and chemotherapy* **50:** 2573-2576

Meberg BM, Paulson AL, Priyadarshini R, Young KD (2004) Endopeptidase penicillin-binding proteins 4 and 7 play auxiliary roles in determining uniform morphology of Escherichia coli. *Journal of bacteriology* **186:** 8326-8336

Monahan LG, Turnbull L, Osvath SR, Birch D, Charles IG, Whitchurch CB (2014) Rapid conversion of Pseudomonas aeruginosa to a spherical cell morphotype facilitates tolerance to carbapenems and penicillins but increases susceptibility to antimicrobial peptides. *Antimicrobial agents and chemotherapy* **58:** 1956-1962

Moya B, Dotsch A, Juan C, Blazquez J, Zamorano L, Haussler S, Oliver A (2009) Beta-lactam resistance response triggered by inactivation of a nonessential penicillin-binding protein. *PLoS pathogens* **5:** e1000353

Moya B, Juan C, Alberti S, Perez JL, Oliver A (2008) Benefit of having multiple ampD genes for acquiring beta-lactam resistance without losing fitness and virulence in Pseudomonas aeruginosa. *Antimicrobial agents and chemotherapy* **52:** 3694-3700

Nelson DE, Young KD (2000) Penicillin binding protein 5 affects cell diameter, contour, and morphology of Escherichia coli. *Journal of bacteriology* **182:** 1714-1721

Nelson DE, Young KD (2001) Contributions of PBP 5 and DD-carboxypeptidase penicillin binding proteins to maintenance of cell shape in Escherichia coli. *Journal of bacteriology* **183:** 3055-3064

Nikolaidis I, Favini-Stabile S, Dessen A (2014) Resistance to antibiotics targeted to the bacterial cell wall. *Protein science : a publication of the Protein Society* **23:** 243-259

Noguchi H, Matsuhashi M, Mitsuhashi S (1979) Comparative studies of penicillin-binding proteins in Pseudomonas aeruginosa and Escherichia coli. *European journal of biochemistry / FEBS* **100:** 41-49

Ostash B, Walker S (2010) Moenomycin family antibiotics: chemical synthesis, biosynthesis, and biological activity. *Natural product reports* **27:** 1594-1617

Papp-Wallace KM, Endimiani A, Taracila MA, Bonomo RA (2011) Carbapenems: past, present, and future. *Antimicrobial agents and chemotherapy* **55:** 4943-4960

Pratt RF (2008) Substrate specificity of bacterial DD-peptidases (penicillin-binding proteins). *Cellular and molecular life sciences : CMLS* **65:** 2138-2155

Pucci MJ, Bush K (2013) Investigational antimicrobial agents of 2013. *Clinical microbiology reviews* **26:** 792-821

Quenee L, Lamotte D, Polack B (2005) Combined sacB-based negative selection and cre-lox antibiotic marker recycling for efficient gene deletion in pseudomonas aeruginosa. *BioTechniques* **38:** 63-67

Ranjit DK, Young KD (2013) The Rcs stress response and accessory envelope proteins are required for de novo generation of cell shape in Escherichia coli. *Journal of bacteriology* **195:** 2452-2462

Reith J, Mayer C (2011) Peptidoglycan turnover and recycling in Gram-positive bacteria. *Applied microbiology and biotechnology* **92:** 1-11

Rodriguez-Martinez JM, Poirel L, Nordmann P (2009) Extended-spectrum cephalosporinases in Pseudomonas aeruginosa. *Antimicrobial agents and chemotherapy* **53:** 1766-1771

Rodriguez-Rojas A, Rodriguez-Beltran J, Couce A, Blazquez J (2013) Antibiotics and antibiotic resistance: a bitter fight against evolution. *International journal of medical microbiology : IJMM* **303:** 293-297

Rosano GL, Ceccarelli EA (2014) Recombinant protein expression in Escherichia coli: advances and challenges. *Frontiers in microbiology* **5:** 172

Sarkar SK, Chowdhury C, Ghosh AS (2010) Deletion of penicillin-binding protein 5 (PBP5) sensitises Escherichia coli cells to beta-lactam agents. *International journal of antimicrobial agents* **35:** 244-249

Sarkar SK, Dutta M, Chowdhury C, Kumar A, Ghosh AS (2011) PBP5, PBP6 and DacD play different roles in intrinsic beta-lactam resistance of Escherichia coli. *Microbiology* **157:** 2702-2707

Sauvage E, Kerff F, Terrak M, Ayala JA, Charlier P (2008) The penicillin-binding proteins: structure and role in peptidoglycan biosynthesis. *FEMS microbiology reviews* **32:** 234-258

Sayers EW, Barrett T, Benson DA, Bryant SH, Canese K, Chetvernin V, Church DM, DiCuccio M, Edgar R, Federhen S, Feolo M, Geer LY, Helmberg W, Kapustin Y, Landsman D, Lipman DJ, Madden TL, Maglott DR, Miller V, Mizrachi I, Ostell J, Pruitt KD, Schuler GD, Sequeira E, Sherry ST, Shumway M, Sirotkin K, Souvorov A, Starchenko G, Tatusova TA, Wagner L, Yaschenko E, Ye J (2009) Database resources of the National Center for Biotechnology Information. *Nucleic acids research* **37:** D5-15

Seddon AM, Curnow P, Booth PJ (2004) Membrane proteins, lipids and detergents: not just a soap opera. *Biochimica et biophysica acta* **1666:** 105-117

Smith JD, Kumarasiri M, Zhang W, Hesek D, Lee M, Toth M, Vakulenko S, Fisher JF, Mobashery S, Chen Y (2013) Structural analysis of the role of Pseudomonas aeruginosa penicillin-binding protein 5 in beta-lactam resistance. *Antimicrobial agents and chemotherapy* **57:** 3137-3146

Smyth DR, Mrozkiewicz MK, McGrath WJ, Listwan P, Kobe B (2003) Crystal structures of fusion proteins with large-affinity tags. *Protein science : a publication of the Protein Society* **12:** 1313-1322

Song J, Xie G, Elf PK, Young KD, Jensen RA (1998) Comparative analysis of Pseudomonas aeruginosa penicillin-binding protein 7 in the context of its membership in the family of low-molecular-mass PBPs. *Microbiology* **144** 975-983

Stover CK, Pham XQ, Erwin AL, Mizoguchi SD, Warrener P, Hickey MJ, Brinkman FS, Hufnagle WO, Kowalik DJ, Lagrou M, Garber RL, Goltry L, Tolentino E, Westbrock-Wadman S, Yuan Y, Brody LL, Coulter SN, Folger KR, Kas A, Larbig K, Lim R, Smith K, Spencer D, Wong GK, Wu Z, Paulsen IT, Reizer J, Saier MH, Hancock RE, Lory S, Olson MV (2000) Complete genome sequence of Pseudomonas aeruginosa PAO1, an opportunistic pathogen. *Nature* **406:** 959-964

Strateva T, Yordanov D (2009) Pseudomonas aeruginosa - a phenomenon of bacterial resistance. *Journal of medical microbiology* **58:** 1133-1148

Tan JS, File TM, Jr. (1995) Antipseudomonal penicillins. *The Medical clinics of North America* **79:** 679-693

Tatusov RL, Fedorova ND, Jackson JD, Jacobs AR, Kiryutin B, Koonin EV, Krylov DM, Mazumder R, Mekhedov SL, Nikolskaya AN, Rao BS, Smirnov S, Sverdlov AV, Vasudevan S, Wolf YI, Yin JJ, Natale DA (2003) The COG database: an updated version includes eukaryotes. *BMC bioinformatics* **4:** 41

Tayler AE, Ayala JA, Niumsup P, Westphal K, Baker JA, Zhang L, Walsh TR, Wiedemann B, Bennett PM, Avison MB (2010) Induction of beta-lactamase production in Aeromonas hydrophila is responsive to beta-lactam-mediated changes in peptidoglycan composition. *Microbiology* **156:** 2327-2335

Terpe K (2003) Overview of tag protein fusions: from molecular and biochemical fundamentals to commercial systems. *Applied microbiology and biotechnology* **60:** 523-533

Tseng YY, Liou JM, Hsu TL, Cheng WC, Wu MS, Wong CH (2014) Development of bacterial transglycosylase inhibitors as new antibiotics: moenomycin A treatment for drug-resistant Helicobacter pylori. *Bioorganic & medicinal chemistry letters* **24:** 2412-2414

Tsutsumi Y, Tomita H, Tanimoto K (2013) Identification of novel genes responsible for overexpression of ampC in Pseudomonas aeruginosa PAO1. *Antimicrobial agents and chemotherapy* **57:** 5987-5993

Typas A, Banzhaf M, Gross CA, Vollmer W (2012) From the regulation of peptidoglycan synthesis to bacterial growth and morphology. *Nature reviews Microbiology* **10:** 14

Usher KC, Blaszczak LC, Weston GS, Shoichet BK, Remington SJ (1998) Three-dimensional structure of AmpC beta-lactamase from Escherichia coli bound to a transition-state analogue: possible implications for the oxyanion hypothesis and for inhibitor design. *Biochemistry* **37:** 16082-16092

Vega D, Ayala JA (2006) The DD-carboxypeptidase activity encoded by pbp4B is not essential for the cell growth of Escherichia coli. *Archives of microbiology* **185:** 23-27

Vollmer W, Bertsche U (2008) Murein (peptidoglycan) structure, architecture and biosynthesis in Escherichia coli. *Biochimica et biophysica acta* **1778:** 1714-1734

Vollmer W, Blanot D, de Pedro MA (2008a) Peptidoglycan structure and architecture. *FEMS microbiology reviews* **32:** 149-167

Vollmer W, Holtje JV (2004) The architecture of the murein (peptidoglycan) in gram-negative bacteria: vertical scaffold or horizontal layer(s)? *Journal of bacteriology* **186:** 5978-5987

Vollmer W, Joris B, Charlier P, Foster S (2008b) Bacterial peptidoglycan (murein) hydrolases. *FEMS microbiology reviews* **32:** 259-286

Vollmer W, Seligman SJ (2010) Architecture of peptidoglycan: more data and more models. *Trends in microbiology* **18:** 59-66

Walsh C (2003) Where will new antibiotics come from? *Nature reviews Microbiology* **1:** 65-70

Weigel LM, Belisle JT, Radolf JD, Norgard MV (1994) Digoxigenin-ampicillin conjugate for detection of penicillin-binding proteins by chemiluminescence. *Antimicrobial agents and chemotherapy* **38:** 330-336

Weiss DS (2013) Escherichia coli shapeshifters. *Journal of bacteriology* **195:** 2449-2451

West SE, Schweizer HP, Dall C, Sample AK, Runyen-Janecky LJ (1994) Construction of improved Escherichia-Pseudomonas shuttle vectors derived from pUC18/19 and sequence of the region required for their replication in Pseudomonas aeruginosa. *Gene* **148:** 81-86

Wiley J, Sons. (1996) Metal-Chelate Affinity Chromatography. *Current Protocols in Molecular Biology*, Vol. 36, pp. 10.11.10-10.11.24.

Wiley J, Sons (2000) Agarose Gel Electrophoresis. In *Current Protocols in Molecular Biology* Vol. 51, pp 2.5A.1-2.5A.9. Wiley Online Library

Wiley J, Sons (2002) Media preparation and bacteriological tools. In *Current Protocols in Molecular Biology* Vol. 59, pp 1.1.1-1.1.7. Wiley Online Library

Wiley J, Sons (2006) One-Dimensional SDS Gel Electrophoresis of proteins. In *Current Protocols in Molecular Biology* Vol. 75, pp 10.12A.12-10.12A.37. Wiley Online Library

Winsor GL, Lam DK, Fleming L, Lo R, Whiteside MD, Yu NY, Hancock RE, Brinkman FS (2011) Pseudomonas Genome Database: improved comparative analysis and population genomics capability for Pseudomonas genomes. *Nucleic acids research* **39:** D596-600

Yang Y, Bhachech N, Bush K (1995) Biochemical comparison of imipenem, meropenem and biapenem: permeability, binding to penicillin-binding proteins, and stability to hydrolysis by beta-lactamases. *The Journal of antimicrobial chemotherapy* **35:** 75-84

Yao X, Jericho M, Pink D, Beveridge T (1999) Thickness and elasticity of gram-negative murein sacculi measured by atomic force microscopy. *Journal of bacteriology* **181:** 6865-6875

Zamorano L, Reeve TM, Deng L, Juan C, Moya B, Cabot G, Vocadlo DJ, Mark BL, Oliver A (2010) NagZ inactivation prevents and reverts beta-lactam resistance, driven by AmpD and PBP 4 mutations, in Pseudomonas aeruginosa. *Antimicrobial agents and chemotherapy* **54:** 3557-3563

Zamorano L, Reeve TM, Juan C, Moya B, Cabot G, Vocadlo DJ, Mark BL, Oliver A (2011) AmpG inactivation restores susceptibility of pan-beta-lactam-resistant Pseudomonas aeruginosa clinical strains. *Antimicrobial agents and chemotherapy* **55:** 1990-1996

Addendum

Addendum

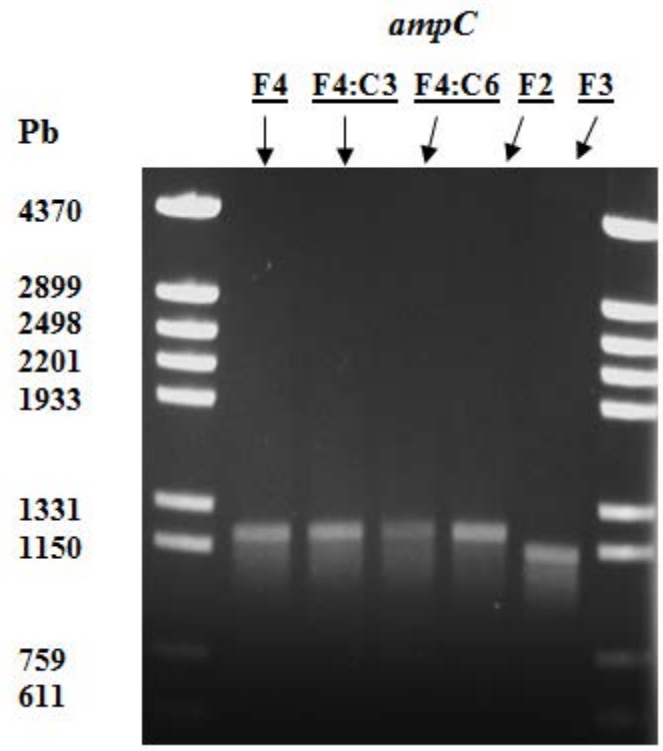

Figure A.1. Colony-PCR amplifications of the different *ampC* forms displaying their DNA fragment sizes.

Agarose gel electrophoresis shows DNA sizes of ampC-F4, ampC-F4:C3, ampC-F4:C6, ampC-F2 and ampC-F3which were amplified by colony-PCR of Bl21(DE3) harboring pET-F4, pET-F4:C3, pET-F4:C6, pET-F2 and pET-F3, respectively. For simplification, only colony-PCR confirmation of some ampC forms were shown while all other ampC were confirmed by the same way in transformants of Bl21(DE3), DV900(DE3) and PAO1 strains; where, ampC-F1 and ampC-F4-TEV displayed a very close size and migration as shown by ampC-F4; ampC-F1:C3 and ampC-F1:C6 displayed a very close size and migration as shown by ampC-F4:C3 and ampC-F4:C6, respectively. All of ampC-F3:C3, ampC-F3:C6 and ampC-F3-TEV displayed a very close size and migration as shown by ampC-F3. Colony PCR of ampC-F1, ampC-F4-TEV, ampC-F1:C3, ampC-F1:C6, ampC-F3:C3, ampC-F3:C6 and ampC-F3-TEV were amplified from the clones pET-F1, pET-F4-TEV, pET-F1:C3, pET-F1:C6, pET-F3:C3, pET-F3:C6 and pET-F3-TEV, respectively, in E. coli; while we cloned only the two forms ampC-F3 and ampC-F4 in PAO1 strains using the vectors pUCP-F3 and pUCP-F4, respectively. All of these clones have been confirmed by DNA sequencing.

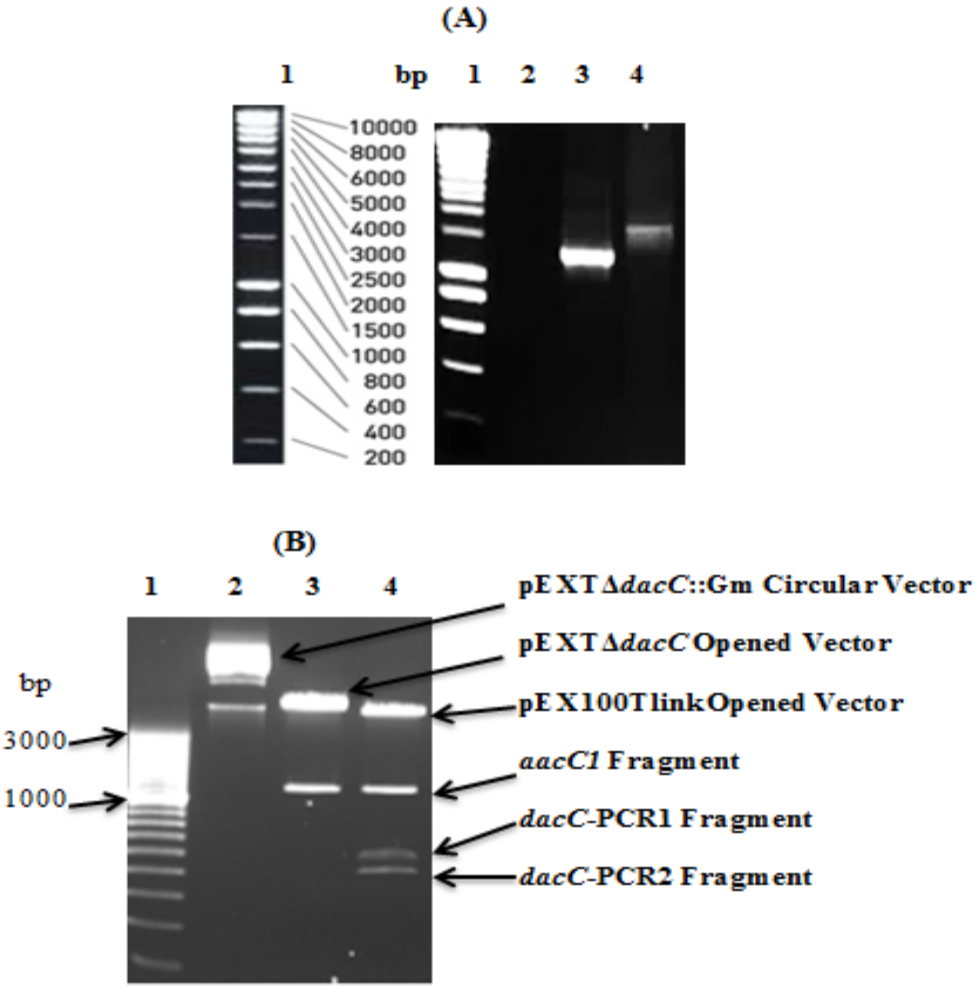

Figure A.2. Confirmation of the constructed *pbpG* and *dacC* gene-specific mutagenesis vectors.

(A) Verification of the constructed pbpG gene-specific mutagenesis vector by colony PCR and agarose gel electrophoresis: lane 1: DNA Ladder (SmartLadder); lane 2: PCR negative control; lane 3: pbpG-PCR positive control; lane 4: colony PCR of E coli XL1 havepEXTΔpbpG::Gm vector. (B) Confirmation of the constructed dacC gene-specific mutagenesis vector by treatment with restriction enzymes: lane 1: 100bp DNA Ladder; lane 2: pEXTΔdacC::Gm circular vector; lane 3: pEXTΔdacC::Gm cleaved with Hind III; lane 4: pEXTΔdacC::Gm cleaved with HindIII, EcoRI and BamHI. All colony PCR and enzyme digestions were visualized by 1% agarose gel electrophoresis.

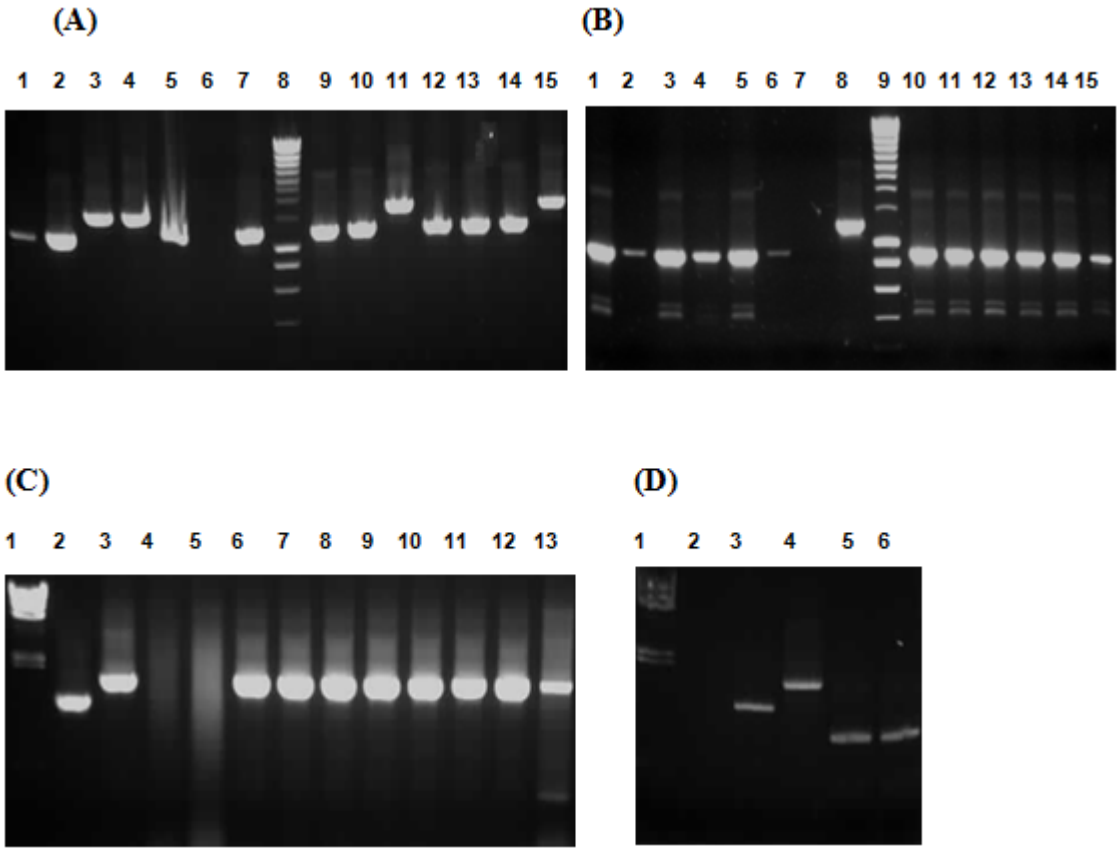

Figure A.3. Verification of the constructed mutants PAOΔ*pbpG*, PAOΔ*dacB* Δ*pbpG* *and* PAOΔ*pbpG*Δ*ampC* by colony PCR and agarose gel electrophoresis.

(A) Confirmation of recombination for PAOΔpbpG::Gm and PAOΔdacBΔpbpG::Gm constructs: lanes 1, 2 and 5: not PAOΔpbpG::Gm genotype; lanes 3 and 4: have PAOΔpbpG::Gm genotype; lane 6: PCR negative control; 7: PCR positive control for PAO1 pbpG; lane 8: DNA Smart Ladder; lanes 9, 10, 12, 13, and 14: not PAOΔdacBΔpbpG::Gm genotype; lanes 11 and 15: have PAOΔdacBΔpbpG::Gm genotype. (B) Confirmation of elimination of Gm resistance cassette; lanes 1→6: have PAOΔpbpG genotype; lanes 7 and 8: pbpG-PCR negative and positive controls; lane 9: smart Ladder; lanes 10→15: have PAOΔdacBΔpbpG genotype. (C) Confirmation of recombination for PAOΔampC ΔpbpG::Gm construct; lane 1: λ HindIII DNA ladder. Lane 2: pbpG-PCR positive control; lane 3: PCR positive control for recombination using pEXTΔpbpG::Gm; lanes 6→13: have PAOΔampCΔpbpG::Gm genotype; (D) Confirmation of elimination of Gm resistance cassette from PAOΔampCΔpbpG::Gm; lane 1: λ HindIII DNA ladder; lanes 2 and 3: pbpG-PCR negative and positive control, respectively; lane 4: PCR positive control for recombination using pEXTΔpbpG::Gm; lanes 5 and 6: have PAOΔpbpG ΔampC genotype.

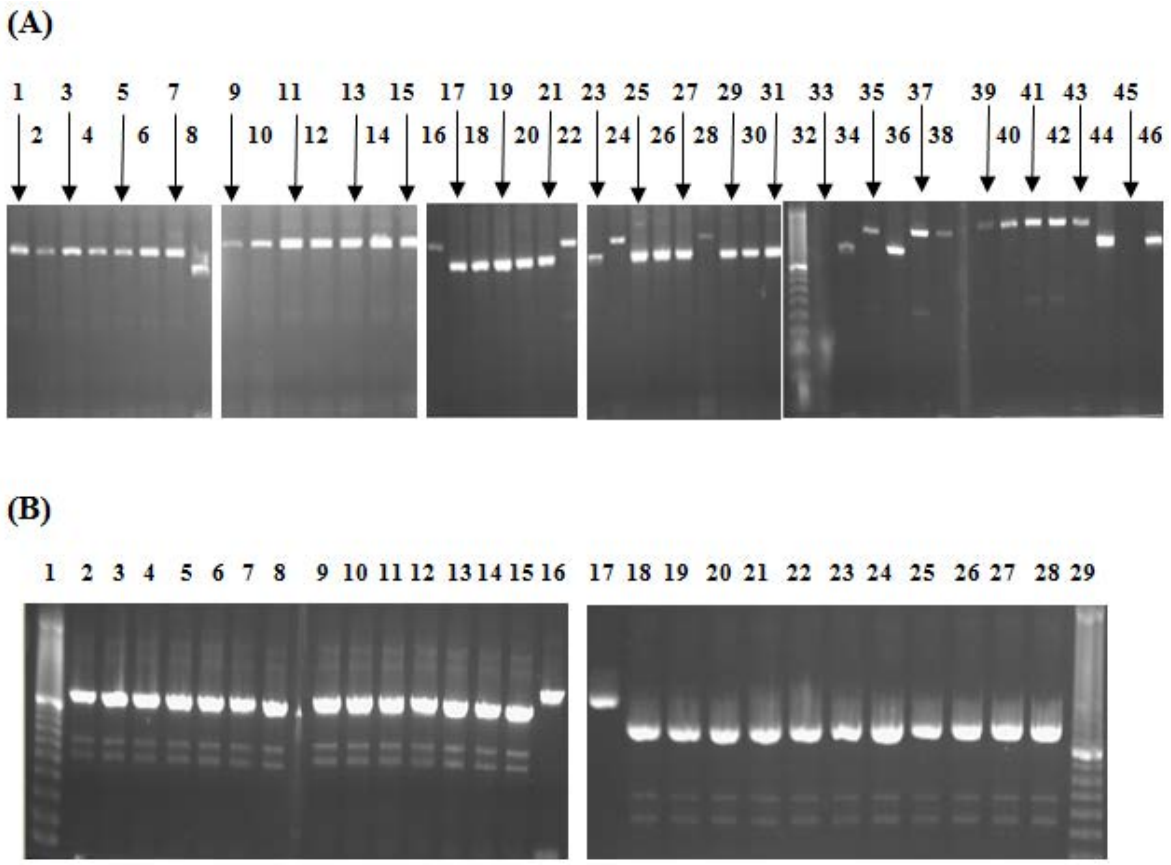

Figure A.4. Verification of the constructed mutants PAOΔ*dacC*Δ*ampC*, PAOΔ*dacC*Δ*pbpG*, PAOΔ*dacC*, PAOΔ*dacB*Δ*dacC* and PAOΔ*dacB*Δ*dacC*Δ*pbpG*.

(A) Confirmation of recombination; lanes 1→7: havePAOΔampC ΔdacC::Gm genotype; lanes 8, 23, 34 and 46: dacC-PCR positive control; lanes 9→15: have PAOΔdacC::Gm genotype; lanes 16 and 22: have PAOΔpbpGΔdacC::Gm genotype; lanes 17→21: not PAOΔpbpGΔdacC::Gm genotype; lanes 24 and 28: have PAOΔdacBΔdacC::Gm genotype; lanes 25→27 and 29→31: not PAOΔdacBΔdacC::Gm genotype; lane 32: 100 bp DNA ladder; lanes 33 and 45: PCR negative control; lanes 35 and 37→43: have PAOΔdacBΔpbpGΔdacC::Gm genotype. (B) Confirmation of removal of Gm resistance cassette; lanes 1 and 29: 100 bp DNA ladder; lanes 2→6: have PAOΔdacCΔampC genotype; lanes 7→11: have PAOΔdacC genotype; lanes 12→15: have PAOΔdacCΔpbpG genotype; lanes 16 and 17: dacC PCR positive control; lanes 18→24: have PAOΔdacBΔdacCΔpbpG genotype; lanes 25→28: have PAOΔdacBΔdacC genotype.

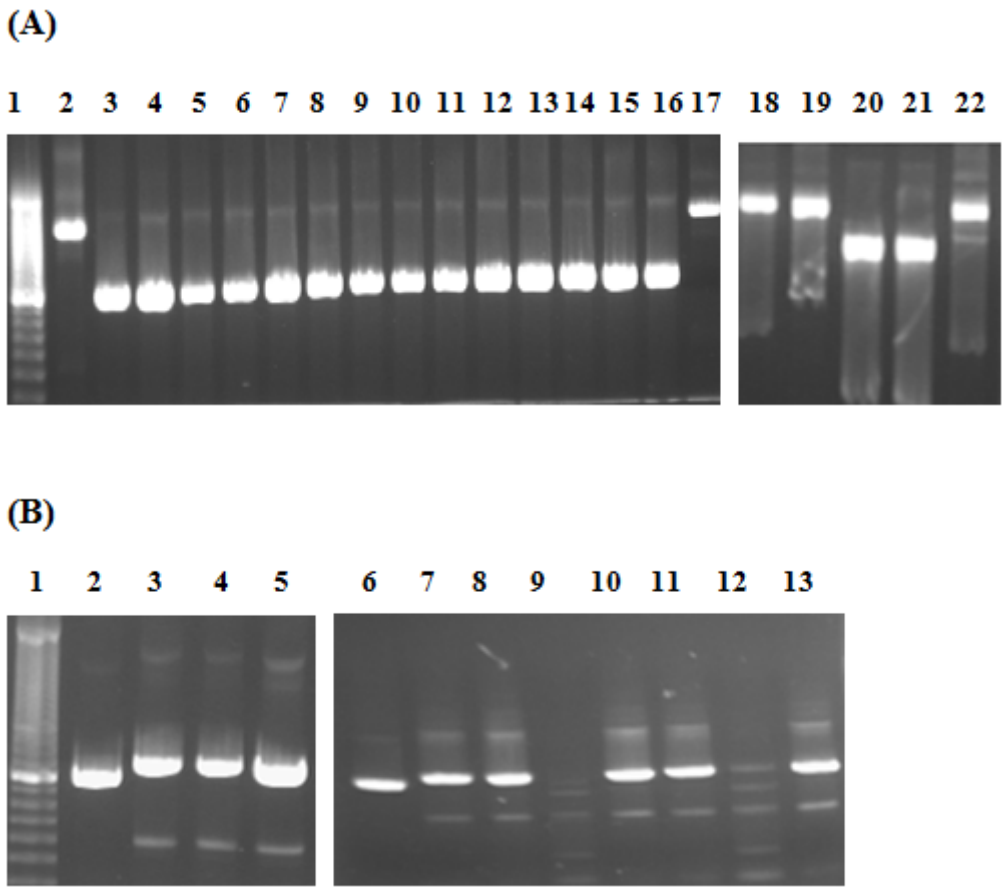

Figure A.5. Verification of the constructed mutants PAOΔ*dacB*Δ*ampC* and PAOΔ*dacB*Δ*pbpG*Δ*ampC*.

(A) Confirmation of recombination of PAOΔdacBΔampC::Gm construct; lane 1: 100 bp DNA ladder; lane 2 and 18: recombination PCR control positive using pEXTΔampC::Gm; lane 3: ampC PCR positive control; lanes 4⟶16: Not PAOΔdacBΔampC::Gm genotype; lane 17: has PAOΔdacBΔampC::Gm genotype; lanes 19 and 22: have PAOΔdacBΔpbpGΔampC::Gm genotype. (B) Confirmation of removal of Gm resistance cassette; lane 1: 100 bp DNA ladder; lanes 3 and 4: have PAOΔdacBΔampC genotype; lanes 5 and 6: ampC PCR positive control; lanes 7, 8, 10, 11, and 13: have PAOΔdacBΔpbpGΔampC genotype.

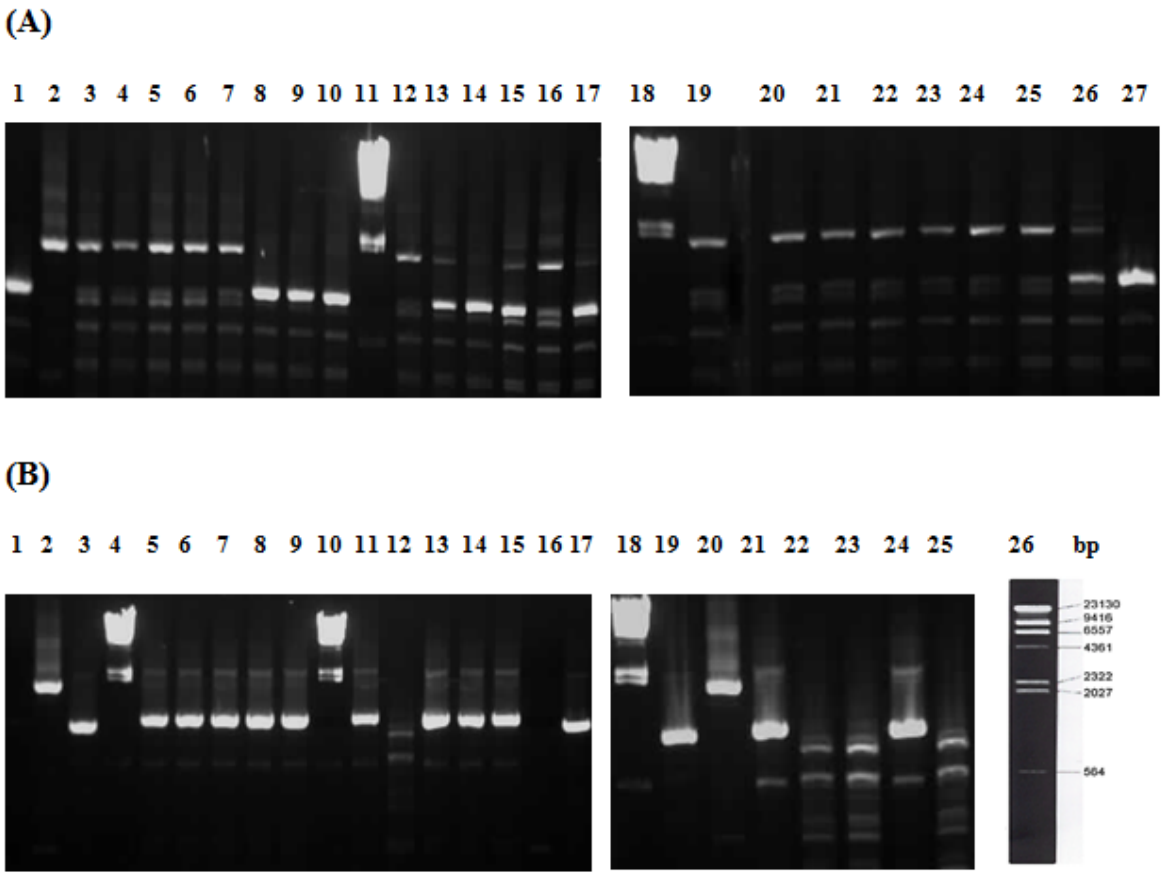

Figure A.6. Verification of the constructed mutants PAOΔ*dacB*Δ*dacC*Δ*ampC*, PAOΔ*dacC*Δ*pbpG*Δ*ampC* *and* PAOΔ*dacB*Δ*dacC*Δ*pbpG*Δ*ampC*.

(A) Confirmation of recombination in PAOΔdacCΔpbpGΔampC::Gm and PAOΔdacCΔpbpGΔ ampC::Gm constructs; lanes 1 and 27: ampC PCR positive control; lane 2: recombination PCR positive control using pEXTΔampC::Gm; lanes 3→7: have PAOΔdacBΔ dacCΔ ampC::Gm genotype; lanes 11 and 18: λ HindIII DNA ladder; lanes 12 and 16: have PAOΔdacCΔpbpGΔampC::Gm genotype; lanes 19→25: have PAOΔdacBΔdacCΔpbpGΔampC::Gm genotype. (B) Confirmation of removal of Gm resistance cassette; lane 1: PCR negative control; lanes 2 and 20: recombination PCR positive control using pEXTΔampC::Gm; lanes 3 and 19: ampC PCR positive control; lanes 4, 10, 18 and 26: λ HindIII DNA ladder; lanes 5→9: have PAOΔdacBΔdacCΔampC genotype; lanes 13→15 and 17: have PAOΔdacCΔpbpGΔampC genotype; lanes 21 and 24: have PAOΔdacBΔdacCΔpbpGΔampC genotype. All colony PCR amplifications were visualized by agarose gel electrophoresis.

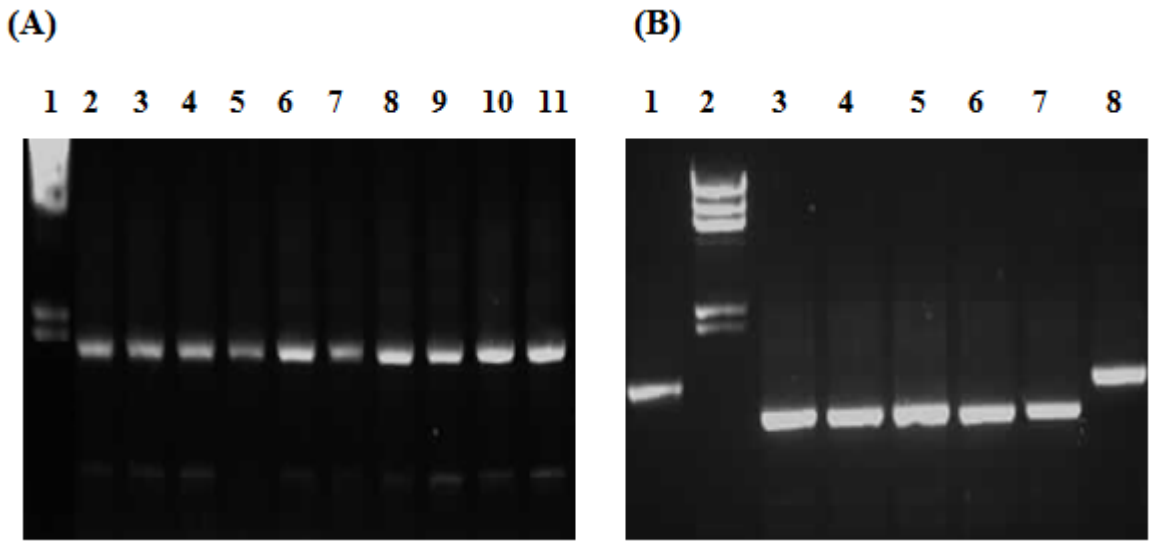

Figure A.7. Verification of the constructed mutant PAOΔ*dacB*Δ*pbpG*Δ*ampC* Δ*dacC*. *(A) Confirmation of recombination in PAOΔdacBΔpbpGΔampCΔdacC::Gm construct; lane 1: λ HindIII DNA ladder; lanes 2→11: have PAOΔdacB ΔpbpGΔampCΔdacC::Gm genotype. (B) Confirmation of removal of Gm resistance cassette; lanes 1 and 8: dacC-PCR positive control; lane 2: λ HindIII DNA ladder; lanes 3→7: have PAOΔdacBΔpbpGΔampCΔdacC genotype.*